Impacts of Pricing Structures on Home Battery Storage Operation and Economics

Michael Campbell

A thesis presented for the degree of
Doctor of Philosophy
in
Electrical and Computer Engineering
at the
University of Canterbury,
Christchurch, New Zealand.

31 January 2021

ABSTRACT

This thesis considers the optimisation of residential battery energy storage system (BESS) operation in order to maximise the financial savings made by the consumer under different pricing structures. It also examines the effect of this financially motivated behaviour on aggregated network loads.

This thesis contributes a mixed integer linear programming (MILP) formulation for the optimisation of the operation of a residential BESS. This method incorporates a BESS efficiency function with both charge/discharge rate dependent and independent components. Driven by common pricing structures in New Zealand, it allows for flexible time varying energy pricing with separate time varying feed-in tariffs. This method, using perfect foresight to produce optimal BESS behaviour, puts an upper bound on the financial savings that could be expected to be made.

A rule-based heuristic method for BESS behaviour is also presented. This goes beyond the common 'greedy algorithm' which maximises photo-voltaic (PV) self-consumption, to instead make decisions based on price thresholds. A primitive day-ahead PV generation forecast is incorporated to inform BESS behaviour. This rule-based method puts a lower bound on the financial savings that could be expected to be made with a simple BESS controller. It is expected that further sophistication of the rules used would serve to narrow the gap between this lower bound and the upper bound of the MILP method.

These methods are applied to three different pricing structures to demonstrate their application to cases where pricing is fixed and known ahead of time, and also to more variable real time pricing structures such as spot price. The presented analysis considers both the financial savings that BESSs provide to customers, as well as the effects that their behaviour has on aggregated peak loads at varying levels of BESS penetration. The capacity of these BESSs to respond to third party signals to provide peak reduction services is also examined.

ACKNOWLEDGEMENTS

I give my sincere thanks and appreciation to following people and groups who have played a part in bringing this research to fruition.

I wish to acknowledge the support of my supervisors throughout the journey of this thesis. Dr Allan Miller for starting the journey, Professor Neville Watson for having been there since the beginning, Dr Alan Wood for stepping in at the halfway mark and pointing me in the right direction, and Dr Radnya Mukhedkar for helping me down the final straight - thank-you. Each of you have a played a role in this journey, and for that I am grateful.

This thesis was made possible through the financial support of the Electric Power Engineering Centre (EPECentre) at the University of Canterbury.

Thank-you to my fellow post-graduates students in the ECE department and EPECentre for the camaraderie, discussions, and distractions. There are those of you I've shared an office with - Thomas Smart, Luke Schwartfeger, Euan McGill, and those that have been down the hallway - Josh Schipper, Parash Acharya, and Scott Lemon. An additional thanks to Scott for providing the PV data.

To my family for your constant love and support - thank-you. If you are reading this then my answer is "yes, I'm finished", and "yes, I'll come and visit now."

To Riley, and the rest of the UCSA technical and production team - I hold you at least partially responsible for adding to my completion time. Nevertheless I've enjoyed putting some electrical engineering skills to use on various projects and schemes.

Finally, and most importantly, I wouldn't be here without Tegan, my partner and best friend. Your support, love, and encouragement has kept me going. I look forward to picking up my share of the housework.

The final 5 months of this thesis journey has seen the world changed by COVID-19. I've been fortunate that the extent of its impact on me was an enforced 6 week lock-down of focussed writing, and supervisory meetings over Zoom. As I reflect on my time as a post-graduate student, I am reminded of the sage words of advice I received before I began my thesis journey from PhD student at the time, Dr Yanosh Irani - "don't do it man, don't do it."

CONTENTS

GLOSSARY

This glossary contains the key notation and abbreviations used in this thesis.

NOTATION

Power Flows

$\boldsymbol{g}$ PV generation power
$\boldsymbol{l}$ load power
$\boldsymbol{x_c}$ charging power
$\boldsymbol{x_d}$ discharging power
$\boldsymbol{x_e}$ export power
$\boldsymbol{x_i}$ import power

Price

$\boldsymbol{p_i}$ import price
$\boldsymbol{p_e}$ export price

State of Charge

$\boldsymbol{\chi}$ state of charge
$\boldsymbol{C}$ battery capacity
$\overline{\mathbf{C}}$ allowable SOC increase from initial value
$\underline{\mathbf{C}}$ allowable SOC increase from initial value

Efficiency

$\boldsymbol{\eta_{RT}}$ round-trip efficiency
$\boldsymbol{\eta_c}$ charge efficiency
$\boldsymbol{\eta_d}$ discharge efficiency
$\boldsymbol{b}$ number of efficiency bands
$\boldsymbol{L_c}$ charge efficiency segment length
$\boldsymbol{L_d}$ discharge efficiency segment length
$\boldsymbol{a_c}$ charge efficiency segment breakpoint
$\boldsymbol{a_d}$ discharge efficiency segment breakpoint

ACRONYMS

AC alternating current
ADHDP action dependent heuristic dynamic programming
BESS battery energy storage system
DC direct current
DP dynamic programming
DSM demand-side management
EDB electricity distribution businesss
ESR equivalent series resistance
ESS energy storage system
EV electric vehicle
GXP grid exit point
HVDC high-voltage direct current
ILP integer linear programming
IoT internet of things
IRR internal rate of return
LCOE levelised cost of energy
LP linear programming
LV low voltage
MILP mixed integer linear programming
MV medium voltage
NIWA National Institute of Water and Atmospheric Research
PV photo-voltaic
QP quadratic programming
RCPD Regional Coincident Peak Demand
SOC state of charge
TOU time of use
TPM Tranmission Pricing Methodology

Chapter 1

INTRODUCTION

1.1 GENERAL OVERVIEW

The electric power supply industry has, for many years, been largely stable. While there have been incremental improvements in technologies, the core concept has remained unchanged: large generators feed power into transmission networks, these transmission networks deliver power to distribution networks which feed end consumers' premises. The power flows are unidirectional, from large generators through to residential, commercial, and industrial loads.

In recent years, however, the development of new technologies has threatened to disrupt the traditional model and its notion of unidirectional power flows. The growth of these technologies is driven not just by technical improvements and falling costs, but also pressures to reduce emissions of greenhouses gases associated with electricity supply and to increase levels of renewable generation. These growing technologies include solar photo-voltaic (PV) generation, electric vehicles (EVs), and home battery energy storage systems (BESSs). The early motivation for this thesis came from attempting to develop an understanding of the impacts which these three technologies would have household on load profiles as their prevalence grew. It became apparent that the effect of BESSs is entirely dependent on the way in which they are operated which, for the rational consumer, means maximising the financial savings a BESS brings.

Of the three technologies identified, PV generation is the most established. Its impact on load profiles can be modelled with techniques which correlate solar irradiance data to expected power generation given location, climatic conditions, and PV system parameters.

Determination of the effect of electric vehicles on household load profiles presents a different challenge due to their impacts being dependent on aspects of human behaviour: the distances people travel in their vehicles, as well as when and where they choose to charge. There is also uncertainty surrounding electric vehicle uptake. Globally, and in New Zealand, EV numbers are growing at an increasing rate [1], [2]. The long term trajectory of such growth is unknown. There is also an expectation that charging

behaviours, and thus the effects on network load, will change as uptake grows. Charging is often undertaken overnight while vehicles are parked at owners' homes, but as the prevalence of public charging infrastructure grows, it is expected that a portion of that overnight charging will be shifted to the daytime while vehicles are parked in public or workplace spaces.

Home BESSs possess many similar attributes to electric vehicles but, by nature of being statically located at a household, have greater freedom in their operation. Unlike an electric vehicle, their operation is not constrained by needing to be at home (or at public charging locations) to be able to charge. The impact of BESSs on household load profiles is dependent on the battery operation methodology. That methodology is not entirely obvious, and could depend on the system owners' intentions and desires as well as more technical considerations. The rational system owner will operate their battery in a way that is most economically beneficial for themselves. What that optimal behaviour entails will depend upon the pricing structure which the system owner is subject to. It is this effect of pricing structure on battery storage economics and operation which this thesis sets out to model and understand.

In order to understand the impact of BESSs it is necessary to understand their operation and charge/discharge schedules. In particular, the operation of BESSs in an economically rational fashion is of greatest interest. That is because mass uptake without significant regulatory intervention will only be seen when it is financially prudent. It is accepted, however, that not every BESS owner will behave in an economically rational fashion - some may only be interested in having a BESS as a backup power source for a grid outage, while others might care only for maximising their PV generation self-utilisation or for reducing CO_2 emissions associated with their electricity consumption.

1.2 THESIS OBJECTIVES

The objective of this thesis is to assess the operation of home energy battery storage systems alongside PV generation under different pricing structures. This assessment is both in terms of the financial savings that BESSs can bring for households and the effect they have on the loads experienced by distribution networks. Additionally, there is the desire to understand and quantify the potential for home BESSs to contribute to peak reduction services in a distribution network.

To achieve these objectives, two modelling methods are developed. The first uses linear programming (LP) and mixed integer linear programming (MILP) optimisation techniques, alongside perfect foresight of PV generation and household load, to put an upper bound on the financial savings able to be made by households. Unlike many existing techniques, these optimisation methods incorporate charge/discharge rate dependent efficiency functions. Steps are also taken to ensure a short computation time such that it is practical to apply the method to a large set of households.

The second modelling method is a heuristic rule-based decision making process with an approximate PV generation forecast rather than complete perfect foresight. This puts on a lower bound on the savings that could be easily achieved by an intelligent battery control system. In reality, modern commercial battery control systems are likely to integrate greater complexity and additional data sources into their decision making. This means they are likely to achieve financial savings within the bounds of the first optimisation method at the upper end, and the rule-based method at the lower end.

In addition to quantifying the financial benefits able to be achieved by BESS owners, these methods are used to assess the impacts this economically motivated operation has on aggregated network load profiles. Of particular interest are peak network loads. There are two aspects to be assessed: the first is the effect of economically rational BESS operation on the peak network loads, and the second is the ability of BESSs to provide peak reduction services to a network. The financial impact on the BESS owner of providing peak reduction services is quantified.

1.3 THESIS CONTRIBUTIONS

The main contributions made by this thesis are:

- Modelling methods utilising LP and MILP optimisation techniques to determine an upper bound on the financial savings a household can make with a BESS. These utilise perfect foresight of household load and PV generation. The key contribution of these methods is the inclusion of charge/discharge rate dependent battery efficiency functions.
- A heuristic rule-based decision making method with an approximate PV forecast which yields a lower bound on the savings that could be made with an intelligent battery control system.
- An assessment of the impacts of the economically motivated operation of BESSs under different pricing structures on aggregated network load profiles. In particular, the effect of BESSs on peak loads is assessed. This considers both the effect of economically motivated operation on network peaks as well as the ability of BESSs to provide peak reduction services. Through this analysis the financial implication of a BESS owner providing peak reduction services is quantified.

1.4 THESIS OVERVIEW

Chapter 2 provides background on a range of new technologies that have the potential to disrupt the electricity industry. BESSs are discussed; this includes the diversity of products available and the benefits they could bring to different segments of the

electricity market. Background on transmission and distribution pricing schemes is given in order explain why peak load control is of such interest. Existing models and optimisations of residential BESSs are reviewed.

Chapter 3 details the development of LP and MILP models of individual households with PV generation and BESSs which optimise battery operation in order to minimise the household's energy bill. These methods use perfect foresight of household load and PV generation. This places an upper limit on the financial savings that could be achieved by consumers. This chapter includes the development of two load dependent efficiency models for battery charge and discharge operations.

Chapter 4 presents an alternative to the LP/MILP models which does not rely on perfect foresight of PV generation and household load. Instead it uses an approximate day ahead PV forecast and rule-based decision tree structure to determine battery operation at each simulation time step. This puts a lower bound on the financial savings a simple battery management system could achieve.

Chapter 5 details the input datasets which are used to produce results from the methods presented previously. It also details considerations that need to be made in applying these two methods to real world data and solving them in a practical time for a large number of individual households.

Chapter 6 presents the results of applying the two methods to real world data under three different pricing structures. These pricing structures cover both known pricing (pricing is fixed and known ahead of time), and unknown pricing (a real-time varying electricity price). The results are presented both in terms of economic results for households, as well as the effect on the peak loads of a network when household loads are aggregated.

Chapter 7 discusses possible improvements that could be made to work in this thesis and suggest areas for future research.

Chapter 8 presents the main conclusions of this research.

Chapter 2

BACKGROUND

2.1 INTRODUCTION

The electric power engineering industry is undergoing a period of change with a number of new technologies being adopted by consumers at increasing rates. As recognised by Transpower, the New Zealand grid owner, in their *Te Mauri Hiko - Energy Futures* white paper, these technologies bring with them the opportunity for a cleaner, more sustainable energy future [3]. Achieving this future, however, depends the ability of the electricity supply industry to understand, plan for, coordinate, and embrace these technologies.

The effect of uptake of some of these technologies can be modelled by applying established techniques to known data. For example, with solar irradiance data, and PV panel and inverter characteristics, the impacts of growing consumer PV generation can be modelled. The modelling of the effects of electric vehicles on the power system is complicated by aspects of human behaviour. People choose when to charge their vehicles, and this choice is impacted by factors such as their daily travel routine, sensitivity to price, and range anxiety [4], [5]. For residential BESSs there is also a significant aspect of operational freedom as to when battery systems charge and when they discharge. If the system owner wants to be able to use the battery system as backup for grid outages then that will result in different behaviour compared with only attempting to maximise financial returns.

Sharma and Shah [6] neatly summarise a number of drivers and barriers to widespread adoption of BESSs. The first identified driver is cost reductions. The growing EV market is driving manufacturer economy of scale for lithium-ion batteries which contributes to the cost reductions alongside the improving technologies. In 2019 BloombergNEF reported an 87% decrease in lithium-ion battery prices since 2010 [7]. Another driver for increasing storage is the general grid modernisation efforts which are occurring in many countries to improve resiliency and efficiency. These efforts are incorporating modern technology to provide two-way communication and advanced control systems which enable opportunities for value to be derived from BESSs. A third

driver is the global shift toward renewable energy and reduction of emissions. A fourth driver is financial incentives being offered by governments. While there are not such financial incentives in New Zealand, [6] recognises that countries with energy security concerns, or countries with an economic stake in battery manufacture, have particularly generous incentives. Low, or declining, feed-in tariffs, as well as net metering are also recognised as drivers for BESSs by consumers trying to maximise the return on their PV generation investments. Other factors beyond economics, such as a desire for self-sufficiency, can also be drivers for consumer uptake.

There are also barriers to more widespread adoption of BESS technologies. The first of these is not just price, but also perception of high prices. With battery prices dropping constantly, consumer's perceptions of pricing and economic feasibility can quickly become outdated. While battery systems are not economic in every case, the perception of price may stop them from even being considered. Another barrier identified in [6] is incomplete definitions and understandings of the value streams that could be derived from battery storage. This is further hampered by outdated regulations and market structures which do not align with the capabilities of modern storage technologies. The capability of modern BESSs to provide different services is discussed in Section 2.2.2.

It is clear from this overview that there are diverse drivers and barriers to the development of widespread BESSs. These factors are not just technical, but also economic, regulatory, environmental, and social. Nevertheless, it is clear that widespread adoption at the residential level will only occur when there is economic impetus to do so.

The remainder of this chapter reviews BESSs - including different types, their potential to benefit different segments of the electricity market, differences resulting from where battery storage is placed in the network, and the efficiency of BESSs.

As part of understanding the potential benefits of BESSs to different market segments, it is necessary to understand pricing structures not just at the consumer level, but also distribution and transmission pricing. These are explored in this chapter along with the use of demand-side management (DSM) in the form of ripple control signalling to provide peak management in distribution networks.

Finally, a review of BESS optimisation literature is presented.

2.2 BATTERY ENERGY STORAGE SYSTEMS

This sections presents an overview of BESSs including the types of commercial products in the market, the services and benefits that BESSs could provide to different segments of the electricity industry, and some common control schemes that systems are operated under.

2.2.1 BESS Market

There is a range of commercial BESS products that exist in the market. Many of them are made by large global electronics manufacturers such as Panasonic, LG, Sony, and Samsung. There are also many that come from manufacturers in the PV industry such as sonnen, SolaX, SMA, and Enphase. Pehraps the most ubiquitous is Elon Musk's Tesla with their Powerwall product.

Residential BESSs can be categorised in a number of ways. One categorisation is the division of all-in-one products such as the Tesla Powerwall, and modular products which separate inverters and batteries into separate products. This allows battery capacity to be customised with the number of battery modules installed. Because of this the BESS can be custom sized to the requirements of a household to ensure the best possible returns are achieved. Another characteristic by which BESSs can be categorised is by the coupling of PV generation into the system. Some systems are DC-coupled, meaning PV generation is coupled to the DC bus, while others are AC-coupled meaning there is a separate inverter for the PV generation. This has the benefit of allowing a BESS to be more easily retrofitted to an existing PV generation installation.

Significant variation exists in the battery capacity and the power ratings of products that exist in the market. At the smaller end exist products such as the Enphase Encharge 3 with a usable storage capacity of 3.36 kWh and rated power of 1.28 kW [8], through to products such as the Tesla Powerwall with a 5 kW continuous power rating and 13.5 kWh of storage capacity [9]. As an example of the range of installed products, Figgener, Stenzel, Kairies, *et al.* [10] review residential BESSs in Germany and finds, that in 2018, the mean usable capacity is 8 kWh, with 75% of all systems having a usable capacity of between 4.5 kWh and 12.5 kWh. Figgener, Stenzel, Kairies, *et al.* [10] shows that the typical usable capacity has been steadily increasing since 2015 as prices fall and technology improves. Beyond this are commercial and utility scale storage solutions where power ratings can be in the hundreds of kilowatts with storage capacities to match.

2.2.2 Benefits of Storage for Different Market Segments

BESSs have the technical potential to bring benefits and services to all segments of the electricity industry. These benefits and services include ancillary frequency keeping and reserve services, energy arbitrage, peak reduction allowing deferral of network upgrades, and increasing PV self-consumption. The location of storage within a network is something explored by Transpower in their 2017 discussion document *Battery Storage in New Zealand* [11]. One of the key conclusions of this report is that batteries offer the greatest value when installed 'behind the meter' where they give benefits to the owner directly, as well as have the potential to provide services upstream in distribution and transmission networks.

Transpower also recognises that the value of these services will not be realised by consumers until there is appropriate market pricing, payment structures, tools, and systems available. Both in New Zealand, and globally, electricity market regulations do not allow for all possible value streams that could be derived from BESS. Work is required to price services in a manner that provides incentives for consumers to use electricity in ways that reduce cost and deliver value for wider society, as well as for pricing that is truly cost-reflective. Development of new market structures and ways to monetise the services which batteries can offer will increase value for end-consumer battery owners [11]. The recognition of the challenge that regulations pose to the establishment of new market offerings to fully utilise the services that BESSs could offer is echoed in [12] and [13]. Sharma and Shah [6] note that nearly every nation they examined is considering changes to their market structure to allow for BESSs to provide capacity and ancillary services, with varying degrees of success.

Transpower [11] identifies 13 possible services that batteries could provide to the electricity industry. These are largely based on the work of Fitzgerald, Mandel, Morris, *et al.* [14]. These services and their applicability at different battery locations within the grid are show in Table 2.1.

Table 2.1 Services which could be provided by BESSs at different locations in the grid.

		Transmission	Distribution	Behind the Meter
Customer Services	Backup Power			✓
	Increased PV Self-Consumption			✓
	Demand Charge Reduction			✓
	Time-of-Use Bill Management			✓
Utility Services	Distribution Deferral		✓	✓
	Transmission Deferral	✓	✓	✓
	Transmission Congestion Relief	✓	✓	✓
	Resource Adequacy	✓	✓	✓
System Operation Services	Black Start	✓	✓	✓
	Voltage Support	✓	✓	✓
	Frequency Regulation	✓	✓	✓
	Spinning/Non-Spinning Reserve	✓	✓	✓
	Energy Arbitrage	✓	✓	✓

An alternative arrangement of these services is to categorise them by their purpose. [11] identifies four categories listed below.

- Back-up functions for power supply failure.
  - Black start
  - Back-up power
- Moving energy - storing energy in times of surplus and low-price to be used when supply is tight and price is high.
  - Energy arbitrage
  - Time of use bill management
  - Increased solar PV self-consumption
- Capacity management - reducing peak demand so that less capacity is needed for generation, transmission, and distribution.

  - Demand charge reduction
  - Transmission constraint relief
  - Transmission deferral
  - Distribution deferral
- Power system operations - evening out variations, restoring balance, or improving voltage.
  - Frequency keeping
  - Instantaneous reserves
  - Resource adequacy
  - Voltage support

For residential consumers it is the second category (moving energy) which relates most to the reasons they would invest in the installation of a BESS under current market and pricing structures. The back-up power that a BESS could provide may also feature in that investment decision. The remaining services do not have a direct bearing on residential consumers. If market structures allowed for financial compensation for behind-the-meter BESSs providing these services, then that would further influence the investment decision.

Battery Storage in New Zealand [11] identifies the potential value offered by each of these services in terms of dollars per kilowatt per annum. Though these figures are reliant on many assumptions, it gives a metric by which to compare the relative value of the services. At the top of the ranking is distribution deferral, peaking capacity, demand charge reduction, increasing PV self-consumption, and frequency regulation. It is also noted by that due to New Zealand's prevalence of flexible hydro generation the procurement of grid services is generally low-cost and therefore the potential revenue from providing some services with batteries is lower than what has been seen in other international examples.

Not all of these services are complementary, nor does current market structure allow for all of them. For example, a battery which is being used to manage capacity or provide peak reduction services may end up fully discharged at which point it has no ability to provide back-up power. Conflicts could also exist with multiple contracted or paid uses. Though batteries could theoretically generate revenue from all these different services, in reality, and under current market structures, their ability is much more limited.

2.2.3 Common Control Schemes

It is important to consider the different control schemes under which these BESSs can operate. The first of these is a simple backup only control scheme; batteries are kept at a high state of charge (SOC) and only used during a grid failure. A typically BESS

installation with back-up power capability designates only a subset of circuits in a house as essential loads which are able to be supplied during a grid outage.

Another simple control scheme is time-based control; the BESS is programmed to charge and discharge at particular times. For consistent load patterns this may lead to reasonable financial savings resulting from BESS operation, however for more variable patterns of generation and consumption this does not guarantee efficient battery operation behaviour.

More complex control schemes consider time of use (TOU) tariffs, PV generation, and household load to make charge/discharge decisions. Exact detail of their operation is not typically disclosed by manufacturers, however many products utilise smart phone or web-based control interfaces. As an example, the Tesla Powerwall allows up to a three tiered pricing structure (peak/shoulder/off-peak) with fixed times for each price. The Powerwall also forecasts load and generation continuously to make its operation decisions, and "learns the patterns of your energy use" [15]. It is not clear however how this forecasting and learning is implemented, nor its level of sophistication.

There are also a number of special control modes that exist in these commercial products. Though not available globally, the Tesla Powerwall has a feature dubbed Storm Watch, where it receives storm forecasts over the internet, and will fully charge when a storm is forecast so as to be able to provide maximum backup power should a grid outage occur.

2.3 ELECTRICITY MARKETS AND PRICING

In order to understand the relationship between electricity distribution businesses and battery storage, the motivations and pressures that these electricity distribution businessss (EDBs) experience need to be understood. The particular relevance of battery storage to EDBs is the effects that batteries could have, both positive and negative, on the peak loads they experience. These loads have the potential to accelerate or defer the need for network investment, and thus could have significant financial implications to EDBs. An understanding how EDBs are charged for the transmission services that deliver electricity to their networks, as well as how they charge their customers, the retailers, is key to understanding those financial implications.

2.3.1 Transmission Pricing

In a perfectly competitive market participants are price takers; they cannot affect prices by their own decisions. Perfectly competitive markets are rare however, and some industries are natural monopolies. Electricity transmission is one such natural monopoly. It is therefore common practice for government regulators to influence pricing with the view to producing a better outcome than an unregulated monopoly.

Green [16] identifies six key principles in designing transmission pricing for economic efficiency and political implementation. These are:

1. promote the efficient day-to-day running of the bulk power market;
2. signal locational advantages for investment in generation and demand;
3. signal the need for investment in the transmission system;
4. compensate the owners of existing transmission assets;
5. be simple and transparent;
6. be politically implementable.

The first three of these all relate to price signalling, as does the fifth. As [16] suggests, there is little point in sending a signal if it too complex to be understood. As identified in Section 2.2.2, BESSs have the potential to provide services which could benefit the transmission sector. These benefits largely relate to the reduction of peak loads through demand shifting. It is therefore important to develop an understanding of approaches to transmission pricing with respect to peak capacity.

Frontier Economics in [17], a report prepared for the New Zealand Electricity Commission, provide a comparison of energy markets and transmission pricing methodologies for different countries. Globally there is a mix of jurisdictions where transmission pricing is fully nodal, generator nodal pricing with weighted-average nodal prices for loads, zonal or regional pricing, or single region pricing. There is also a mix of jurisdictions with energy only markets, or also capacity markets, as well as a variety of ways in which costs are allocated. The following sections present key aspects of transmission pricing in the New Zealand context, as well as more globally.

2.3.1.1 Transmission Pricing in New Zealand

Transpower, as grid owner, operates as a monopoly. This means that their total regulated revenue is dictated by the Commerce Commission, however the Electricity Authority is responsible for approving the methodology by which those revenue requirements are apportioned to its customers. These requirements are set out in the Tranmission Pricing Methodology (TPM) which is a schedule to the Electricity Industry Participation Code.

The TPM comprises the recovery of two costs - the costs associated with Transpower's alternating current (AC) network, and the costs associated with its high-voltage direct current (HVDC) assets. The AC network costs comprise of two components - connection charges, and interconnection charges. Connection charges relate to the cost of providing connection assets. This connection charge recovers the annual cost of assets supplying specific customers whether they are injection or take-off customers.

The second part is the interconnection charge which relates to the customer's contribution to Regional Coincident Peak Demand (RCPD). RCPD is defined as "Average of the 'n' $\frac{1}{2}$ hour net offtakes during the regional coincident peak periods for

the region for a customer at a connection location during the capacity measurement period (CMP)" [18].

For all the regions (Upper North Island, Lower North Island. Upper South Island), and Lower South Island) n=100, however, for the North Island and Lower South Island the months of November to April are excluded from CMP. That is to say, the interconnection charge for each grid exit point (GXP) is based on the the average demand of that GXP during the top 100 regional peaks in the measurement period. For the 2019/20 pricing year this interconnection rate is $109.38 per kW.

This interconnection charge provides one incentive to EDBs to manage and reduce their peak demand.

2.3.1.2 Transmission Pricing Internationally

Internationally there are a range of market structures, and measures by which transmission network costs are allocated. Many of these relate to a load's contribution to peak demand. In Argentina a capacity charge component is passed to participants based on a weighting of their share of usage at system peak as determined through load flow modelling. Norway has a load charge component based on average consumption during the peak hour of the last five years. Great Britain considers the three half-hours of peak system demand in the year [17]. Unlike New Zealand, many countries have a locational pricing element to transmission prices alongside locational pricing in the energy market. This could give downstream EDBs an incentive to be able to reduce the load they present to the transmission network so as to reduce constraints and subsequent locational price separation.

While transmission pricing structures vary significantly between countries, in general they include components which are impacted by a load's contribution to peak demand. Because of this, these loads have the potential for financial gain from the ability to manage and reduce the peak demand they present to the transmission network.

2.3.2 Distribution Pricing

EDBs, by simple economies of scale, are natural monopolies just as transmission providers are. Some EDBs in New Zealand are consumer owned - these are exempt from Commerce Commission price-quality paths. The others, however, not being subject to market pressures or consumer input, are regulated by the Commerce Commission. This regulation includes limits on the revenue the businesses can earn, as well as requiring them to deliver services at a level that could reasonably be expected. It also places certain information disclosure expectations on EDBs. One of these is for their distribution pricing methodology which must demonstrate how their pricing is consistent with the pricing principles and explain any inconsistency [19].

Recently there has been significant discussion around distribution pricing in New Zealand given that the predominant flat per kWh charges do not reflect the costs of providing network services. There is also growing recognition that the scope of poor outcomes from inefficient price signals is growing as new technologies (PV, EV, storage) become more affordable.

The Electricity Authority identify a number of principles for electricity pricing which revolve around to concept of accurately and transparently reflecting the economic cost of service provision [20]. Distribution companies must set their pricing so as to cover all of their costs, including pass through costs such as transmission charges, while complying with these principles and regulations. They aim to provide a pricing structure that is economically efficient. This means that customers using their network face the appropriate cost of that service and are incentivised to weigh up that service against the cost of alternatives. It also provides for appropriate investment in the network over time being driven by the needs of customers.

Using Orion, the EDB for the Canterbury region, as an example, there are three different charges levied to an electricity retailer for a standard household connection. The first is a fixed daily charge ($/connection/day), the second is a peak charge ($/kW/day), and the third is a volume charge ($/kWh).

The peak charge is based on the average real power loading during network peaks occurring during winter. These peak periods are occur when, in the absence of load management, the network load would exceed set trigger points, and are signalled via the ripple system, as well as text messages and emails. Orion's goal is to focus on the highest peaks by targeting 100-150 hours per year of peak period by adjusting the trigger points. This charge is calculated from each retailer's reconciled real energy at each GXP.

This charge gives retailers an incentive to manage the peaks that their customers impose on the system. In New Zealand, tariffs are composed by the retailers, with distribution and metering costs bundled into the pricing presented to consumers. It is therefore a decision of the retailer as to the extent which they reflect the distribution charged to the consumer [21]. All of the EDBs surveyed in [21] report that the biggest barrier they face to enabling demand response from consumers is this rebundling and diluting by retailers of the price signals they offer.

2.3.3 Demand Side Management

Electricity distribution businesses (EDBs) are largely concerned with the peak loads that their networks experience as it is these peaks that determine network sizing. For most networks in New Zealand, system peaks occur on winter mornings and evenings. A small number of rural networks, however, experience summer peaks due to irrigation pump loads.

One option to deal with these generally short duration peaks is to increase network capacity to support the peak demand. The investment required for this is often excessive when considering that this additional capacity is not needed 98% of the time. Network capacity upgrades are typically large projects that need to provide long into the future. The nature of distribution assets does not allow for small incremental upgrades. This forces network operators to invest more, and earlier, than is required. The economies of scale mean that new network assets will be initially oversized. Consequently, any reduction in peak load requirement can enable substantial delays in investment. As such, EDBs have a significant interest in load control methods.

For many EDBs in New Zealand this comes in the form of ripple control which was introduced to New Zealand in the 1950s [22]. Some areas of the country use a pilot wire system rather than a ripple system [23].

The extent to which ripple control is used varies by EDB. Orion, for example, serving the Canterbury region uses ripple control signalling for a number of purposes. The first of these is peak control. These signals are sent only when load is peaking. Typically, the load that is switched is residential and commercial hot water. It is normally a requirement of the connection agreement with the EDB that ripple relay equipment is installed. Consumers may, however, chose their pricing plans to receive a lower rate by allowing the EDB to switch their controllable load. Or they may give the EDB emergency control only, and in return pay a higher distribution charge.

A second use is fixed time signals. These are sent at a fixed time each day to turn things like hot water cylinders and night store heaters on at times when loads are always low. Much like the first use, this shifts loads away from peak time periods.

The third way in which Orion uses ripple signalling is providing signalling of pricing incentives to larger commercial consumers to reduce consumption during high price periods. Some of these customers use backup generation during these high price periods to lower their electricity bills [24].

There are also other uses for ripple control beyond demand management, such as switching meter registers and switching street light.

BESSs provide another resource by which EDBs could manage the load in their networks. This could be through direct control, as existing ripple load control is, or through price signalling. As identified in the previous section however, rebundling of pricing by retailers presents a challenge to those price signals effectively reaching consumers.

2.3.4 EDB Summary

EDBs incur transmission charges which have a peak load component. EDBs have scope to choose how these charges are passed on to their customers, which are retailers, as well as being able to add their own peak demand based charges. Retailers can then

choose how they present pricing to their customers. This means that in many cases the entire aspect of peak charging is hidden from the end consumer, and as such, does not provide suitable signalling and incentive for battery operation behaviours which aid controlling system peaks. Automated BESS control systems offer a way for household loads to respond to price signals that has no impact on the consumers and requires no intervention on their part.

2.4 OPTIMISATION OF BESS

There are many published works on the optimisation of BESSs in various contexts, with various objectives, and using various techniques. This section presents an overview of the field relating to the optimisation of residential BESSs alongside PV generation. Weitzel and Glock [25] present a comprehensive review of literature surrounding energy storage systems (ESSs), including BESSs. A framework for the classification of models and optimisation methods is proposed. The proposed framework consists of 3 main groupings of characteristics as follows:

What is considered? These are the contextual characteristics of the work. Four key characteristics are identified in this category:

- **System scope and ojectives** refer to the number and type of participants in the system being modelled. For example, a single BESS arbitraging variable pricing compared to a micro-grid with multiple forms of generation and storage which is being optimised for multiple objectives.
- **System characteristics** deals with the type of load, generation, storage, and markets.
- **Time horizon** simply refers to the time horizon which is being modelled. This could range from a single day through to the entire lifetime of an ESSs.
- **Control architecture** relates to how different participants communicate with each other and where in the system that optimisation occurs.

How it is modelled? This category relates to the mathematical characteristics of the models that are developed. This is broadly composed of the storage model, the load mode, the market model, the generation model, and the grid model. Weitzel and Glock [25] considers only the storage and load models as key focus areas for its comparison of published works.

How is it solved? This category relates to the characteristics of the optimisation employed. This is divided into three categories:

- **Solution techniques** are largely informed by the contextual and mathematical characteristics. Weitzel and Glock [25] recognises that many models require special techniques to be able to be solved within a reasonable time.

Uncertainties refers to if, and how, uncertainties in the input data are dealt with.

Multi-objectivity defines if there are multiple objectives and how they are handled. Some models not only have objectives for individual economic gain, but also wider environmental or technical objectives.

This framework provides a useful guide into aspects to be considered when reviewing existing models, as well as highlighting the diversity of modelling and optimisation techniques that exist within the field of ESSs. Models and optimisation techniques are framed by the contextual characteristics by which the research was motivated. This leads to significant variation in aspects which are ignored, modelled to a basic degree, or more comprehensively modelled between different works.

While not delving into the specifics of each work, [25] provides an interesting overview of the 202 papers which it reviewed. In consumer-oriented applications it was found that the most popular objective was reducing cost. This is not unexpected considering that return return on investment will be the key driver of ESS uptake without substantial regulatory intervention. BESSs were the most popular form of ESS considered by the reviewed papers by a substantial margin.

Of the different types of solution techniques which were observed, the most popular were exact solution techniques (107 out of 202 publications), where the optimal solution can be found subject to the assumptions made. Of those 107, 87 applied standard solution methods using existing tools, and 66 of those 87 were formulated as LP/integer linear programming (ILP)/MILP problems. CPLEX was the most popular solver used.

Hesse, Schimpe, Kucevic, *et al.* [26] provide another comprehensive review specifically focussed on lithium-ion storage for the grid. They cover aspects of the performance and degradation of lithium-ion battery cells, the design of lithium-ion battery storage systems, and applications of BESSs. Of particular interest to the work in this thesis is the review of modelling and optimisation methods. A key observation of [26] mirrors that of [25] which is that no present state-of-art BESSs modelling tools include all aspects of a system to a high level. Instead studies selectively include aspects dependent on the specific goal of that work. These aspects includes factors such as power electronic losses, cell ageing, or economic factors. The specific use case of a BESS requires dedicated analysis in order to understand the distinct operation patterns which are required to maximise its value.

This approach of different models for different focuses is highlighted by the specific modelling tools which are reviewed by [26]. One of these is *PerModAC* which was developed at the University of Applied Sciences Berlin. This has a focus on modelling efficiency of PV BESS systems including batteries, inverter, stand-by, and control system losses. This uses a temporal resolution of one second and includes the effect of control system dead time and steady state error. Converter efficiency is modelled as

varying with power, however a constant mean battery efficiency is utilised. Temperature, voltage, and SOC efficiency dependencies are not modelled [27]. While *PerModAC* is one of the more detailed efficiency models reviewed, it is not an optimisation tool which can determine battery behaviour under variable pricing conditions.

An alternative focus taken by some models is battery system ageing and degradation. A well known tool that focuses on this is *BLAST* (Battery Lifetime Analysis and Simulation Tool) from the US National Renewable Energy Laboratories (NREL). *BLAST* comes in multiple variants; *BLAST-V* pertains to EV battery degradation, *BLAST-S* pertains to stationary BESSs at a utility scale for peak shaving, and *BLAST-BTM* pertains to behind the meter energy storage. The battery model employed by *BLAST* uses an open circuit voltage dependent on SOC, and a series resistance dependent on SOC and temperature. Lookup tables are used for these values. Temperature is determined by a battery thermal model where heat generation is a function of battery current. Power converter efficiency is deemed to be constant and symmetrical for charge and discharge operations. The optimisation component of *BLAST-BTM* optimises system size for the maximum internal rate of return (IRR). The possibility of feed in tariffs is not considered though, and the documentation is unclear on the exact operational behaviour that is employed [28].

2.4.1 Contextual Characteristics of Optimisation Methods

This section considers some of the contextual characteristics of BESSs modelling and optimisation in the reviewed literature. There are three main applications of optimisation discussed by [26]. These are system sizing, placement, and dispatch. One technique for optimising system sizing, utilised by Magnor and Sauer [29], is genetic algorithms. This optimises PV array size, tilt angle, azimuth angle, PV inverter size, battery converter size, battery capacity, and SOC limits in order to give the best levelised cost of energy (LCOE). The optimisation is applied only to a single load profile of an individual household. Its computational complexity makes it infeasible for sizing multiple individual systems. While system sizing is not the direct focus of this thesis, optimisation of system sizing does require some operation modelling in order to determine the system's LCOE or financial results. Typically, a simple maximisation of PV self-consumption method is used [29]–[31]. When there is surplus of generation the battery is charged, and when load exceeds generation the battery is discharged. This is commonly referred to as the 'greedy algorithm' in the literature. No regard is given to time varying electricity of feed-in tariffs.

Ru, Kleissl, and Martinez [32] approaches the sizing problem from an economic optimisation perspective. The BESS operation is optimised to minimise the household energy cost in a situation where import and export prices are equal, and the battery size at which costs no longer decrease is identified. This method allows for time varying

tariffs.

Van der Kooij [33] explores the financial results of a standalone BESS, as well as a household with a BESS, though not with PV. The pricing model used in [33] is one where the sell and buy price are symmetrical with the exception of tax and fixed costs being added to the price of purchasing electricity from the grid.

It is important to recognise that some pricing structures consider generation separately from load and all generation is exported to the grid. Under other pricing structures, classed as net-metering scenarios, only excess generation is exported [34]. In many net-metering scenarios the import and export prices are set to be equal. Ratnam, Weller, and Kellett [35] presents a LP model for battery storage alongside PV generation in a residential context with net metering. A consequence of this is that there are large reverse power flows (net export) during peak price periods as the BESS discharges beyond just that required to meet household load. An alternative quadratic programming (QP) method is used to optimise consumer savings while penalising reverse power flows. In the New Zealand context, where the cost of consumers purchasing electricity far exceeds the rate at which they are compensated for excess generation, this is not of such concern.

Conversely, there are a number of works which consider time varying price without considering load and generation. An example is Kwan and Maly [36], which is one of the earliest works to look at battery storage optimisation. It presents a dynamic programming (DP) method for optimising charge scheduling of a lead acid battery based on two and three part time of use tariffs. This is an optimisation based solely on price arbitrage rather than battery operation alongside generation. This is a significant work because it considers both an energy component to price, and a power component. This power component is based on the pricing structure in Taiwan, where there is a penalty charge for exceeding contract power limits. The power limits are time varying. Though this is a pricing structure which was not seen in other literature, the possibility of net export and the pricing implications of this are not discussed.

2.4.2 Mathematical Characteristics of Optimisation Methods

This sections considers the mathematical characteristics of BESS optimisation methods in the reviewed literature. A particular focus is given to handling of losses and efficiency. There is significant variation in the treatment of efficiency. Some models do not consider efficiency at all which means that all power that flows into the battery system is later able to be extracted [35], [37]–[39]. Weitzel and Glock [25] identify that the most common approach was that charging and discharging efficiencies were considered constant. This observation correlates well with the specific models studied [26], [32], [34], [40]–[43]. Van der Kooij [33] utilise a constant round trip efficiency with losses only settled at discharge. This means that there would be some inaccuracy in the

battery SOC limits compared when losses are accounted for in both charge and discharge operations. There are some methods, however, where more complex efficiency models are used. Arghandeh, Woyak, Onen, *et al.* [44] model a community energy storage system and consider efficiency varying with the square of power by modelling the BESS as a constant voltage source with a series resistance. A quadratic efficiency function is also utilised by [45]. Kwan and Maly [36] progresses further by modelling a non-linear battery loss function which depends on both current and SOC. This is a notable work for the fact that it is from much earlier than others reviewed and consequently is for a lead acid battery rather than lithium-ion which is more common in modern BESSs. Power converter losses do no appear to be considered by [36] however.

Braun, Büdenbender, Magnor, *et al.* [46] explore using storage to increase PV self-consumption in response to a new tariff option introduced in Germany in 2009 with a more detailed efficiency model than seen in other work. A DC-coupled topology is used with DC/DC converters between both the PV array and battery system, alongside a single DC/AC converter. Losses are modelled as three components:

- constant losses due to self consumption,
- voltage losses proportional to power, and
- ohmic losses proportional to the square of the power.

These loss function are parameterised for three different voltage levels on the PV and battery link sides, with a linear interpolation between the curves for voltages that deviate from the three specified levels. Only one curve is used for the DC/AC converter as both the AC and DC buses are of a fixed voltage level. A complex battery RC impedance model is used based on manufacturer data that incorporates elements for electrical conductivity of current collectors, the active materials, and the electrolyte, alongside ohmic charge transfer resistance, and diffusion effects, amongst others. These parameters all vary with SOC and temperature. While the converter and battery models display a high level of sophistication, the battery operation strategy does not. The operation strategy mirrors that discussed for [29], where electricity pricing is not a factor, and battery charging from the grid is not considered.

Lifshitz and Weiss [47] take an alternate approach and show that a "bang-off-bang" strategy is optimal for a storage only system. That is, an ESS is either charging at full power, resting, or discharging at full power. This relies on a constant efficiency value and cannot hold for a system with a power dependent efficiency function. It also has difficulty when considering a storage system alongside load and generation where pricing may make it attractive to only dispatch storage energy to meet current load, but not to export power to the grid. This result is agreed with by Steffen and Weber [48] who consider optimal operation of pumped storage. Steffen and Weber [48] goes further to conclude that price thresholds for starting and stopping storage operations produces

optimal results under their assumptions. While it makes use of complex optimal control theory to prove it, an intuitive understanding is possible; if considering a standalone storage system where efficiency is constant and not rate dependent, then either the current price is attractive for storing/charging, or it is not. There is no reason to run at a partial rate.

2.4.3 Solving Characteristics of Optimisation Methods

Hesse, Schimpe, Kucevic, *et al.* [26] identify that a large range of techniques have been used for optimising BESSs. These include deterministic optimisation techniques such as LP/ILP/MILP/DP [42], [49], [50], as well as other techniques such as fuzzy logic control, genetic algorithms [29], [41], particle swarm optimisations [51], and model predictive control [52]. Furthermore, there are a number of studies which take a more heuristic based approach [31], [53]–[55].

Hassan, Cipcigan, and Jenkins [49] simulate a household with a BESS and PV generation using a MILP problem formulation. They focus on simulation with feed-in tariffs and time varying tariffs. This feed-in tariff considered involves both a payment for energy generated, as well as a payment for energy exported. As with many of the reviewed models, efficiency is treated as a constant value. They also perform a sensitivity analysis considering the effect of battery capacity on financial benefit for the single household which is studied. Under their specific set of inputs, no benefit was gained by increasing battery capacity beyond 3 kWh.

Another MILP formulation is presented by Wang, Meng, Dong, *et al.* [50]. They provides interesting contribution where a controllable load, in the form of air conditioning (for cooling only), is included in a MILP optimisation for PV and BESS alongside household load. The model structure does not allow for the kinds of behaviour that would accurately represent BESS behaviour and maximise savings however. Power from the BESS cannot flow to the grid and to the house simultaneously. It is unclear how battery power could ever be exported unless the household had a load of zero. Additionally, there is no consideration made for any efficiency loss in either battery charging or discharging.

A commonly recognised problem when applying deterministic optimisation to ESSs is the end-value problem. This is where the system, with no knowledge of anything existing beyond the end of the optimisation horizon, uses all stored energy thus resulting in an empty ESS at the end of the last time step. Weitzel and Glock [25] recognises that there are two techniques typically used to deal with this. The first is a receding horizon technique; continuously advancing the time horizon renders that empty storage at the end a less favourable outcome. The second is fixing the SOC at the start and end of the optimisation horizon. This is an approach used by [35], and examined in more detail by [56]. These fixed points in the SOC trajectory can have a particularly

pronounced effect in short time horizon optimisations where storage capacity is large compared to power capability. This results in a period of forced behaviour to meet the constraint which may be not be optimal behaviour.

[33] explores a price threshold based control methodology where thresholds are set symmetrically around the mean price such that the return on investment is zero if energy is sold and bought on the thresholds. This is a simple methodology which guarantees a positive return. It is less practical however in cases with variable charge/discharge rates and rate dependent efficiency functions.

Another heuristic approach is presented by Young, Bruce, and MacGill [53], who examine both the financial results for consumers as well as analysis of the effects battery operation on network peaks. The examination of the wider network effects of multiple BESSs is a key contribution of [53]. It uses a rule-based control scheme and examines flat rate tariffs and time-of-use tariffs. Like many others, it incorporates constant round trip efficiency and does not account for battery degradation. While [53] considers the interplay of load and PV with time varying pricing, it does not allow for charging from the grid during low price periods. The network peak load analysis considers only a single peak load of the year rather than wider consideration of the loads during peak periods.

A heuristic approach is taken by Suppers [54], who presents a publicly accessible modelling tool for household load, PV generation, and a BESS. This is a New Zealand focussed tool using local data and pricing structures. Three different rule-based strategies are used; a load levelling strategy, a financial saving strategy, and a hybrid strategy that combines the two. Under the load levelling strategy battery operation is determined by household load thresholds, while under the saving strategy price thresholds are used for decision making. This model also uses a single constant value for round trip efficiency.

A different approach is taken by Kucevic, Tepe, Englberger, *et al.* [57]; instead of optimising storage they create a framework and set of standard storage profiles to compare different technologies. Two methods of BESS charging are used. The first is a simple 'greedy algorithm' where excess PV generation is sent to the battery, and discharged as soon as load exceeds generation. The second spreads the charging over the period for which generation is expected to exceed load in order to reduce the magnitude of power exported to the grid. Neither are particularly sophisticated and are not price responsive. This uses a similar battery model as *BLAST*. Converter efficiency is treated as a function of power however the detailed implementation is not specified. While variable pricing is discussed as a driver for peak shaving, the battery behaviour is not determined on price, but instead by optimal peak shaving. A household consumer is not motivated by their BESS investment providing optimal peak shaving unless there is the financial incentive to match it.

In a departure from more conventional optimisation methods, Fuselli, De Angelis,

Boaro, *et al.* [58] uses action dependent heuristic dynamic programming (ADHDP) utilising two neural networks that are pretrained using particle swarm optimisation procedures for optimising household battery operation with load and PV generation. This work extends that of [59] by allowing battery charging from the grid as well as from excess PV generation. While excess PV generation is able to to be exported, battery power is not allowed to be exported to the grid. This is justified as being "in compliance with the existing regulations in many western countries." This prevention of price arbitraging battery operation is at odds with much of the other reviewed literature. While time varying prices are used, it is not clear how compensation for net export is calculated. BESS efficiency is treated as a constant round trip value.

2.4.4 BESS Efficiency

Battery charge and discharge efficiency is an important parameter for the modelling of a BESS. This section gives a more general overview of BESS efficiency compared to the specific models which feature in the previously reviewed literature. While it has been shown that the literature typically considers BESS efficiency as a single constant value, more nuanced models recognise that there are two components; the power electronic converter has losses, as does the battery itself. A constant efficiency value implies a linear dependence between power and losses [60].

Considering first the converter, there are two components to the losses: conductive losses, which vary approximately with the square of the load, and switching losses, which are approximately constant [61]. Though literature on stationary BESS efficiency is limited, [62] presents a series of efficiency measurements made on a bi-directional EV charger which is a similar product. Power measurements were made on both the AC side and direct current (DC) side of the converter while it was connected to a Nissan Leaf and providing a frequency keeping reserve service. This gave measurements over a wide range of power values. While the overall trends of both charge and discharge efficiency followed the expected approximate behaviour, significant spread in efficiency values for a given power level were observed. This was particularly noticeable at low power levels. This highlights that there are additional factors in a commercial product which play a role in determining overall efficiency beyond the approximate theoretical models.

The second component to be considered is the efficiency of batteries themselves. Their high efficiency is one key reason why lithium-ion batteries dominate the BESS market. Renewable power sources such as solar or wind generation display high degrees of variability, this means that the charge profiles of BESSs connected to this generation are not always predetermined, and are not controllable. In other contexts, such as consumer electronic products, batteries are charged under controlled conditions. This means charging is conducted in a way that it is efficient and battery degradation is

minimised [63]. In the case of BESSs, the charging conditions are unable to be controlled and charge rates are likely to vary across the full range of rated power capabilities.

Much of the research on battery behaviour focusses on battery performance under a given discharge behaviour. When research does focus on charging behaviour, it usually considers the use of variable charge rate to improve efficiency rather than it being an externally varying variable. Elena Marie Krieger [63] presents modelling work where losses are modelled as a series resistance. In the idealised case, the battery voltage and the resistance are constant values, this gives losses proportional to the square of the current. In a more detailed model, however, both resistance and battery voltage are complex functions of SOC and temperature. Further complications to efficiency modelling are brought by charge and discharge efficiencies not being simple inverses of each other. A important recognition of this work is that charging and discharging efficiencies are not simple inverses of each other.

2.5 SUMMARY

This chapter has given a brief overview of the diversity of commercial products that are available in the market. The different benefits which BESSs could bring to various segments of the electricity market were identified. It was noted that BESSs placed behind the meter could provide the widest range of services, however there are hurdles that would prevent many of those benefits being realised due to current regulations and market structures. A range of common control schemes for modern commercially available BESSs were discussed.

An overview of transmission and distribution pricing was given alongside EDBs approaches to load control. This gives additional context as to why EDBs could benefit from BESSs providing reductions to the peak loads experienced by networks. These benefits come not just as simple investment deferral for network upgrades, but also in reductions in the transmission interconnection charges which they pay.

A number of key points and reoccurring themes in literature surrounding residential BESS optimisation were identified:

- Optimisations of BESS can be divided into those that focus on the sizing of systems such as [30], [32], [34], [51], and those that focus on the operation of systems such as [35], [37], [38], [41]. Typically sizing optimisations rely on simple heuristic methods to calculate the financial returns resulting from battery operation. It is more common for operation focussed optimisations to use deterministic optimisation techniques to identify optimal BESS operation.
- Some optimisation methods consider only price arbitraging using battery storage, others consider maximising PV generation self-consumption. There are few that combine both.

- Feed-in tariffs which are much smaller than electricity purchase costs, as is typical in the New Zealand market, are not always considered. Much more commonly a net metering scheme with equal buy and sell prices is used [32]. This has significant impact on BESS operations.
- BESS efficiency is generally treated as a constant value, either a single round trip efficiency which is accounted for at either charge or discharge [26], [32]–[34], [40], or separate values for charge and discharge [41]–[43], [51], [52]. Some optimisations neglect efficiency altogether [35], [37]–[39], [56], while others implement more complex models where efficiency depends on some combination of power, SOC, and temperature [36], [44], [46], [64].
- The reviewed works consider either the financial returns for a BESS owner, or they incorporate components to optimise BESS to benefit the wider distribution network. They do not examine the effect that purely economically motivated operation has on the aggregated load profiles experienced by the distribution network.

Chapter 3

BATTERY OPERATION OPTIMISATION WITH PERFECT FORESIGHT

This chapter presents the LP and MILP methods used for optimisation of battery behaviour with perfect foresight of household load and PV generation. It introduces the notation used to define household load, PV generation, and BESSs and covers two approaches for modelling the battery charge and discharge efficiency. The first approach uses a single equivalent series resistance representing losses that are solely dependent on charge/discharge rate, while the second approach considers a rate independent loss component. The formulation of a LP problem incorporating the first efficiency model is elaborated. The LP problem is then extended to a MILP problem, so as to be able to incorporate the second efficiency model. These optimisations, through using perfect foresight, represent the upper limit of achievable household savings and the likely impact on network operation.

3.1 MODEL OVERVIEW AND NOTATION

A method is developed to determine the optimal battery charge/discharge behaviour with the objective of minimising the energy cost component of a consumer's electricity bill given the load profile, battery characteristics, and solar PV generation (if any).

The physical system for an individual household is illustrated in Figure 3.1. It presents some of the notation used in this thesis. The notation is based on [38] and [35], modified to fit the particular requirements of this model.

The charging and discharging power of the battery (in kW) over the kth time interval of length Δ (in hours) is denoted by $x_c(k) \geq 0$ and $x_d(k) \geq 0$ respectively. The battery charge or discharge power over a time window of $[0, T]$, is represented by a vector of length s, where s is the number of time intervals of length Δ. Thus, the length of the time window over which the battery usage is being optimised is denoted as $T = s\Delta$ (in hours). Subsequently, the power charging the battery over the complete period $[0, T]$ is denoted by $x_c := [x_c(1), ..., x_c(s)]^T \in \mathbb{R}^s$. x_d can be represented by a similar expression.

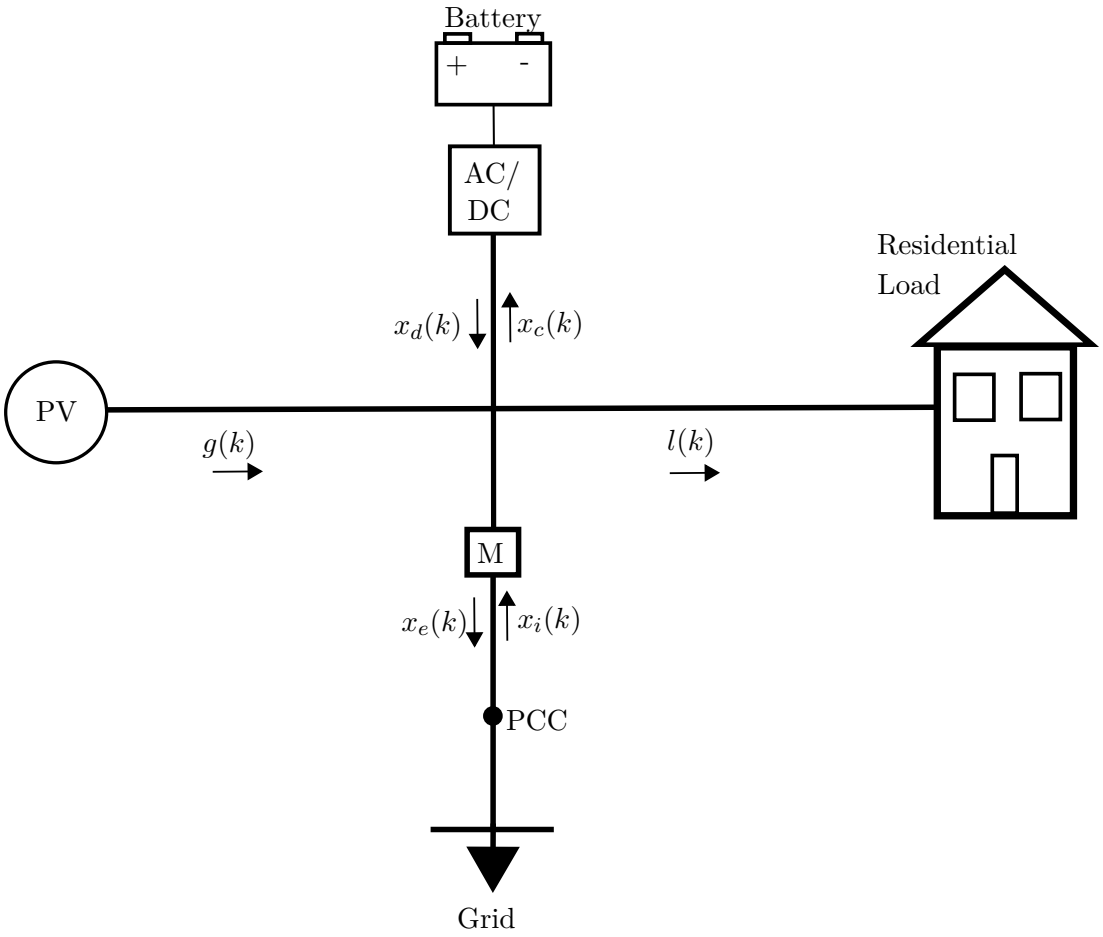

Figure 3.1 Battery system topology with residential load and PV generation.

The average power exported from the household to the grid over a period $((k-1)\Delta, k\Delta)$ is represented by $x_e(k) \geq 0$ for all $k \in \{1, ..., s\}$. The power imported by the household from the grid is similarly represented by $x_i(k) \geq 0$ for all $k \in \{1, ..., s\}$.

The average power imported from (or exported to) the grid at the meter M, is billed (or compensated) according to a time varying price. The electricity billing for imported power (in $\$/kWh$) at meter M over the period $((k-1)\Delta, k\Delta)$ is defined by $p_i(k) \geq 0$ for all $k \in \{1, ..., s\}$, and the electricity billing profile over $[0, T]$ is $p_i := [p_i(1), ..., p_i(s)]^T \in \mathbb{R}^s$. Likewise, the compensation price for exported power (in $\$/kWh$) at meter M over the period $((k-1)\Delta, k\Delta)$ is denoted by $p_e(k) \geq 0$ for all $k \in \{1, ..., s\}$ and the electricity compensation price profile over $[0, T]$ by $p_e := [p_e(1), ..., p_e(s)]^T \in \mathbb{R}^s$. Thus, the energy component of a household's electricity bill can be calculated by multiplying the import price profile (p_i) with the power flow captured in x_i and the export price profile (p_e) with x_e.

The variables, shown in Figure 3.1, are related to each other through Kirchoff's

current law at the central node. This gives

$$g(k) + x_d(k) + x_i(k) - l(k) - x_c(k) - x_e(k) = 0. \tag{3.1}$$

3.1.1 Battery System Efficiency

One of the key characteristics of BESSs included in the optimisation method is battery charge and discharge efficiency; in particular the variation of efficiency with charge or discharge rate. The efficiency of charge and discharge operations is important not only because it affects the financial savings that a BESS can provide, but also because optimal battery operation will consider the efficiency function in order to reduce losses. Two models of load dependent battery efficiency are considered. The first, a simpler model is where efficiency depends only on battery current and is represented by a simple series resistive loss component (Figure 3.2). The second, a more complex approach, is a combination of load dependent and independent losses.

3.1.1.1 Load Dependent Loss Model

The first efficiency model depends only on the battery current. As an example to illustrate the approach, consider the Tesla Powerwall with a round trip efficiency of 90% at a charge/discharge rate of 3.3 kW [9].

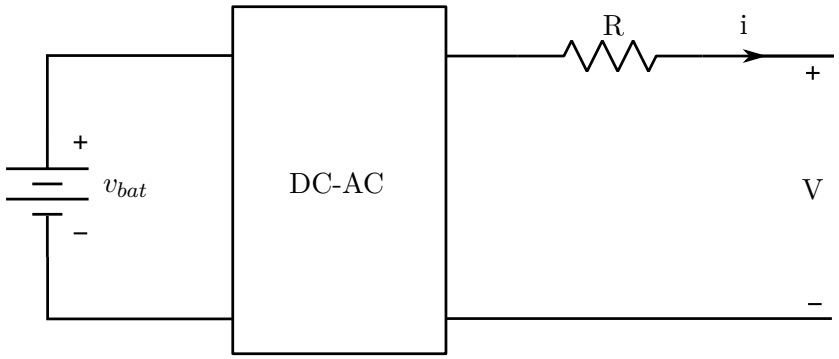

Figure 3.2 Basic topology of equivalent series resistance model.

Because efficiency varies with power, and charge and discharge operations are not guaranteed to be be symmetrical, the efficiency of the two operations must be considered separately rather than as a single round trip efficiency. The round trip efficiency, η_{rt}, is the product of the charging efficiency, η_c, and discharging efficiency, η_d [65]. Charging

efficiency is defined as the ratio of power, resulting in energy, stored in the battery to the terminal input power:

$$\eta_c = \frac{P_{\text{stored}}}{P_{\text{terminal}}}. \tag{3.2}$$

In this example with a Tesla Powerwall the terminal voltage is fixed at a nominal mains voltage of 230 V and the terminal power is specified as 3.3 kW. Assuming sinusoidal voltage and current, and unity power factor, the current can be calculated and equation 3.2 can be rewritten as

$$\eta_c = \frac{VI - I^2R}{VI}. \tag{3.3}$$

Similarly, the discharge efficiency is defined as the ratio of the terminal output power to the power depleted from the energy stored within the battery:

$$\eta_D = \frac{P_{\text{terminal}}}{P_{\text{depleted}}} = \frac{VI}{VI + I^2R}. \tag{3.4}$$

Combining equations 3.3 and 3.4 yields an expression for the round trip efficiency which can be solved for R given a terminal voltage of 230 V and a terminal power of 3.3 kW:

$$\begin{aligned} \eta_{\text{RT}} &= \eta_c \cdot \eta_c \\ 0.9 &= \frac{VI - I^2R}{VI} \cdot \frac{VI}{VI + I^2R} \\ R &= 0.844\,\Omega. \end{aligned} \tag{3.5}$$

It is important to note that constant terminal power, along with the fixed resistance, means that while the losses are the same when charging or discharging at a given rate, the efficiency values differ given the difference in definition of the two efficiencies. This difference between charge and discharge efficiencies, with an assumed constant terminal voltage, is illustrated in Figure 3.3.

The implementation of efficiency in the linear programming optimisation requires that the efficiency function be decomposed into a piecewise function of b bands. This is because efficiency is implemented as a scaling factor for the effect of charge/discharge power on the battery state of charge. This also requires the conversion of the efficiency values to incremental efficiency values. This means the value of power that is being stored in, or discharged from, the battery is the integral of the incremental efficiency curve. This is illustrated, for the piecewise approximation, by considering the area under the curve of Figure 3.4.

A simple algorithm is used to determine the size of these bands which give the minimum mean squared error for the calculated efficiency values. This is achieved by discretising the range of charge/discharge powers in steps of 100 W and calculating all the feasible combinations of efficiency breakpoints. For each feasible combination

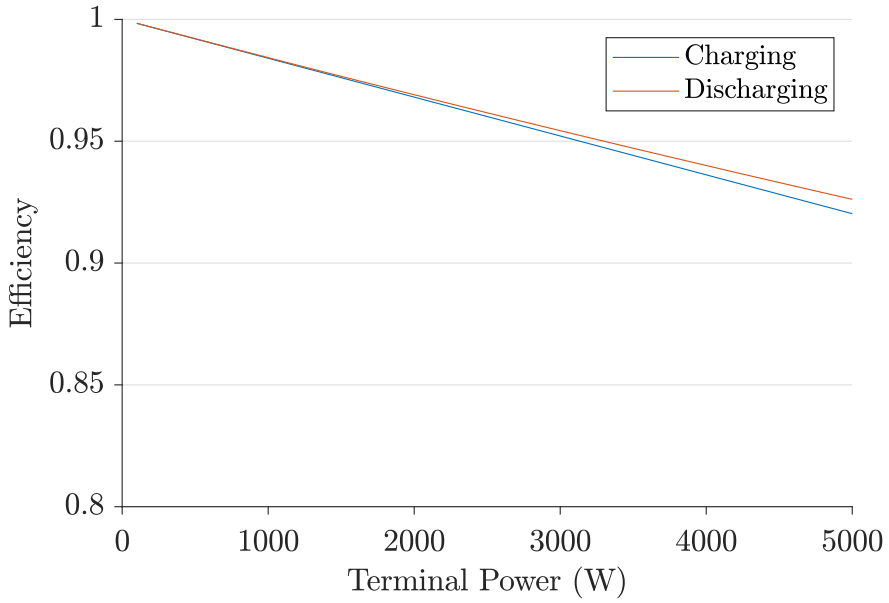

Figure 3.3 Charge and discharge efficiency across varying powers using simple series resistance loss model.

the mean efficiency value is identified across each step and the mean square error is calculated. This is repeated for each set of feasible breakpoints in order to find the set of breakpoints giving the minimum mean squared error.

The output of this algorithm is a vector of charge and discharge incremental efficiencies: $\eta_c = [\eta_c^1, \eta_c^2, \ldots, \eta_c^b]$ and $\eta_d = [\eta_d^1, \eta_d^2, \ldots, \eta_d^b]$. These efficiencies have corresponding vectors of breakpoints a_c and a_d,

$$a_c = \begin{bmatrix} a_c^1 \\ a_c^2 \\ \vdots \\ a_c^b \end{bmatrix} \qquad a_d = \begin{bmatrix} a_d^1 \\ a_d^2 \\ \vdots \\ a_d^b \end{bmatrix}. \tag{3.6}$$

The breakpoints of the piecewise efficiency curve are used to calculate the length, L^j, of each segment such that

$$\begin{aligned} L_c^1 &= a_c^1 \\ L_c^2 &= a_c^2 - a_c^1 \\ &\vdots \\ L_c^b &= a_c^b - a_c^{b-1}. \end{aligned} \tag{3.7}$$

The efficiency curve is broken down into a piecewise constant function of b pieces, or efficiency bands. The piecewise function is illustrated in Figure 3.4, which demonstrates

the relationship between efficiency breakpoints and segment lengths.

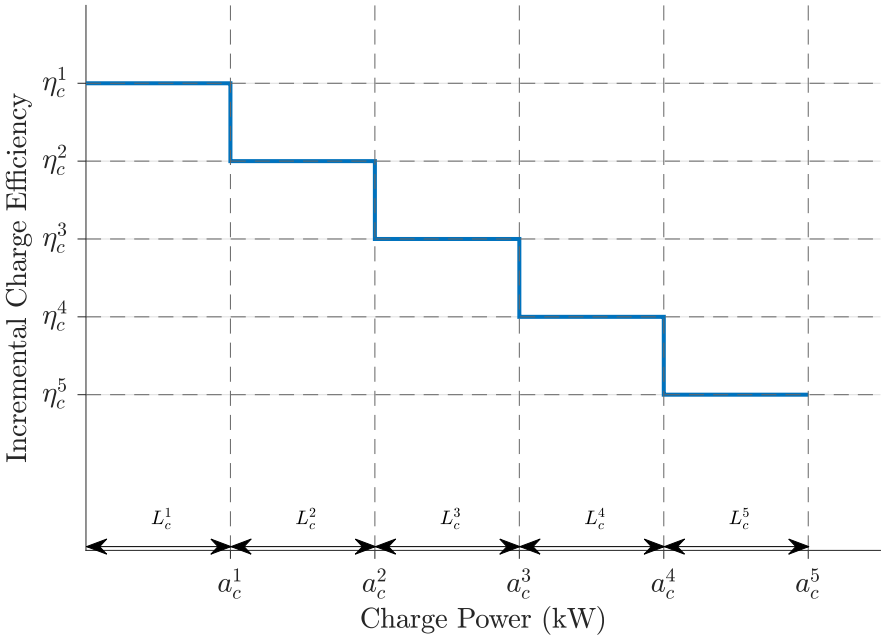

Figure 3.4 Generalised efficiency function illustrating breakpoints and segment lengths ($b = 5$).

In order to calculate the overall efficiency of a charge or discharge operation, the battery power at time step k is further divided into separate components defined by the breakpoints a_c and a_d such that

$$\begin{aligned} x_c(k) &= x_c^1(k) + x_c^2(k) + ... + x_c^b(k) \\ x_d(k) &= x_d^1(k) + x_d^2(k) + ... + x_d^b(k) \end{aligned} \tag{3.8}$$

where

$$\begin{aligned} 0 \leq x_c^1(k) \leq L_c^1 \qquad & 0 \leq x_d^1(k) \leq L_d^1 \\ 0 \leq x_c^2(k) \leq L_c^2 \qquad & 0 \leq x_d^2(k) \leq L_d^2 \\ \vdots \qquad & \vdots \\ 0 \leq x_c^b(k) \leq L_c^b \qquad & 0 \leq x_d^b(k) \leq L_d^b. \end{aligned} \tag{3.9}$$

This gives the power that is being stored by the battery system during a charging operation in time step k as

$$x_{stored}(k) = x_c^1(k)\eta_c^1 + x_c^2(k)\eta_c^2 + ... + x_c^b(k)\eta_c^b. \tag{3.10}$$

Similarly, for a battery discharge operation, for a terminal terminal power of $x_d(k)$, the

power being drawn from and depleting the battery is

$$x_{depleted}(k) = \frac{x_d^1(k)}{\eta_d^1} + \frac{x_d^2(k)}{\eta_d^2} + ... + \frac{x_d^b(k)}{\eta_d^b}. \tag{3.11}$$

3.1.1.2 Load Dependent and Independent Loss Model

An alternative loss model, which incorporates a standing loss component along with a current dependent component, is considered. Due to limited manufacturer data regarding BESSs, some assumptions must be made. The first assumption is that the published efficiency data corresponding to a specified charge/discharge rate is the point of maximum efficiency. In the case of the Tesla Powerwall, the assumption is that the maximum round trip efficiency of 90% is achieved at a power of 3.3 kW. It is assumed that it follows that this maximum efficiency is achieved when the standing loss is equal to the load dependent loss. Figure 3.5 shows how these losses are implemented.

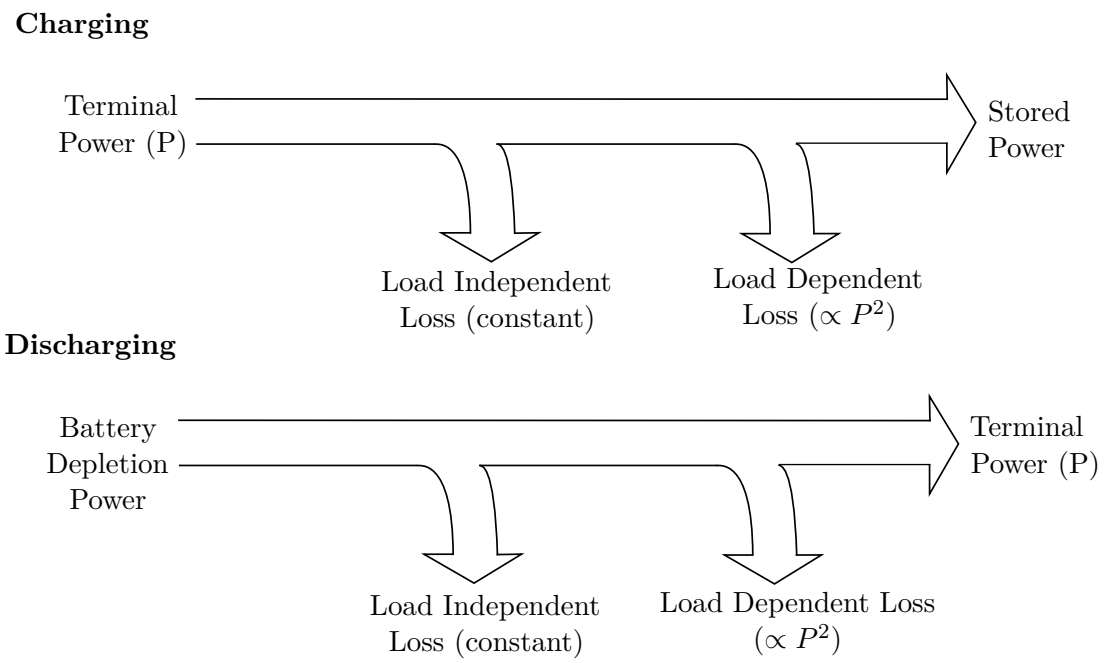

Figure 3.5 Loss model for a combination of standing and rate dependent losses.

The definition of charging efficiency as the ratio of the power stored to the terminal power remains as previously. Its calculation now accounts for the new standing loss component such that

$$\begin{aligned} \eta_c &= \frac{P_{\text{stored}}}{P_{\text{terminal}}} \\ \eta_c &= \frac{VI - I^2R - P_{\text{standing}}}{P_{\text{terminal}}}. \end{aligned} \tag{3.12}$$

An equivalent expression for the discharge efficiency is

$$\begin{aligned} \eta_d &= \frac{P_{\text{terminal}}}{P_{\text{depleted}}} \\ \eta_d &= \frac{P_{\text{terminal}}}{VI + I^2R + P_{\text{standing}}}. \end{aligned} \tag{3.13}$$

In the previous loss model with only a current dependent loss, the battery charging at a rate of 3.3 kW produces losses of 174 W. Halving this gives a constant standing loss of 87 W and a rate dependent loss of 87 W. This rate dependent loss is produced by the terminal current through an equivalent series resistance (ESR) of half the previous value, or 0.42 Ω. Calculating and plotting these efficiency values across the full range of possible charge and discharge rates produces Figure 3.6. The standing self-consumption loss of 87 W corresponds to losses of 1.75% of rated capacity. Given the absence of detailed efficiency data, it is difficult to asses whether this is accurate.

As identified in [66], inverter losses, to a good approximation, can be modelled as constant load-independent component and load dependent component. This mirrors the approach taken to the combined inverter and battery efficiency for the Tesla Powerwall. It is recognised that different inverter designs favour reduced constant losses against increased losses at higher loads and vice versa. For the inverters modelled in [66], the constant loss component varies between 0.88% and 1.45% of rated power. This is lower than the 1.75% calculated for the Tesla Powerwall; however, the 1.75% also includes battery efficiency alongside the inverter. Thus, while not verified with manufacturer data, the constant loss assumptions appear to be plausible.

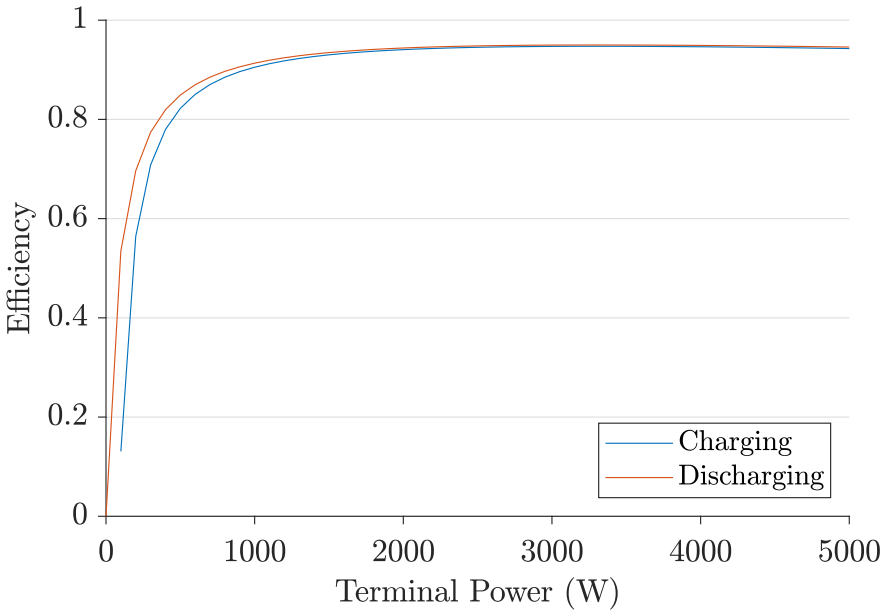

Figure 3.6 Charge and discharge efficiency across varying powers.

As before (Section 3.1.1.1), the minimum mean square error algorithm is applied

to approximate this efficiency curve with a constant piecewise function of b bands. Figure 3.7 shows both the charge and discharge efficiencies across the operating power range of the Tesla Powerwall, calculated with both the continuous efficiency function and the piecewise function found with the mean square error algorithm. There is a distinct error in the range 0 kW to 0.2 kW where the constant piecewise nature is dominant and observable. Throughout the remainder of the operating power range, the continuous function is well matched with the calculated piecewise function.

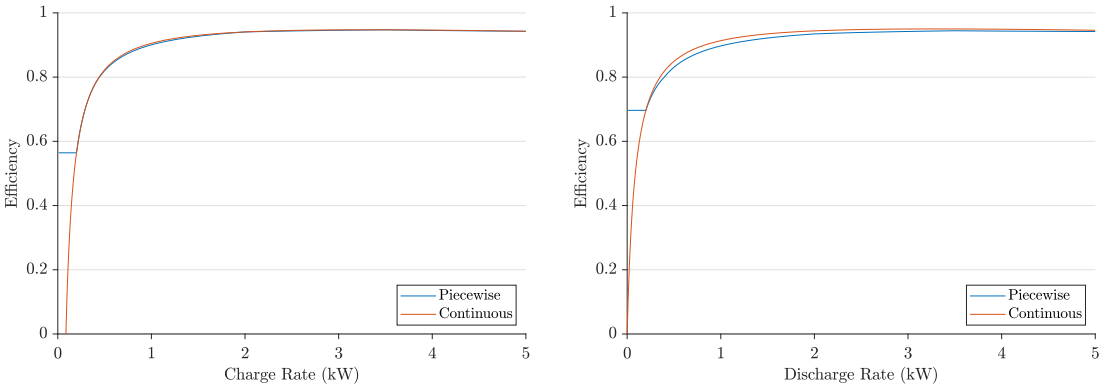

(a) Charge Efficiency (b) Discharge Efficiency

Figure 3.7 Charge and discharge efficiency curves calculated using the continuous efficiency function and piecewise efficiency function for the Tesla Powerwall example ($b = 5$).

Unlike with the case of simple series resistance, the efficiency does not monotonically decrease with increasing power; this significantly increases the optimisation complexity. It requires additional constraints to ensure that the efficiency function is correctly applied. The formulation of these constraints is discussed in Section 3.3.

3.2 LINEAR PROGRAMMING OPTIMISATION PROBLEM

In this section, a LP optimisation problem is formulated using the load dependent efficiency model to optimise battery system behaviour in order to reduce household energy costs. In Section 3.3, this is extended to a MILP problem which removes the requirement for the efficiency curve to be monotonically decreasing with increasing charge/discharge rate. This allows the use of the second loss model (Section 3.1.1.2), which includes both charge/discharge rate dependent and independent loss components.

In addition to the notation presented in Figure 3.1, it is important to introduce the notation which is used to simplify and condense the formulation of the optimisation problem. Recall that s is the number of time periods over which battery system behaviour is be optimised. Let $\mathbb{R}^s$ denote an s-dimensional vector of real numbers. The s-by-s identity matrix is denoted $\mathbf{i}$, and $\mathbb{1}$ is the all-1s column vector of length s. $\mathbf{0}$ denotes an all-zero matrix or column vector, and $\mathbf{T}$ is a lower triangular s-by-s matrix

of 1s such that

$$T^{s\times s} = \begin{bmatrix} 1 & 0 & \dots & 0 \\ 1 & 1 & \dots & 0 \\ \vdots & \vdots & \ddots & 0 \\ 1 & 1 & \dots & 1 \end{bmatrix}. \tag{3.14}$$

The standard form of an LP problem, given by [67], is

$$\begin{aligned} &\text{maximise } c'x \\ &\text{subject to } \begin{cases} Ax = b \\ x \geq 0 \end{cases} \end{aligned} \tag{3.15}$$

with the understanding that it is a maximisation problem containing non-negativity constraints for all variables, with all remaining constraints being equality constraints, and having a non-negative right hand side vector, b. For clarity of explanation, this thesis uses a modified representation of the problem which separates equality and inequality constraints, as well as separately identifying lower and upper bounds that elements of the decision variable may take. It must be noted that this representation can be transformed to the standard form with sign changes and the addition of slack variables. The definition of the LP problem used henceforth is that given vectors f, lb, and ub, matrices A and A_{eq}, and corresponding vectors b and b_{eq}, a vector x is found to solve:

$$\min_x f^T x \text{ subject to } \begin{cases} A \cdot x \leq b \\ A_{eq} \cdot x = b_{eq} \\ lb \leq x \leq ub \end{cases}. \tag{3.16}$$

The decision variable, x, comprises all of the power flows which are influenced by battery behaviour. These are the charge and discharge powers, x_c, and x_d, arranged by efficiency band, as well as the grid import and export powers, x_i and x_e, which take values required to satisfy the power balance of the system. Recall that the charging power vector for efficiency band b over the optimisation timespan is defined $x_c^b = [x_c^b(1), x_c^b(2), ..., x_c^b(s)]^T$, with a similar expression for the discharge power vector. These vectors for each efficiency band are arranged sequentially within the single decision variable, as shown in Equation (3.17). The decision variable, x, has length of $2sb + 2s$

and is defined as

$$x = \begin{bmatrix} x_c^1 \\ x_c^2 \\ \vdots \\ x_c^b \\ x_d^1 \\ x_d^2 \\ \vdots \\ x_d^b \\ x_i \\ x_e \end{bmatrix}. \tag{3.17}$$

3.2.1 Constraints

The operation of a BESS is limited by a number of constraints which must be implemented in the LP problem formulation. These constraints include adherence to the power balance equation (Equation (3.1)), battery system charge/discharge power ratings, and limiting the battery SOC. The charging and discharging efficiency curves are also built into the optimisation problem through formulation of constraints. This section outlines how each of these constraints are formulated into the general LP problem structure.

3.2.1.1 Power Balance

The first constraint is represented by the power balance equation (Equation (3.1)). It is this constraint which forces the grid import power or grid export power to take the required value to ensure household load, PV generation, and any battery operation results in a valid solution at every time step.

The power balance constraint is implemented as a single equality constraint for each time step. The s-by-s identity matrix, $\mathbf{i}$, is used as a constructor to create a constraint for each time step. This means that the first s rows of the equality constraint structure are defined as

$$\begin{gathered} A_{eq} \cdot x = b_{eq} \\ \Big[\underbrace{-\mathbf{i} \quad \ldots \quad -\mathbf{i}}_{a} \quad \underbrace{\mathbf{i} \quad \ldots \quad \mathbf{i}}_{b} \quad \underbrace{\mathbf{i} \quad -\mathbf{i}}_{c} \Big] \cdot x = \Big[l - g \Big]. \end{gathered} \tag{3.18}$$

Section a of A_{eq} relates to the charging power bands with the s-by$s$ identity matrix repeated b times, section b to the discharge power bands, and section c to the grid import and export power. The power balance constraint is clearly seen when the kth

row of Equation (3.18) is expanded to give

$$-x_c^1(k) - ... - x_c^b(k) + x_d^1(k) + ... + x_d^b(k) + x_i(k) - x_e(k) = l(k) - g(k). \tag{3.19}$$

3.2.1.2 Charge/Discharge Rate

A BESS has limited charge and discharge power capability. In the case of the Tesla Powerwall, which is used here as an example, that is a continuous power rating of 5 kW. In addition to this total power limit, each efficiency band has limits defined by the breakpoints, a_c and a_d, which when enforced also serve to limit the charging or discharging power.

These limits on the charging and discharging powers are previously expressed in Equation (3.9). As an example, a simple illustrative charging efficiency curve where $b = 5$ is shown in Figure 3.8. It is observed that the values of the charge power bands must be constrained such that

$$\begin{aligned} 0 \leq & x_c^1 \leq 0.5 \\ 0 \leq & x_c^2 \leq 1 \\ 0 \leq & x_c^3 \leq 1.5 \\ 0 \leq & x_c^4 \leq 1 \\ 0 \leq & x_c^5 \leq 1. \end{aligned}$$

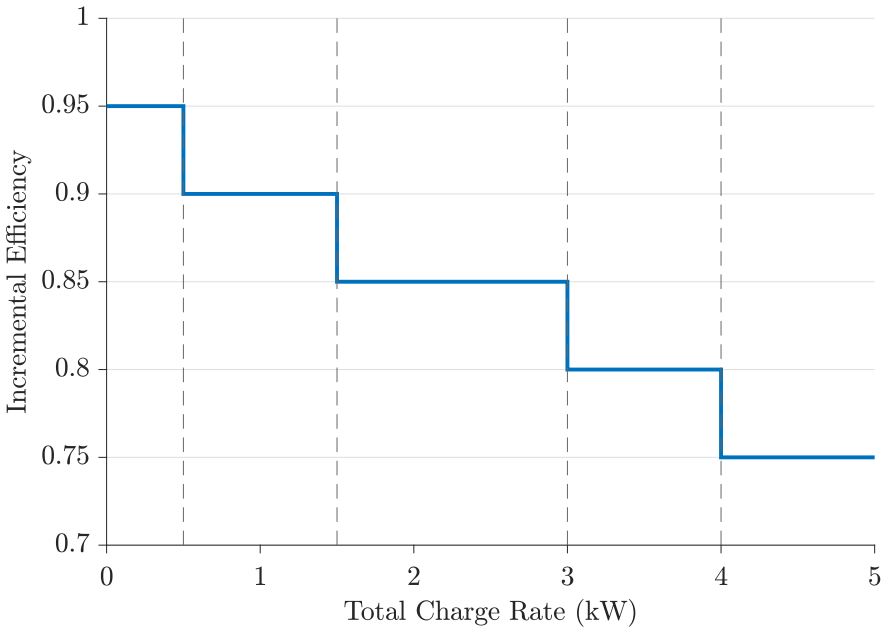

Figure 3.8 Example piecewise constant incremental charging efficiency curve for $b = 5$.

For this definition to be valid, $x_c^1 = 0.5$ whenever $x_c^2 > 0$ and $x_c^2 = 1$ whenever

$x_c^3 > 0$, and so on. Because the efficiency curve in Figure 3.8 represents a series (load dependent) loss component and is monotonically decreasing, the optimal solution will always comply with these constraints. The first band (x_c^1) has the highest efficiency so an optimal solution will always always reach its maximum value before x_c^2 becomes non-zero. This observation is not valid for an efficiency model including both load dependent and load independent loss components, as the efficiency is not guaranteed to be monotonically decreasing. Instead, additional constraints are required to ensure that the previous efficiency band reaches its maximum value before the next band becomes non-zero. The associated formulation using binary constraints is presented in Section 3.3 as an extension from a LP problem to a MILP problem.

These limits on the maximum and minimum values for each charge/discharge power mirror the form of the lower and upper bound constraints of the LP problem structure (Equation (3.16)) and are easily incorporated as such.

3.2.1.3 State of charge (SOC)

There are limits to the SOC of a BESS, which must be reflected in the LP problem formulation. Given the charge and discharge profiles x_c and x_d, as well as the efficiency profiles η_C and η_D, the SOC of the battery (in kWh) at time step k is denoted by $\chi(k)$ where

$$\chi(k) = \chi(0) + \sum_{i=1}^{k} \left(\sum_{j=1}^{b} x_c^j(i) \Delta \eta_c^j \right) - \sum_{i=1}^{k} \left(\sum_{j=1}^{b} x_d^j(i) \Delta \frac{1}{\eta_d^j} \right) \tag{3.20}$$

and $\chi(0)$ denotes the initial SOC of the battery. The full SOC profile of the battery over the entire optimisation time space is therefore represented by $\chi = [\chi(0), \chi(1), ..., \chi(s)]^T \in \mathbb{R}^{s+1}$.

A BESS has a physical limit as to how much energy can be stored, which is represented by $C \in \mathbb{R}_{\geq 0}$ (in kWh). As $\mathbb{1}$ is the all-1s column vector of length s, this physical storage limit leads to the state of charge profile, χ being constrained such that

$$\mathbf{0} \leq \chi \leq C \begin{bmatrix} 1 \\ \mathbb{1} \end{bmatrix}. \tag{3.21}$$

For an initial state of charge which satisfies $0 \leq \chi(0) \leq C$, two vectors of length s are defined to represent the amount by which the SOC can increase from $\chi(0)$ and the amount by which it can decrease from $\chi(0)$. These are $\overline{\mathbf{C}}$ and $\underline{\mathbf{C}}$ respectively:

$$\overline{\mathbf{C}} = (C - \chi(0))\mathbb{1} \tag{3.22}$$

$$\underline{\mathbf{C}} = \chi(0)\mathbb{1}. \tag{3.23}$$

These constraints are implemented in the LP problem as linear inequality constraints in two parts. The first part ensures that at each time step the net increase in state of charge from the start of the optimisation time span is less than the defined maximum. The second part ensures the reverse - that the net decrease in state of charge is less the maximum allowed. In order to do this, the current SOC must be calculated at each time step. This requires incorporation of the previously discussed efficiency factors.

The linear inequality constraints ($Ax \leq b$) where $A \in \mathbb{R}^{2s \times (2sb+2s)}$, and $b \in \mathbb{R}^{2s}$ are defined as:

$$A = \begin{bmatrix} \underbrace{\begin{matrix} \eta_c^1\mathbf{T} & \eta_c^2\mathbf{T} & \dots & \eta_c^b\mathbf{T} \\ -\eta_c^1\mathbf{T} & -\eta_c^2\mathbf{T} & \dots & -\eta_c^b\mathbf{T} \end{matrix}}_{a} & \underbrace{\begin{matrix} -\frac{1}{\eta_d^1}\mathbf{T} & -\frac{1}{\eta_d^2}\mathbf{T} & \dots & -\frac{1}{\eta_d^b}\mathbf{T} \\ \frac{1}{\eta_d^1}\mathbf{T} & \frac{1}{\eta_d^2}\mathbf{T} & \dots & \frac{1}{\eta_d^b}\mathbf{T} \end{matrix}}_{b} & \underbrace{\begin{matrix} \mathbf{0} & \mathbf{0} \\ \mathbf{0} & \mathbf{0} \end{matrix}}_{c} \end{bmatrix} \tag{3.24}$$

$$b = \begin{bmatrix} \overline{C} \\ \underline{C} \end{bmatrix}. \tag{3.25}$$

As in Equation (3.13), the annotated section a relates to battery charging, section b to battery discharging, and section c to grid import and export. The first s rows of Ax give the amount by which battery SOC has increased from its initial value at each time period, while the following s rows give the amount SOC has decreased from its initial value. This means that a battery which experiences a net increase in SOC will have a negative value for the amount by which its SOC has decreased, and vice versa. These values are constrained such that they do not exceed $\overline{C}$ and $\underline{C}$.

The final element of the SOC constraints is ensuring the SOC at the end of the optimisation period is equal to the initial SOC. Given the computational complexity of long time span optimisations, this method will generally be applied to consecutive optimisation time spans. For example, optimising battery operation over a full year would be achieved by a series of single day-ahead optimisations. Without a constraint requiring the final SOC to be equal to the initial SOC, the optimal solution would result in complete discharge of the battery by the end of the optimisation time span (given a non-zero buyback rate). This would force the initial SOC for the next optimisation timespan to be zero, causing sub-optimal results. The two ways in which this can be mitigated are constraining the final SOC to be equal to the initial SOC, or modification to the optimisation time span, which is discussed in Chapter 5.

The constraint where final SOC is equal to initial SOC is implemented with the addition of one final row to the equality constraint formulation ($A_{eq}x = b_{eq}$), such that row $s+1$ of A_{eq} is set to

$$\begin{bmatrix} \eta_c^1\mathbb{1}^T & \eta_c^2\mathbb{1}^T & \dots & \eta_c^b\mathbb{1}^T & -\frac{1}{\eta_d^1}\mathbb{1}^T & -\frac{1}{\eta_d^2}\mathbb{1}^T & \dots & -\frac{1}{\eta_d^b}\mathbb{1}^T & \mathbf{0} & \mathbf{0} \end{bmatrix} \tag{3.26}$$

and the corresponding element of b_{eq} is set to 0. This formulation means that the net

change in the battery SOC over the entire time span is constrained to be equal to zero.

3.2.1.4 Electricity Pricing

The final element of the LP problem formulation is the coefficient vector f. This vector contains the costs which are applied to the power flows represented by the decision variable, x, in order to calculate the objective value which is being minimised. The only elements of the decision variable which have a financial cost associated with them are the grid import and grid export elements. This results f being defined

$$f = \begin{bmatrix} 0 \\ \vdots \\ 0 \\ p_i \\ p_e \end{bmatrix} \tag{3.27}$$

where the first $2sb$ elements, which are associated with battery charging and discharging, are zero.

3.3 MIXED INTEGER LINEAR PROGRAMMING OPTIMISATION PROBLEM

This section details the extension of the LP problem to a MILP problem featuring binary constraints, which remove the requirement for a monotonically decreasing efficiency function. What the constraints must achieve, as well as how the constraints are formulated in the MILP problem structure, is elaborated here.

To model the BESS efficiency curve, the charge or discharge rate is expressed as the sum of b bands, with each band having a different efficiency. In Section 3.2, efficiency was monotonically decreasing with increasing charge/discharge power, and as such was able to be modelled as a simple LP problem. If this is not the case, such as for a combination of load dependent and independent losses, then additional binary variables are needed to formulate the problem. This shifts the problem from being a LP to a MILP problem.

The equality constraints, $A_{\text{eq}} \cdot x = b_{\text{eq}}$, which incorporate the power balance constraints at each time step, and the start/end SOC constraint, remain as they are for the LP problem (Section 3.2). The MILP problem includes an additional constraint, that a subset of the decision variable, x, must take integer values. The definition of the

MILP problem is updated to:

$$\min_x f^T x \text{ subject to } \begin{cases} x(i) \text{ are integer for some, or all, i=1,2,...,n} \\ A \cdot x \leq b \\ A_{eq} \cdot x = b_{eq} \\ lb \leq x \leq ub. \end{cases} \tag{3.28}$$

Recall that the charging power for a single time step is the sum of a number of efficiency bands (Equation (3.8)), and the total stored power for a given $x_c(k)$ is given by:

$$x_{stored}(k) = x_c^1(k)\eta_c^1 + x_c^2(k)\eta_c^2 + ... + x_c^b(k)\eta_c^b.$$

For this interpretation to be valid it is required that $x_c^1(k) = L_c^1$ whenever $x_c^2(k) > 0$, and $x_c^2(k) = L_c^2$ whenever $x_c^3(k) > 0$, and so on. Without this requirement, the optimal solution will fill whichever band has the highest efficiency first, rather than the bands being filled incrementally. These restrictions are enforced through the addition of binary variables and constraints.

First, binary variables are defined to indicate when a charge or discharge variable is at its maximum value. These binary variables exist for each time step and for all but the last efficiency band. Allowing for both charge and discharge, there are $2s(b-1)$ additional binary variables. They are defined such that, for the charging case,

$$w_c^1(k) = \begin{cases} 1 & \text{if } x_c^1(k) = L_c^1 \\ 0 & \text{otherwise} \end{cases}$$

$$w_c^2(k) = \begin{cases} 1 & \text{if } x_c^2(k) = L_c^2 \\ 0 & \text{otherwise.} \end{cases}$$

This continues until the $(b-1)$ efficiency band is reached:

$$w_c^{b-1}(k) = \begin{cases} 1 & \text{if } x_c^{b-1}(k) = L_c^{b-1} \\ 0 & \text{otherwise.} \end{cases}$$

The static upper and lower bound constraints on the charge/discharge elements of the decision variable in the LP problem can then be replaced with conditional constraints

formulated with these binary variables. They are formulated such that

$$\begin{aligned} L_c^1 w_1(k) \leq x_c^1(k) \leq L_c^1 \\ L_c^2 w_2(k) \leq x_c^2(k) \leq L_c^2 w_c^1(k) \\ \vdots \\ 0 \leq x_c^b(k) \leq L_c^b w_c^{b-1}(k). \end{aligned} \tag{3.29}$$

Binary constraints to force sequential filling of the charge/discharge bands are implemented as a part of the inequality constraint formulation ($Ax \leq b$). These inequality constraints are the same as those for the LP problem (Equation (3.24)) with two additional sets of constraints. The first new set comprises $2sb$ constraints on the upper bounds of each charge/discharge element of x. These are implemented in two slightly different ways: the constraints of the first efficiency band are formulated in a manner differing from the remaining. The constraints for the first efficiency band are represented as follows:

$$\begin{aligned} Ax \leq b \\ x_c^1(k) \leq a_c^1. \end{aligned} \tag{3.30}$$

For the subsequent efficiency bands, the constraint formulation is:

$$\begin{aligned} Ax \leq b \\ x_c^j(k) - L_c^j w_c^{j-1} \leq 0. \end{aligned} \tag{3.31}$$

The second set represents another $2sb$ constraints associated with the lower bounds of Equation (3.29). These constraints also feature two slightly differing formulations; in this instance the final efficiency band is different to the others. The constraints for the first $b-1$ efficiency bands are represented as:

$$\begin{aligned} Ax \leq b \\ -x_c^j(k) + L_c^j w_c^j(k) \leq 0. \end{aligned} \tag{3.32}$$

The lower bound constraint for the final efficiency band is simply formulated as:

$$\begin{aligned} Ax \leq b \\ -x_c^j(b) \leq 0. \end{aligned} \tag{3.33}$$

Along with the constraints that remain from the LP problem, a total of $2s + 4sb$ linear inequality constraints are specified for the MILP method. Furthermore, definition of the binary variables results in the MILP solver internally creating additional inequality

constraints.

3.4 SUMMARY

This chapter has presented two models for BESS charging and discharging efficiency. One is purely charge/discharge rate dependent, which is represented as a simple series resistance model, while the other incorporates a constant standing loss component. A LP problem is formulated to optimise battery operations under the first efficiency model. This LP is then extended to a MILP problem in order to accommodate the second model, or in general any arbitrary efficiency curve. The generalised MILP method is used, along with measured household load data and PV generation data (Chapter 5), to produce analysis of the financial benefits to households, as well as assessments of the effects on aggregated network loads, that BESSs could produce under different pricing structures (Chapter 6).

Chapter 4

FORMULATION OF RULE-BASED METHOD

The MILP optimisation covered in Chapter 3 gives an upper bound on the savings that could be made by a household. It is not, however, a realistic control algorithm that could be practically implemented, as it is based on perfect foresight. It is necessary to develop and assess a simple and implementable control scheme. Such a practicable method puts a lower bound on the achievable financial benefits. It is expected that future commercially produced control systems could have a greater level of sophistication and would therefore produce financial results that fall within the region bounded by this rule-based method at the lower end, and the MILP model at the upper end.

This chapter presents the structure of this rule-based control method. Under this method, battery operation decisions are made at each time step based on the present state of the system as well as an approximate forecast of the upcoming PV generation. This method therefore does not rely on perfect foresight of the household load and PV generation, as assumed in the MILP method.

The following sections give an overview of the method and how price decision thresholds are implemented under different pricing structures. Also detailed is the application of approximate PV generation forecasts to inform SOC constraints in order to improve battery operation. Third party control signalling to provide network load management is also discussed.

4.1 RULE-BASED METHOD OVERVIEW

This section outlines the rule-based battery control methodology. At each time step, a decision tree is used to determine battery operation. This decision is based on present household load, PV generation, and pricing. The decision interval is defined by the time resolution of the data. As the data used for testing all methods in this thesis has a half-hour resolution, the decisions are made with the same time interval.

The decision tree used to determine battery operation for each half hour is illustrated in Figure 4.1. Its primary objective is maximisation of PV self-consumption, and the secondary objective is to take advantage of temporal pricing variations. This is achieved

by prioritising the use of PV generation in excess of household load for battery charging as opposed to export to the grid.

When PV generation does not exceed the load, the import price is used to make operational decisions. Two pricing thresholds are considered: a high price threshold and a low price threshold. If the import price exceeds the high price threshold ,it is classed as a high price period. This means it is worthwhile discharging energy from the battery in order to reduce the power being imported. Similarly, the low price threshold determines when the import price is low enough that it is worthwhile charging the battery from the grid. The selection of these thresholds under different pricing structures is discussed in Section 4.2.

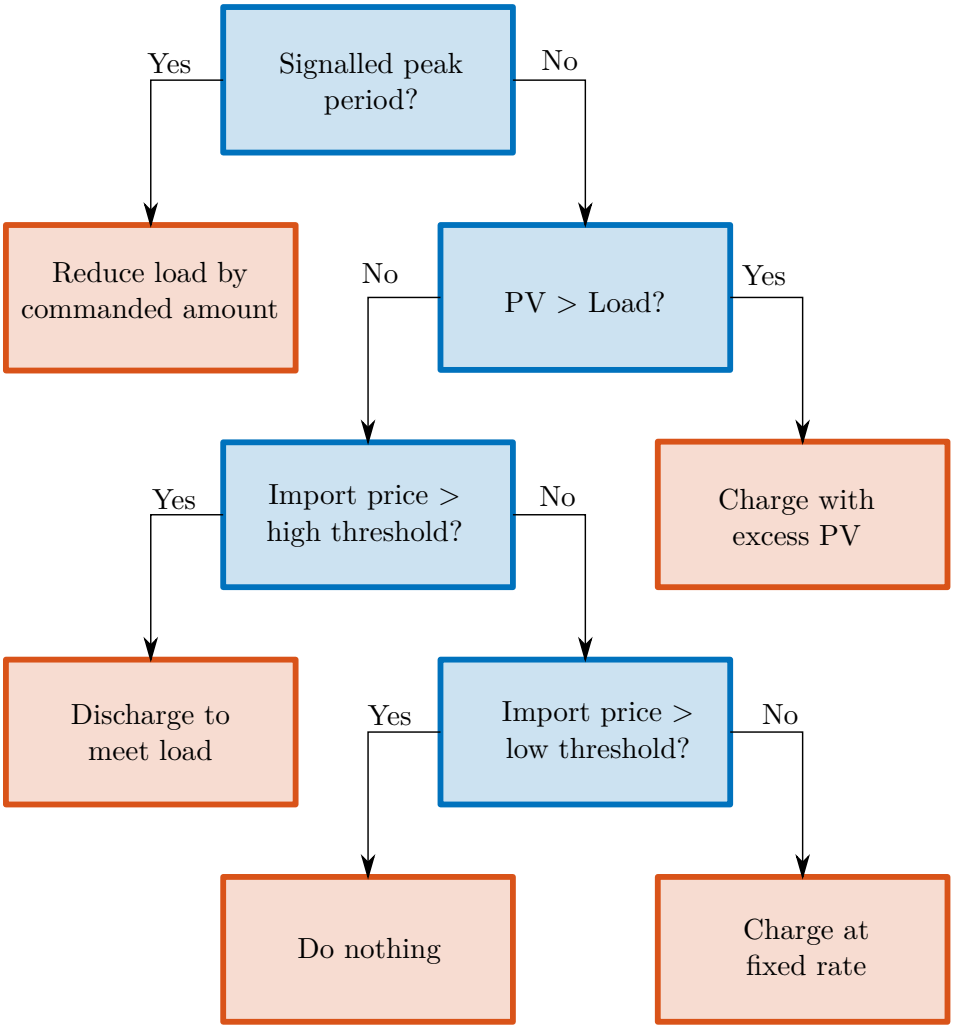

Figure 4.1 Outline of rule-based battery management decision structure.

During PV charging, or high price triggered discharging, the charge/discharge rate is determined by the relationship between the household load and the PV generation.

However, this is not true for grid-charging which permits a greater degree of freedom. There are two aspects to be considered: the rate at which the charging occurs and the SOC at which this charging is terminated. Unlike charging with excess PV generation, where it is logical to charge with only the available excess PV power, charging from the grid could occur at any rate within the capabilities of the battery system. This could be a low rate to minimise grid impacts, the system's peak efficiency rate, or a high rate to minimise charging time.

With regard to termination of grid charging, if the battery is fully charged from the grid during, for example, a low priced overnight period before a sunny day, then the battery will not have the capacity to store excess PV generation. This will result in the battery system providing sub-optimal financial results for the owner. Alternatively, if the grid charging mode is entirely prevented, then during winter periods when PV generation is low and household load is high, the battery may not offer any energy for extended periods and certainly not for the daily cycling for which it is intended. A method of optimising this charge quantity based on an approximate PV generation forecast is described in Section 4.3.

As in the MILP optimisation, there are constraints on both the power ratings of the BESS, as well as the SOC of the battery, which are enforced in the rule-based method. The charge or discharge power is restricted by the rating of the battery irrespective of the operation recommended by the decision tree. Any difference is made up by grid import or export to ensure the power balance equation is satisfied.

Equally, if the decision would result in the battery exceeding the SOC limits at the end of the present time step, then the charge or discharge power is reduced so that SOC constraints will not be violated. This recalculation takes into account the same efficiency function as the MILP method Section 3.1.1. This means that the charge or discharge power is calculated so that the SOC is brought exactly to its limit at the end of the time step. accounting for charge or discharge efficiency.

4.2 PRICING THRESHOLDS

Two distinct categories of energy pricing have been identified. These have been termed known pricing and unknown pricing. Known pricing is when the prices are fixed and known ahead of time, such as a fixed rate, or day/night pricing. This could also include more complex TOU pricing, subject to it being a fixed pricing schedule. Conversely, unknown pricing is not known ahead of time. The prime example is a pricing structure where the spot price is passed onto consumers. Pricing structures containing real time demand reflective components would also fall into the unknown pricing category.

The relevance of these two pricing structures is in the approach towards the battery operation price thresholds. A known pricing structure allows for simple fixed thresholds to be set, while an unknown pricing structure like spot pricing requires the definition of

a dynamic threshold to cater to changes and trends over a longer timespan than the daily battery cycling.

Known pricing can be allowed for with fixed thresholds. As long as there is sufficient price differential, the operating methodology is to set the thresholds to allow charging during low price periods and to restrict discharge to high price periods. In a two tiered pricing structure, such as day/night pricing, the two thresholds reduce down to a single threshold - the price is either high or it is low. Other multi-tiered pricing structures, such as peak/shoulder/off-peak, allow for a differential between the two thresholds, which creates a dead-band where the battery is commanded to neither charge nor discharge.

In the case of unknown pricing, such a spot pricing scenario, a fixed price threshold may not be appropriate. This is due to the fact that daily cycling is desired from the battery system, which a fixed threshold may not enable as spot pricing often displays significant variation over time spans longer than a day. A fixed threshold would not align well with seasonal variations in price in order to obtain daily cycling. As an example of this, the half-hourly spot price at the ISL2201 node across the entirety of the year 2012 is shown in Figure 4.2. This spot price data is used later in Section 6.2 which presents the results of both the MILP method and this rule-based method under a spot pricing structure.

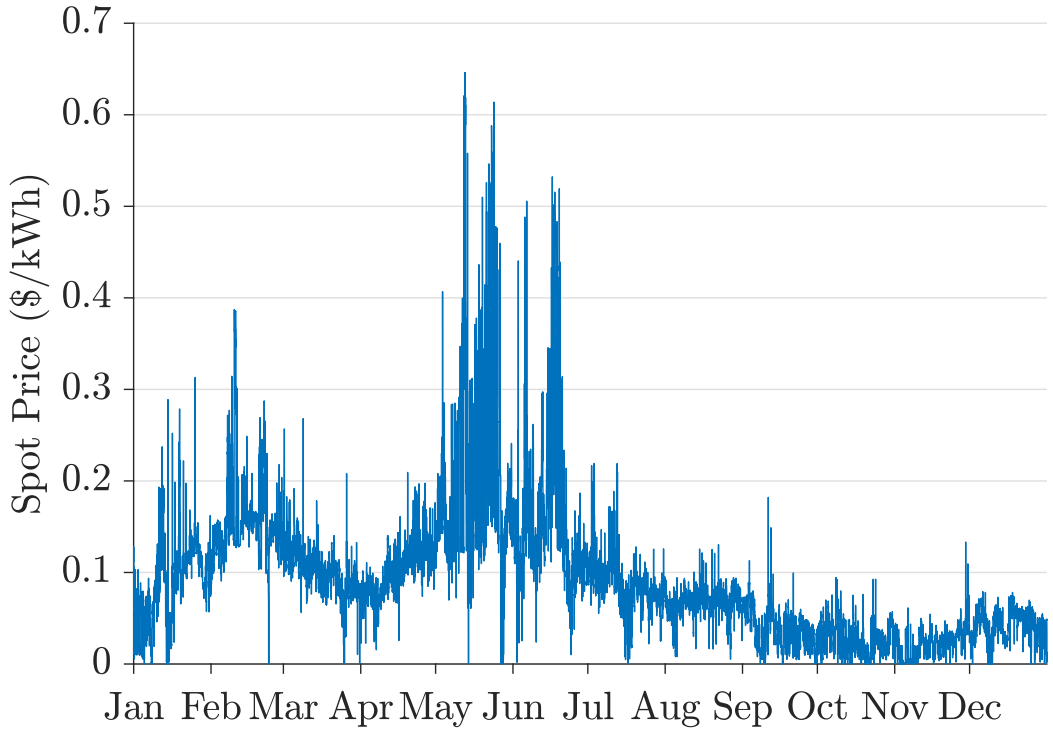

Figure 4.2 Half-hourly spot price at node ISL2201 for 2012.

A method has been developed in which the fixed threshold is replaced by a moving average of the past week's pricing in combination with a margin. Where the import price at time step k is given by $P_i(k)$, the moving average for the last n time periods at

time k, $\bar{P}_i(k)$ is given by

$$\bar{P}_i(k) = \frac{1}{n}\sum_{i=1}^{n} P_i(k-i). \tag{4.1}$$

The price threshold below which the battery is charged, $T_C(k)$, is given by,

$$T_C(k) = \bar{P}_i(k) \cdot (1-\alpha) \tag{4.2}$$

where $\alpha \in [0, 1]$ is the margin. If the present price is less than the moving average minus some definable margin then the battery will charge from the grid. The purpose of the margin, α, is to create a dead band around the average price where the battery will neither charge or discharge. The discharge threshold, the price above which the battery system will discharge its stored energy, $T_D(k)$, is calculated as

$$T_D(k) = \bar{P}_i(k) \cdot (1+\alpha). \tag{4.3}$$

The margin, α, can be tuned for a desired level of price arbitrage depending on the objectives of the battery owners. If they desire to maximise short term gains, then α could be a small value, meaning the battery management system attempts to exploit minor variations in price. If the owner wants to reduce energy cycling, then α can be increased so that only large price deviations from the average result in battery charge or discharge operation.

4.3 PV GENERATION FORECAST

The objective of the rule-based model is to reduce the consumer's electricity bill. Because, in the cases considered in this thesis, the compensation for exporting power to the grid is less than the cost of importing from the grid, this means the objectives are to firstly maximise PV self-consumption, and secondly to create benefit from price differentials. These objectives make many of the battery operation decisions readily apparent and simple. The desired behaviour that is least clear is when the PV generation does not exceed the household load and import prices are low. There is a desire to charge during these low priced periods in order to be able to reduce consumption during higher priced periods. A decision needs to be made as to what extent the battery is charged during the low price periods. If no constraint is placed on the charging, then under a day/night pricing structure, for example, the battery will charge fully overnight. This means there is minimal capacity for any excess PV generation to be stored during the daylight period. Such battery behaviour will impact financial savings, as the objective of increasing PV self-consumption is not being met.

In the age of readily accessible data and the internet of things (IoT), a commercially implemented battery management system could have access to a day-ahead PV generation forecast to inform its decision making. This would allow the system to make

use of low priced power for charging overnight when the day ahead is expected to have low levels of excess PV generation. Similarly, if the day ahead is expected to have high levels of PV generation, then overnight charging may not be utilised.

PV forecasts can be implemented with varying degrees of sophistication in numerous ways. Of key interest is the quantity of excess PV generation above household load rather than the gross generation. A forecast of the excess PV generation is more complex than the gross generation because it also requires a forecast of household load. Instead, a forecast of the gross PV generation, along with a consumer's historical load information, is used to make the charging decision. In the New Zealand context, it is reasonable to assume that data regarding a consumer's historical load will be available. Consumers' smart meter usage data is required to be made available to consumers (or their agents) by request under a 2014 amendment to the Electricity Industry Participation Code [68]. This historical data would allow for configuration parameters of a BESS to be set at the time of installation, which could then be improved over time as the battery management system collects its own data.

For the purposes of this rule-based model, each day is classified as one of three types: a good PV day, an average PV day, and a poor PV day. The intention is that on a good PV day, prior to the daytime PV generation period, the system will not undertake any grid charging. For an average PV day, the system may undertake some grid charging but will maintain enough spare capacity to store the typical quantity of excess PV energy. For a poor PV day where there is not expected to be any significant quantity of excess PV generation, then no additional limit is put on grid charging. A poor PV day is defined as one where the quantity of excess PV generation is less than 1 kWh, while a good PV day is defined as one where excess PV generation exceeds the battery capacity.

Days are classified based on a forecast value of total energy generated for the coming day, along with two thresholds which have been set for each household's battery management system. For this model, it assumed such a forecast is made available to the battery management system. Given the age of smart and internet connected appliances, this seems a reasonable assumption to make.

The relationship between gross and excess PV generation is approximated by fitting a first order polynomial to the year's worth of data for each household. This is shown in Figure 4.3 for one example household. For each day of the year, the household's gross PV generation is plotted against the excess generation, where excess generation is energy exported to the grid if there is no storage. From this fitted function the gross generation for which excess generation is expected to be 1 kWh and 13.5 kWh are identified. For this example household, it is expected that a forecast gross generation of less than 2.6 kWh will result in an excess generation of less than 1 kWh, while a forecast gross generation greater than 16.5 kWh will result in an excess generation

greater than 13.5 kWh. Additionally, for all average PV days, the mean excess PV generation is calculated. This mean value is used as the spare battery capacity which must be preserved after any grid charging leading up to an average PV day.

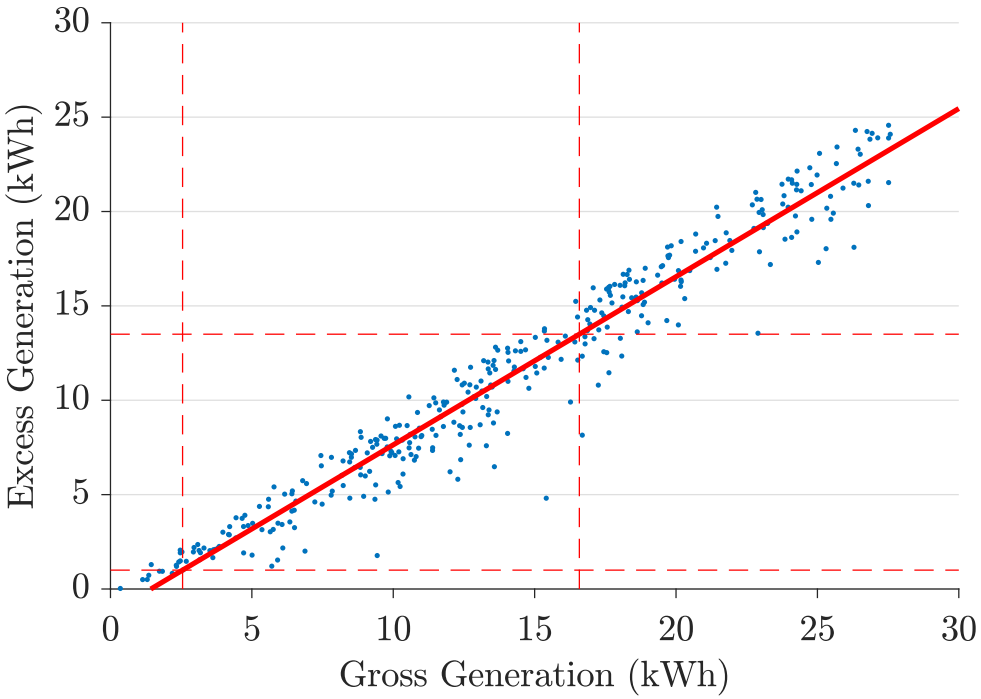

Figure 4.3 Determining day type classification thresholds for an example household.

To summarise how this forecast is implemented in the modelling, for this example household if the forecast gross PV generation for the next daylight period is less than 2.6 kWh then it is classified as a poor PV day. As a result of this, the maximum SOC under grid charging is constrained to the full battery capacity of 13.5 kWh. If the forecast generation is greater than 2.6 kWh but less than 16.5 kWh, it is classified as an average day and the constraint is set to the capacity less the mean excess generation. If the forecast is greater than 16.5 kWh then grid charging is prevented entirely.

4.4 THIRD PARTY CONTROL

The effect of BESSs on peak network loads is of particular interest to EDBs. These effects include both the ability of battery systems to be leveraged to reduce peak network loads, as well as peak loads being increased through a lack of charging diversity. One possible method in which battery storage could be used to reduce peak loads is a centralised control signalling system. This is much like existing ripple control switched water heaters. With a centralised signalling scheme, an EDB (or other market player) would provide a signal to households indicating that the BESSs should be used to reduce the load the household presents to the network.

This concept of using privately owned BESSs for network load management raises some questions. Firstly, how effective is this centralised signalling at controlling and reducing network peak loads? And secondly, if battery systems are being asked to undertake behaviour for network load management, then what is the financial implication of that behaviour for the battery system owner?

Under present, and potentially future, pricing structures, battery system owners are not always incentivised to behave in a way that reduces system peaks. Even being exposed to the market spot price does not necessarily incentivise consumer behaviour that is beneficial at a local distribution network level. There are many factors that contribute to spot prices, including generation costs, seasonal climatic conditions, outages, locational pricing effects, transmission constraints, and security of supply constraints [69]. Local distribution loads and constraints do not factor into spot prices, while these are precisely the things which battery systems have the potential to reduce.

One option for achieving distribution network peak load reduction benefits from battery systems would be a load reflective real time pricing component. In the New Zealand case, distribution companies providing real time pricing signals to residential consumers would be a large shift in operational paradigm. A second approach could be signalling system peak load periods to battery management systems and requiring them to discharge (if having suitable SOC) while that signal persists. In exchange, consumers would be given a lower distribution charge. This could have the benefit of being better understood by consumers, as it is very similar to controllable hot water heating and ripple control signalling already operated by some distribution companies in New Zealand.

This third party signalling method is implemented in the model by by defining a vector, S, where $S(k)$ is the power at which the battery system is being signalled to reduce the household load by. Referring to Figure 4.1, the first decision point at time step k can be seen to be that if it is a signalled period, meaning $S(k) > 0$, then take the action required to reduce the load presented to the grid by $S(k)$ if able to do so.

By conducting simulations using this rule-based model both with and without this third party controlled discharge, the effect on aggregate network peak loads can be assessed, as can the financial implications for the system owners. The following sections detail how the signalled periods are identified and how battery behaviour is modified under load reduction signalling.

4.4.1 Selection of Signalled Periods

The implementation of this control signalling in the rule-based method requires a network load threshold to be set; this could be considered a target peak network load. When the aggregate network load exceeds this threshold at any time step, it is deemed

a signalled peak period. BESSs will then be signalled to reduce the load they present to the network by a specific amount if they are able to do so.

There are two approaches that could be taken to determining this load threshold. The first is simply setting it to a particular fixed value. The second is to identify a target number of time steps, κ, to be signalled periods. For example, as discussed in Section 2.3.2, Orion targets a total of 50-100 hours annually signalled as peak pricing periods to general consumers. To convert this to a load threshold, the aggregate network load is found with no third party control signalling. From this aggregate network load, the top κ peak loads are identified and the $\kappa + 1$th peak can be taken as the load threshold. This means that there would be κ time periods where peak signalling was active with the intention of reducing the aggregate network load to the level of the $\kappa + 1$th peak. In reality, once BESSs respond to a signalled period, their storage trajectory from that point forward is altered. This means the household loads presented to the grid will differ from what was calculated originally with no control signalling. As such the exact number of time steps which exceed the price threshold may differ slightly from κ.

This results in a two-step modelling process. At each time step, the aggregate load is found with no control signalling active. This is then compared to the threshold. If it is less than the threshold, then calculation advances to the next step. If it exceeds the threshold, then the quantity of load reduction to reduce the aggregate load down to the threshold is calculated. The time step is then repeated with control signalling active before continuing to the next time step. This two-step process exists because the model must calculate the aggregate load rather than simply measure it as it would in a practical implementation. This process is illustrated in Figure 4.4.

4.4.2 Battery System Behaviour when Signalled

This section outlines the behaviour undertaken by the BESSs when a load management control signal is received. Recall that the signal received by the BESS is $S(k)$, which is the amount by which the system is being asked to reduce the load presented to the grid by the household. The first step in reducing this load is to stop any charging that would otherwise be occurring. A new value for the battery charging power $X'_c(k)$ is calculated to replace what charging power would be in the absence of a control signal ($x_c(k)$), such that:

$$x'_c(k) = \begin{cases} x_c(k) - S(k) & \text{if } S(k) < x_c(k) \\ 0 & \text{if } S(k) \geq x_c(k). \end{cases} \tag{4.4}$$

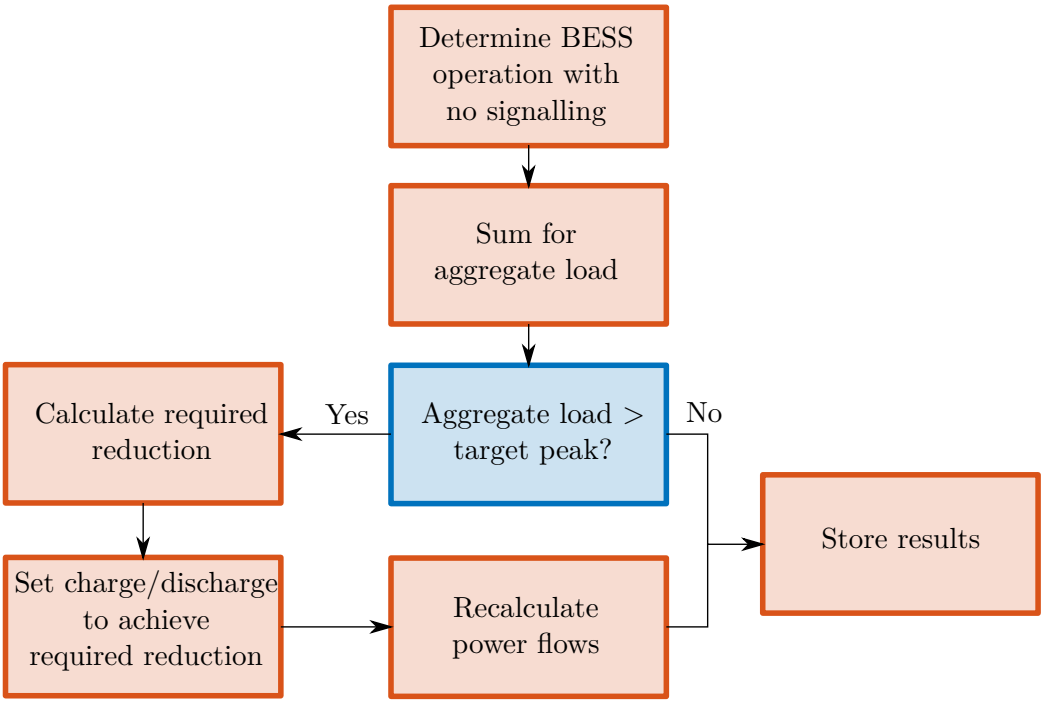

Figure 4.4 Modelling process for a single time step in the presence of third party signalling.

From this, a remaining signalled reduction, $S'(k)$, is calculated such that

$$S'(k) = S(k) - \Big(x_c(k) - x'_c(k)\Big). \tag{4.5}$$

From this, if further reduction is required, the quantity of battery discharge power, $x'_d(k)$, can be calculated from what the discharge power, $X_d(k)$, would otherwise be, such that

$$x'_d(k) = x_d(k) + S'(k) \quad \text{subject to SOC and power contraints.} \tag{4.6}$$

With these new behaviours under control signalling found, new values for grid import/-export are calculated, as is the battery's SOC. Simulation then proceeds to the next time step.

4.5 SUMMARY OF RULE-BASED MODEL

In contrast to the MILP method, which provides optimal day-ahead battery behaviour and requires perfect foresight of household load and PV generation, the method presented in this chapter is simple and implementable without relying on perfect foresight. Battery operation decisions are made at each time step based on the current system state, along with a simple and approximate PV generation forecast.

While there are improvements that could be made to the calculation of pricing

decision thresholds and sophistication that could be added to PV forecasting, this method serves to put a lower bound on easily achievable financial benefits that can be made from a BESS.

Additionally, this method allows exploration of centralised network load management signalling schemes. The method can be used to assess the availability and efficacy of privately owned BESSs to contribute to network peak load reduction. The financial cost to battery system owners of engaging in these load management behaviours is also able to be assessed.

Chapter 5

INPUT DATA AND CONSIDERATIONS

This chapter details the relevant considerations that must be made in order to produce the results of Chapter 6 using the MILP method (Chapter 3) and the rule-based method (Chapter 4). Firstly, consideration must be given to the input datasets which are used for both household load and PV generation (Section 5.1). Secondly, consideration must be given to how the MILP problem is actually solved, as well as ensuring that it is solved in a reasonable time (Section 5.2).

5.1 INPUT DATA

There are two large datasets which are used to produce results for the example pricing structures in Chapter 6. The first dataset is a collection of household smart meter load measurements provided by an electricity retailer. The second dataset is solar PV generation data based upon the solar irradiance data collected and kept by the National Institute of Water and Atmospheric Research (NIWA). Additionally, spot price data is obtained from the New Zealand Electricity Authority which for one of the pricing structures considered in Chapter 6.

5.1.1 Household Load Data

The household load dataset is obtained from the smart meters of of 2212 households in Christchurch, New Zealand. This data was provided to the GREEN Grid Project by an electricity retailer. The dataset contains half hourly electricity consumption data for each household for the year of 2012. This was a leap year, so there are 366 complete days of data available.

Within the dataset, households are anonymised such that the only information available for each household is whether the household is on a fixed rate pricing structure or a day/night pricing structure, and the household's energy consumption for each half hour period of the year. Of the 2212 households, 31% are on the day/night pricing structure while the remaining 69% are on the simple fixed rate pricing structure.

The Electricity (Low Fixed Charge Tariff Option for Domestic Consumers) Regulations 2004 require retailers to offer a low fixed charge tariff option. This requirement benefits consumers who have electricity usage less than the average consumer. For households in the lower South Island, the average user is defined as 9000 kWh annually, while for the rest of the country it is 8000 kWh. The dataset has a mean annual usage of 8241 kWh, which is less than the defined average consumer in the lower South Island. Figure 5.1 shows the distribution of annual household electricity consumption with the red line indicating the low user definition. 65% of the households in the dataset fall into this low user category. This aligns with the Electricity Network Association's 2018 estimate of 60% of households nationwide meeting the low user definition [70].

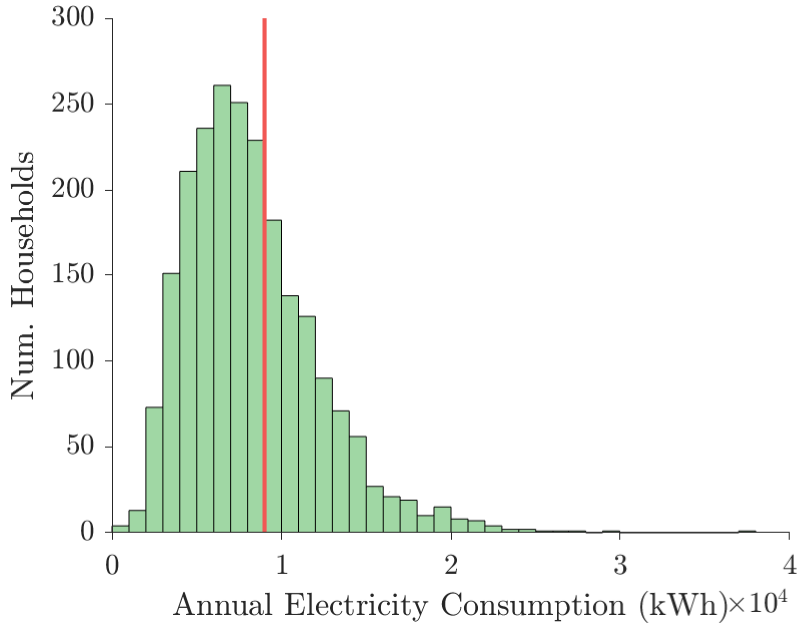

Figure 5.1 Distribution of annual household electricity consumption.

In the results presented in Chapter 6, there is no division of households into low use and standard use categories with differing pricing structures. Instead they are treated uniformly with a single pricing structure. The example cases presented in Chapter 6 are chosen to highlight the application of the methods to different forms of pricing structure and as such are already divorced from reality, because a single pricing structure is applied to all households. The additional consideration of low fixed price structures adds complexity without any particular benefit.

The intention of these regulations, when introduced by the Government in 2004 was to "provide low-use consumers with a tariff option that is more equitable for low energy usage and compatible with the Government's energy-efficiency objectives" [71]. Recent announcements from both major political parties in New Zealand, however, indicate that there is support for the removal of this requirement for retailers to offer a low fixed

price option. Reasons for its removal are outlined in [72] which include that it:

- reduces costs only to some households in need,
- promotes inefficient choices for the adoption and use of new technologies, and
- increases complexity of pricing structures and adds to consumer confusion. This makes it difficult for consumers to pick the best plan, which subsequently hampers retail competition.

With the removal of the regulations requiring low fixed charge pricing structures expected in the near future, it would be unwise and unnecessary to complicate the selection of pricing structures to be used as examples with the inclusion of low fixed charge pricing. The New Zealand electricity industry is undergoing a journey towards more cost reflective pricing in which a low fixed charge tariff option appears unlikely to feature.

Figure 5.2 shows an example of the typical daily household load profile contained in this dataset. This is synthesised from multiple load profiles as the conditions placed upon the use of this dataset prevent the publication of any individual household's data. The load data is quantised to the nearest 100 W, which can be observed in the sample load profile.

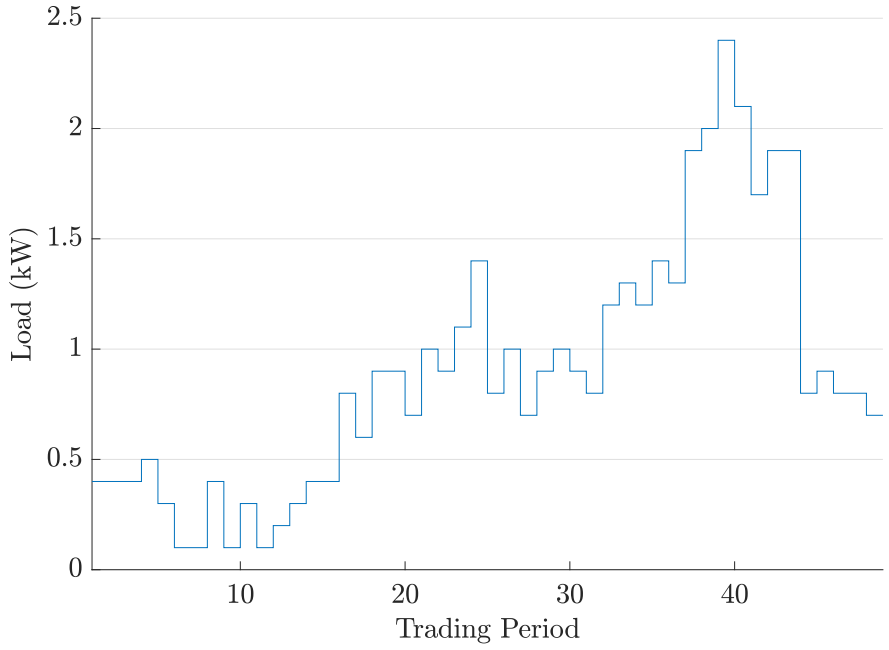

Figure 5.2 Example household load profile for one day.

5.1.2 PV Generation Data

The PV generation data is sourced from a large dataset which covers 16 regions of New Zealand for a period of 15 years (2000-2015) at a time resolution of 10 minutes. The

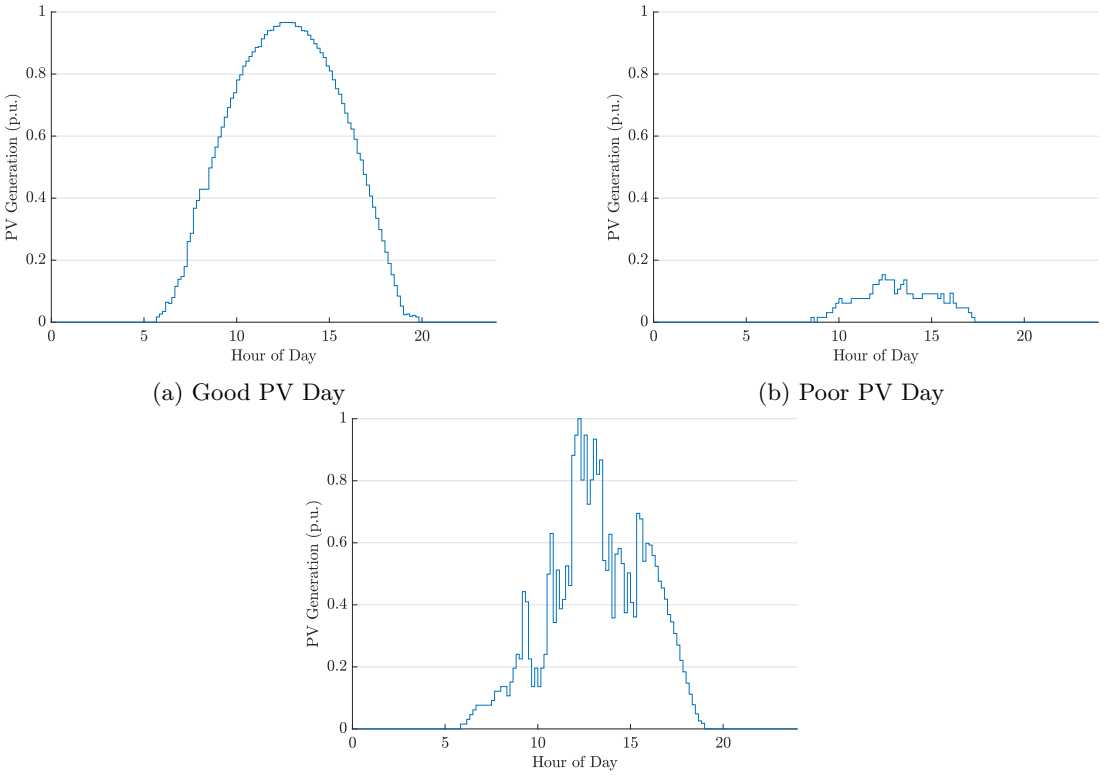

(a) Good PV Day

(b) Poor PV Day

(c) Variable PV Day

Figure 5.3 Sample daily PV generation data.

results presented in this thesis use the data for the Canterbury region which contains the city of Christchurch from which the household load data is sourced. The dataset was generated as part of the GREEN Grid Project.

The initial data source is solar irradiance data collected by NIWA. This raw solar irradiance data was then processed using the SoL model [73] to produce values for Watts generated per Watt of installed capacity. The SoL model encompasses the processing of irradiance data, decomposition and transposition of the irradiance onto the plane of the PV array, converting the incident irradiance to generated power from the array and inverter, and control of the resulting real and reactive AC power. There are a number of assumptions that have been made in the preparation of this dataset. These assumptions include that the PV arrays are North facing, that they have a tilt of 30°, and that the PV modules are sized to the inverter with no over sizing. Three sample days from this dataset are shown Figure 5.3. These show the per-unit PV generation across the day for a good clear sky day, a poor day with low levels of generation, and a day with highly variable generation.

In the case of a BESS such as a Tesla Powerwall, the fact that this PV data accounts for inverter efficiency is not an issue due to a Tesla Powerwall being an AC-coupled system. There are losses both in the PV inverter, which are accounted for in the PV data, and then also losses in the BESS rectifying and charging, which are accounted

for in the battery operation optimisation. For BESSs which are DC-coupled with PV generation, more careful consideration would need to be given to the data and models used.

As the chosen optimisation time step is 30 minutes but the PV dataset is at a 10 minute resolution, the PV data is downscaled to a resolution of 30 minutes. This is calculated such that the integrated energy over each half hour period is equal under both time resolutions.

5.1.3 Spot Price Data

Spot price data is obtained from the New Zealand Electricity Authority's Electricity Market Information (EMI) data source [74]. Half-hourly spot price data from the year 2012 is used in order to align with the household load and PV data.

The city of Christchurch is fed by two GXPs, Islington and Bromley. Islington is the larger of the two, with three times the capacity and measured demand of Bromley [75]. It is also often used as a reference node for the Mid-South Island region. For these reasons, spot price data for year of 2012 from the ISL2201 node is used in order to align temporally and spatially with the other data sources.

As was shown previously in Figure 4.2, there is significant volatility in the spot price. The distribution of this spot price data is showing as Figure 5.4. The long tail demonstrates the relative rarity of particularly high prices.

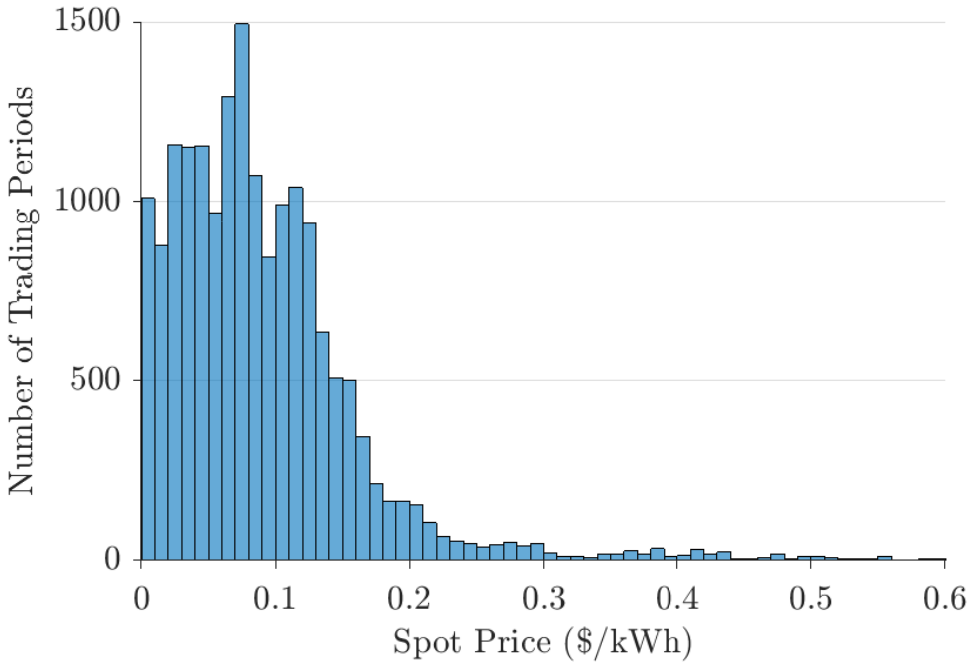

Figure 5.4 Distribution of half-hourly spot price at node ISL2201 for 2012.

Spot prices in New Zealand, with the large proportion of hydro generation, display different characteristics to those in a market dominated by thermal generation [76]. In New Zealand spot price is largely driven by seasonal variation in hydro reservoir storage levels. This results in seasonal pricing variations dependent on hydrological conditions. In general this means higher prices in the late winter, and lower prices in early summer. Thermal generation is used to maintain hydro storage levels, which is used to meet peaks in a low cost way. This means that spot prices are not strongly correlated with daily load peaks.

This lack of correlation is shown in Figure 5.5 which plots the aggregated demand from the household load dataset against the spot price for each half-hour of 2012. While there is a slight lower limit observable where the price is not typically below \$0.05/kWh for total demand greater than 4000 kW, there is such variation in the remainder that there is no clear relation between the two variables.

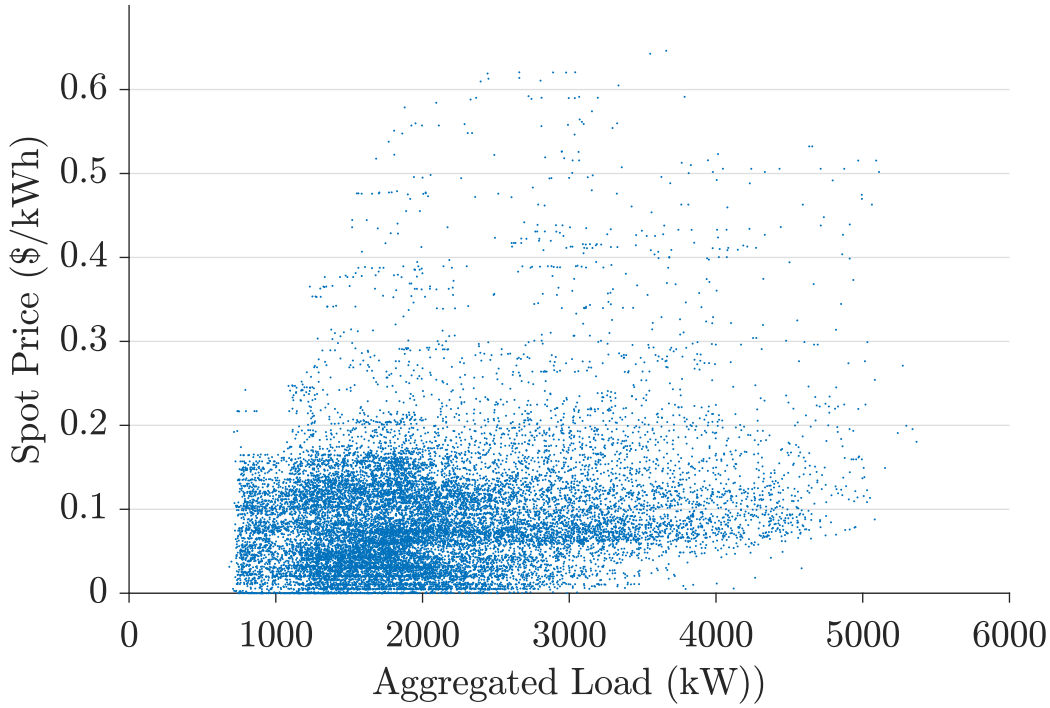

Figure 5.5 Correlation of aggregated residential demand to half-hourly spot price at node ISL2201 for 2012.

The operation of residential BESSs is more concerned with daily cycling and intra-day variations in pricing than long term seasonal variation. The correlation between daily peaks in price and daily peaks in residential load is assessed in Figure 5.6. A seven day moving average is taken of both aggregate load and spot price, and the difference between the value at each half-hour and the moving average at that half-hour is calculated. Positive values of load deviation indicate periods where load is above the average, while negative values indicate periods where load is below the average. The same applies to the price deviation. No clear relationship is observable; this shows that

there is little correlation between daily price peaks and daily residential load peaks.

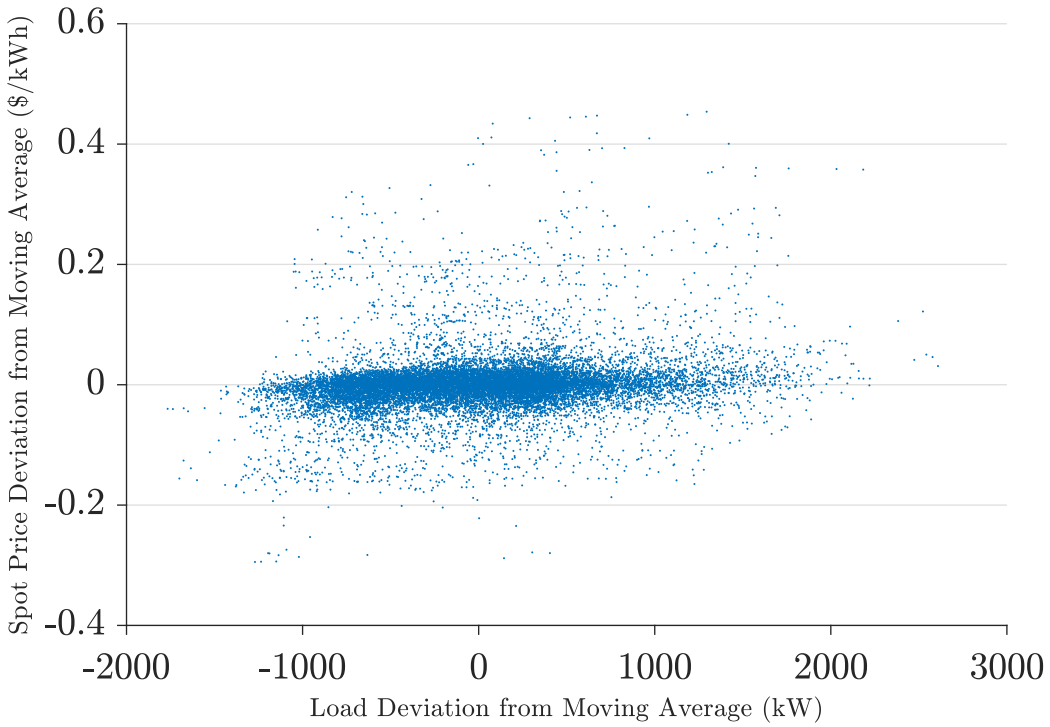

Figure 5.6 Correlation of aggregate load deviation from moving average to spot price deviation from moving average.

5.2 SOLVING OF MILP PROBLEM

This section presents detail of how the MILP problem is solved within a practical computation time. Data handling, pre-processing, MILP problem formulation, and result processing and storage are handled by MATLAB. The actual solving of the MILP problem is completed by IBM CPLEX, which is an advanced commercial optimisation solver [77]. CPLEX is used largely with its default configuration values. The relative gap tolerance is set to 0.2%. This means that the optimisation is stopped when a feasible integer solution is found that falls within 0.2% of the best bounding solution.

As discussed in Section 5.2.1, the MILP problems cover a period of 2 days (96 time steps). These have a typical computation time of less than one second, however there are a small number of cases that do not solve in such a short time. These cases comprise less than 1% of the total number of optimisations required for the complete 2212 households spanning an entire year. In these cases, where the solve time exceeds 15 seconds, the relative gap tolerance is expanded to 2%.

Table 5.1 Variation in computation time for different time spans.

Number of Days	Time for single problem(s)	Time to optimise entire year (s)
1	0.2	73
2	0.7	128
4	1.4	128
6	3.5	214
8	75	3431
10	103	3770
12	167	5090
14	306	8000
16	525	12000

5.2.1 Rolling Horizon Optimisation

The previously discussed LP and MILP problems have been formulated for the purpose of optimising battery system operation over an entire year. An entire year is necessary in order to fully capture the interplay of seasonal variations in PV generation and household loads. To optimise an entire year at the desired half-hour resolution presents a significant computational challenge. The time step chosen is 30 minutes, in order to match both the household load data and the trading periods of the New Zealand Electricity Market. This computational challenge is compounded by the desire for the optimisation to be repeated for more than two thousand individual households.

The computational challenge is a recognised problem in the MILP optimisation of energy systems, where both a short time period, to capture intra-day variation, and a long time span, to capture inter-day and seasonal variations, are needed. While an LP problem is a well understood and convex problem, adding integer constraints turns it non-convex and NP-hard [78]. The computational burden grows exponentially with the number of integer variables and rapidly becomes difficult to solve within a reasonable time [79]. The increasing computation time is highlighted in Table 5.1. This shows the variation in computation time depending on the number of days formulated into a single optimisation problem, as well as the time that would be required to optimise an entire year's battery operation at that rate. The computation time increases significantly as the problem size grows. It rapidly reaches a point where the computational burden is too great to be repeated for the 2212 households in the dataset utilised in this thesis.

[80] recognises that there are two commonly applied approaches to reducing the burden of a long time span energy system optimisation. The first is reducing the problem to only optimise for a series of typical days which are found with some clustering algorithm. The second common method is to use a rolling horizon approach to reduce the computational complexity. Instead of solving a complex problem considering the full time span, the problem is divided into smaller successive sub-problems which are more easily solved.

When dividing a longer time span into shorter sub-problems, the boundary between

these problems must be considered. As an example, take the constraint detailed in Section 3.2.1.3 where the BESS SOC at the end of the optimisation period must be equal to the SOC at the start of the optimisation period. If the optimisation period is reduced from the entire year to a series of single days, then there is a fixed point in the SOC profile every 24 hours. This can shift the battery behaviour from what its optimal operation would be given a longer time span. In the rolling horizon technique, each sub-interval comprises the time period to be solved, as well as an overhang which is discarded and then solved in the successive sub-problem. This distancing of the end constraint from the battery operation being saved serves to reduce its impact on the final combined results. The overhang prevents each consecutive sub-problem from being entirely independent of the others [81]. The battery SOC at the end of the saved period is used as the initial condition for the next successive sub-problem. This rolling horizon approach is illustrated in Figure 5.7.

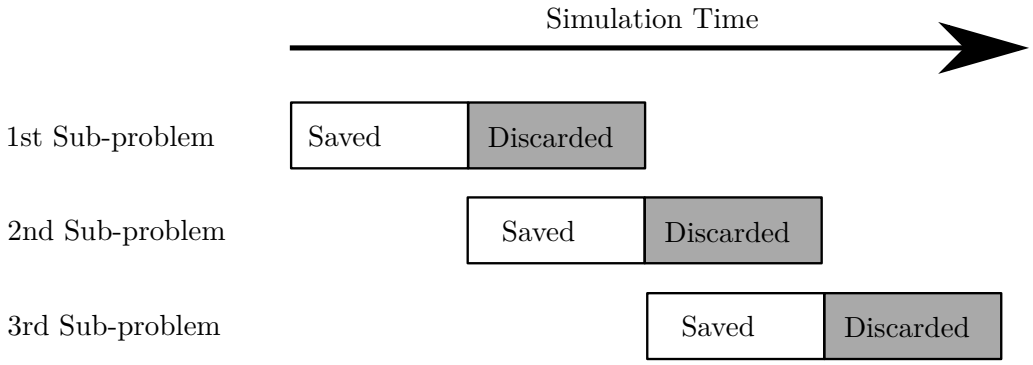

Figure 5.7 Simple diagram of rolling horizon technique.

For this thesis, each sub-problem is 2 days, or 96 half-hour trading periods, with the saved length being 1 day, or 48 trading periods. Optimising for a time span less than one day does not align well the the intended daily cycling of batteries, while increasing to longer time spans creates a significant computational challenge. While it is acknowledged that the MILP method is not a realistic implementable BESS control algorithm due to its perfect foresight nature, the use of this rolling horizon approach brings it closer in alignment to what a realistic method could be. The rolling horizon technique reduces the impact of the perfect foresight nature of the MILP method. Optimising an entire year as a single time span uses the full year-ahead household load and PV generation information. A year-ahead forecast of either of these is unrealistic, but by decomposing it into sub-problems, only 2-day-ahead household load and PV generation is needed.

5.3 IMPACTS OF EFFICIENCY MODEL ON BATTERY OPERATION

As presented in Chapter 3, two different efficiency models have been developed. The first has battery charge/discharge efficiency, and therefore losses, dependent entirely on battery charge/discharge rate. The second has a constant standing loss component alongside the rate dependent component. There are two aspects to be compared between the two models. The first is the effect they have on the battery operation obtained, and thus the load presented to the network. The second is the impact the efficiency model has on the financial result (objective value).

It was hypothesised that the difference between these models in terms of the objective value would be minimal as, though there is some variation between them, they are based on the same published manufacturer data. Conversely, the impact on the actual battery behaviour which leads to that objective function value could be significant. This is particularly important to understand because it is not just the financial results (objective function) that are of interest, but also the aggregated effect of battery behaviour on distribution system loads.

The impact of the efficiency model on battery behaviour when charging during an overnight low priced period is easily observable. Figure 5.8 shows the battery charge/discharge operation for a single household for a single day under a day/night pricing structure. The grey background indicates the low night pricing period. A positive power value represents battery charging and a negative value represents battery discharging.

Under the first efficiency model, the BESSs are incentivised to charge slowly across a longer time period in order to reduce losses. While under the second efficiency model, batteries are incentivised to charge at a more efficient, higher rate for a shorter period of time. It is seen that under the first efficiency model, charging during the night period is of a lower magnitude and longer duration than under the second efficiency model.

This highlights that the battery operation obtained with the LP/MILP methods shows a significant sensitivity to the efficiency model used. While the difference in energy cost to the household between the two efficiency models is 1.5% in this example, when the effects are examined more widely it becomes apparent that the effect on the financial results achieved by the optimisation are more than minor. Figure 5.9 shows the difference in the achieved annual electricity bill for a sample of 100 households under the two efficiency models.

This difference is attributed to the assumptions made in choosing the values for the efficiency models (Section 3.1.1). In general, the battery charge/discharge operations observed are less than the 3.3 kW value of greatest efficiency. This makes the second model consistently less efficient than the first, producing a difference in the financial

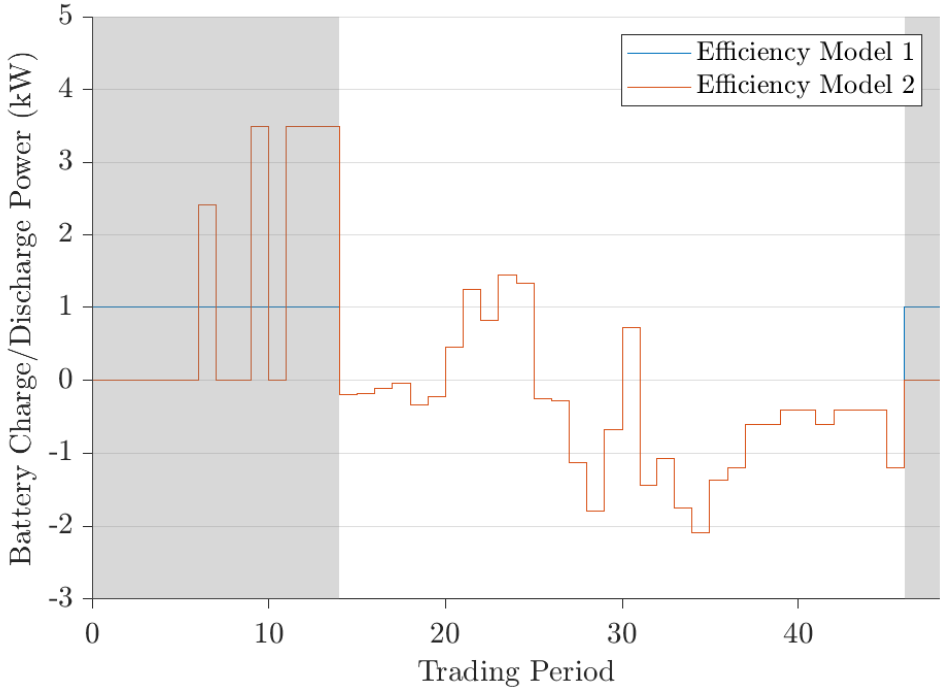

Figure 5.8 Variation in battery charge/discharge operation for a single household and single day under the two efficiency models.

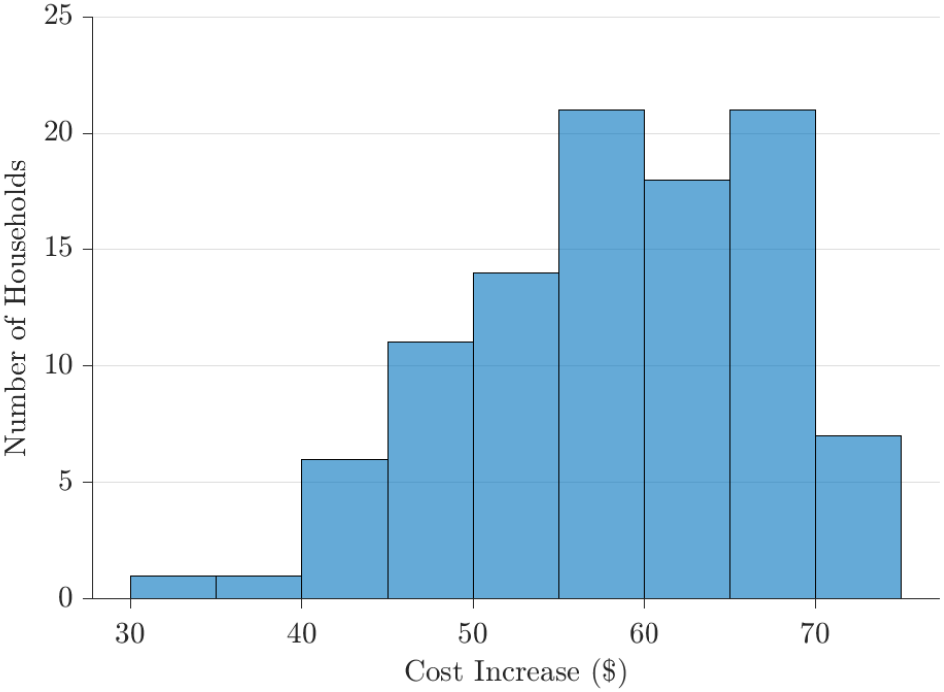

Figure 5.9 Increase to annual electricity bill from efficiency model 1 to efficiency model 2 for 100 households.

results achieved by the optimisation method. As noted in Section 3.1.1, the assumptions which lead to the efficiency values used are unverified, but appear plausible. Nevertheless, the sensitivity of the results to the efficiency values used is demonstrated.

Not only does the difference between the two models cause changes in the battery operation, but the actual values used for the efficiency curves have a direct effect on battery behaviour during periods when there is increased freedom of battery operation. During low priced grid charging operations, the charge rate under both models is affected by the efficiency model. When considering the aggregated effect of BESSs on the peak loads experienced by distribution networks, it is important that the charging operation of these systems during low price periods is understood and modelled.

Chapter 6

RESULTS

In this chapter, three different pricing cases are presented to illustrate the use of the modelling methodologies and highlight the metrics by which the results are analysed.

Between differing distribution charges amongst the 27 EDBs in New Zealand and the many electricity retailers, there are hundreds, if not thousands, of potential pricing structures that residential consumers could be subject to. The widespread nature of advanced metering infrastructure in New Zealand allows for time varying tariff structures from basic day/night pricing through to half-hourly spot pricing [82]. These pricing structures can be broadly divided into either known pricing, or unknown pricing. Known pricing refers to a fixed pricing structure where the price is known ahead of time. This is sometimes known as a fixed price variable volume tariff. Unknown pricing refers to pricing that varies in real time. This could be varying with the spot market or as a factor of load or some other metric.

The first case chosen is a simple day/night pricing structure, which represents an example of known pricing. The second case utilises spot price as an example of unknown pricing. The third presents a peak/shoulder/off-peak pricing structure. This is a structure which has been discussed widely in the New Zealand market as a method of delivering more cost-reflective distribution pricing and has seen some uptake [83]. Additionally, it is expected that this pricing structure could improve the network peak load reductions from BESSs due to shortening the time period at which battery discharge is optimal compared to the day/night case.

These three pricing cases have a number of parameters which are held constant. These are shown in Table 6.1.

Table 6.1 Inputs common to all three pricing structures.

Variable	Value
PV system size	3.5 kW
Maximum charge/discharge rate	5 kW
Maximum SOC	13.5 kWh
Minimum SOC	0 kWh
Battery efficiency	Efficiency model 2 (Section 3.1.1.2)
Fixed charge rate for grid charging[1]	1 kW

The PV system size is chosen as 3.5 kW based on data published by the New Zealand Electricity Authority. Over the period of August 2013 to December 2019, the average capacity of a residential PV installation in New Zealand has fluctuated between 3.4 kW and 3.8 kW, with a mean value of 3.5 kW [84]. The battery parameters are based upon the second generation Tesla Powerwall system, which has a usable storage capacity of 13.5 kWh and a continuous power rating of 5 kW [9]. The Tesla Powerwall is chosen as it is one of the best known home BESSs products in the market.

6.1 CASE 1 - KNOWN PRICING

The first pricing structure is used to demonstrate the application of the methodologies to a pricing structure in which prices are fixed and known ahead of time. In this case a day/night tariff is used. The parameters specific to this case are shown in Table 6.2. The pricing parameters are based on a plan published by electricity retailer Meridian Energy in February 2018 as an example of a day/night tariff available in Canterbury, New Zealand.

Table 6.2 Case 1 - Known Pricing Inputs.

Variable	Value
Day import price	27 c/kWh
Night import price	11 c/kWh
Export price	8 c/kWh
Night rate period	11pm-7am

In the following sections, the results of this pricing case are analysed and presented. These include financial results for households and the effect on the aggregate load experienced by the networks, as well as an exploration of the capability of the BESSs to provide reductions to peak loads.

[1] Applicable to rule-based method only

6.1.1 MILP Optimisation Method

The input parameters from Table 6.1 and Table 6.2 are applied to the MILP optimisation method covered in Chapter 3. This section presents the output of the MILP optimisation method, including both the financial benefits to households and the aggregated load effects. This represents a one-day-ahead perfect foresight optimisation and indicates the best savings that could be achieved without any consumer driven load shifting.

6.1.1.1 Household Benefits

This first set of results examine the financial benefits of the PV and battery systems to households. This analysis of the financial benefits considers only the impact of the PV generation and BESSs on the energy component of the household's electricity bill; it does not consider the CAPEX or OPEX associated with these systems. BESSs are largely seen as an addition to a PV generation system and not something to be installed stand-alone.

Distributions of the household annual energy costs for three scenarios are presented in Figures 6.1 to 6.3. The first plot shows the annual energy cost of just the household load, the second adds PV generation to the household load, and the third adds a battery system alongside the PV generation.

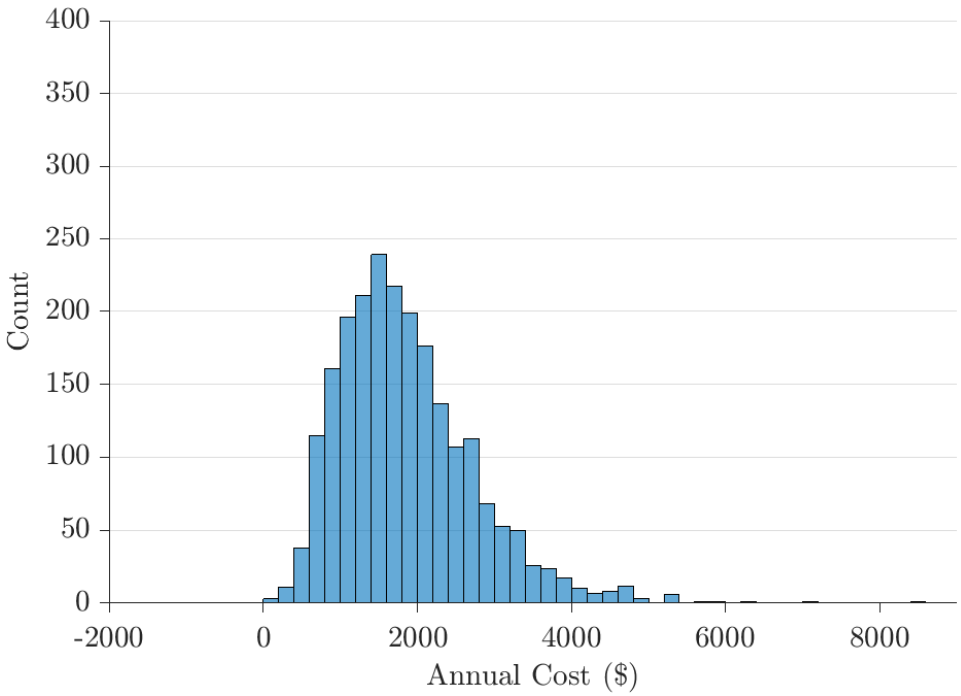

Figure 6.1 Distribution of annual household energy cost incorporating only household load.

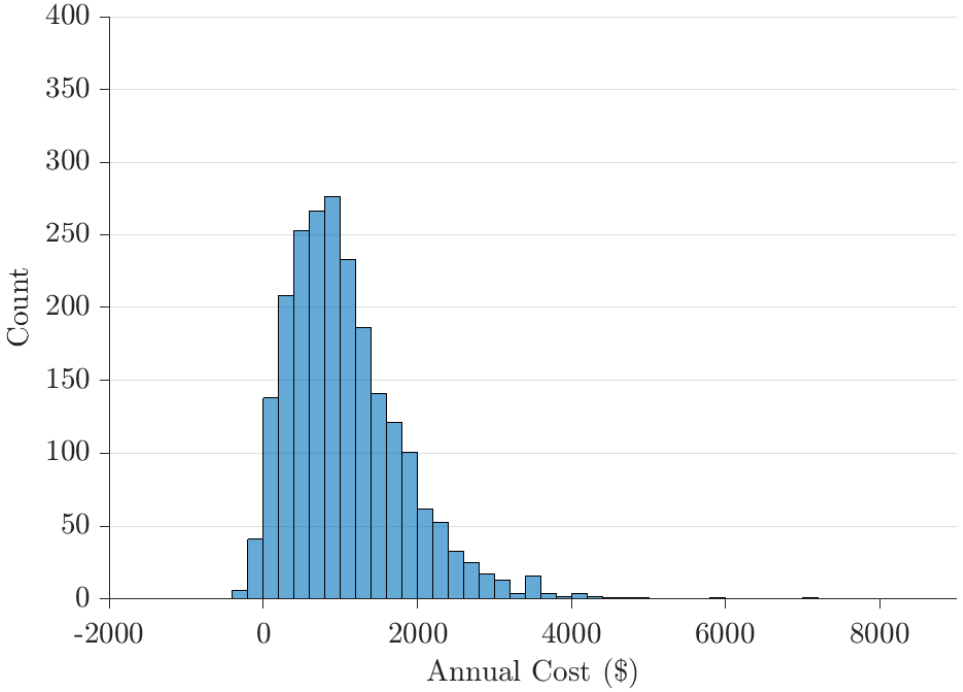

Figure 6.2 Distribution of annual household energy cost incorporating household load and PV generation.

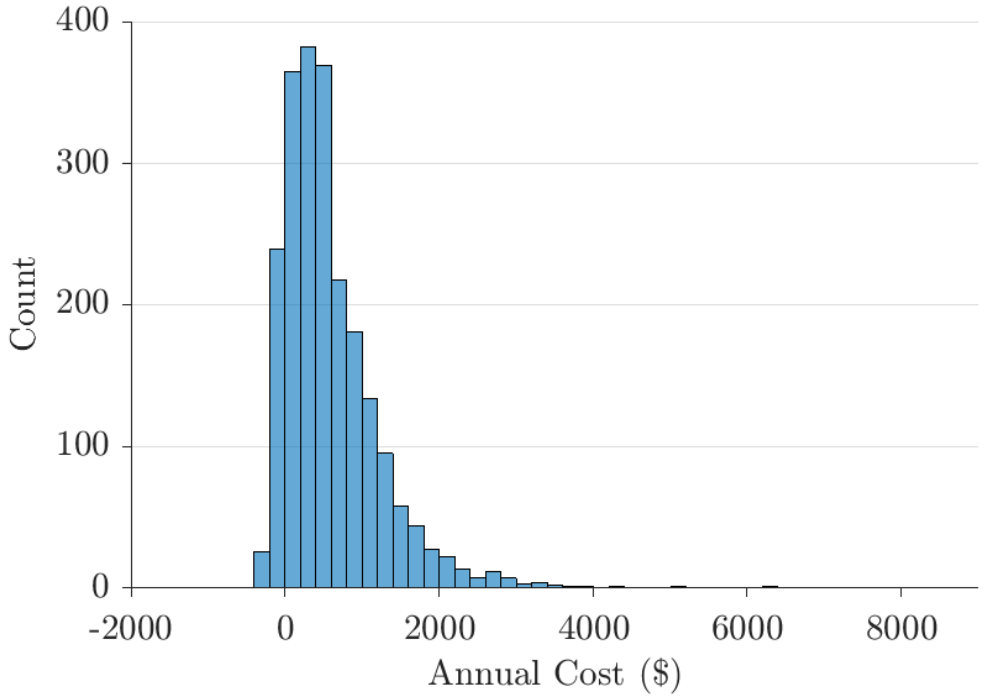

Figure 6.3 Distribution of annual household energy cost incorporating household load, PV generation, and battery storage systems.

These results are summarised and compared in Figure 6.4 which shows the cost distribution for the three scenarios. It can be seen that the annual energy costs decrease with the addition of PV generation, and then decrease further with the addition of the BESS.

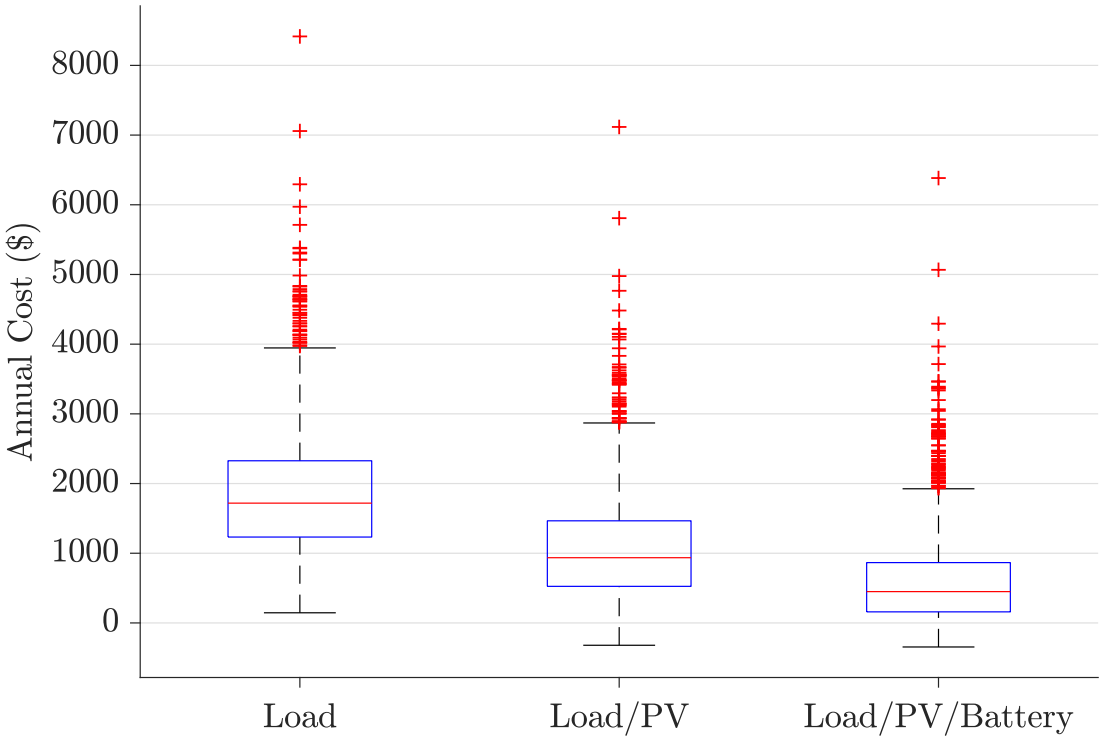

Figure 6.4 Distributions of annual household energy costs under different scenarios. The extent of the box represents the 25th percentile (q_1) and 75th percentile (q_3). The maximum bounds of the whiskers are calculated as $q_3 + 1.5(q_3 - q_1)$ and $q_1 - 1.5(q_3 - q_1)$. Any values exceeding the whisker maximum bounds are plotted as outliers.

A consumer considering investment in PV and battery systems is primarily concerned with the financial savings these will bring: firstly the financial savings that can be achieved by installing the PV generation, and secondly the savings that are achieved by adding a battery storage system. The incremental savings of going from a traditional load only household, to a household with PV generation system, to a household with PV generation and battery storage are plotted in Figure 6.5.

The median annual saving from the installation of PV is $780, or a saving of 55% of the annual energy cost. Installation of a battery system results in a further median annual saving of $500. It can be seen from these results that the savings obtained through installation of PV generation are greater than those achieved by adding a battery system to an existing PV installation.

It should also be noted that there are some households in the dataset which achieve close to no financial benefit from the installation of a battery system alongside their PV generation. Further investigation into these cases shows that these are households in the dataset with very low total annual energy consumption. With such low levels of

load, PV generation nearly always exceeds household load and thus is exported. Given that the pricing structure features a constant price for electricity exported to the grid, there is little financial benefit from a battery storage system.

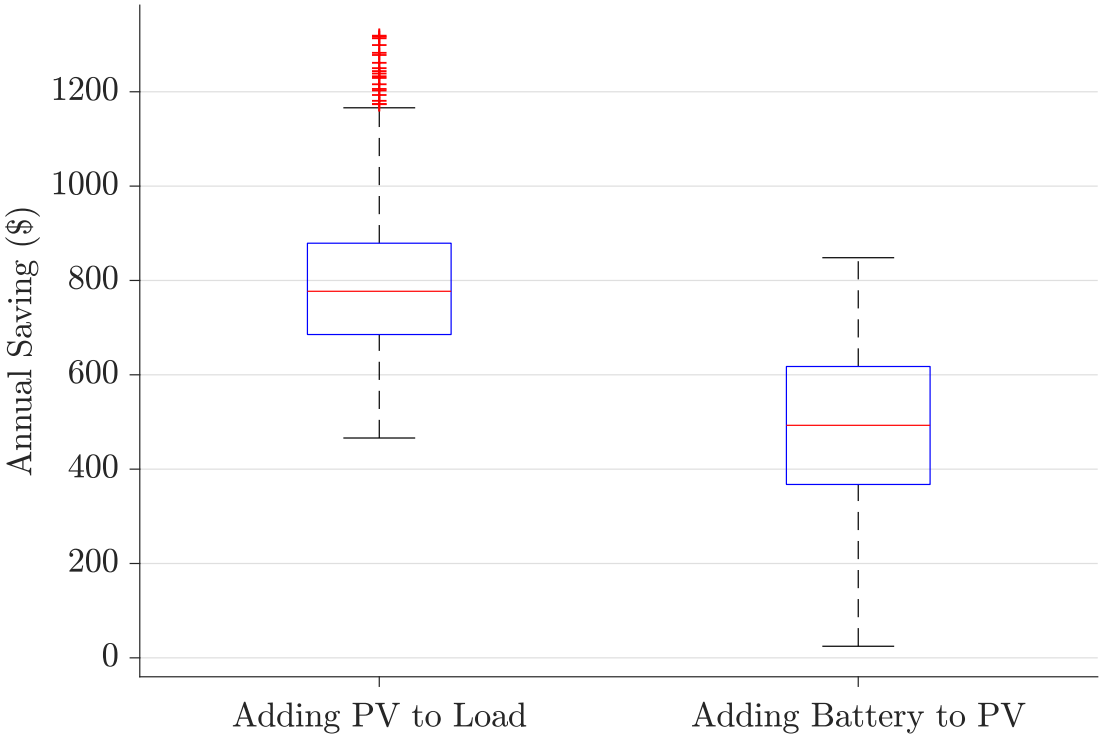

Figure 6.5 Distributions of annual household savings achieved through the installation of new technologies.

Electric heating is present in 80% of private dwellings in New Zealand which makes it the most popular form of space heating [85]. Considering this prevalence of electric heating, as well as decreased PV generation during winter, it is expected that daily energy costs will peak in winter and PV generation will contribute less to reducing this than it might during the summer period. This is observed in Figure 6.6, which shows the mean daily household energy cost across the year - both the raw daily energy cost, as well as a smoothed trace. Note that with New Zealand being in the Southern Hemisphere the winter season is in the middle of the year, between June and August.

The underlying household load case, in blue, shows a clear increase in cost (directly related to energy volume) during the winter period. When PV is introduced (orange trace), there are three observations to be made. The first is that volatility increases substantially as a result of variations in PV generation combined with the variations in household consumption. The second is that the mean daily cost decreases across the year. The third is that the reduction in mean daily cost is significantly less during winter. With the addition of the battery storage system, the mean daily cost reduces further, as expected.

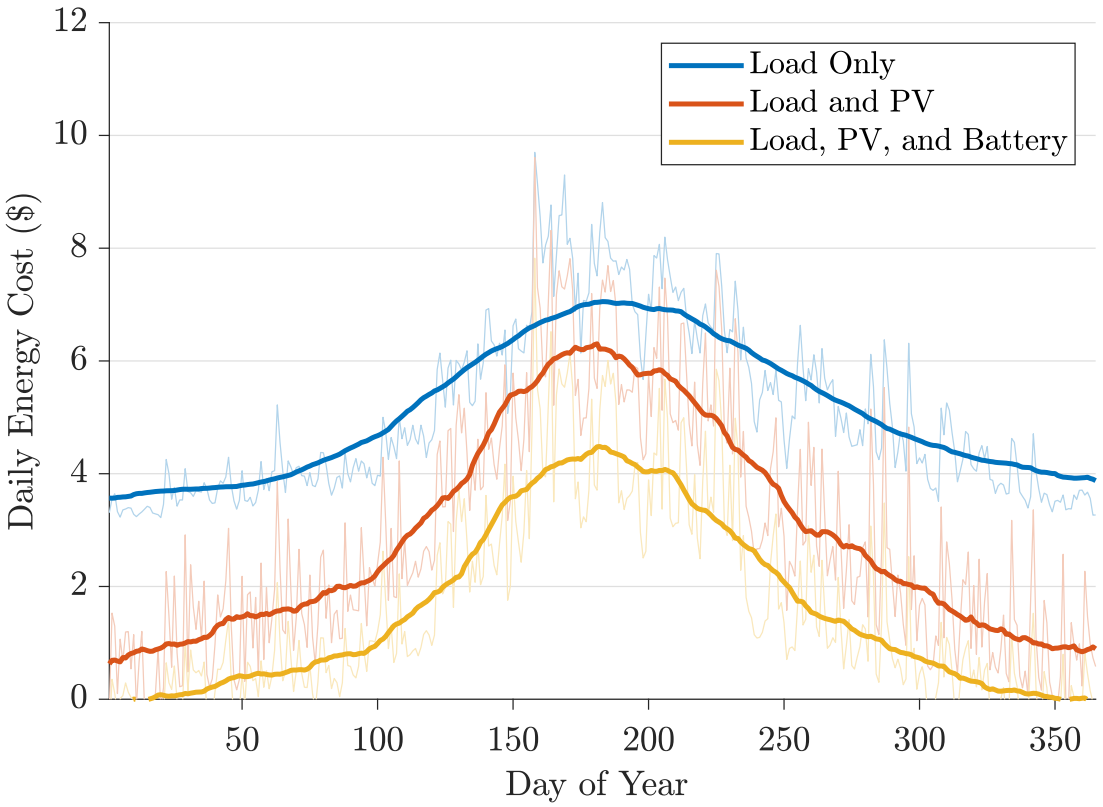

Figure 6.6 Mean daily household energy cost across the year under different scenarios.

6.1.1.2 Network Effects

This section presents results on the network effects of the MILP model under day/night pricing. In particular, the effect of PV and battery systems on network peak loads at different penetration levels is examined.

At penetration levels less than 100%, the allocation of PV and battery systems to households introduces an element of uncertainty. To quantify this, the random allocation of systems to households is repeated a number of times to produce a distribution of results. In this situation, the allocation of systems to households is repeated 500 times and the top 100 aggregate load periods are identified for each allocation. This yields 500 distributions of 100 points each for each penetration level. It is important to describe the spread of these distributions and the significance of the impact of a particular allocation on the results. A method is needed to compare these distributions and identify if there is significant variation between them. Analysis of peak reduction capabilities is simplified if a single allocation of systems to households can be used.

One method for comparing the similarity between two distributions is the two sample Kolmogorov-Smirnov test [86]. This test has the benefit of being non-parametric and distribution free. This generality means that it can be applied to data irrespective of its underlying distribution, unlike many other statistical tests which require the data to be normally distributed. The two sample Kolmogorov-Smirnov test is a test of whether

Table 6.3 Number of random allocations for which the null hypothesis is rejected by the Kolmogorov-Smirnov test with 5% significance level for allocations with the minimum null hypothesis rejections.

	Penetration level										
Number of households	**5%**	**10%**	**15%**	**20%**	**25%**	**30%**	**35%**	**40%**	**45%**	**50%**	**75%**
50	4	40	35	50	85	125	133	138	123	131	40
100	0	2	6	13	32	76	109	118	94	89	30
200	0	0	0	1	8	37	52	54	42	37	0
400	0	0	0	0	1	4	10	9	8	9	0
600	0	0	0	0	0	0	0	0	0	0	0
800	0	0	0	0	0	0	0	0	0	0	0
1600	0	0	0	0	0	0	0	0	0	0	0
2212	0	0	0	0	0	0	0	0	0	0	0

two samples are likely to be from the same, not necessarily known, probability density function, which is the null hypothesis (H_0), or different probability density functions which is the alternative hypothesis (H_1). This test is implemented by performing a calculation on the samples to produce a real scalar statistic, D, which is compared against a published critical value. This critical value is a function of both the desired confidence level and the sample size [87]. To find the test statistic, D, given the two cumulative distribution functions of the samples, $F_{n1}(x)$ and $F_{n2}(x)$, the maximum absolute difference between them across all values of x is found:

$$D = \max_x(|\hat{F}_1(x) - \hat{F}_2(x)|). \tag{6.1}$$

For a specified significance value and sample size, a critical value D_{crit} is defined for which the null hypothesis (that the two samples are from the same distribution) is rejected if $D > D_{crit}$ [87].

In this case, however, there are not two samples but instead 500. Later results, looking at the ability of BESSs to provide peak reduction services, are computationally intensive and it would be prohibitively time consuming to repeat these calculations for large numbers of allocations of systems to households. It is necessary to understand the impacts of network size and penetration level on the variation of these distributions of peaks.

In order to do this, the allocation which is most reflective of all 500 allocations is found. To do this, each allocation has the Kolmogorov-Smirnov test performed against each other allocation. From this, the allocation which has the fewest rejections of the null hypothesis is identified. This is the allocation of systems to households that produces aggregate load peaks significantly different to the least number of other random allocations. For this chosen best allocation, the number of random allocations for which the null hypothesis is rejected (at a 5% significance level) is shown in Table 6.3.

It can be seen that with a sample size of 600 or greater, there is sufficient diversity such that a random allocation of PV generation and BESSs to households can be found which is representative of all 500 random allocations, as determined by the Kolmogorov-

Smirnov test to a 5% significance level. However, distribution networks commonly have fewer than 100 households. A typical low voltage (LV) urban network in the Canterbury region has 68 residential loads [88]. While choosing the most representative allocation may work for aggregation at the medium voltage (MV) network level, for the smaller LV networks , it is difficult to achieve a truly representative single allocation of PV and battery systems. If analysis of small network sizes is desired, then a statistical approach would need to be taken to capture the range of potential peak load impacts.

Continuing to assess the impact of BESSs on peak aggregate loads, it is necessary to examine how peaks may change from a growing penetration of PV and battery systems. Figure 6.7 shows the distributions of the single greatest half hourly load from the aggregated dataset of 2212 households across the entire year. Note that penetration levels of 0% and 100% are entirely deterministic and a single value is plotted rather than a distribution. It is seen that penetration levels of up to 20% of households having PV and battery systems causes a reduction in the peak aggregate load experienced by the network. At a penetration level of 25% and above, the single peak load experienced by the network in the year begins to increase. By 40%, it has exceeded the peak load of the 0% penetration base case.

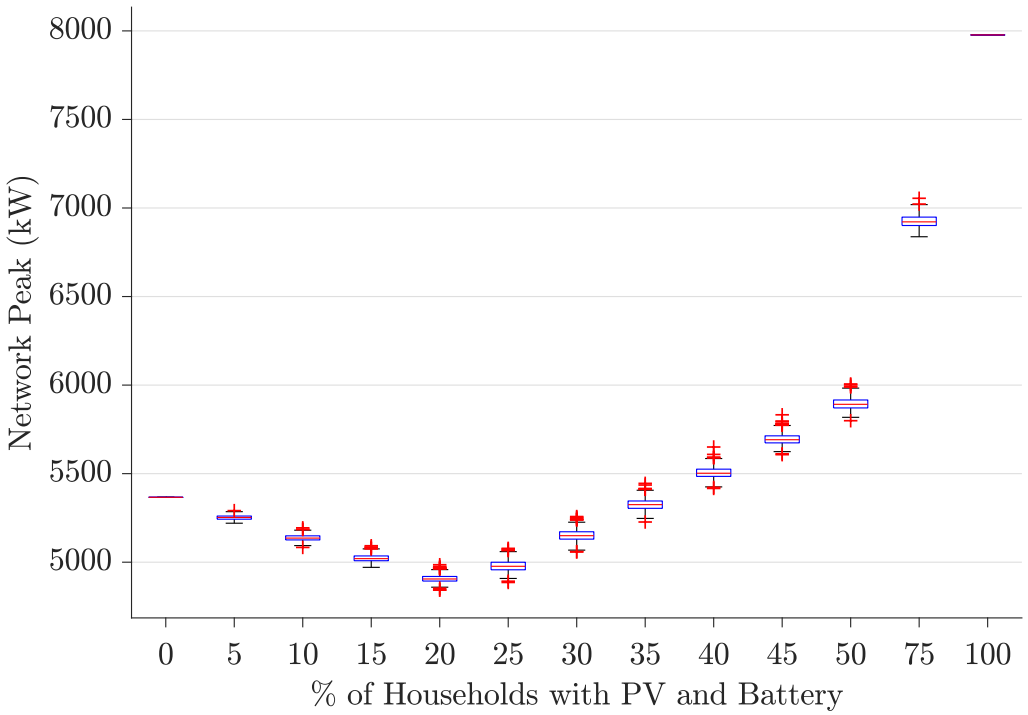

Figure 6.7 Distributions of single largest half-hourly aggregate load for differing penetration levels of PV and battery technology.

Figure 6.8 shows the distributions of the reductions to the top 100 load peaks experienced by the network as the penetration level increases. As the penetration

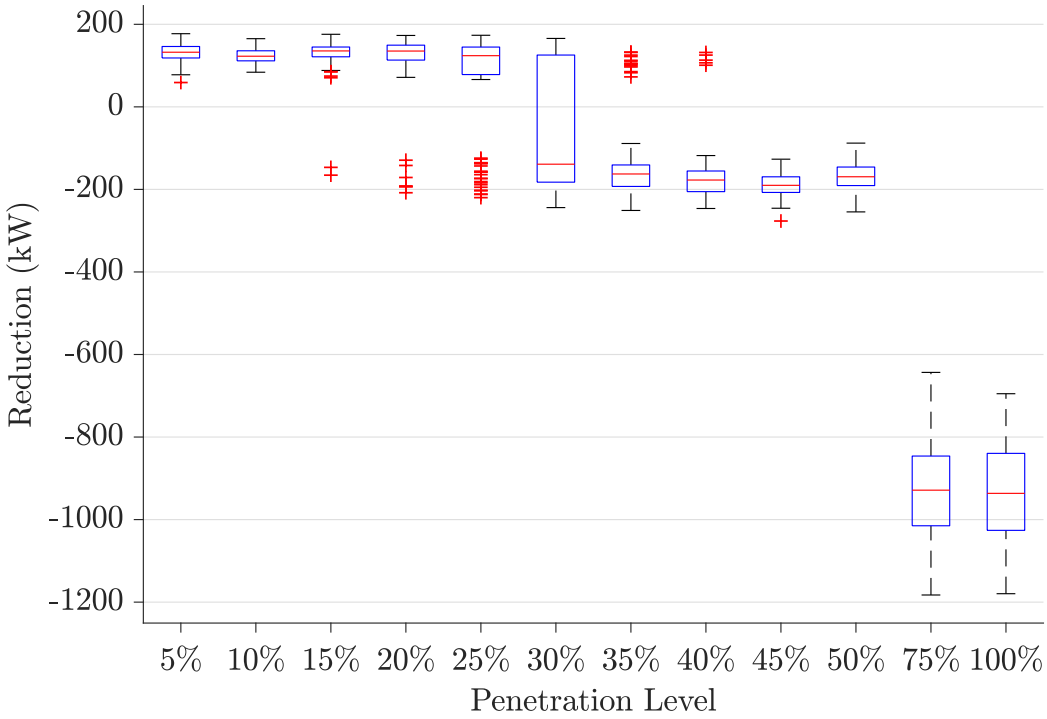

Figure 6.8 Incremental peak reduction from natural battery behaviour.

level increases, where the peaks occur also shifts. For this reason, the reductions are calculated from the top 100 peaks of the previous penetration level. This enables an understanding of the penetration levels which serve to decrease the peak loads experienced by a network, and the penetration at which the BESSs begin to cause an increase in peak loads. A cumulative allocation of systems to households is used. This means that as the penetration increases it is only the additional households that are randomly sampled. Households that have already had a BESS allocated retain that system. The cumulative allocation, rather than fully random allocation at each penetration level, is important to reflect reality. Households with BESSs retain them and new households are added as penetration grows. Failure to account for this results in impractical results where growing penetration levels can result in apparent slight increases in peak loads due to variation in households' loads. The results presented here are for a network with the full data set of 2212 households.

At penetration levels from 5% through to 25% there is largely a reduction across all 100 of the measured peaks; that is to say that the growing penetration level causes a decrease in the peak loads. Beginning at 15%, there are a small number of outlying data points where the increasing penetration level causes an increase in a small number of those top 100 peaks. As the penetration level increases further, these cases where the increasing penetration causes an increase in peak loads become the majority.

It is not only the magnitude of system peaks that is of interest, but also their timing. It is an exploration of this timing that provides the explanation for this observed

increase in system peak load.

Figure 6.9 shows the distribution of the top 100 annual loads that result from one specific allocation of systems to households. These 100 peaks are grouped by the month in which they occur. As would be expected, these top 100 half hourly loads occur during winter months at all penetration levels.

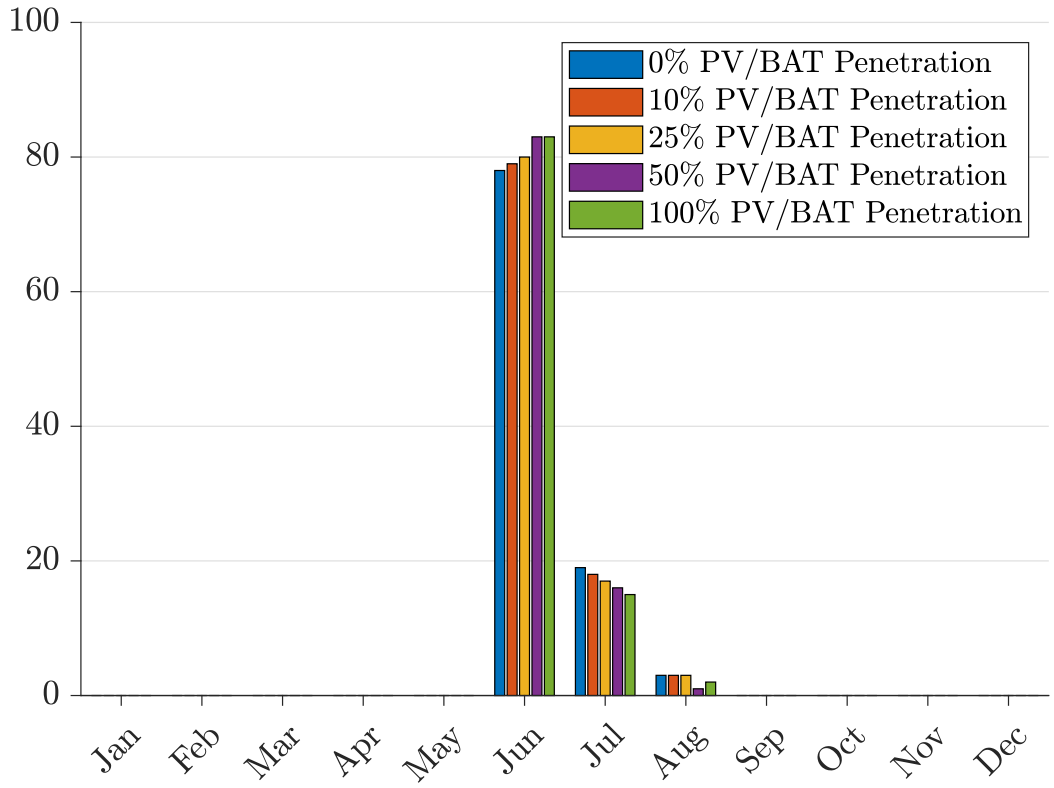

Figure 6.9 Number of top 100 half-hourly network aggregated loads occurring by month under different penetration levels.

Figure 6.10 clarifies the maximum system load increases between a penetration level of 25% and 50%. This plot takes the same 100 peak half hours from Figure 6.9 and groups them by time of day rather than month. The New Zealand electricity system is a winter evening peaking system and, as expected the peaks in the "household load only" data generally occur during trading periods 35 to 40, which correlates to 6:00pm-9:00pm. This pattern remains similar for low penetration levels, however at 25% penetration there is a change. At 25% penetration it is observed that these peak half hours are split between the traditional evening period of 6:00pm - 9:00pm, and also 11:00pm - 12:00am, and 6:00am - 7:00am.

These new time periods correlate to the start and end of the low night tariff period. The traditional load peaks have been surpassed by battery charging during low priced periods. It is an artefact of the MILP solver that these are clustered around the start and end of that low tariff period. In reality, there is no financial benefit to the consumer whether that battery begins charging when the low price period begins at 11:00pm, or

whether it begins later in the night, as long as it has reached the desired state of charge by the end of the low price period. As previously discussed in Section 3.1.1, the efficiency model used in the MILP optimisation has a peak charging efficiency at a charge rate of 3.3 kW. This charge rate would completely charge the battery in approximately 4 hours, so there is the potential for a control algorithm to shift charging within the 8 hour low price period to create a better diversity of charging load presented to the network with minimal impact on the consumers. These results do, however, serve to illustrate that at high penetration levels with uncoordinated or uncontrolled charging, battery systems have the potential to increase network peak loads rather than provide any of the desired peak reduction benefits.

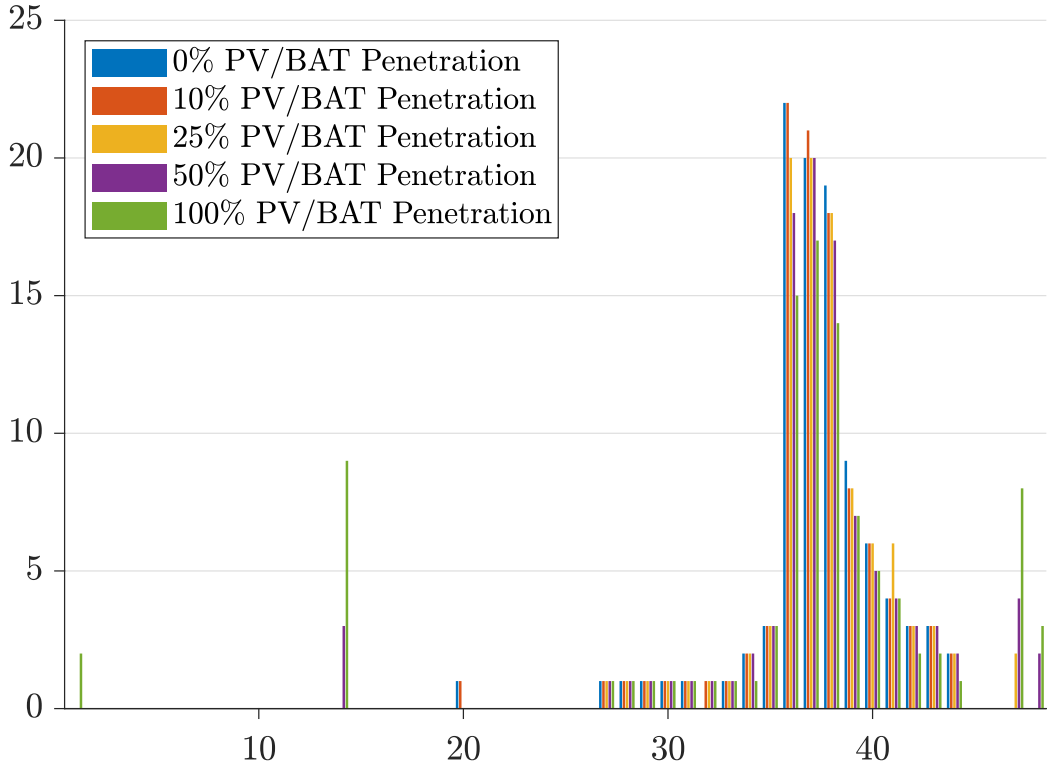

Figure 6.10 Number of top 100 half-hourly network aggregated loads occurring in a trading period under different penetration levels, demonstrating a shift of the peaks to low priced overnight period.

6.1.2 Rule-based

This section presents the results for the same pricing case (Section 6.1) but applying the rule-based methodology and compares the results with those from the MILP method. This provides a more realistic assessment of consumer benefits and network effects, as perfect foresight is not achievable.

The distributions of annual costs with just load and PV are not repeated, as they are unchanged from those previously shown (Section 6.1.1.1). Figure 6.11 presents the distribution of annual household energy costs with load, PV, and battery storage

included.

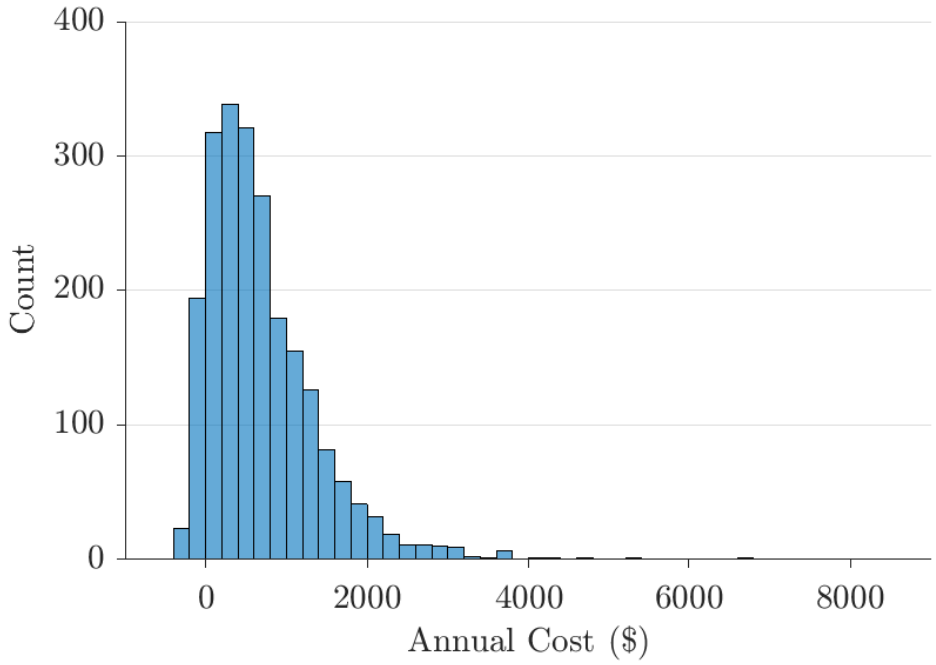

Figure 6.11 Distribution of annual household energy cost with PV and batteries under the rule-based control method.

As can be observed in Figure 6.12, the rule-based method yields slightly higher household annual energy costs than the MILP method with its inherent perfect foresight. That is to say, the results are as expected where the rule-based method is slightly sub-optimal.

This slight sub-optimality of the rule-based method can also be observed in Figure 6.13, where the mean daily energy cost under the rule-based method is seen to be above that of the MILP method.

Figure 6.14 shows the distribution of percentage decrease in annual savings between the MILP method and the rule-based method as a measure of how close to optimal the rule-based method results are. This is calculated as the saving under the MILP method less the saving under the rule-based method divided by the saving under the MILP method. The median difference in savings is 8%, which seems reasonable going from a case where there is perfect foresight of both load and PV generation, to a case where load is unknown and PV is a coarse forecast. It would also be expected that a commercial battery system controller could add more intelligence to the rules used, however this serves to show that a simple set of rules achieves close to the optimal result.

As with the MILP method, another area of interest is the effect of increasing penetration levels on the load peaks experienced by the distribution network. As before, the variation in top 100 peak loads is assessed with various random allocations of PV

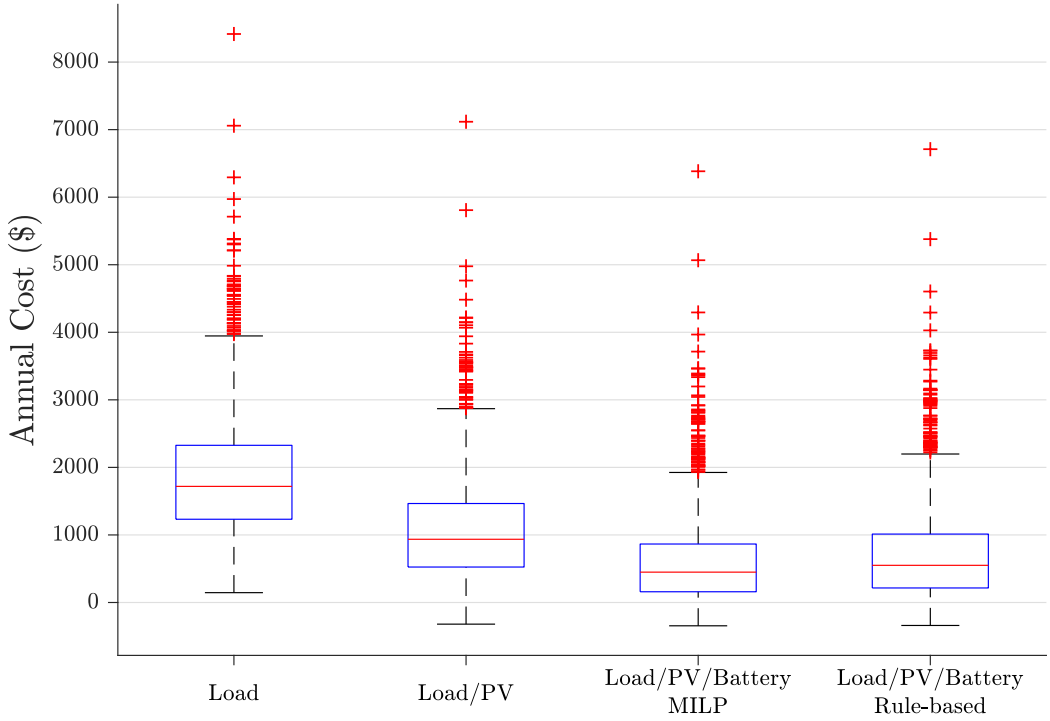

Figure 6.12 Distribution of annual household energy costs under different scenarios and both battery control methods.

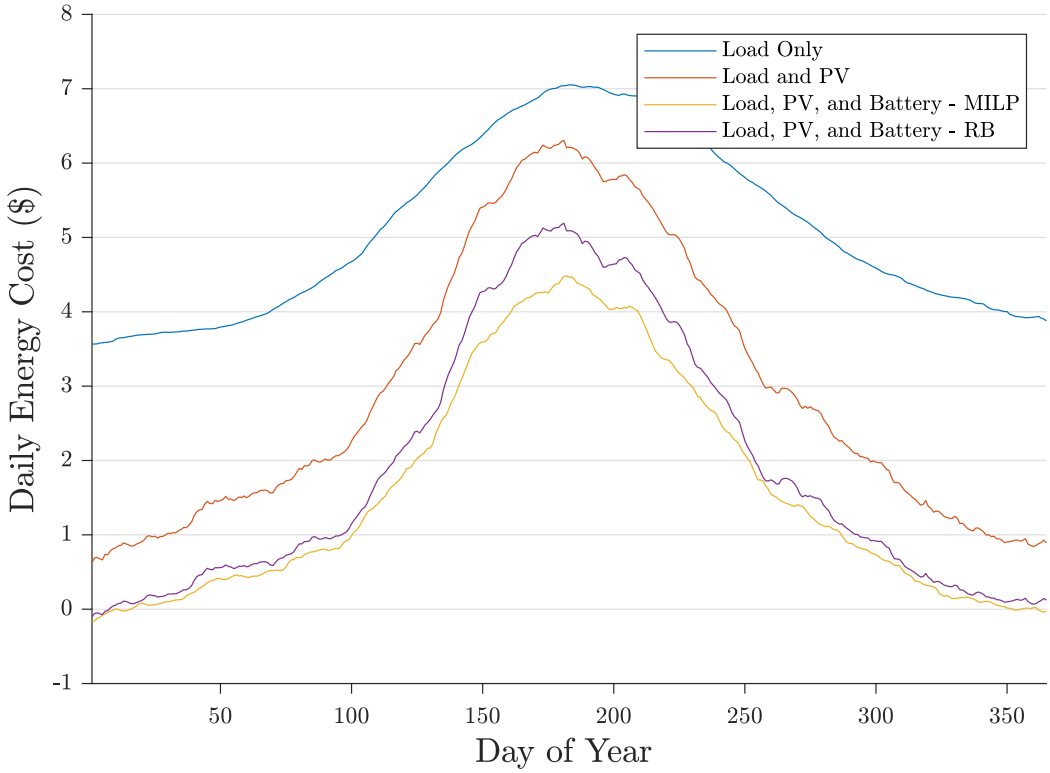

Figure 6.13 Smoothed mean daily energy cost across the year under different scenarios including rule-based control.

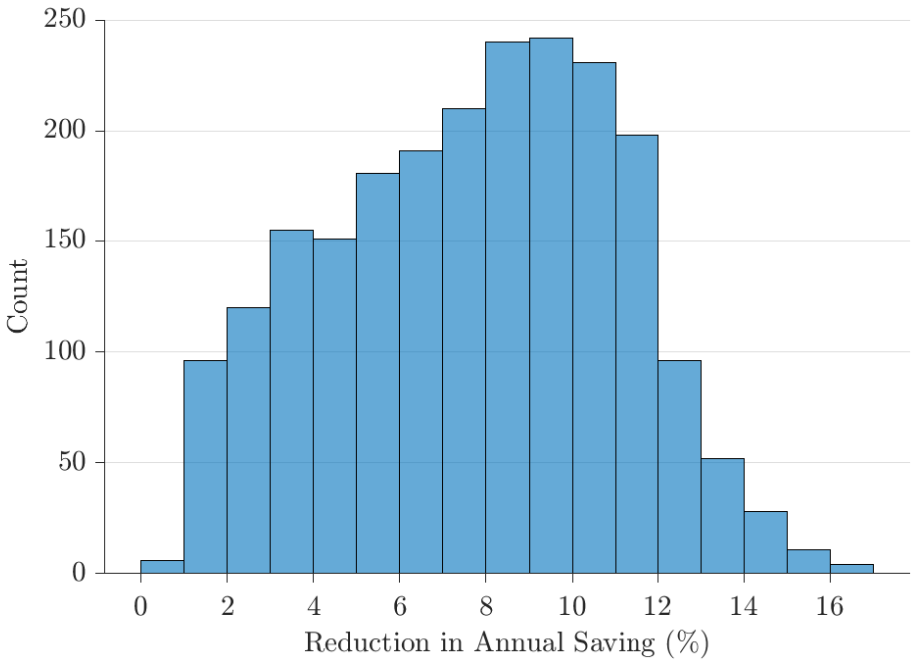

Figure 6.14 Percentage decrease in annual saving from perfect foresight MILP to rule-based control.

Table 6.4 Number of random allocations for which the null hypothesis is rejected by the Kolmogorov-Smirnov test with 5% significance level for the allocation with the minimum null hypothesis rejections.

	Penetration Level										
Number of Households	**5%**	**10%**	**15%**	**20%**	**25%**	**30%**	**35%**	**40%**	**45%**	**50%**	**75%**
50	0	0	0	0	0	0	0	0	0	0	1
100	0	0	0	0	0	0	0	0	1	0	0
200	0	0	0	0	0	0	0	0	0	0	0
400	0	0	0	0	0	0	0	0	0	0	0
600	0	0	0	0	0	0	0	0	0	0	0
800	0	0	0	0	0	0	0	0	0	0	0
1600	0	0	0	0	0	0	0	0	0	0	0
2212	0	0	0	0	0	0	0	0	0	0	0

and BESSs to households. The assessment methodology, using the Kolmogorov-Smirnov test, remains the same as previously discussed for the MILP case (Section 6.1.1.2). The results of this are shown in Table 6.4.

There are only two combinations of sample size and penetration level in which the most representative random allocation causes the null hypothesis to be rejected at the 5% significance level for any of the 499 other random allocations. In these two combinations, there is only one rejection. To be clear, in each combination of penetration level and sample size, there are distributions of top 100 network peaks which are statistically significantly different from each other. For all but two combinations, however, there exists at least one random allocation which produces a distribution of top 100 peaks loads that is not significantly different from all 499 other random allocations. This is chosen as the representative allocation and used in further analysis.

These Kolmogorov-Smirnov results differ significantly from those in the MILP case and show that there is less variability in the effect on network peak loads dependent on system allocation in the rule-based method. This aligns with all households following the same rules, and so there is less variance in battery behaviour between households when compared with the perfect foresight MILP method.

The effect of varying penetration rates on the annual highest peak load is shown in Figure 6.15. In comparison to the MILP control method (Figure 6.7), it is seen that the increase in peak load at 50% penetration is a decrease under the rule-based method, and at 100% penetration the increase is of a much smaller magnitude. This is due to the decreased low price charge rate. In the MILP case, when charging from the grid during low priced periods, the batteries will charge at their most efficient charge rate (3.3 kW), which creates significant network load. Under the rule-based method, the grid charge rate was set at 1 kW, which significantly lowers the grid impact.

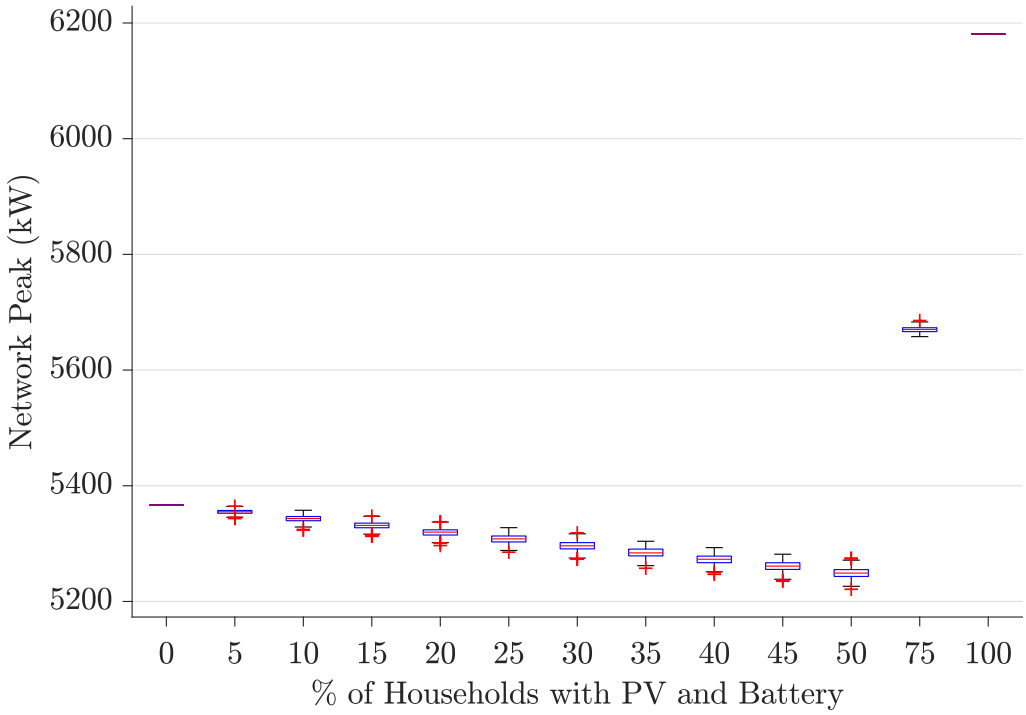

Figure 6.15 Distributions of single greatest aggregate load for all 2212 households with 500 allocations of systems to households at each penetration level.

Also of interest is not what a certain penetration of BESSs will do to the peak loads experienced by a network without BESSs, but instead the incremental changes in peak loads as penetration levels gradually increase. This incremental impact of network peak loads is shown in Figure 6.16.

At low penetration levels, it is seen that the peak reduction is at or very near zero, for half of the identified peaks. Beginning at a penetration of 25%, there are one or two

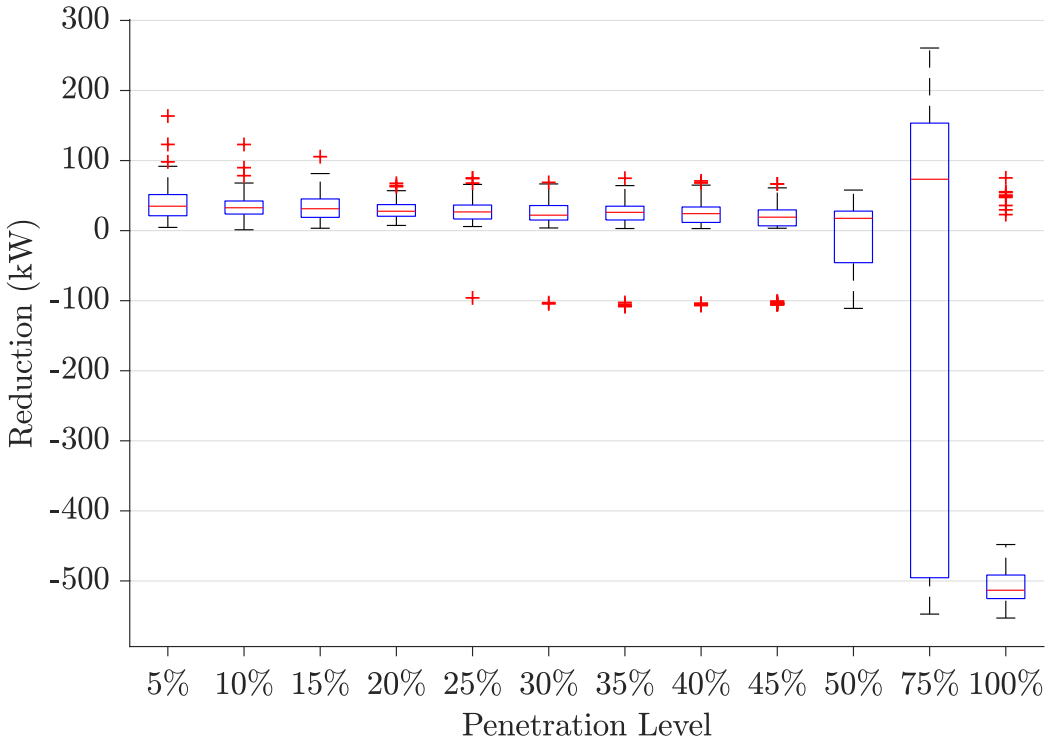

Figure 6.16 Incremental peak reduction of top 100 peaks of the previous penetration level with no third party control.

outlying data points which show a negative reduction (an increase), in load. Further investigation reveals that these peaks occur during night rate hours, when some charging is taking place causing the increase.

The first significant change is seen with the step from 45% to 50% penetration, as peaks from BESS charging begin to overtake typical evening peak loads. This trend continues for the shift from 50% to 75% penetration which, though it appears dramatic, is simply a scaled response similar to those before, but five times greater because of the increment of 25% compared to the previous 5% increments.

Another significant change is observed with the increment from a penetration level of 75% to 100%. At a penetration level of 75%, over half of the top 100 peaks experience a decrease, while at 100% all but a few outliers experience a considerable increase in magnitude. If this low price period charge rate was not limited to 1 kW, such as with the MILP where the most efficient charge rate was 3.3 kW, then this point of change would occur at lower penetration levels, and would also be of greater magnitude.

6.1.3 Third Party Control

Another key area of interest is the use of these home battery systems to provide peak reduction services to a distribution network. The analysis of battery system capability to provide these peak reduction services can be divided into two parts. The first assesses

the power reduction which is available at any particular time independently of any response actually being dispatched.[1] The second examines the response achieved for a given signalling and control method, along with the financial implications for the system owner.

6.1.3.1 Available Reduction

In order to identify the peak reduction capability, it is first determined whether aggregate load, at that time step, is positive or negative. Then, the capability of battery systems to move that aggregate load toward zero is calculated. For time steps where aggregate load is positive, this means household grid import is minimised (and export maximised) within the constraints of the battery system. In order to achieve this, any battery charging activity is halted and battery discharge at the maximum rate possible within the constraints of the battery system is calculated. The effect of this is that in cases where the battery would otherwise be charging, the achievable reduction by a single household can be in excess of the discharge that is possible from the battery.

For time steps where there is an excess of PV generation and thus negative aggregate load, the desired objective is increased consumption. This means stopping any battery discharge and charging at the maximum rate permitted by the constraints on the battery system.

Figure 6.17 shows how the available power reduction varies with aggregate load for the case of 100% penetration of PV and BESS in a network of 2212 households. The trends and behaviours observed here are also displayed, albeit more subtly, at lower penetration levels (Appendix A.1).

At negative values of aggregate load, that is when household load is low and PV generation is high, the available reduction power decreases with increasing load magnitude. This follows logic; it is preferable that PV generation is used for meeting household load and charging battery systems. It is only excess power beyond these needs that is exported to the grid. The fact that aggregate load is negative means there is excess PV generation that is not needed to meet household load and which cannot be utilised for battery charging because batteries are already fully charged. If battery SOC is already constrained, then they are unable to be used to increase consumption and reduce the negative aggregate load.

This behaviour is confirmed by examining the plots of aggregate load against charging power and total stored energy, Figure 6.18 and Figure 6.19 respectively. Looking first at the total charging power (Figure 6.18), as the magnitude of the negative aggregate load increases (greater net export from households), the total charging power decreases. Considering that there is a dependency between the two, this makes sense.

[1] Reduction is defined as a reduction in magnitude of a power flow. That is, a reduction in aggregate load is a shift towards zero.

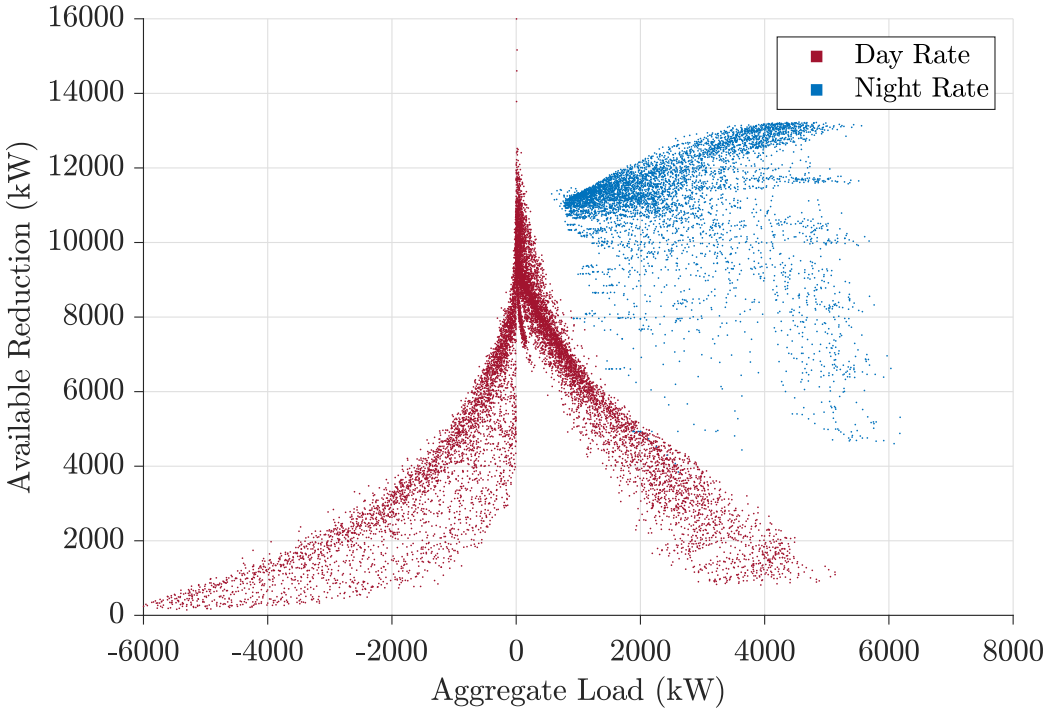

Figure 6.17 Total aggregate load against available reduction capacity for a network of 2212 households with 100% PV and BESS penetration level.

Aggregate load depends on household load, PV generation, and battery behaviour. If batteries are being charged, they are either consuming PV generation that would otherwise be exported or they are being charged with power imported from the grid, both of which increase the total aggregate load. High levels of negative aggregate load require either high levels of excess PV generation or battery discharge, which align with low levels of charging power.

Equally, at those points of greatest excess PV generation, total stored energy (Figure 6.19) is at, or near, its maximum possible value of 29.8 MWh. Under this pricing structure, it is preferable to use excess PV generation to charge the battery rather than exporting it to the grid. As such, the greatest values of negative aggregate load are only seen when storage capacity is full.

Returning back to Figure 6.17, there is a strong clustering around the 0 kW aggregate load where a significant range of reduction powers are available. That means there are many time periods where the available reduction power is in excess of what is required to reduce the aggregate load to zero. As expected, however, during daytime pricing, as aggregate load increases, the available reduction power decreases. At periods of greater load, more battery discharge capacity is committed to meeting household load, meaning less is available for reduction. The timing of when these top aggregate loads occur is also a factor – they are winter evening peaks, and the extreme values are likely to occur on days of poor weather with low PV generation. This means batteries will have used what energy they do have earlier in the day, leaving little for peak reduction in

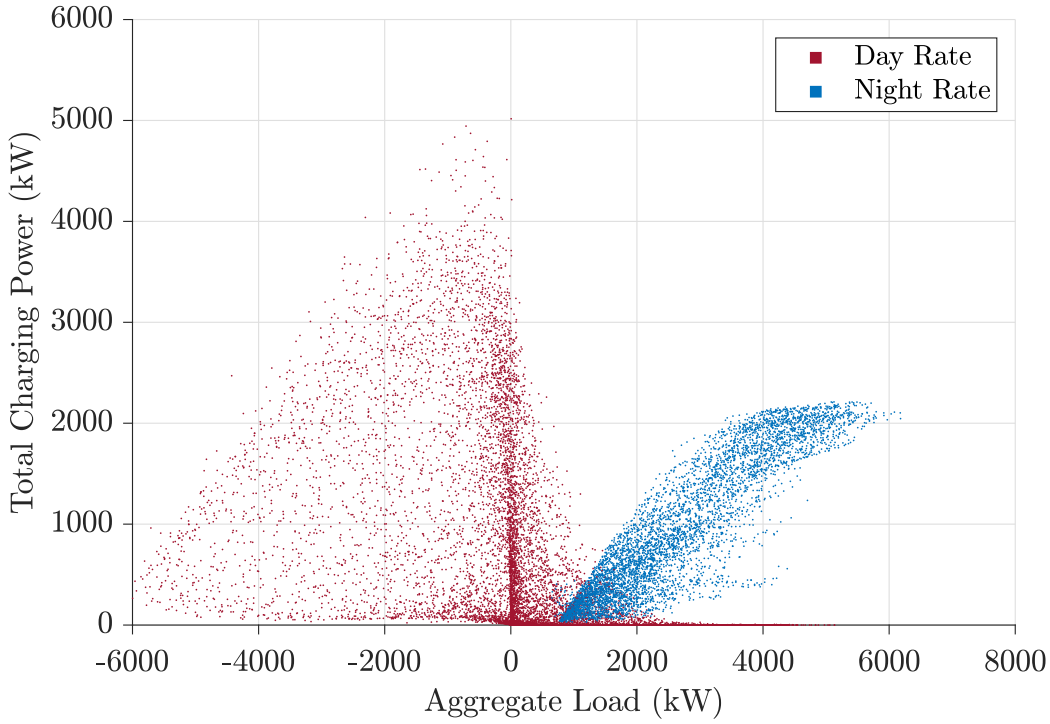

Figure 6.18 Total aggregate load against total charging power for the dataset of 2212 households with 100% PV and BESS penetration level.

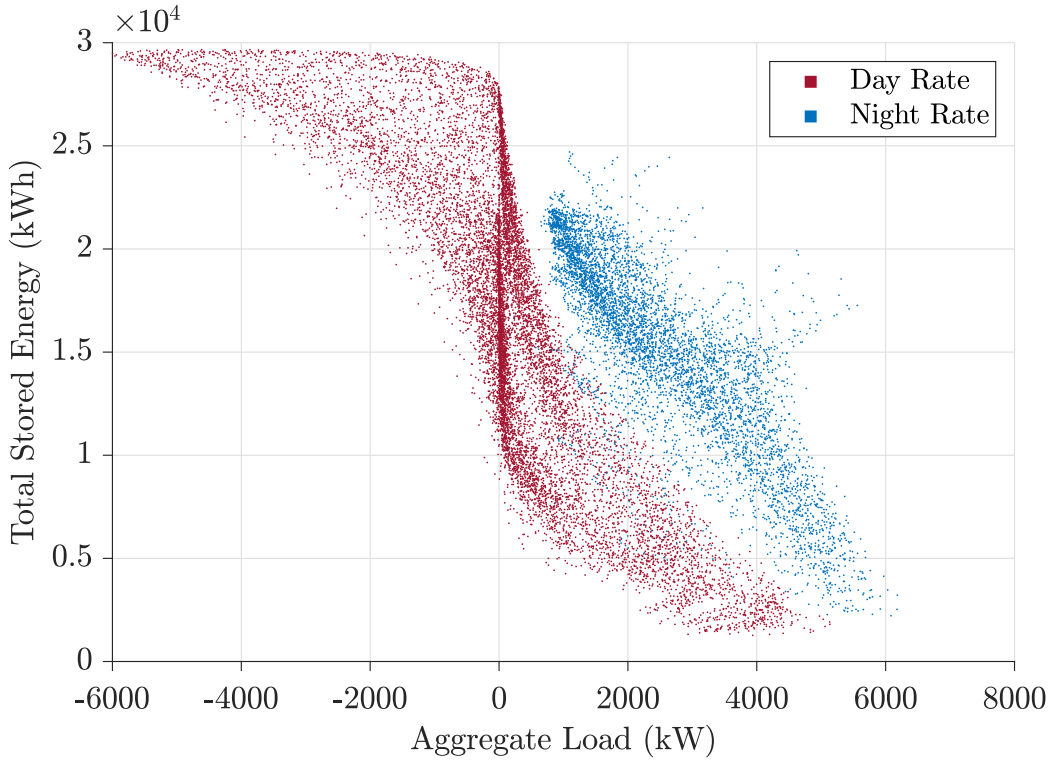

Figure 6.19 Total aggregate load against total stored energy for a network of 2212 households with 100% PV and BESS penetration level.

the evenings. This is confirmed in Figure 6.19, which shows that total stored energy decreases with increasing aggregate load.

The final aspect in Figure 6.17 is related to the night rate data (blue). Night charging occurs from the grid at a fixed rate. In this example it was set at 1 kW. The available reduction reaches a maximum of 13 272 kW. This correlates to 6 kW of reduction for each of the 2212 households. This 6 kW comprises of 1 kW of charging that is stopped and discharging at the maximum rate of 5 kW.

It can also be observed that a strong cluster of night rate points exists where available reduction increases with aggregate load. Again, this is logical when considering that both available reduction power and aggregated load have a component dependent on charging power.

What can be drawn from these results is that the operation of BESSs under a day/night tariff results in battery behaviour where the capacity to reduce aggregate network load over and above any natural reduction from normal operational strategy is lowest at the time it would be most needed. These periods of peak load, the highest aggregate network loads, occur when BESSs are not discharging; not because it isn't economically prudent for them to do so, but because they do not have the stored energy to be able to do so.

6.1.3.2 Sufficiency of Stored Energy to Meet Peak Reduction Requirements

There are both technical and financial incentives for EDBs to control peak loads on their networks. As discussed in Section 2.3.2, the EDB Orion, from which this household load data is taken, targets the very top peak loads of the year through peak signalling. This section revolves around the premise that it is desirable to utilise the peak reduction capability (if any) of BESSs to reduce the top 100 half-hourly annual loads to the level of the 101st half-hour. This section analyses the reduction power available from BESSs specifically at the times of the top 100 aggregate load peaks in the year.

In order to do this, for each penetration level both the top 100 half-hour aggregate loads and the reduction required to reduce that load to the level of the 101st peak are identified. This required reduction can then be compared to the available reduction power and thus a decision of sufficiency is made. As before, these results are presented for one particular allocation of systems to households.

These results are binned by required reduction and presented as two bars for each bin; one bar shows the number of half-hours for which the required reduction falls within the range of that bin, and the second shows the number of half-hours for which there is sufficient reduction capacity for the peaks that fall in that bin.

Figure 6.20 shows these results for a 5% BESS penetration level. 47 of the top 100 peaks require a reduction between 0 kW to 200 kW to bring them to the level of

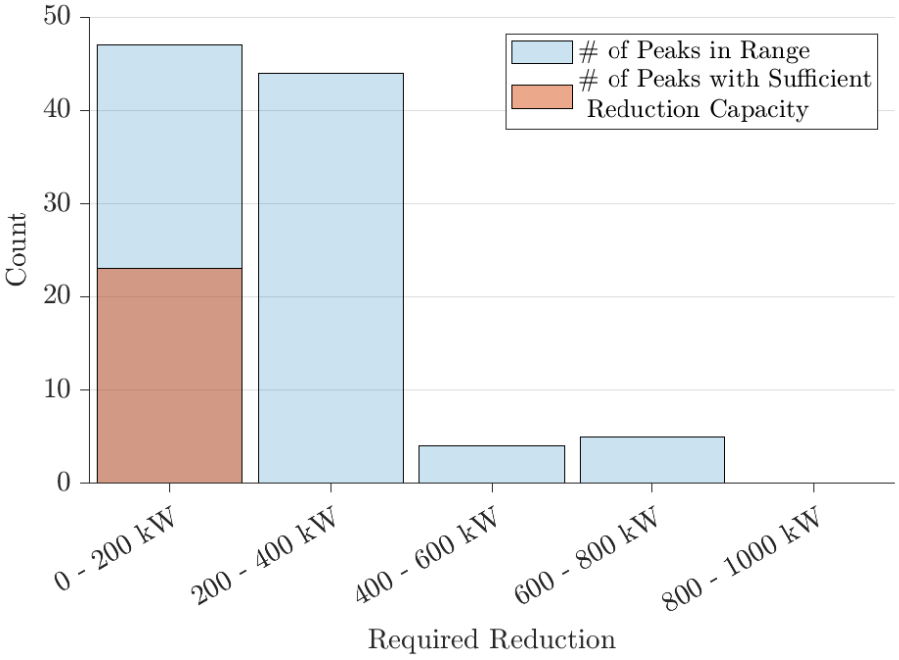

Figure 6.20 Sufficiency of available reduction power to meet required reduction to reduce the top 100 peaks to level of 101st peak for 5% penetration level in a network of 2212 households.

the 101st peak. There is sufficient reduction capacity during only 23 of those half-hour periods. The remaining 53 peak loads require a reduction of between 200 kW to 800 kW, and it is shown that there is not sufficient reduction capacity for these cases.

As the penetration levels increase, there is an increase in the number of half-hours for which there is sufficient reduction capacity. For example by 25% penetration (Figure 6.21), there are 88 half hours where there is sufficient capacity. However for the half-hours that require the greatest reductions, there is insufficient capacity to meet those requirements.

At high penetration levels, such as 100%, there is sufficient reduction capacity for all 100 half-hours. This is because these peaks are caused by low priced night charging, and thus are able to be reduced by not charging. The required reduction capacity is not dependent on battery SOC.

6.1.3.3 Effectiveness of Peak Reduction Signalling

This section examines how effectively network peak loads could be reduced if the BESSs are signalled to discharge at a specified rate. There are many approaches that could be taken when determining the discharge behaviour that is signalled to battery systems. This could include dividing the desired load reduction evenly amongst all battery systems in the network and signalling each system to provide its fair share of load reduction. A downside to this approach is that if any battery system is unable to

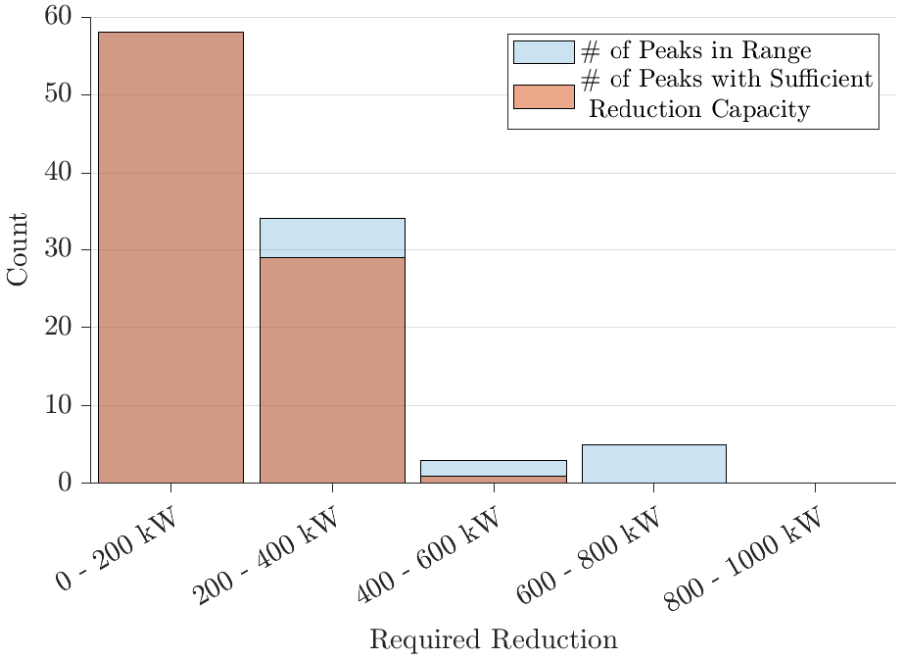

Figure 6.21 Sufficiency of available reduction power to meet required reduction to reduce top 100 peaks to level of 101st peak for 25% penetration level in a network of 2212 households.

behave as requested due to SOC or power constraints, then the desired response will not be achieved. Alternative approaches could include increasing the requested response by a scaling factor to account for some portion of battery systems being unable to respond, or instead requesting battery systems to provide their maximum possible response.

The previous section has shown that there are many instances of peak aggregate load where there is insufficient capacity to provide the desired peak reduction. However, this is demonstrative of the potential and is not comparable to the effective response achieved. The earlier section examines each time period individually for the potential reduction, without any reduction behaviour actually taking place. When the battery operation is changed by responding to a peak reduction signal, this alters the battery's SOC trajectory from that point forward.

As before, the goal is to reduce the top 100 aggregate load peaks to the level of the 101st peak. However, because responding to control signals influences all future battery system behaviour, the top 100 load peaks cannot be identified ahead of time. Instead, the 101st load peak is identified when there is no third party signalling present and this is used as a proxy for the target network load peak. Then, with third party signalling enabled, if the aggregate load exceeds this identified target value, the control signal is sent. This means that the actual number of controlled periods in the year may differ from the target 100.

This analysis considers two signalling methods. The first is where desired response is split evenly between the battery systems. This is shown to be largely ineffective in

producing the desired results. The second is where each battery system is signalled to provide a reduction of significantly more than its fair share, in this case by multiplying by a factor of ten. It is recognised that for battery systems able to respond, this will cause a greater deviation from their natural behaviour and therefore impose a greater cost on the system owner. These financial implications are quantified in the following sections. This approach serves to explore the types of response that can be achieved under different signalling methods.

Figure 6.22 plots the required reduction against the achieved reduction for the 103 periods in which peak reduction behaviour was evenly signalled with a penetration level of 5%. There are 103 periods because that is the number of times that the set load threshold is exceeded (Section 4.4.1). It can be seen that in all cases, the achieved reduction is significantly less than that required to reduce the aggregate load to its target value. In the worst cases, 0% of the required reduction is achieved, through to 50% in the best cases.

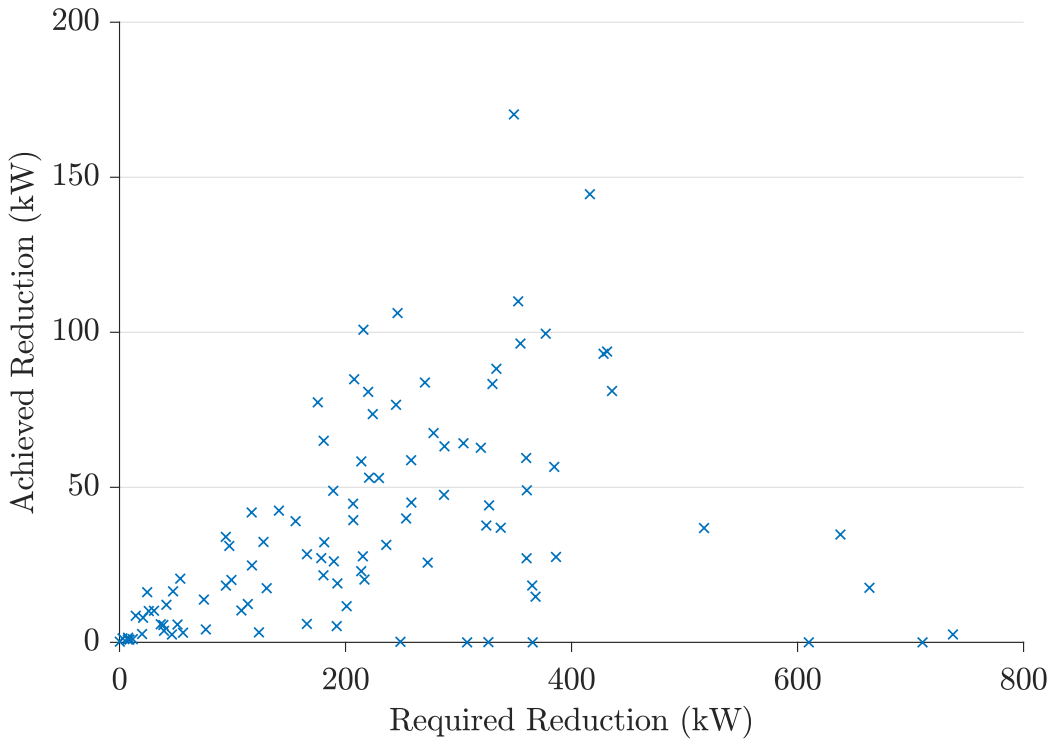

Figure 6.22 Desired reduction against achieved reduction for a network of 2212 households with a 5% penetration level and desired response being evenly divided between battery systems.

In comparison, when the magnitude of the required reduction is increased to ten times that required to reduce the aggregate load to the target, the desired response is achieved for 14 periods. As before, this scaled signalling is divided evenly between the battery systems. These 14 periods are, however, some of the smallest required reductions. None of the largest peaks are reduced at all. This is shown in Figure 6.23.

This same analysis is repeated for a penetration level of 50% and shown in Figure 6.24.

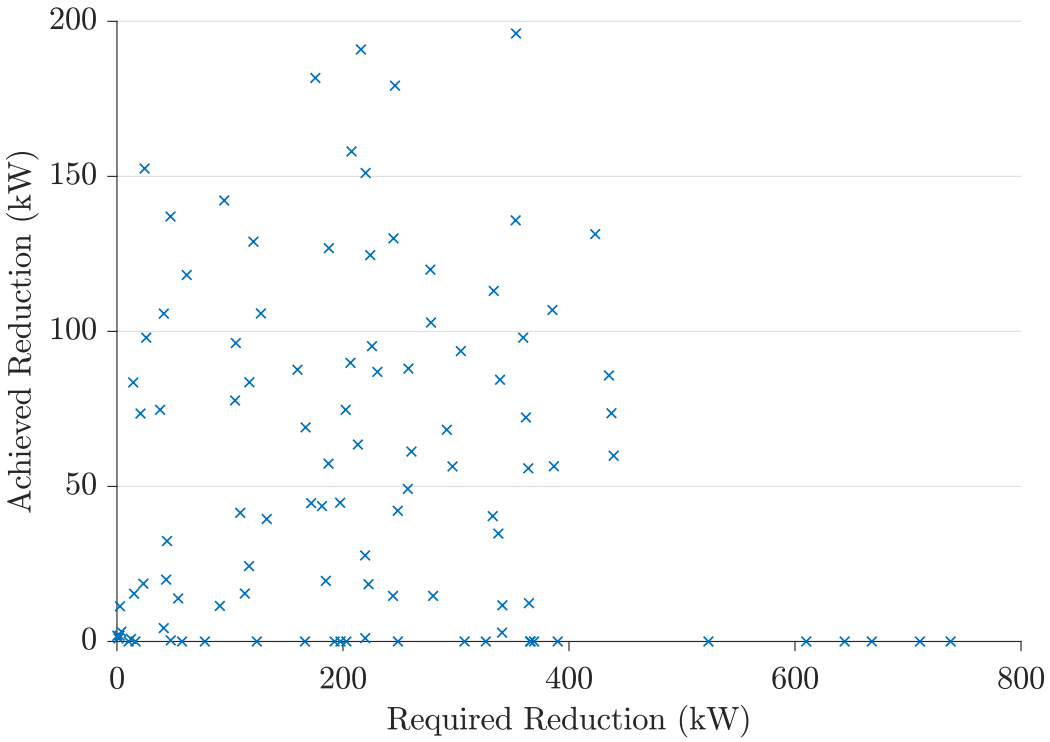

Figure 6.23 Desired reduction against achieved reduction for a network of 2212 households with a 5% penetration level and desired response being scaled by a factor of 10.

In this case, there are 108 periods in which load reduction signalling occurs. There are two clear sections to these results. The first is a series of points on a line with a gradient of 1 through the origin which corresponds to 100% of the desired response being achieved. These are points at which the peak load is the result of the battery charging behaviour, and as such the required response is achieved through changing charging behaviour and is not dependent on battery SOC. The second is a much lower clustering of points where the achieved response does not exceed 100 kW, with up to 800 kW being required. These are cases where it is not battery charging but instead household load that is contributing to the peak. As such, battery SOC and power constraints factor into the ability of these systems to respond as signalled.

At a penetration level of 100%, the desired reduction is achieved in every case. This is because all instances of the network maximum load target being exceeded are caused by low price period grid charging of batteries.

6.1.3.4 Economic Implications of Third Party Control

The other area of interest is the economic implications of third party control. These vary with the penetration level. Engaging in peak reduction behaviour shifts battery operation away from what may be financially optimal for the households. These increases in annual energy cost, for the signalling method where desired reduction is divided

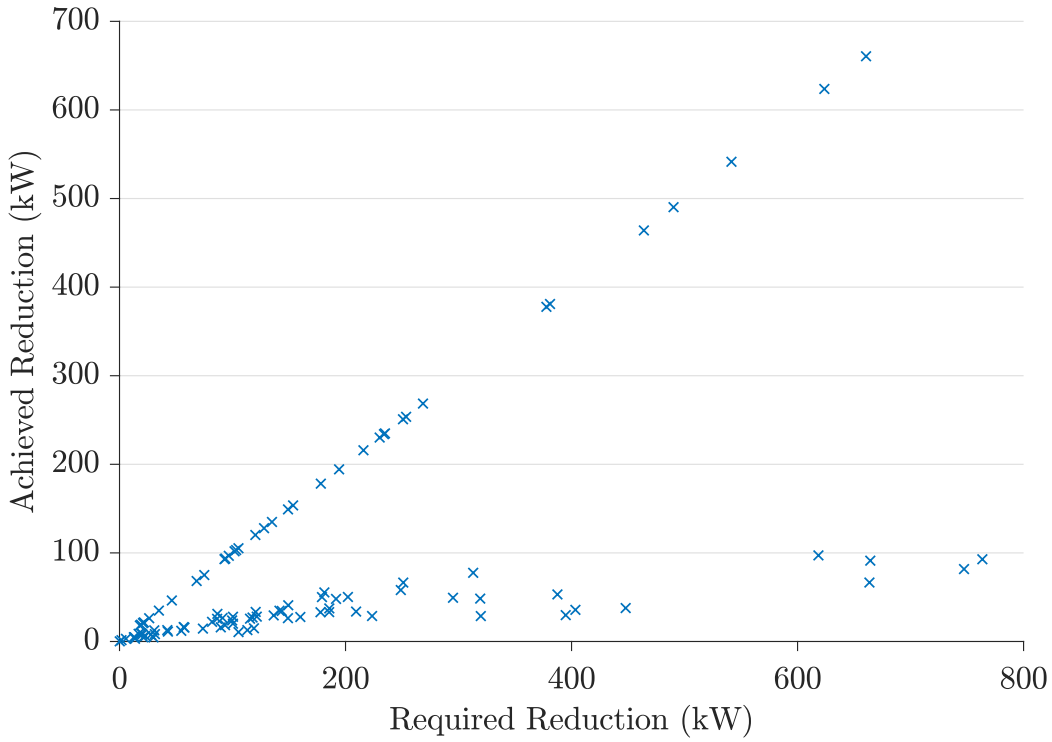

Figure 6.24 Desired reduction against achieved reduction for a network of 2212 households with a 50% penetration level and desired response being evenly divided between battery systems.

evenly between between battery systems, are quantified in Figure 6.25.

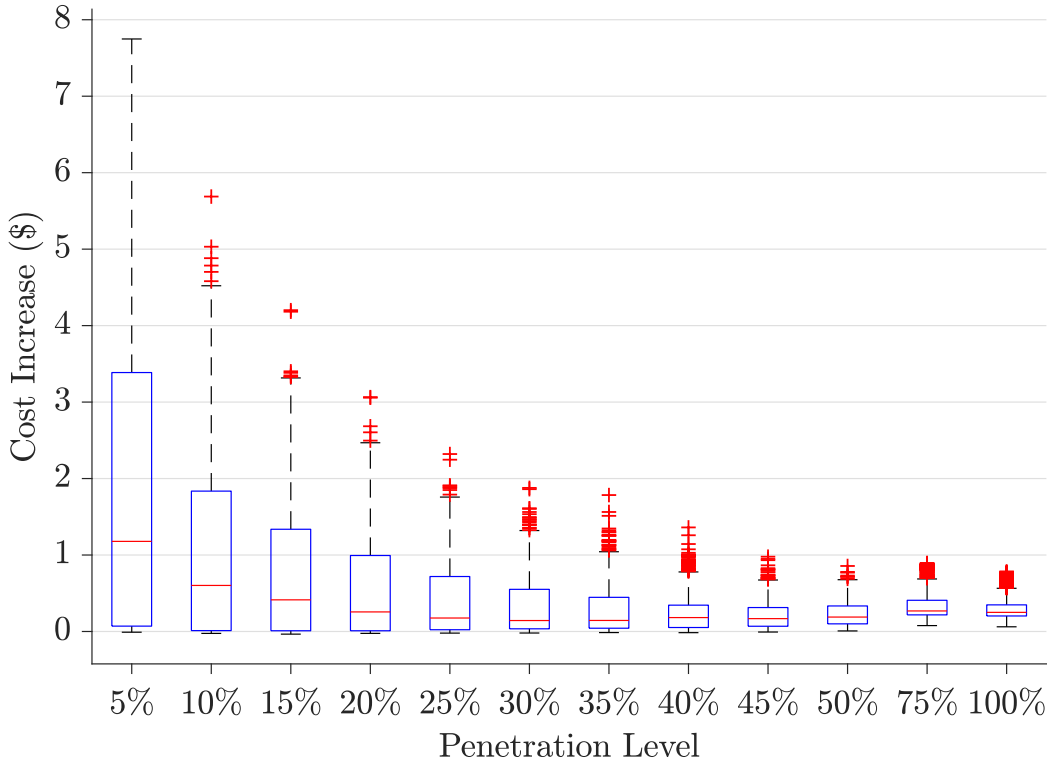

Figure 6.25 Annual costs to BESS system owners of allowing third party peak reduction signalling.

Where the network load peaks are caused by household demand and not battery charging, the lower the penetration level, the more each battery is being signalled to provide. This causes greater deviation from its natural behaviour, which is reflected in the cost to the owner. Note that the maximum annual cost is less than $8. As penetration levels increase, the magnitude of response required from each battery is less and the response can be achieved through charging behaviour. As such, the cost of this behaviour decreases with increasing penetration. The relatively minor cost of the third party control is expected, as only 0.6% of all half-hour periods are being signalled as peak periods.

6.1.4 Summary of Day/Night Pricing

Under day/night pricing, the biggest financial saving to consumers comes from the installation of a PV generation system, with the median annual saving being $780. Under the MILP control method, the addition of a BESS to the PV system results in a further saving, with a median value of $500. It is noted that similar to like household loads, the savings that can be achieved vary significantly.

With respect to the effect on the aggregated network loads, at low penetration levels, small decreases in network peaks are observed. At penetration levels greater than 25%, some of the traditional evening peaks are surpassed by battery charging activity during low priced night periods. For penetration levels less than 100%, there is a non-deterministic element to the results from the allocation of the PV generation and BESS to households. With the complete dataset of 2212 households, there is enough diversity such that a particular allocation causes insignificant variation in the top 100 half-hourly loads experienced by the network.

The rules-based method is compared with the perfect foresight MILP method and shown to produce, on average, a reduction in savings of 7.6%. This puts a small bound between savings achievable by a modern smart battery management system and the idealised maximum possible savings.

The effect of rules-based battery system operation on network peak loads is analysed in detail and it is shown that, without additional peak reduction control, there are only minimal reductions across the top 100 peak half hour loads of the year. Additionally, it is shown that not only is there minimum peak reduction from the batteries operating according to their own rules, this operation results in a behaviour where there is minimal capacity to reduce loads at peak times, even with some form of a third party peak control.

Two methods of signalling desired peak reduction behaviour to the battery systems are identified. The key result is that there is limited potential for BESSs to provide meaningful peak reduction services to a network under the two control methods when the peak loads are not caused by battery charging. Where the peak loads are caused

by battery charging from the grid, there is scope for these peaks to be mitigated with insignificant financial implication to the system owners.

6.2 CASE 2 - UNKNOWN PRICING

The second pricing case is one of unknown pricing, where pricing varies between trading periods and this variation is not known ahead of time. In this case, a spot pricing plan of New Zealand electricity retailer Flick Electric is used. The MILP has perfect foresight of this spot price data.

In this plan, a household in Christchurch is charged a fee plus the spot price for energy they consume. The fees cover network charges, metering charges, the Electricity Authority levy, and Flick Electric's charges. The fee is 17.282 c/kWh for peak times and 3.771 c/kWh for off-peak periods for customers connected to the Orion network [89].

Under Flick Electric's generator trial, the consumer is paid the spot price for any energy they export without any additional fees. However, this is subject to change at the end of the trial as it moves into a standard pricing product [90]. This pricing structure is summarised in Table 6.5.

Table 6.5 Case 2 - Unknown Pricing Inputs

Variable	Value
Import price	Spot price + fees
Export price	Spot Price
Off-peak time	11pm-7am
Peak time	7am - 11pm

6.2.1 MILP Optimisation Method

Similar to the day/night tariff structure, the common inputs of Table 6.1 and the pricing case specific inputs of Table 6.5 are applied. The following results show both the financial benefits to households and aggregated network effects for this one-day-ahead perfect foresight optimisation.

6.2.1.1 Household Benefits

The distribution of annual household energy costs under the three scenarios of load only; load and PV generation; and load, PV generation, and battery systems is shown in Figure 6.26. The median annual energy cost for meeting household load is $1500, which reduces to $800 with the installation of PV generation. This median cost reduces further, to $350, with the addition of BESSs.

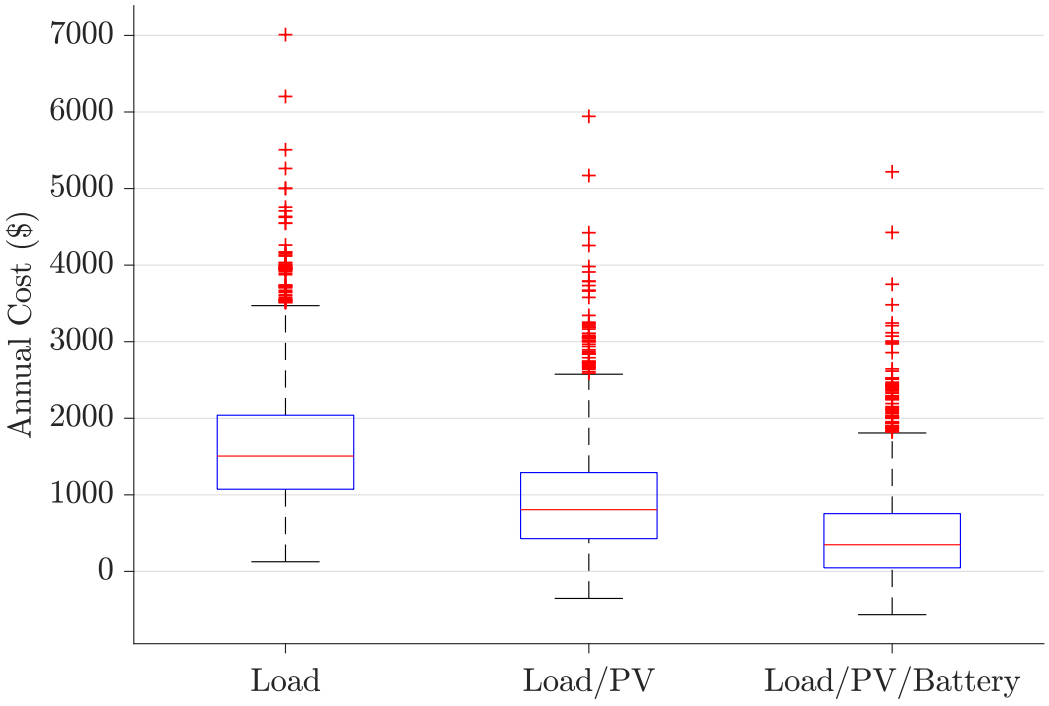

Figure 6.26 Distributions of annual household energy costs under spot pricing.

These costs are presented instead as incremental savings in Figure 6.27. This shows a median annual saving from the installation of PV generation of $700, with an additional $450 saved by the inclusion of a battery system.

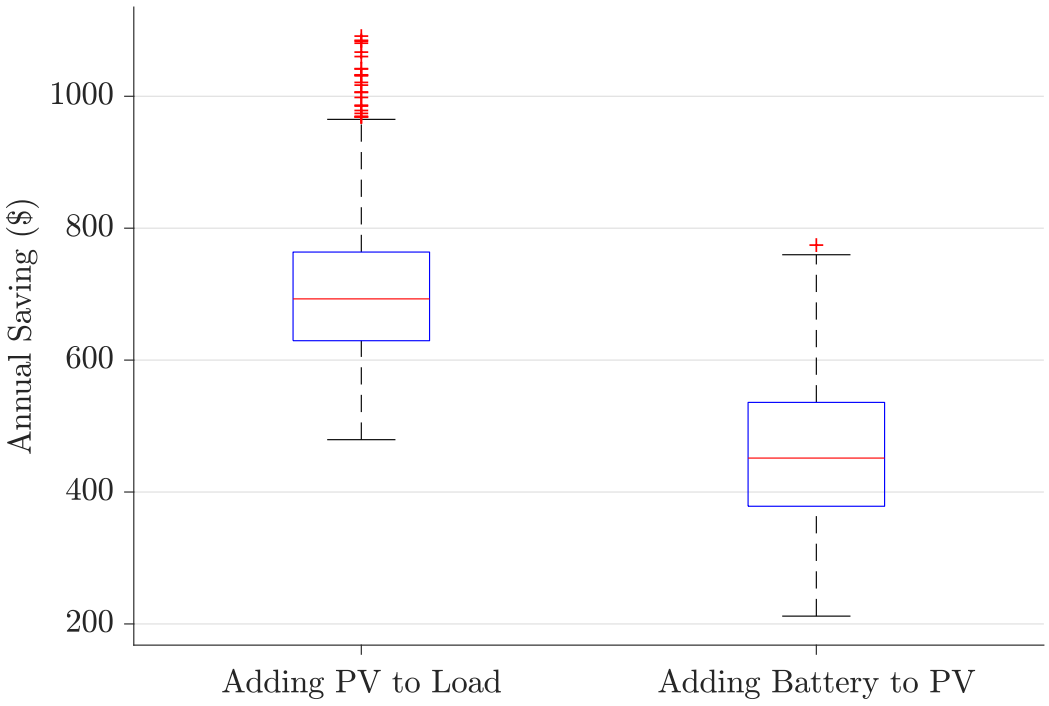

Figure 6.27 Incremental savings under spot pricing.

The examination of daily energy costs across the year, in Figure 6.28, shows that daily costs peak in winter, as is expected. Comparing the raw data and the smoothed data it can be seen that there is significant short time period variability. Of particular note is the large spike at the point with the highest cost, the full magnitude of which is hidden by the smoothing.

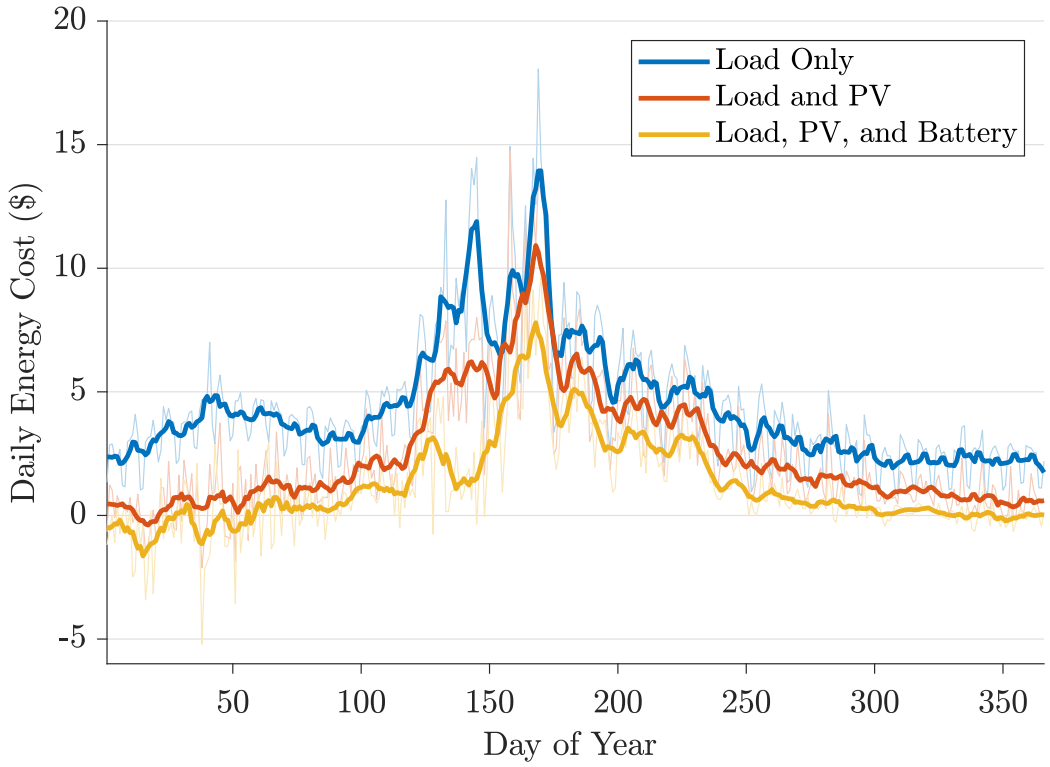

Figure 6.28 Mean daily household energy cost under spot pricing.

6.2.1.2 Network Effects

This section presents the effects of PV and battery systems operating under the spot pricing structure on the distribution networks. As before, the Kolmogorov-Smirnov test is used to assess the effects of the allocation of systems to households on the top 100 annual peak aggregate loads experienced by a network. The results of this are shown in Table 6.6.

For all but four combinations of number of households and penetration level, there exists an allocation of systems to households that does not significantly differ from all others. In small networks sizes of 50 and 100 households with penetration levels of 10% and 15%, the most representative allocation fails the Kolmogorov-Smirnov test for one other allocation. This shows that the impact of battery systems on top 100 half-hourly loads is much less dependent on system allocation for this spot price case compared to the day/night rate case.

Table 6.6 Number of random allocations for which the null hypothesis is rejected by the Kolmogorov-Smirnov test with 5% significance level for the allocation with the minimum null hypothesis rejections.

	Penetration Level										
Number of Households	**5%**	**10%**	**15%**	**20%**	**25%**	**30%**	**35%**	**40%**	**45%**	**50%**	**75%**
50	0	1	1	0	0	0	0	0	0	0	0
100	0	1	1	0	0	0	0	0	0	0	0
200	0	0	0	0	0	0	0	0	0	0	0
400	0	0	0	0	0	0	0	0	0	0	0
600	0	0	0	0	0	0	0	0	0	0	0
800	0	0	0	0	0	0	0	0	0	0	0
1600	0	0	0	0	0	0	0	0	0	0	0
2212	0	0	0	0	0	0	0	0	0	0	0

This behaviour is also further observed in the distribution of the single greatest annual network load peak of all 2212 households across different penetrations (Figure 6.29). As the allocation of systems to households is entirely deterministic at penetration levels of 0% and 100%, these are represented by single data points. However, at all other penetration levels there is minimal spread of the magnitude of this peak load. Spot price, with its significant variability, becomes the dominating factor in battery system behaviour at the time of peak load, rather than household load, resulting in the small spread seen within the distributions. The peak load experienced by the network decreases for a penetration level of 5%; beyond this, however, an increase in peak load is observed. This highlights a poor correlation between peak residential electricity demand and spot price.

Figure 6.30 looks at the effects on network peak loads with increasing penetration levels. As covered previously for the day/night pricing case, due to the change in load profiles caused by the increasing numbers of PV and battery systems, the timing of the top 100 peak loads will change. As such, for each penetration level, the reduction is calculated against the top 100 trading periods of the prior penetration level. For penetration levels of 5% and 10%, there is a reduction in the magnitude of the majority of the top 100 peak loads. For penetration greater than 10%, however, an increase is seen for most, if not all, of the top 100 peak loads.

In terms of the timing of the top 100 peak loads, there are small changes in both the time in the year and day as penetration levels increase. At low penetration levels, the peak loads occur in June and July, while at higher penetration levels some shift earlier in the year, to May. With regards to time of day, increasing numbers of peaks are seen in the morning between 8:00am and 10:00am, as well as some occurring in late evening between 10:00pm and midnight, for higher penetration levels.

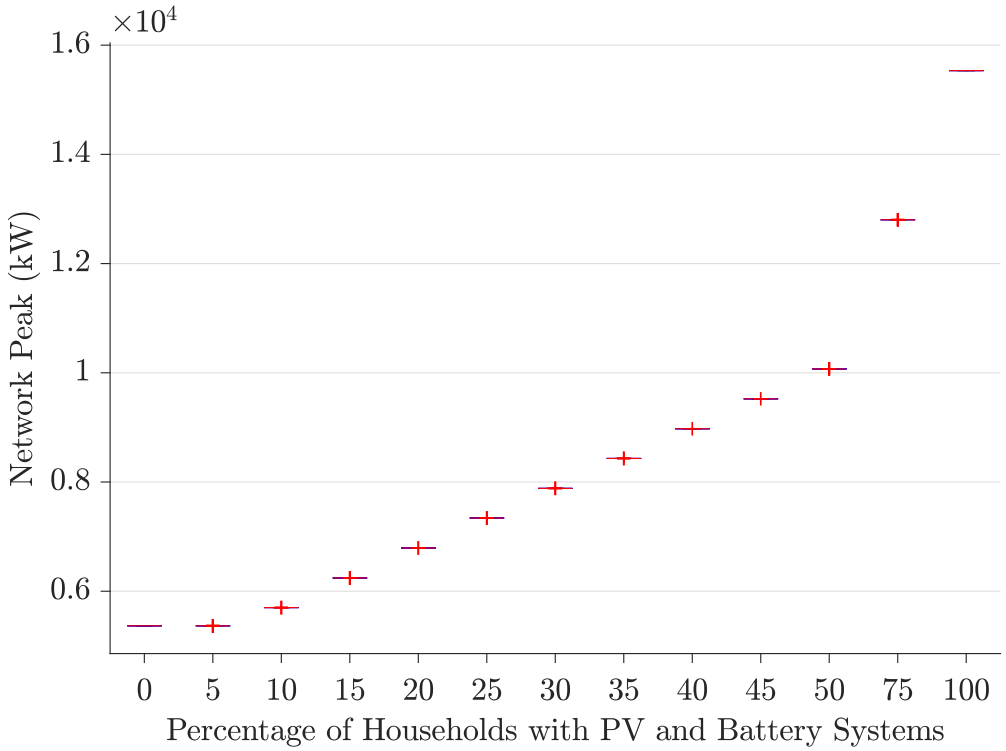

Figure 6.29 Distribution of single largest half-hourly aggregate load for differing penetration levels of PV and battery technology.

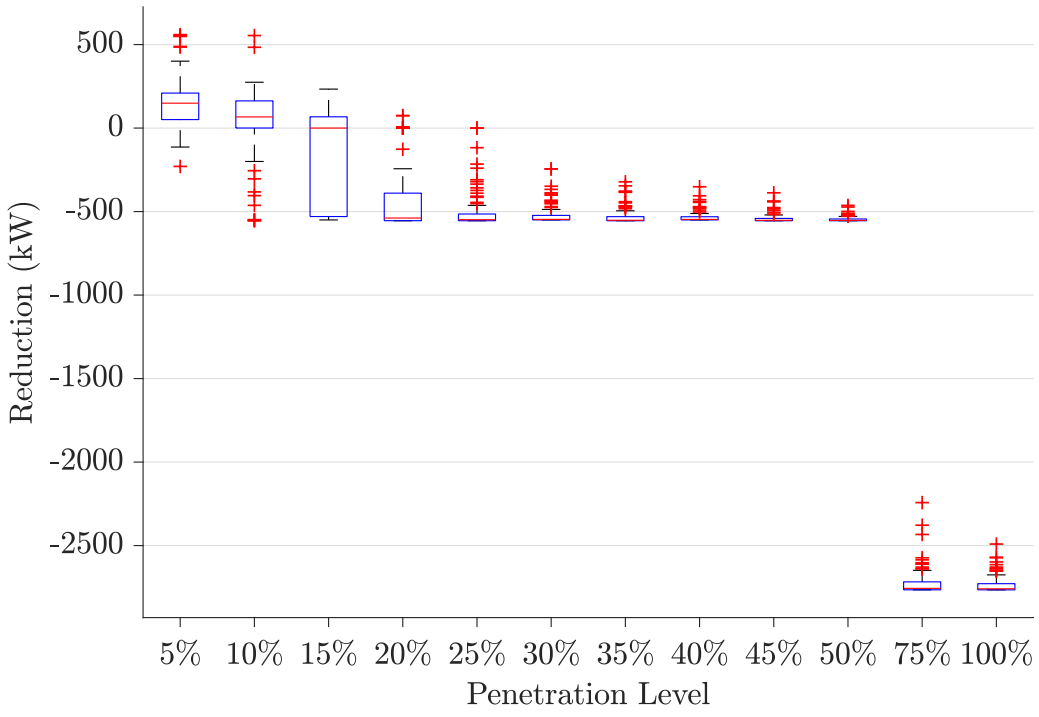

Figure 6.30 Incremental peak reduction from natural battery behaviour.

6.2.2 Rule-based

This section compares the results obtained using the MILP method (Section 6.2.1), to the results obtained using the rule-based method. This highlights some of the challenges created by highly variable pricing.

The difference in annual household energy costs between the MILP method and the rule-based method is highlighted in Figure 6.31. This shows that the rule-based method yields higher annual energy costs than the MILP method due to its sub-optimality and lack of perfect foresight. It does, however, provide savings beyond those achieved by PV generation alone.

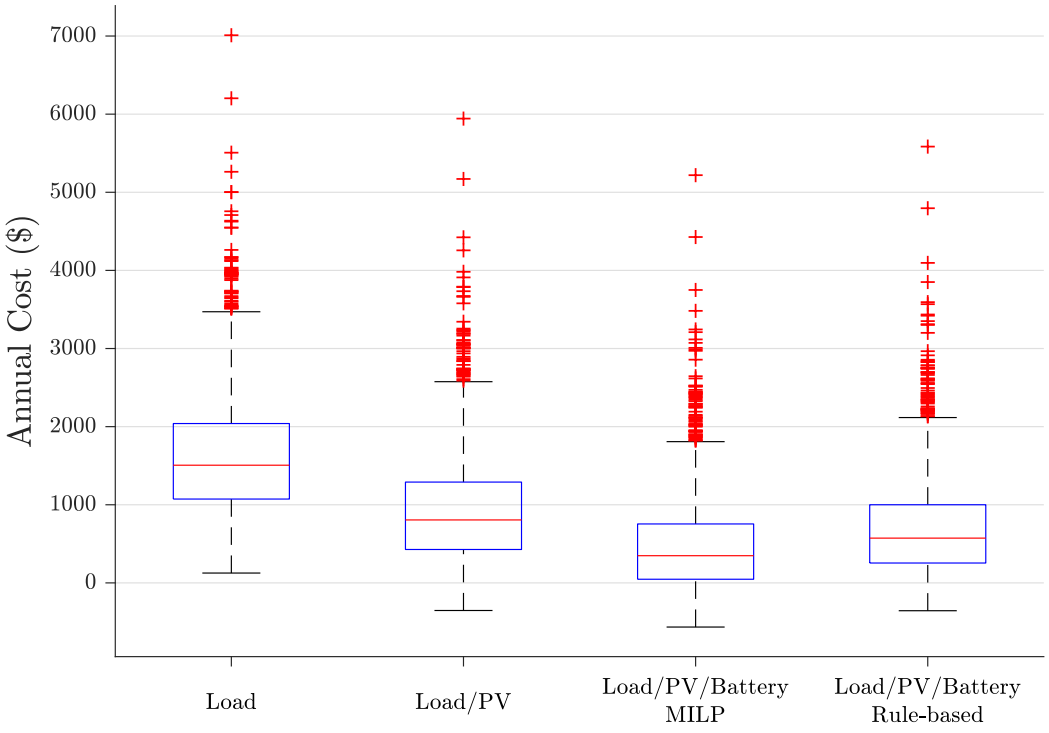

Figure 6.31 Distribution of annual household energy costs under different scenarios and both battery control methods.

The volatility of the spot price data can be observed from the mean daily household energy cost under the three system configurations shown in Figure 6.32. There is significant spread in the raw data around the smoothed lines. Also, there are short time periods when the mean cost of a system including a battery is greater than a system with PV only. That is, there are days where the average household will spend more on energy because they have a battery system than they would without it. This is seen most prominently in days 150 to 153. Further investigation shows that a period of relatively high spot prices preceded this period, which means that the seven day moving average price threshold lies right around the average daytime price when this odd phenomenon occurs. This results in battery discharge only in the evening, which is

followed by cost incurred by overnight charging, and high levels of excess PV generation the following day.

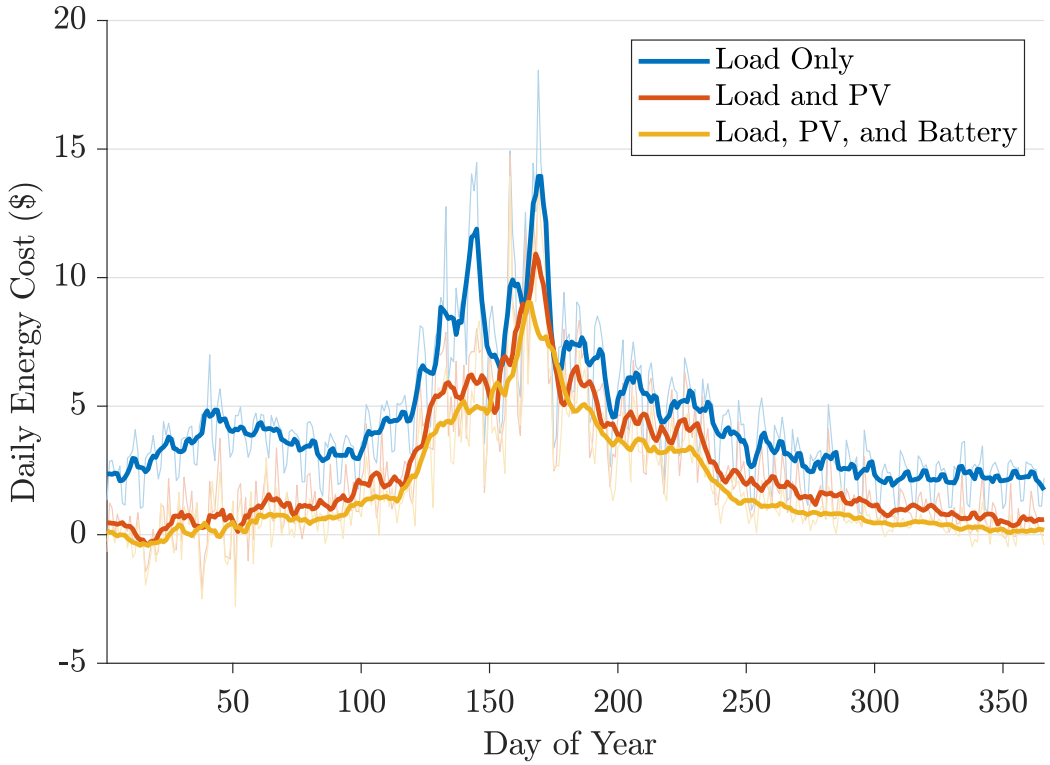

Figure 6.32 Mean daily energy cost across the year under spot pricing with the rule-based method.

The degree by which the rules-based method differs from the MILP method is shown as the percentage decrease in annual household savings from the MILP method to the rule-based method in Figure 6.33. The median reduction in annual savings is 20% when compared with 8% for the day/night pricing structure. This highlights the complexity and challenge of designing simple battery operation rules under such volatile pricing.

Next to be considered are the network effects that result from this rule-based battery behaviour. Figure 6.34 shows that the single biggest peak load experienced by the network of 2212 households across the year decreases only slightly for penetration levels of up to 45%, after which the network peak increases significantly as charging load exceeds any household load. There is little spread in these results, which indicates little variation in the network peaks as a result of the particular allocation of systems to households. This is behaviour aligns with the Kolmogorov-Smirnov test results in Table 6.7, which show that a representative allocation of systems to households is possible at all combinations of network size and penetration levels.

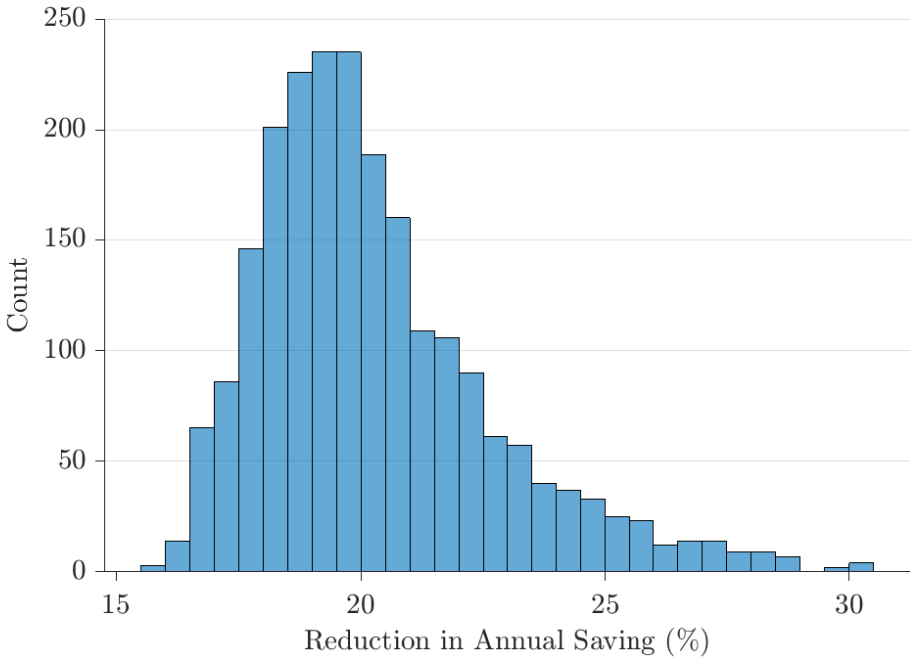

Figure 6.33 Distribution of the percentage reduction in annual household energy cost savings between the MILP method and rule-based method.

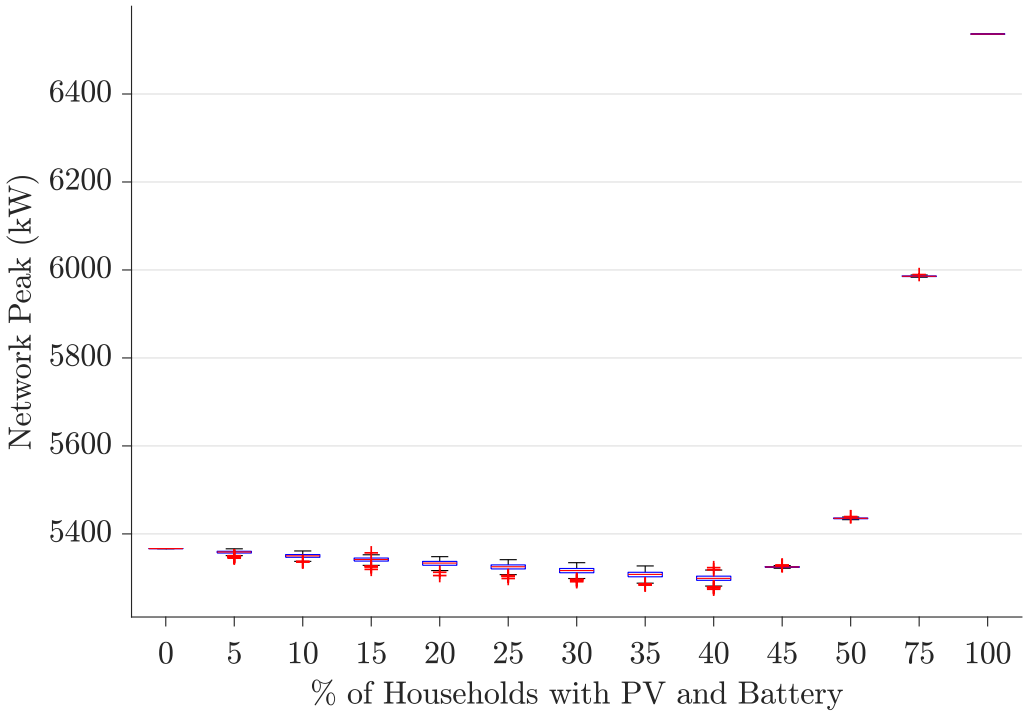

Figure 6.34 Annual peak load experienced by network of 2212 households operating with the rule-based method under spot pricing.

Table 6.7 Number of random allocations for which the null hypothesis is rejected by the Kolmogorov-Smirnov test with 5% significance level for the allocation with the minimum null hypothesis rejections.

	Penetration Level										
Number of Households	**5%**	**10%**	**15%**	**20%**	**25%**	**30%**	**35%**	**40%**	**45%**	**50%**	**75%**
50	0	0	0	0	0	0	0	0	0	0	0
100	0	0	0	0	0	0	0	0	0	0	0
200	0	0	0	0	0	0	0	0	0	0	0
400	0	0	0	0	0	0	0	0	0	0	0
600	0	0	0	0	0	0	0	0	0	0	0
800	0	0	0	0	0	0	0	0	0	0	0
1600	0	0	0	0	0	0	0	0	0	0	0
2212	0	0	0	0	0	0	0	0	0	0	0

6.2.3 Third Party Control

This section discusses the results of using BESSs for network peak reduction services under a third party control scheme. As with the day/night case, this involves firstly looking at the available reduction power in relation to the aggregate load, secondly the sufficiency of that reduction power to meet peak load targets, and thirdly the effective response achieved by a signalling method and the financial implication that has for the system owner.

6.2.3.1 Available Reduction

Figure 6.35 shows the available reduction power against aggregate load for the case of 100% penetration across the full 2212 households under spot pricing. It displays similar characteristics as the day/night pricing structure (Figure 6.17). The notable exception is a strong band of points at 11 000 kW of available reduction power. This correlates to the maximum battery power of 5 kW for all 2212 households. The spot pricing structure introduces a dead band of prices where the battery will neither charge nor discharge. This causes a strong clustering of points where the available reduction per household is 5 kW. This is caused by the batteries being able to discharge at their full rate but with no charging taking place.

6.2.3.2 Sufficiency of Stored Energy to Meet Peak Reduction Requirements

As before, the magnitude of available reduction power at the times of the top 100 half-hourly aggregate load is analysed in order to gain a better understanding of the battery systems' ability to reduce peak network loads.

Figure 6.36 shows the spread of reduction magnitudes required to reduce the top 100 peaks down to the level of the 101st peak over and above any reduction occurring from natural battery behaviour. It also shows for how many of those peaks there is sufficient reduction capacity. It can be seen that 45 of the top 100 peak loads require

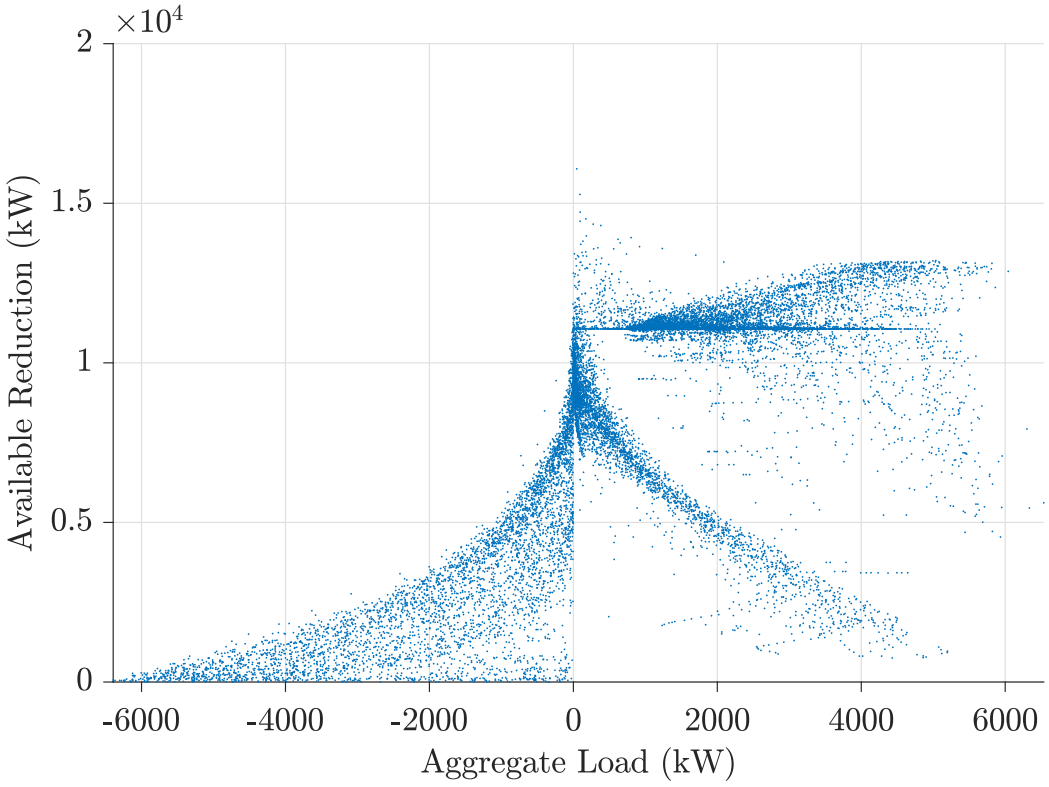

Figure 6.35 Available reduction power for 100% penetration in a network of 2212 houses under a spot pricing structure.

a reduction between 0 and 200 kW, which is achievable for 34 of them. For the peak loads for which the largest reductions of 600 kW and greater are required, there is not sufficient reduction capacity for any of them to be achieved.

At higher penetration levels, where peak loads are caused by battery systems charging during low price periods, it is seen that the proportion of peak periods with sufficient reduction capacity increases. At a penetration level of 100%, all 100 peak periods have sufficient reduction capacity to meet the required reduction.

6.2.3.3 Effectiveness of Peak Reduction Signalling

This section shows the effectiveness of peak reduction signalling when BESSs are signalled to discharge at a specified rate. This includes the effects that responding to one signalled period has on BESSs' SOC trajectory from that point forward. Figure 6.37 shows the achieved response against the requested response when each system is signalled to provide an even share of the required aggregate response for a penetration level of 5% in a network of 2212 households. Of the 104 signalled periods, the required response is achieved 16 times. The majority of other points lie well under that line, showing there is a poor response to the requested load reduction. The responses are particularly low at the 5 greatest required reductions. Overall, this shows a generally poor correlation

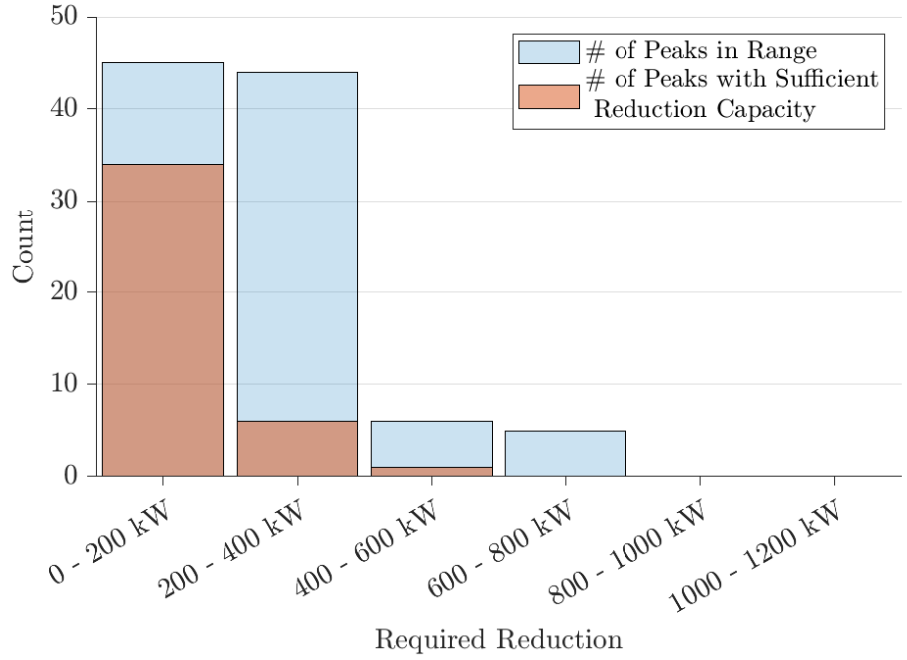

Figure 6.36 Sufficiency of available reduction power for 5% penetration in a network of 2212 houses under a spot pricing structure.

between spot price induced battery behaviour and load reduction capability.

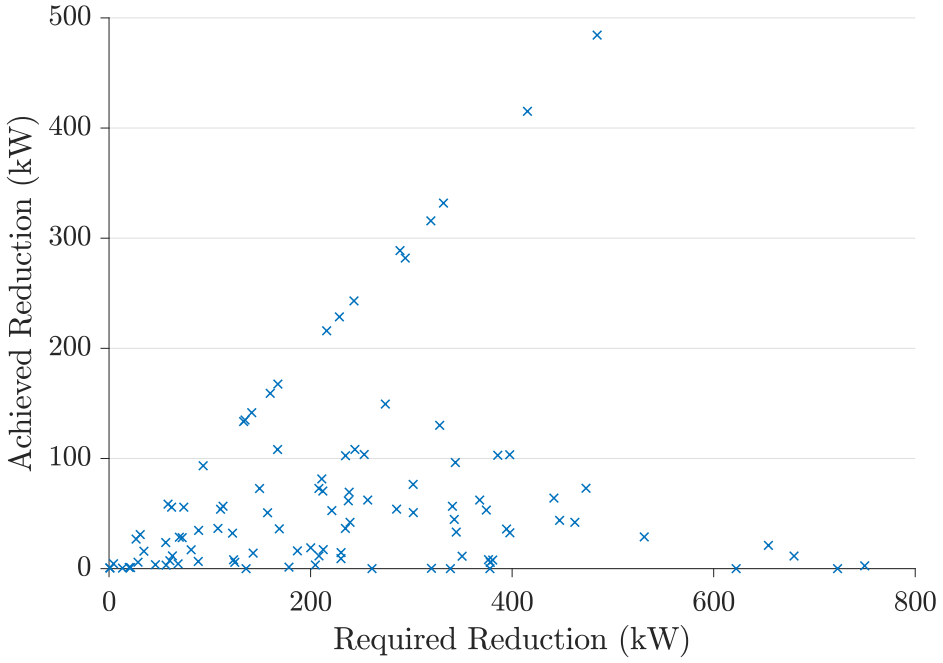

Figure 6.37 Achieved reduction against signalled reduction for 5% penetration in a network of 2212 houses under a spot pricing structure.

When the magnitude of the requested response is scaled by a factor of 10, it is seen

that the success rate increases to 36 out of 112 signalled periods. It can also be seen that there are a small number of cases in which the achieved response is far in excess of what is required. This is shown in Figure 6.38. As before, the greatest required reductions which relate to the largest network loads are of particular interest. Under both signalling methods, there are five half-hour periods which have a required reduction greater than 600 kW. Under the first signalling method, there is a minor reduction for two of those five. However, when the signalled reduction is increased by a factor of ten with the idea of increasing the achieved response, response actually decreases and there is no response achieved for all five of those half-hour periods. By increasing the requested response, the storage trajectory of the battery systems is changed and accordingly they are no longer able to respond at the periods of greatest load. This highlights the complex and interlinked behaviour of these battery systems, as well as the difficulty in predicting what their response capability might be.

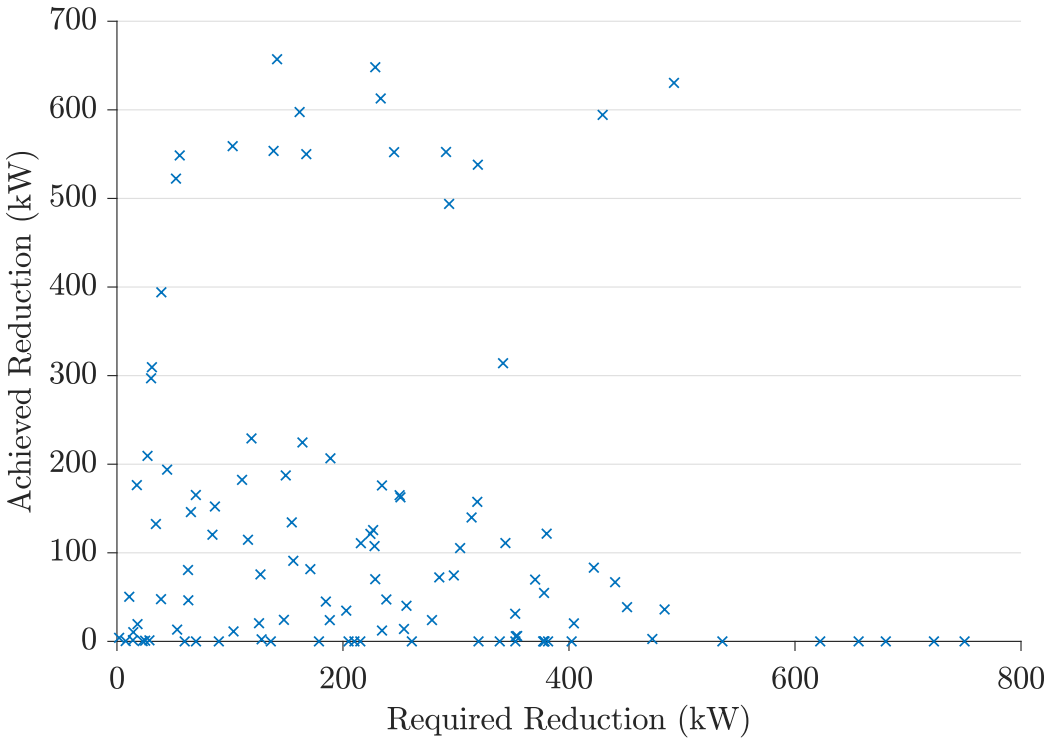

Figure 6.38 Achieved reduction against signalled reduction for 5% penetration in a network of 2212 houses under a spot pricing structure with signal magnitude scaled by 10.

As the penetration level increases, the same behaviour is observed for this case as for the day/night pricing case; as peak loads begin to be caused by battery behaviour, the ability of the battery systems to control and reduce those peaks increases. However, it remains difficult for peak loads which result from household load to be reduced to the extent desired.

6.2.3.4 Economic Implications of Third Party Signalling

This section examines the economic implication of third party control on the system owner. The distribution of cost increases for households is shown in Figure 6.39. Of interest is the fact there are a small number of households at which the cost is negative. This means there are some households which achieve a lower energy bill through responding to these third party signals than they would by just behaving according to their own rules. This once more highlights the sub-optimality of this particular rule set compared to the perfect foresight optimal result.

It is seen that under any penetration level, the cost increase never exceeds \$4 and is largely less than \$1 which, when considered against the capital expense of a battery system, is insignificant.

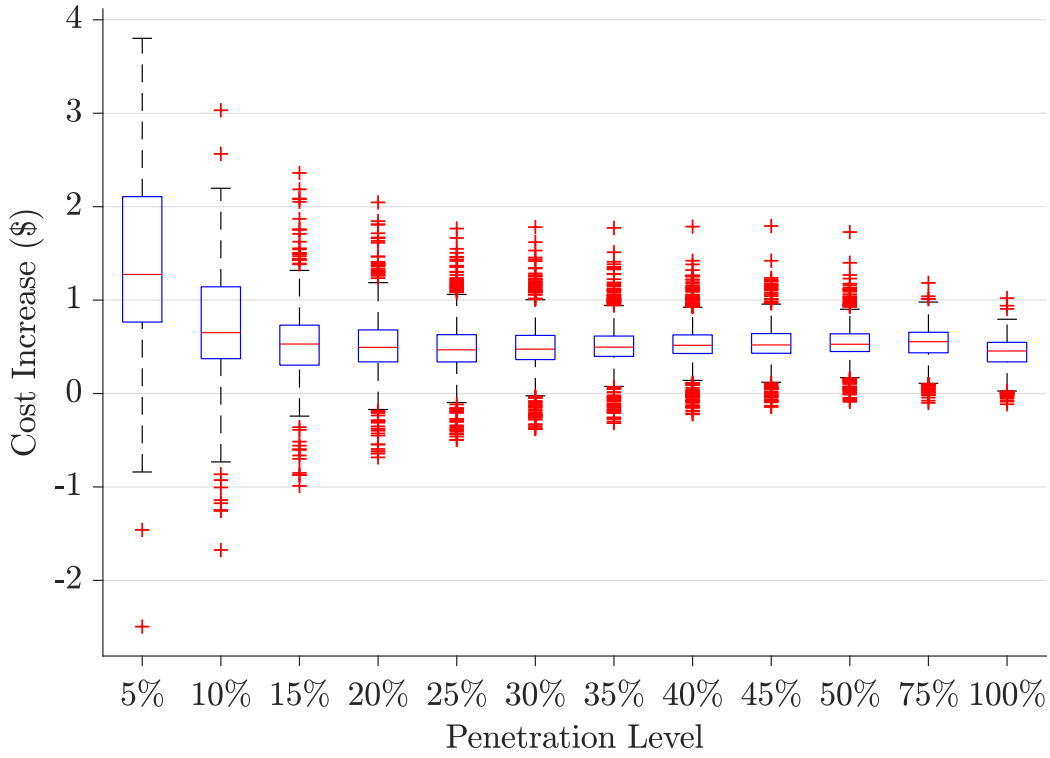

Figure 6.39 Cost implications of third party signalling.

6.2.4 Summary of Spot Pricing

Under spot pricing, with perfect foresight, there are significant financial gains to be made from a BESS. As with fixed pricing, bigger savings result from the installation of the 3.5 kW PV system than from the BESS. The volatility of the spot price combined with the peak/off-peak fee structure allows for financial benefits to be realised from price arbitrage as well as from the maximisation of PV self-consumption. Spot pricing does little to incentivise battery behaviour that reduces network peak loads. Under the

MILP method, network peak loads were seen to increase for penetration levels greater than 10%.

The rule-based method was shown to reduce the household savings by 15-30%. Further sub-optimality was observed where, under certain pricing conditions for short periods, the cost of having a battery system was greater than not having a battery system. This highlights the challenge of designing a rule set for such volatile pricing and it is acknowledged that a refined and more complex set of rules could improve upon this.

The ability of battery systems operating under this spot pricing structure to provide peak reduction services beyond their natural behaviour was explored. It was shown that while some potential does exist, the signalling methodology has a large impact on the result achieved. Asking for too little from each battery system results in less than the desired response being achieved, due to some systems not being able to behave as requested. Conversely, asking for too much from each system limits its ability to provide peak reduction services for the full duration of the peak and for future peaks.

6.3 CASE 3 - PEAK/SHOULDER/OFF-PEAK PRICING

This case makes use of a three tiered pricing structure consisting of peak, shoulder, and off-peak periods. Having a shorter peak rate period compared to the day/night structure focusses the times that there is economic incentive to discharge batteries and thus should produce beneficial network effects. It is also a tariff structure that has been adopted by some parties in the New Zealand Electricity Market in recent years.

As noted previously, there are hundreds of possible tariff structures in the New Zealand electricity market. One particular available structure is chosen to be used for this case. The timings of the different price periods are shown in Table 6.8 and the pricing in Table 6.9.

Given this is the third case and the methods and analysis remain constant, a brief summary highlighting only key observations is presented for this case.

Table 6.8 Definition of peak, shoulder, and off-peak time periods.

	Peak	**Shoulder**	**Off peak**
Weekday	0700-0930 1730-2200	0930-1730 2000-2200	2200-0700
Weekend	-	0700-2200	2200-0700

Table 6.9 Case 3 - Peak/Off-peak/Shoulder Pricing Inputs.

Variable	Value
Import price - peak	25.5 c/kWh
Import price - shoulder	18.8 c/kWh
Import price - off-peak	16.7 c/kWh
Export price	8 c/kWh
Low price fixed charge rate	1 kW

6.3.1 MILP Optimisation Method

This section highlights some of the key results of the day-ahead perfect foresight MILP optimisation method under this peak/shoulder/off-peak pricing structure.

6.3.1.1 Household Benefits

The distributions of annual household energy costs are shown in Figure 6.40. The key observation under this pricing structure is that the addition of a BESS to a household that already has PV generation results in a significantly smaller cost saving when compared with the installation of the PV generation. Figure 6.41 shows the mean daily

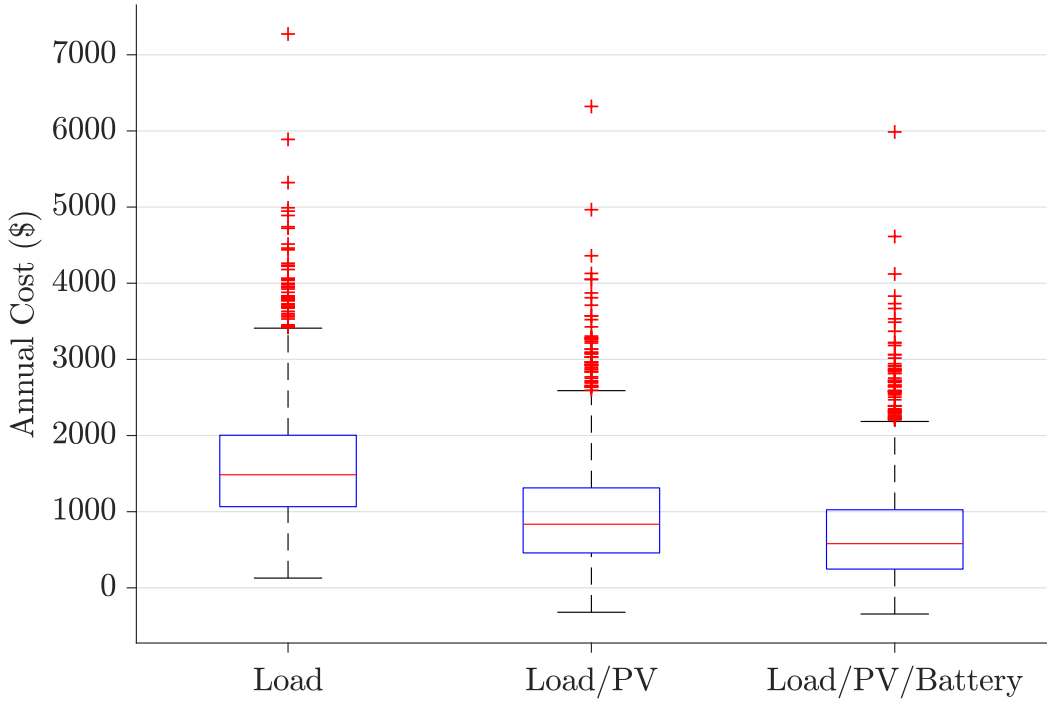

Figure 6.40 Distribution of household annual energy costs under peak/shoulder/off-peak pricing.

household energy cost across the year. An increase in the price differential between a household with PV generation only and system with both PV generation and battery storage is seen in the middle of the year. This is the winter period where energy volumes are higher, which allows for greater benefit to be gained from the battery system.

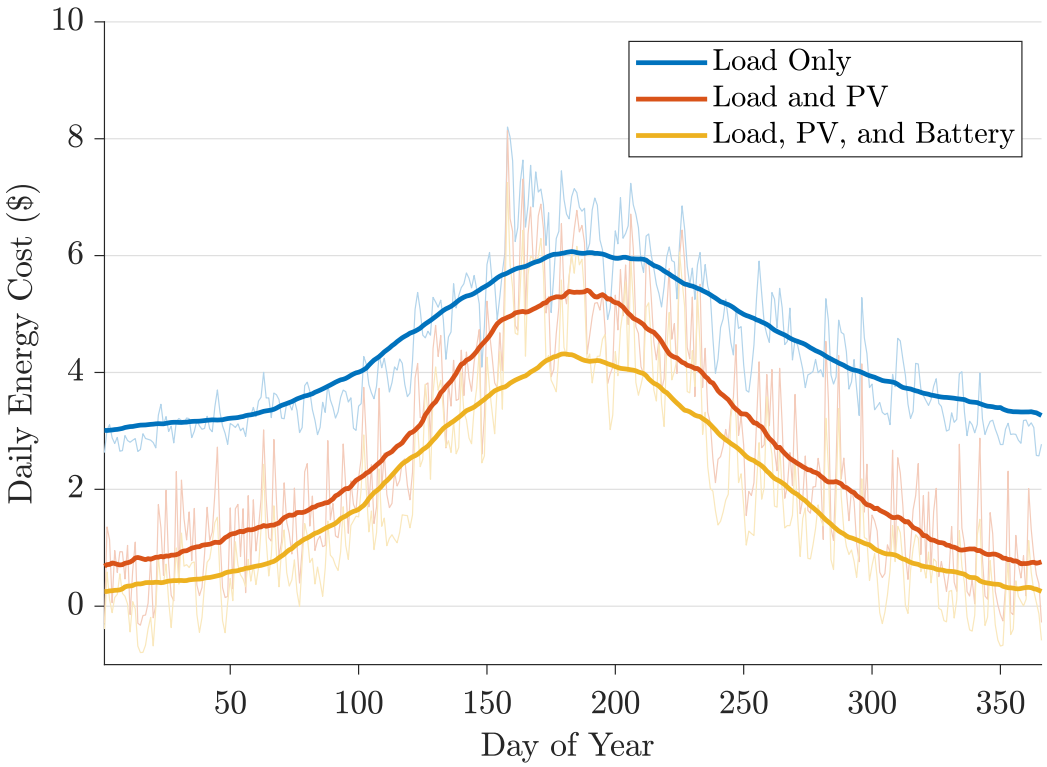

Figure 6.41 Mean daily energy household energy cost across the year under peak/shoulder/off-peak pricing.

6.3.1.2 Network Effects

Intuitively, it seems that the narrowed peak pricing period of peak/shoulder/off-peak pricing compared to day/night pricing should result in behaviour that will have a more positive impact on network peak loads. Figure 6.42 shows that this may not be the case. This plot shows the distributions of magnitudes of the greatest single network peak load of the year, with 500 random allocations of systems to households at each penetration level. Unlike day/night pricing, for which a decrease in peak load was observed for penetration levels from 5% to 25%, this pricing structure shows an increase in peak load magnitude right across the spectrum of penetration levels. This increase is minor at low penetration levels but grows at the high penetration levels. For the low penetration levels, this single highest load peak of the year occurs in a shoulder priced period rather than a peak period and as such the battery systems are not being incentivised to use their stored energy to discharge.

When considering all of the top 100 peak loads from the most representative allocation of systems to households, as in Figure 6.43, it can be seen that the BESSs under this pricing structure provide generally positive peak reductions at lower penetration levels. However, like the other pricing structures, at high penetration levels an increase in many of the peak loads occurs due to charging during low priced periods.

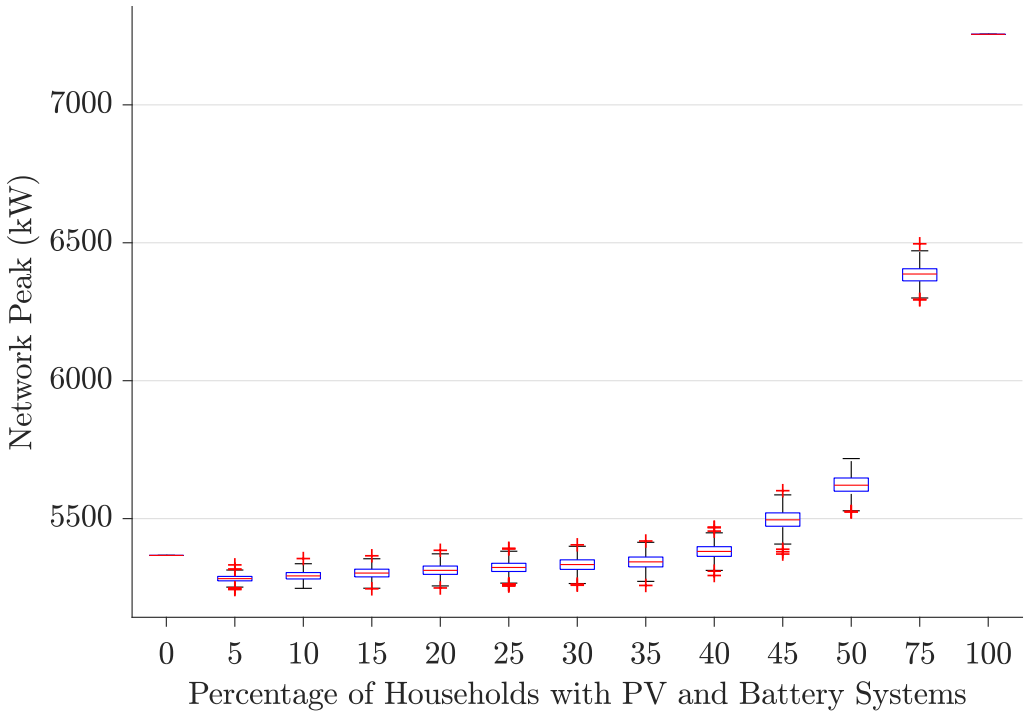

Figure 6.42 Distributions of magnitude of single largest aggregate load peak for a network of 2212 households with 500 random allocations of systems to households.

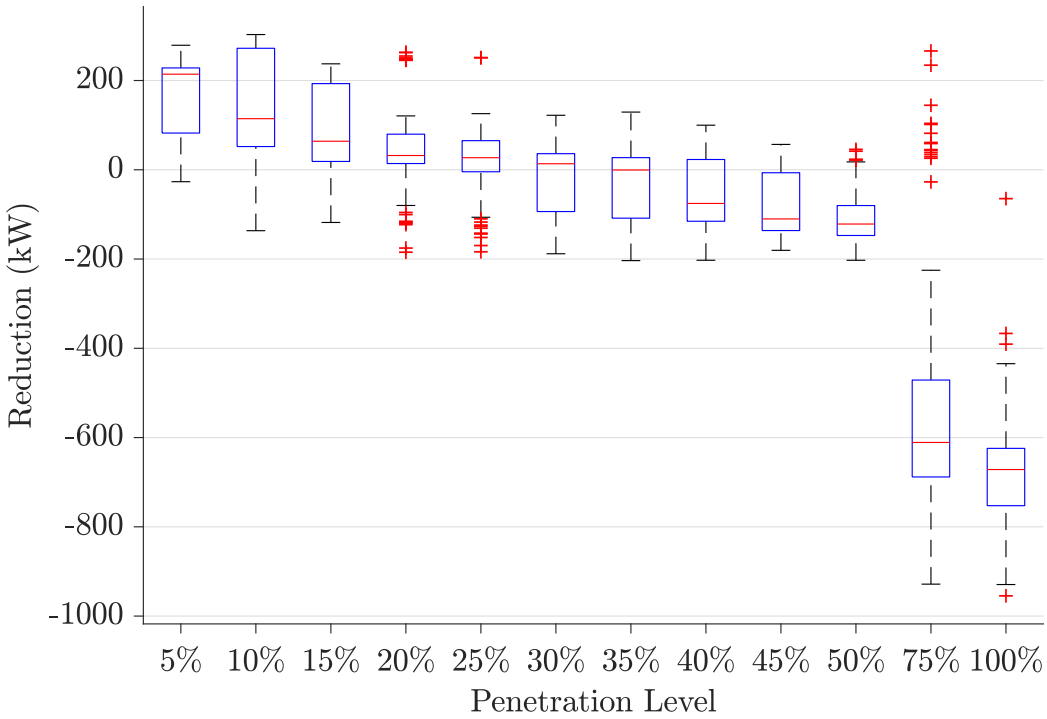

Figure 6.43 Distributions of incremental reductions experienced by top 100 peak loads.

6.3.2 Rule-based

The first indicator that this rule-based method may not perform as well as expected is seen in Figure 6.44. The mean daily energy cost for a household with both PV generation and a battery system is only slightly less than a household with only PV generation. In particular, during the winter period the rule-based method performs poorly compared to the MILP method. There is little financial benefit from the battery system.

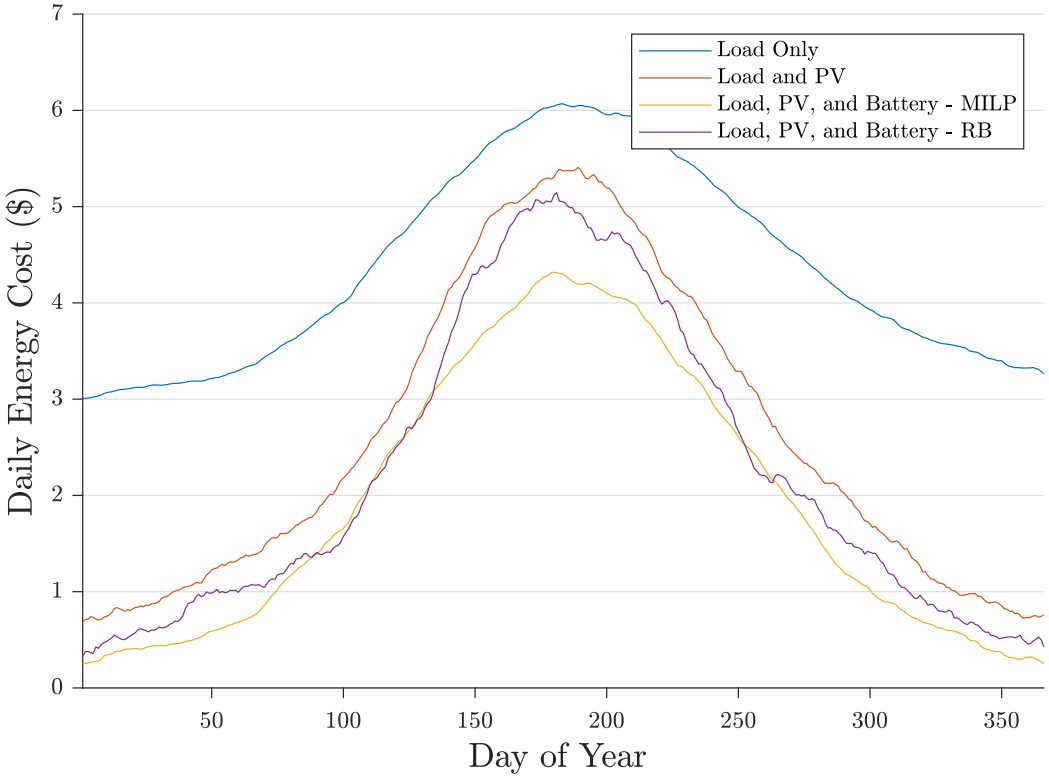

Figure 6.44 Comparison of mean daily energy costs

This definite sub-optimality is also seen in Figure 6.45, which shows the distributions of annual household energy cost. There is a slight reduction in cost compared to the load and PV only case, but a marked increase in cost compared to the MILP method. The median incremental saving from adding a BESS to a household that already has PV generation is $255 under the MILP method, while under the rule-based method this decreases to only $140, a decrease of 45%.

Further investigation reveals the reasoning behind this sub-optimality. With the rules chosen, battery discharge occurs only during peak price periods. This severely underutilises the batteries. The median stored energy across all batteries for the year is 84% of the capacity. Figure 6.46 shows the distribution of total stored energy as a percentage of capacity for each half-hour period of the year. The batteries are spending the majority of the time at a high state of charge, only discharging partially during the

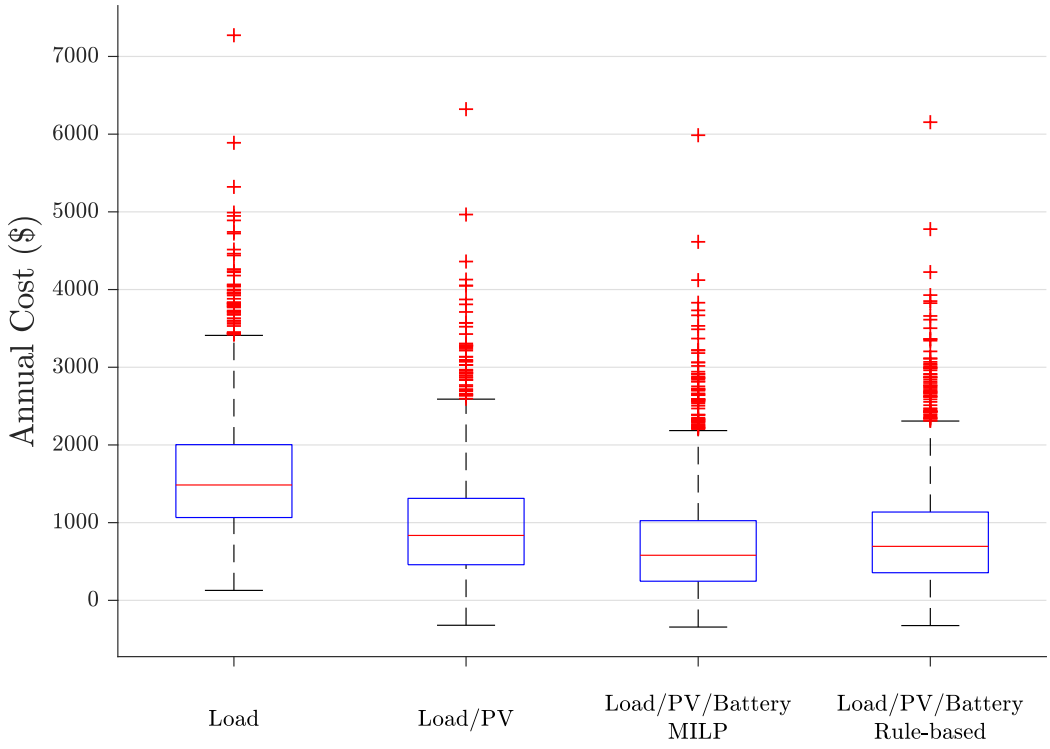

Figure 6.45 Distributions of annual household energy costs under peak/shoulder/off-peak pricing.

peak price period, before being recharged by excess PV generation or by low priced grid energy. If an improved set of rules were to be created, this would better utilise the batteries by prioritising having capacity available to meet household load during peak price periods, but also allowing some battery discharge during shoulder periods.

The focussed approach of this set of rules on peak pricing periods provides a better reduction in network peak loads from natural battery behaviour than the other pricing structures. Examining the effect of increasing penetration on the single greatest load peak of the year masks the true behaviour. At a penetration level of only 5%, the greatest single half-hour load peak occurs in the shoulder pricing period and so is not reduced by this rule set. Examining the incremental effects on the top 100 peaks, as in Figure 6.47, does show the benefits that these systems bring to reducing network load peaks. As with the other pricing structures, there is a combination of peak loads which are reduced by battery systems and peak loads which are increased by, and caused by, battery systems. For penetration levels of up to 15%, many of the top 100 peak loads are reduced by growing PV and BESS penetration levels. There are small numbers of these top 100 peak periods which see an increase in load, and these are generally outliers. It is only at penetration levels greater than 50% that a significant shift is seen to where the peaks are being caused by battery system charging.

Also of interest is the clustering around a reduction of 0 kW which can be seen right up to a penetration level of 75%. When a top 100 peak load occurs in the shoulder pricing period, it will not be reduced by battery behaviour, but equally, low price grid

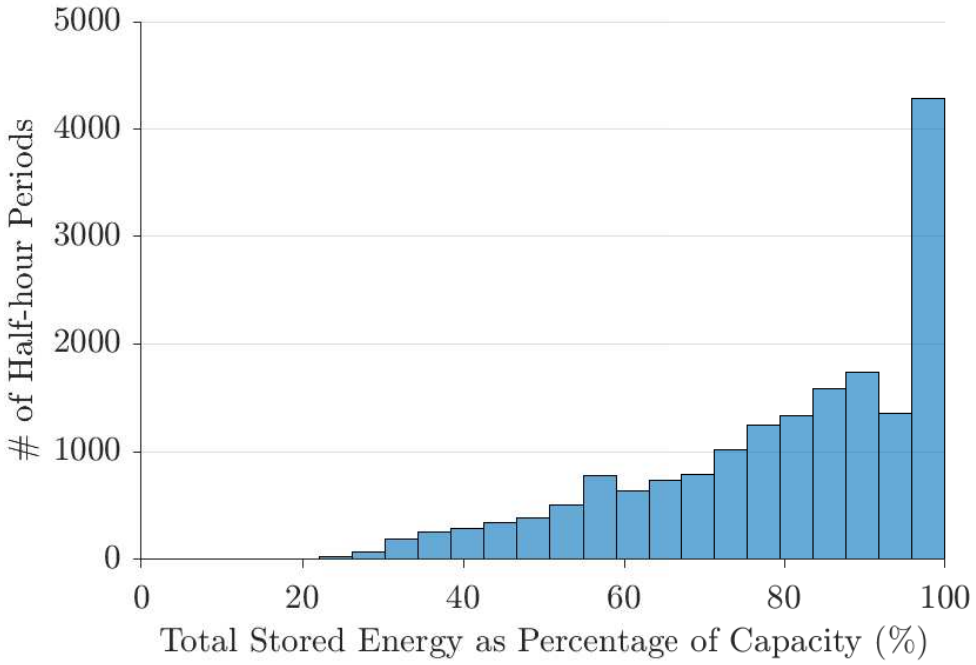

Figure 6.46 Distribution of total stored energy in all batteries for all half-hour periods of the year as a percentage of total storage capacity.

charging will not occur either. For periods falling in the price dead-band, the load is neither increased nor reduced by battery systems.

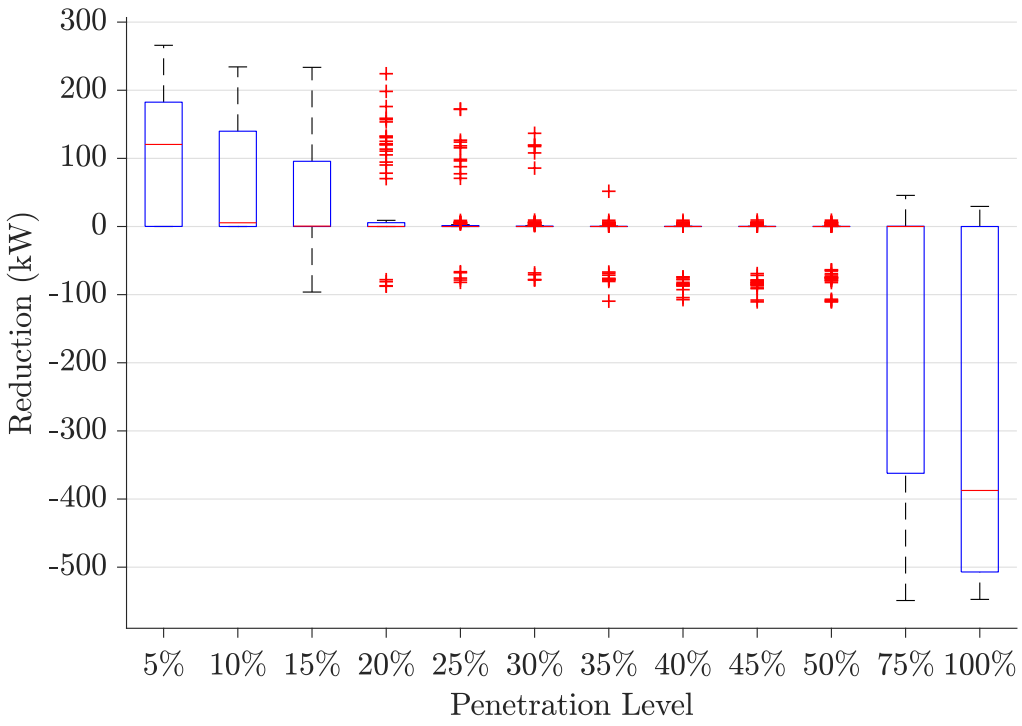

Figure 6.47 Incremental reduction in top 100 peak loads under peak/shoulder/off-peak pricing.

6.3.3 Third Party Control

The on-average high levels of stored energy explored in the previous section indicate that, under this pricing structure, battery systems may have a much greater capacity to respond to third party load reduction signalling than has been seen previously. It could also be expected that responding to third party signalling will increase battery utilisation and subsequently increase the financial savings that the battery system provides.

At a penetration level of 5%, there is sufficient available reduction power to reduce 81 of the top 100 peak half-hourly loads to the level of the 101st peak. This increases to 99 at 10% penetration. For penetration levels of 15% to 100%, there is sufficient available reduction for all 100 of the top 100 aggregate loads. With batteries operating under a peak/shoulder/off-peak pricing structure and with this particular set of rules, there exists significant potential for third party signalling to be used to reduce network peak loads.

6.3.3.1 Effectiveness of Peak Reduction Signalling

As was done previously, the target maximum aggregate load is selected by finding the magnitude of the 101st largest peak load with no third party signalling. The required reduction at any point that exceeds the target is divided evenly amongst the battery systems. For a penetration level of 5%, this results in 103 signalled periods for which the required response is achieved 22 times. Looking at Figure 6.48, which shows the required reduction against the achieved reduction, there are many points that, while not achieving the required reduction, are close to doing so.

When the magnitude of the reduction signal is increased by a factor of ten, the number of periods for which the target is achieved or exceeded increases to 55. There are signalled periods where more than five times the required response is achieved. This highlights the need for an intelligent and optimised signalling system; just because the available response exceeds the requirement does not mean that every system has the available response to contribute equally. Conversely, there is risk in counteracting that by increasing the response asked of each system; the achieved response may end up being much greater than required. This risks reducing the reduction able to be achieved at future times.

As the penetration level increases, so too does the number of periods for which the desired response is achieved. At a penetration level of 50% with an even sharing of signalled reduction, the target is achieved 66% of the time. This increases to 98% at a penetration level of 100%. The effect of this peak reduction signalling on the network load is well illustrated in Figure 6.49, which shows the network load both with and without third party signalling for a penetration level of 50%. The shaving of peak winter

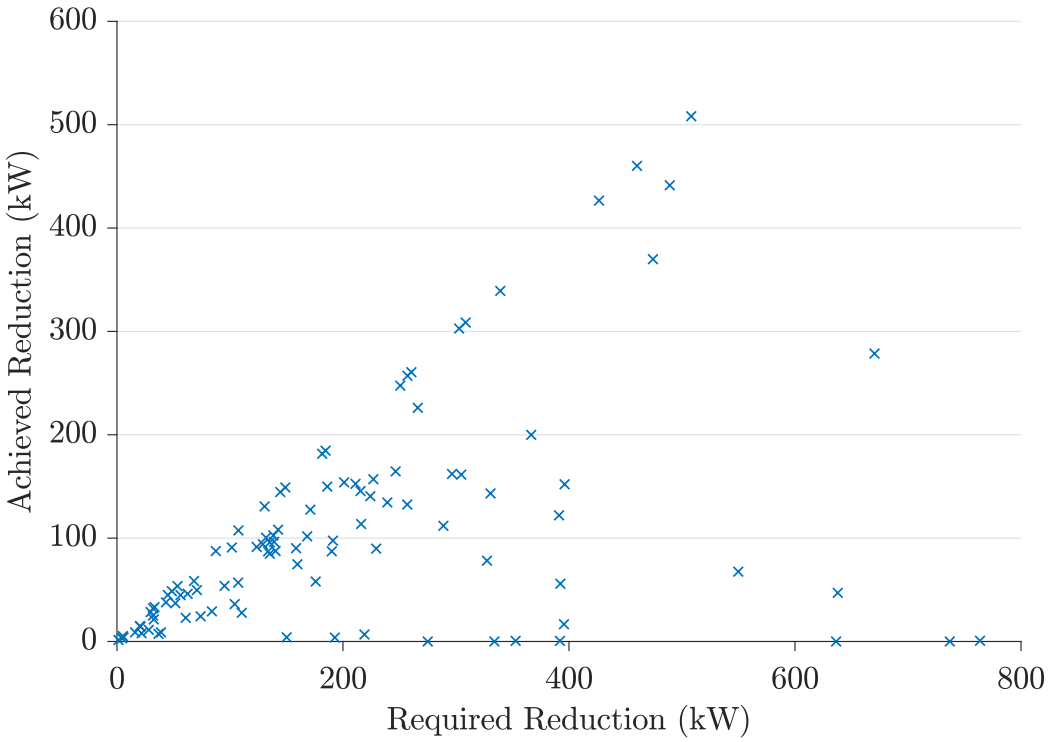

Figure 6.48 Required reduction against achieved reduction for a 5% penetration level in a network of 2212 households under peak/shoulder/off-peak pricing.

loads is clearly visible.

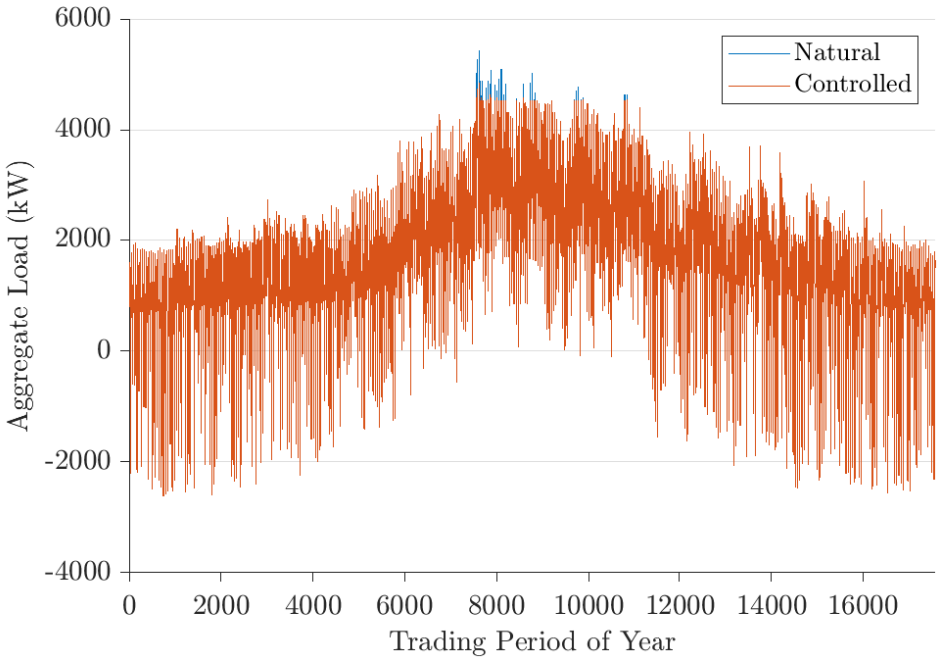

Figure 6.49 Aggregate network load for 50% penetration in a network of 2212 households both with and without third party signalling.

6.3.3.2 Economic Implication of Third Party Control

This section presents the economic implication of third party control for the system owners. The cost increases associated with responding to a signal that is an even share of requested response is shown in Figure 6.50. It follows the same trend as has been seen with the other pricing structures: a higher cost at low penetration levels which decreases as the penetration level increases. From penetration levels of 20% through to 100%, there are outlying households that experience a cost decrease as a result of responding to this peak reduction signalling. Given the low battery utilisation that results from this particular rule set, this is not entirely unexpected. Much like the other pricing structures, these cost increases are minor when considered against the total annual energy bill. However, this third party signalling has been shown to offer some success reducing and limiting network peak loads.

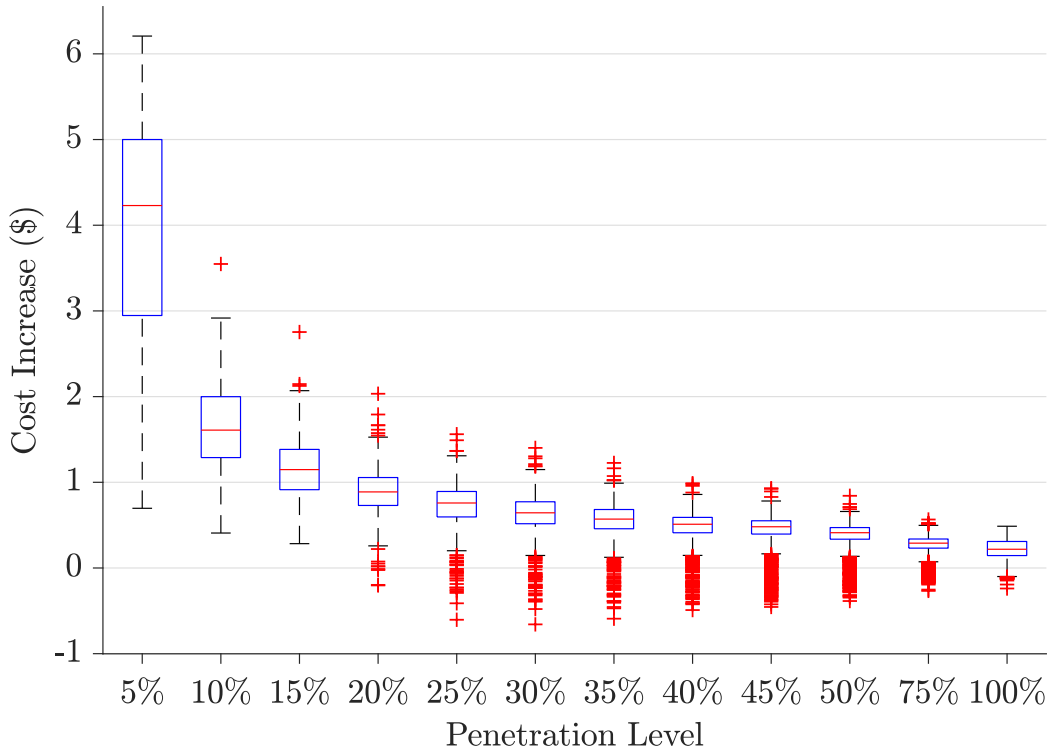

Figure 6.50 Cost increases for households that result from responding to third party load reduction signalling.

6.3.4 Summary of Peak/Shoulder/Off-peak Pricing

Peak/shoulder/off-peak pricing was chosen as a test case because it was hypothesised that it would create battery behaviour that would provide positive network effects. By having a shorter high priced peak period than a simple day/night pricing, it was thought that battery discharge activity would be focussed on this time and subsequently network peak loads would be decreased to a greater extent than the day/night case. The flaw in

this logic is that it is dependent on peak loads falling within the peak price periods. The results have shown that this is not always the case, and there are a number of peak load periods which do not experience a reduction from natural battery system behaviour.

In some aspects, the rule-based method provided more desirable results than the MILP method in that across penetration levels of less than 50%, there was less increase in the magnitude of top 100 peak loads than under the MILP method. This can be attributed to the dead-band where shoulder pricing results in neither battery charge nor battery discharge. The drawback of the dead-band is the reduction in financial savings achieved for the system owner. The short peak period results in underutilisation of the batteries. They spend large periods of time at, or near, their maximum SOC. A more intelligent rule set would prioritise discharge in peak pricing periods but would also allow for some discharge during shoulder pricing.

The generally high SOC results in high levels of available reduction power that can respond to third party signalling in order to reduce network load. It is shown that the cost of this to an individual system owner is minor, while the aggregate effect on the network can be significant.

6.4 SUMMARY

This chapter has presented results for the two methods being applied to three different pricing structures. It was found that, in general, the financial returns resulting from the installation of a BESS are less than those achieved through installation of PV generation.

It was found that under the day/night pricing structure, for penetration levels of less than 25%, the natural BESS behaviour resulted in reductions of network peak loads. On average, each BESS contributed 1.1 kW of peak reduction across the top 100 annual peaks. Above 25% penetration, loads from charging during the low priced periods begin to cause aggregate loads above the existing network peaks. At 100% penetration the single largest network load was increased by 45% compared with 0% penetration. In the spot pricing case this occurred for penetration levels greater than 10%.

The financial returns under the rule-based method for day/night pricing compare well to the optimal results obtained with the perfect foresight MILP method, with a reduction of only 7.5%. The rule-based method for spot pricing and peak/shoulder/off-peak pricing performs less well however. This highlights the challenge of designing rule sets to deal with high volatility of the spot price, as well as reflecting the poor rule set chosen for the peak/shoulder/off-peak case which resulted in underutilisation of the BESS.

Further analysis considered the ability of BESSs to provide peak reduction services

above and beyond any reduction that results from their natural behaviour. It was shown that under the day/night pricing structure BESSs have little capability to provide any additional peak reduction. Under a spot pricing structure the BESSs have the capacity to respond to additional peak reduction signalling however a sensitivity to the dispatch method was demonstrated. As an artefact of the chosen rule set, the peak/shoulder/off-peak pricing structure showed high levels of available reduction capacity due to the high SOC that the rule maintained.

These results have shown that the pricing structure a household is subject to influences, not only the economics of a BESS, but also the behaviours these systems display and the subsequent effects on aggregate network loads. It was also shown that the capacity of BESS to provide additional peak reduction services to a distribution network is sensitive to the pricing structure under which the BESS is operated.

Chapter 7

FUTURE WORK

7.1 OVERVIEW

This chapter presents a number of areas which could be improved upon and that could serve as directions for future research. One of the most significant areas is the determination of the efficiency functions used for both the MILP and rule-based methods. While the MILP method developed in this thesis would remain applicable to an efficiency function of any arbitrary shape, the determination of the function itself could be better validated. Additionally, there is no bound to additional complexity and sophistication that could be added to the rule-based method in order to bring its financial savings closer to the upper bound of the optimisation method. This includes improvements to how the price thresholds for decision making are selected. A more diverse PV generation dataset could be utilised to include the effects of spatial diversity across the households modelled. Finally, there is scope for further investigation into battery system operation characteristics that could be desired by distribution network operators beyond simple peak reduction.

7.2 EFFICIENCY

The MILP method (Chapter 3) allows any arbitrary charge/discharge efficiency to be utilised, subject to it being approximated as a piecewise constant function. The efficiency model which was used included both a constant component and a charge/discharge rate dependent component. Given limited manufacturer data, the actual values used were reliant on significant assumptions.

Further work could be undertaken to ensure the efficiency model accurately reflects not only the losses of the power electronic converter associated with a BESS, but also the electrochemical losses of a battery. There are numerous equivalent circuit models for both power converters and batteries into which further exploration is required to determine the form of model that both accurately represents the real world efficiencies achieved and that is suitable for implementing in a MILP optimisation. One example of

an extension that could be made is the dependence of the series resistance component on SOC and temperature, rather than using a constant resistance value [57].

It was shown that the efficiency model is critical to the battery behaviour obtained during low priced grid charging periods. As such, improvement of the efficiency model to better reflect the real world operation of BESSs will increase the accuracy and relevance of the results obtained under the methods developed in this thesis.

Further improvement to the BESS model could include elements of battery self-discharge, ageing, and degradation. Calendric ageing and degradation due to cycling could be incorporated into the method. The rolling horizon approach allows for model parameters to be updated between sub-problems. These battery ageing and degradation effects are of particular importance when considering the total lifetime of a BESS rather than a single year only.

7.3 RULE-BASED METHOD

The rule-based method was purposefully kept reasonably simple to identify how close a simple operation strategy can get to the upper bound of the perfect foresight MILP optimisation. There is no shortage of ways in which complexity and sophistication could be added to the rule-set in order to close the gap between the two methods.

One clear aspect of improvement is the determination of the price thresholds at which charging and discharging occurs. The improvement that this could bring is most clearly demonstrated in the spot price case, where the gap between the savings achieved under the perfect foresight MILP method and the savings achieved by the rule-based method was significantly greater than for the day/night case. In the spot price case, the mean reduction in annual savings from the MILP method to the rule-based method was 20%, compared to only 8% for the day/night pricing case. Additionally, as discussed in Chapter 6, the thresholds used for the peak/shoulder/off-peak pricing structure could be improved in order to increase battery utilisation and provide network peak load reduction during shoulder periods as well as peak periods.

Furthermore, the PV generation forecast could be expanded beyond the 3 category model, as well as including forecasting of household load to better inform battery operation decisions.

7.4 APPLICATION OF METHODS TO REALISTIC SCENARIOS

It is recognised that the cases chosen do not fully encapsulate realistic real-world scenarios. Nevertheless, they have been chosen to demonstrate the application of the methods to different types of pricing structures, to present the types of analysis that can be undertaken with the results, and to highlight some of the key BESS behaviours that result from the chosen pricing structures.

More realistic scenarios would incorporate greater diversity. Diversity would be seen in different pricing structures for different households in order to be reflective of the significant consumer choice that exists in the retail electricity market. Diversity would also be seen in PV system sizing, PV generation profiles, and BESS sizing and parameters. To include that level of diversity requires assumptions to made about likely future uptake scenarios, and the realistic distributions of these parameters. In order to use the methods developed in this thesis to produce likely future scenarios for both EDBs and consumers, appreciation and consideration needs to be given to the selection of those parameters.

7.5 DISTRIBUTION NETWORK ANALYSIS

A final area of potential future work is the expansion of the analysis on network peak load effects to include other factors which may be of interest to EDBs. As identified in [57], one such factor could be the ability of BESSs to provide feed-in damping. This means battery management systems would spread their charging across the high PV generation period rather than reaching a full SOC early in the day, which results in a sharp increase in exported power fed to the grid.

Chapter 8

CONCLUSION

This thesis began by outlining new technologies which, driven by technological advancement and environmental pressures, threaten to disrupt the traditional electricity supply industry and present problems, but also opportunities, that have not been seen before. Existing BESS modelling and optimisation methods were presented and reviewed.

LP and MILP optimisation methods for battery behaviour under different pricing structures were developed, which incorporate rate-dependent battery charge/discharge efficiency models. The optimisation methods utilise perfect foresight of household load and PV generation in order to produce an upper bound on the savings that could be achieved by a consumer. By implementing a rolling horizon technique, with a problem length of 2 days, the optimisations for a full year of battery operation for a single household could be solved in 128 seconds. This ensures it is feasible to model a large number of individual households in a practical time. The rolling horizon technique also reduces the impact of the end of optimisation SOC constraint.

A heuristic rule-based method for simulating BESS operation was developed which does not rely on perfect foresight, but instead uses a basic PV forecast. This puts a lower bound on the financial savings easily achievable by a battery management system. It is expected that a commercial battery management system could produce equal, if not better, savings for consumers.

These modelling methods were applied to three different pricing structures (day/night, spot price, and peak/shoulder/off-peak) in order to demonstrate their application to both known fixed pricing structures, as well as unknown real time varying pricing structures. It was shown, that under all pricing structures, there are greater savings to be made through the installation of PV generation than there are from installing a BESS alongside PV generation. Under day/night pricing the median annual saving from the installation of PV generation was $780 compared to $500 for the installation of a BESS.

It was shown that the heuristic rule-based method can achieve close to the optimal savings when the pricing structure is simple, and a clear operation strategy is apparent, such as for the day/night pricing case. This was highlighted by a mean reduction in

household savings of only 7.5% when moving from the perfect foresight MILP method to the rule-based method. Under more complex pricing structures, with a less apparent optimal strategy, it is more challenging to create a rule set which achieves savings near the bounding perfect foresight case. This was demonstrated by the spot pricing case where the reduction in household savings from the optimal method to the rule-based method was 15-30%.

In particular, the effect of battery behaviour on network loads during low priced periods when BESSs are charging from the grid was observed. These results highlighted the significance that the efficiency models hold in determining battery behaviour during these periods. Under the MILP method, the greatest efficiency was achieved at a charge/discharge rate of 3.3 kW, while under the rule-based method low price period charging was set at 1 kW. The effect of this difference is that under the MILP method an increase in the annual peak was observed for a penetration level greater than 20%. Under the rule-based method, however, an increase was not observed until penetration levels of 50% were exceeded. If aggregated battery behaviour is to be modelled, then it is critical that consideration is given to charge rate during low priced periods. This could be determined by charging at the most efficient rate, as would be purely economically rational, or it could be artificially constrained by a battery management system.

The ability of BESSs operating in an economically rational fashion to provide network peak reduction services was simulated, and methods of analysis to capture and present this capability were shown. It was demonstrated that BESSs operating under day/night pricing had little capacity to provide any peak reduction beyond that which occurred from their natural behaviour. The annual peak loads occur on days on poor weather in winter where PV generation is low. This means that BESSs have depleted their stored energy during the day leaving little available to contribute toward reducing the evening peak.

When considering the ability of BESSs to reduce the top 100 annual loads to the level of the 101st peak it was shown that under day/night pricing the only points at which the greatest loads could be reduced was when they were caused by low price charging.

Under the spot pricing scenario, network peak loads were seen to increase for any penetration greater than 10%. This is due to the lack correlation between the spot prices and the distribution network load. This highlights the importance which pricing structure design holds in unlocking the potential of BESSs to provide useful peak reduction to distribution networks. The systems themselves do not inherently provide positive network benefits, but instead will rely on incentivisation to produce behaviour which positively impacts network loads. A key aspect of this will be the correlation of pricing to peak loads.

The financial implications for system owners of participating in signalled peak

reduction services was also analysed. It was shown that in general, when peak reduction is signalled only for the greatest 100 half-hourly loads annually, the annual cost to a system owner is less than $2. This is because these peak periods constitute only 0.6% of the total annual trading periods.

Finally, areas for potential future work were identified. In particular, the need for a clear vision of likely future uptake and pricing structures is required to be able to use the methods developed in this thesis to produce results that are reflective of likely real-world scenarios.

Design of operational strategies and tariff structures relating to domestic BESSs is a key future challenge for EDBs; this thesis proposes a methodology for assessing their impacts, and shows its importance using some current strategies being considered.

Appendix A

CASE 1 - DAY/NIGHT PRICING

The following appendices present a wider range of results than were shown in Chapter 6. These present the available reduction capability, peak reduction sufficiency, and achieved peak reduction for each of the three pricing structures across the full range of penetration levels (0-100%). While the observed behaviour is often similar between penetration levels, comparing results across penetration levels gives an insight into the rate at which the observed behaviours change.

A.1 AVAILABLE REDUCTION CAPABILITY

The following figures show the available reduction power as a function of aggregate load across different penetration levels for a network of 2212 households.

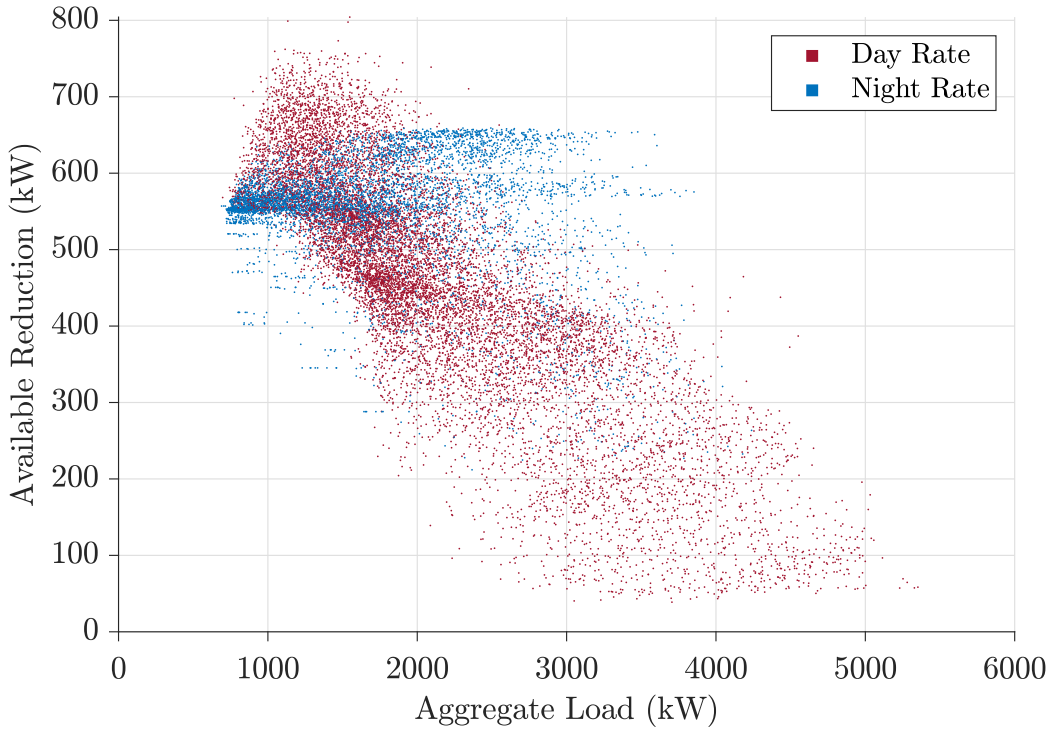

Figure A.1 Total aggregate load against available reduction capacity for a network of 2212 households with 5% PV and BESS penetration level.

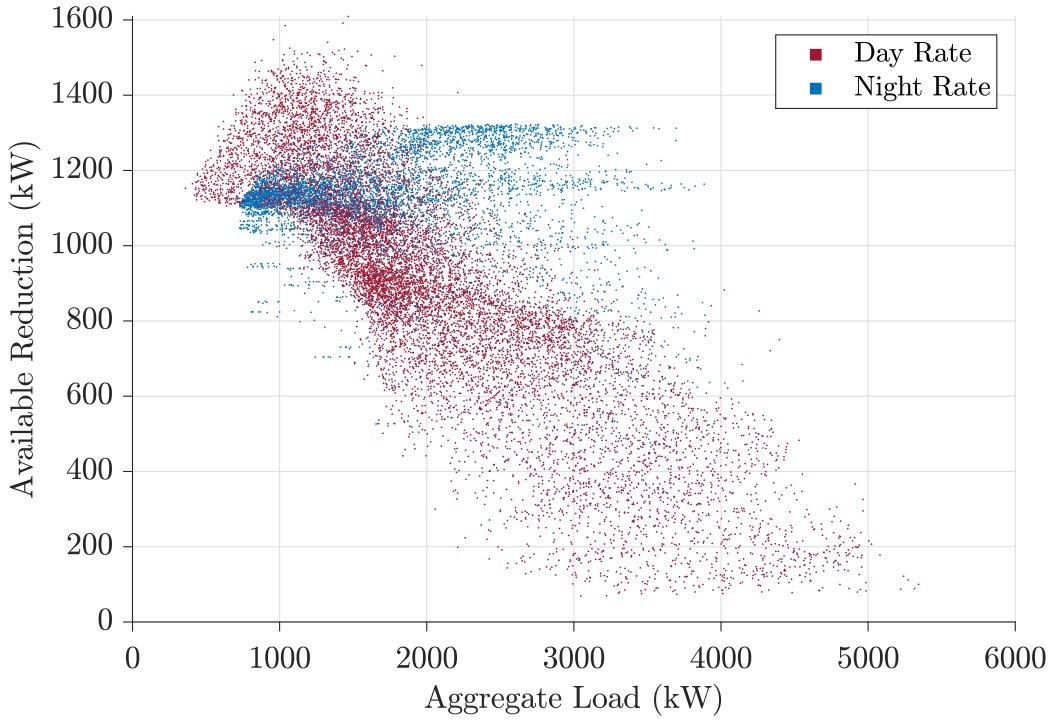

Figure A.2 Total aggregate load against available reduction capacity for a network of 2212 households with 10% PV and BESS penetration level.

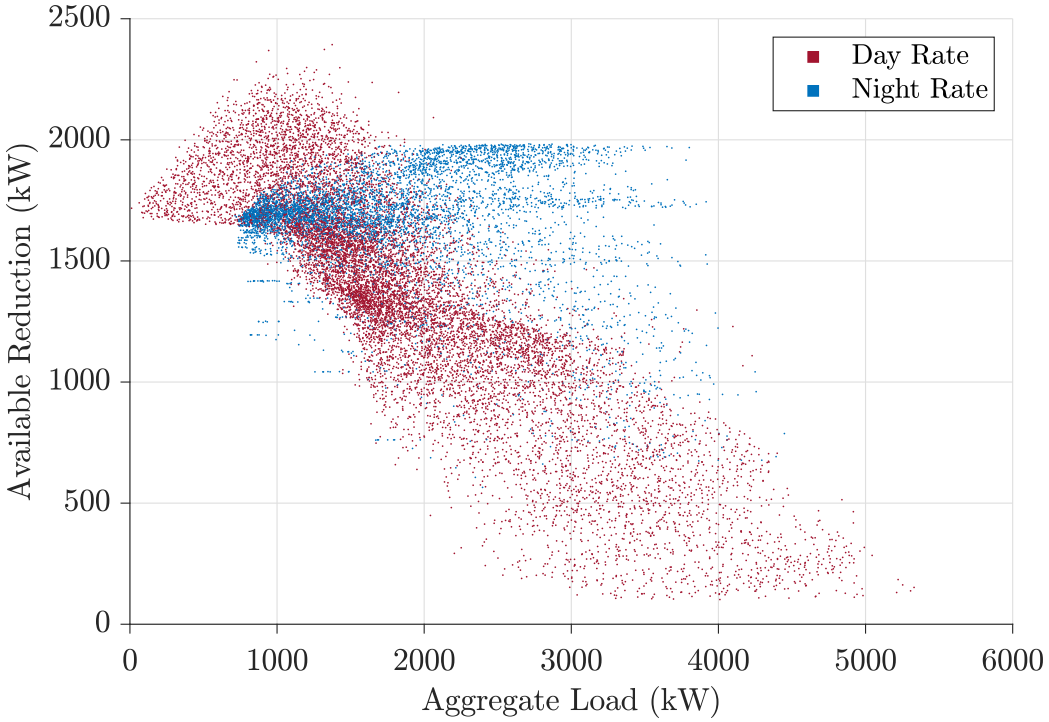

Figure A.3 Total aggregate load against available reduction capacity for a network of 2212 households with 15% PV and BESS penetration level.

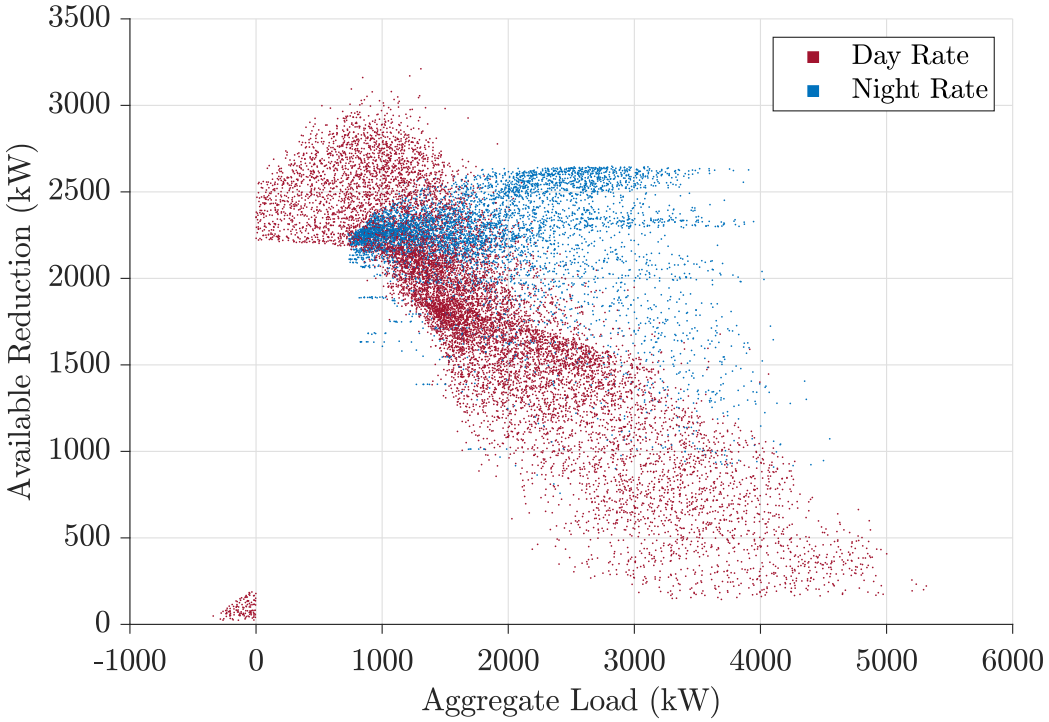

Figure A.4 Total aggregate load against available reduction capacity for a network of 2212 households with 20% PV and BESS penetration level.

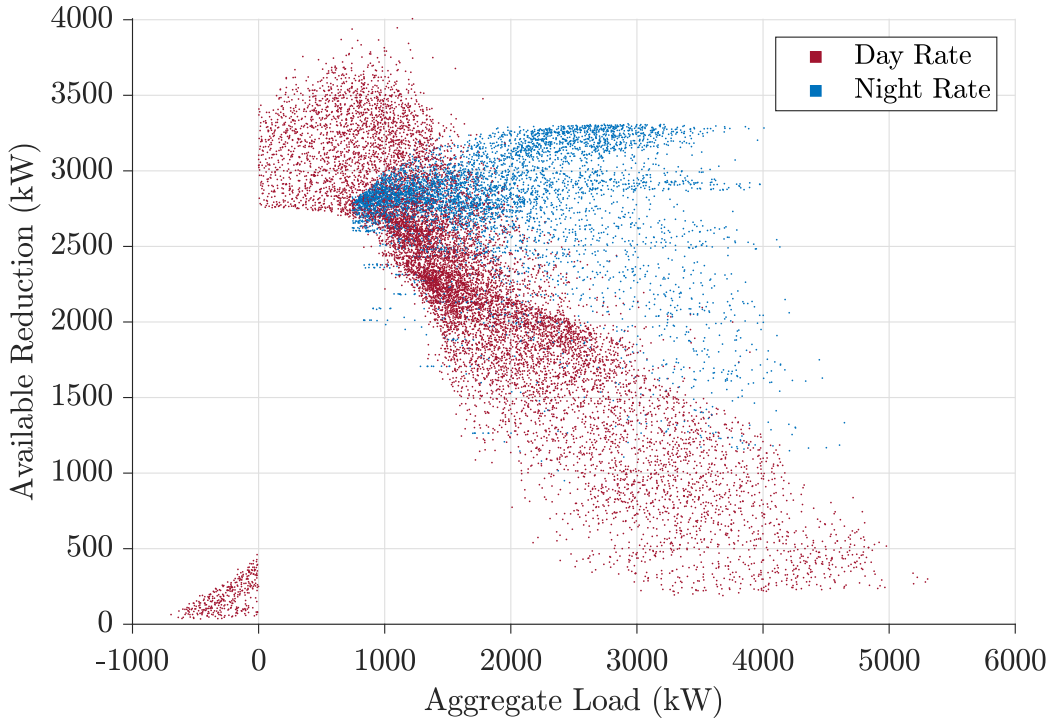

Figure A.5 Total aggregate load against available reduction capacity for a network of 2212 households with 25% PV and BESS penetration level.

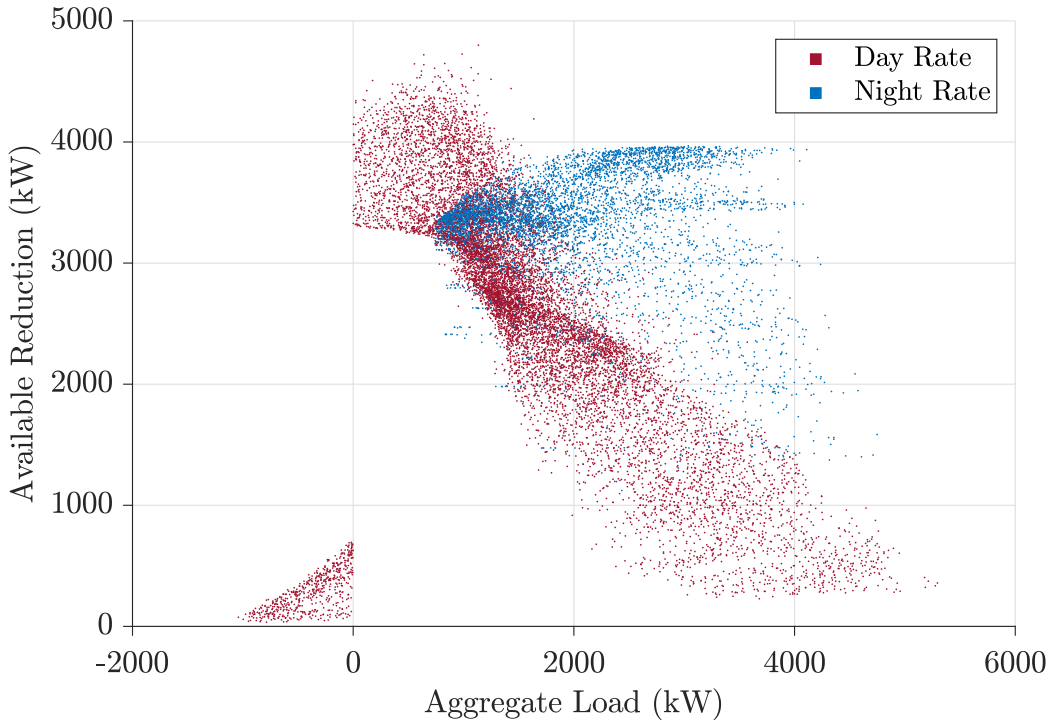

Figure A.6 Total aggregate load against available reduction capacity for a network of 2212 households with 30% PV and BESS penetration level.

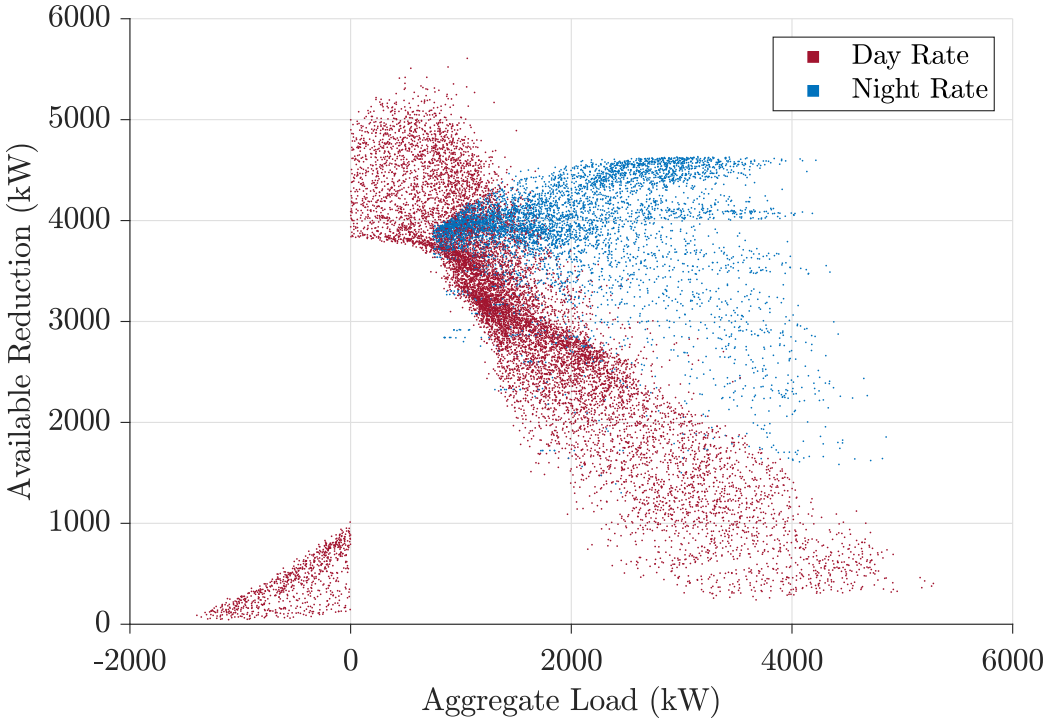

Figure A.7 Total aggregate load against available reduction capacity for a network of 2212 households with 35% PV and BESS penetration level.

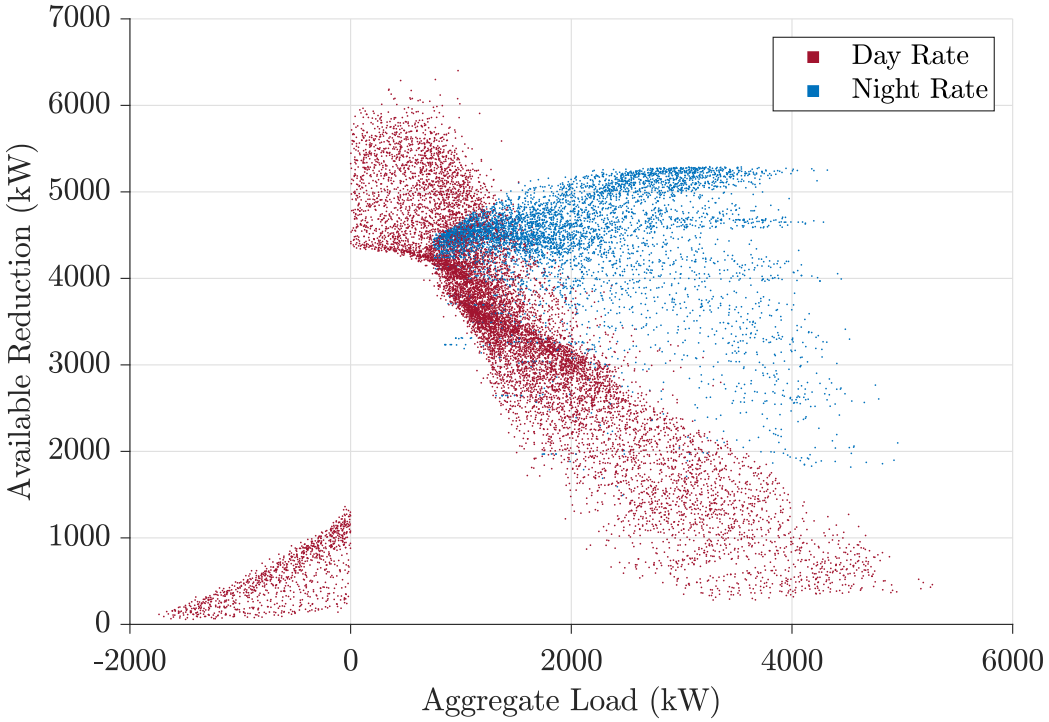

Figure A.8 Total aggregate load against available reduction capacity for a network of 2212 households with 40% PV and BESS penetration level.

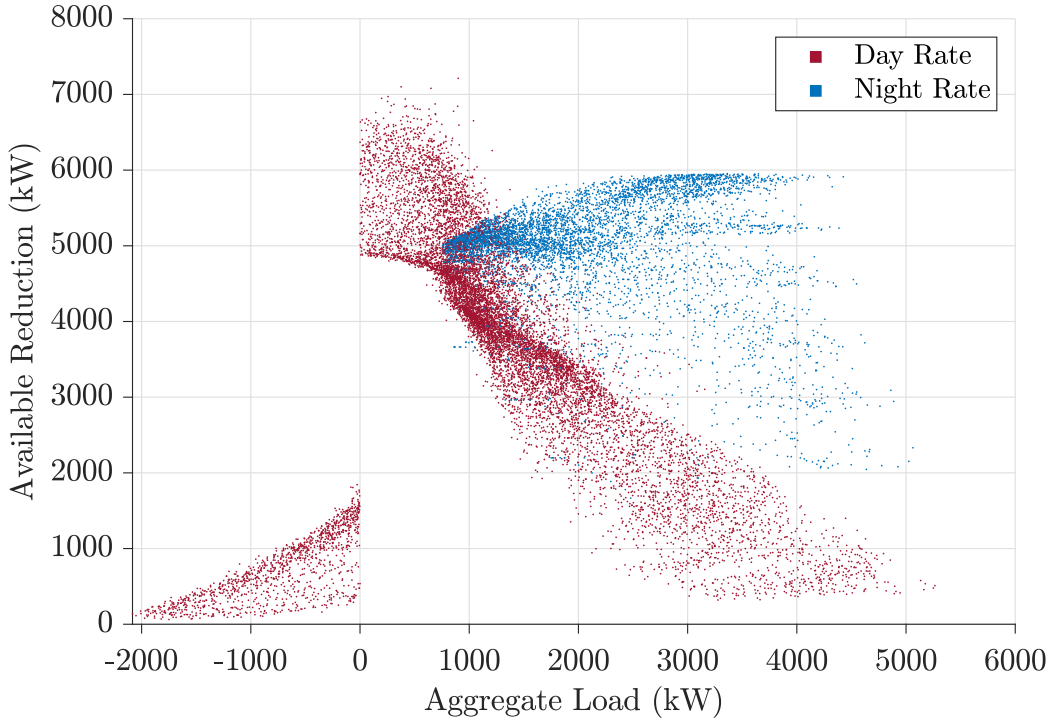

Figure A.9 Total aggregate load against available reduction capacity for a network of 2212 households with 45% PV and BESS penetration level.

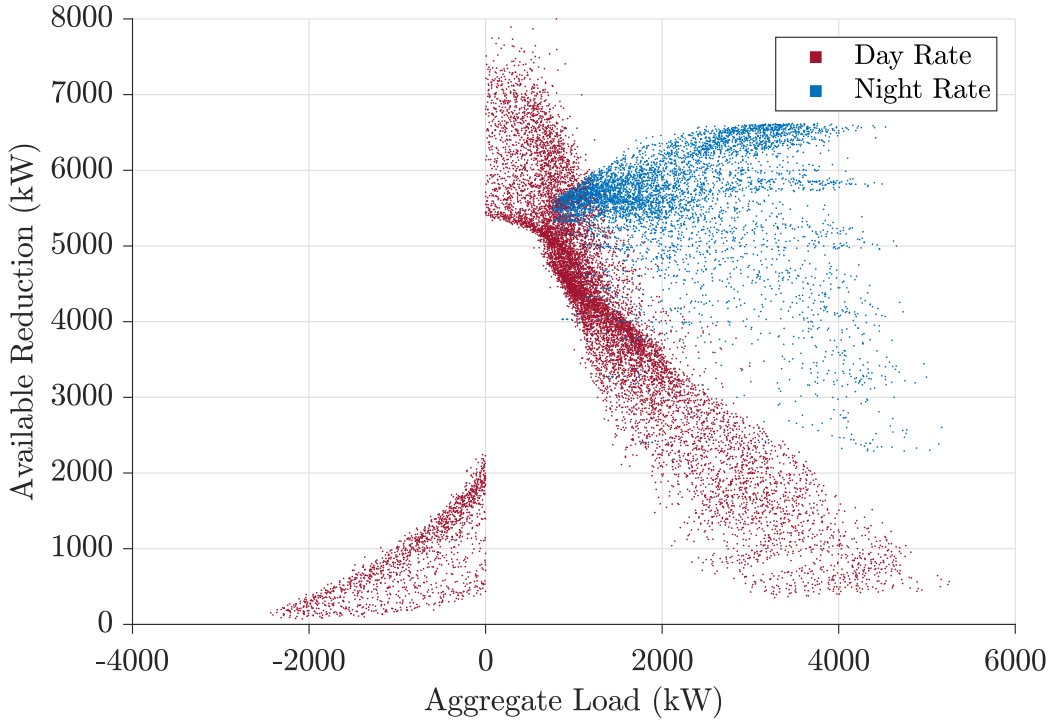

Figure A.10 Total aggregate load against available reduction capacity for a network of 2212 households with 50% PV and BESS penetration level.

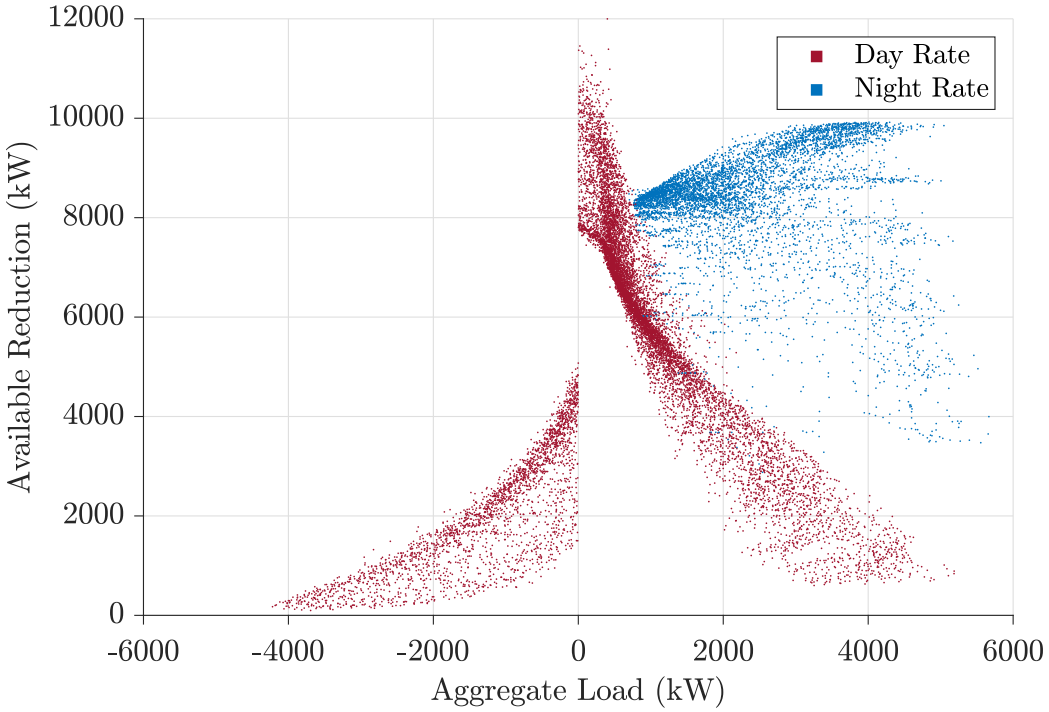

Figure A.11 Total aggregate load against available reduction capacity for a network of 2212 households with 75% PV and BESS penetration level.

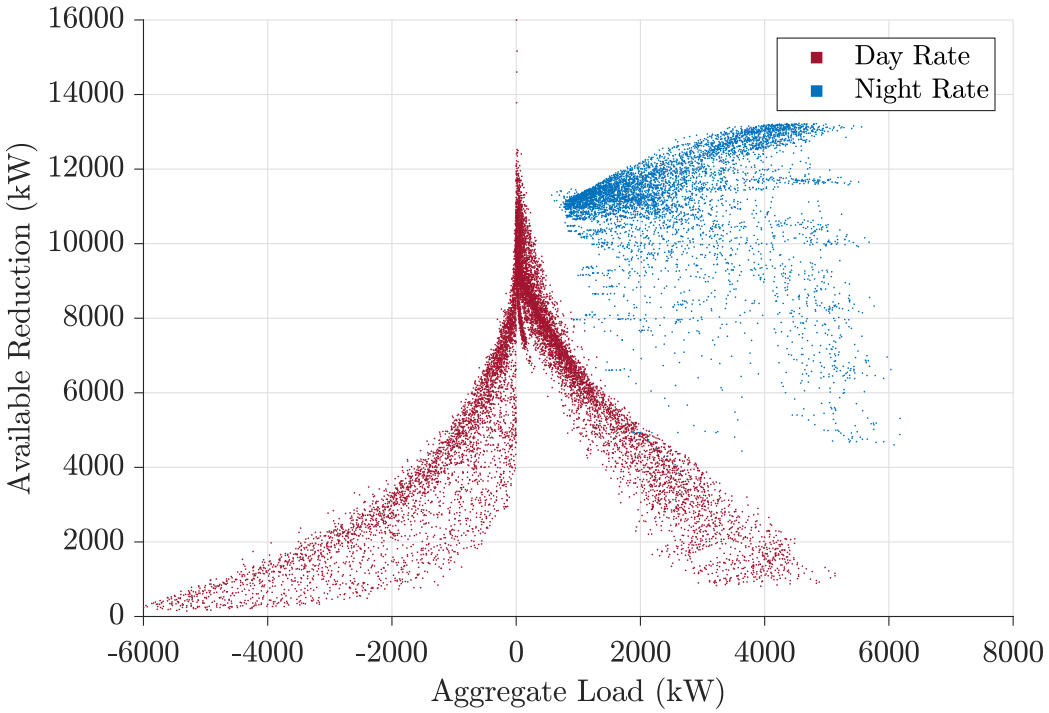

Figure A.12 Total aggregate load against available reduction capacity for a network of 2212 households with 100% PV and BESS penetration level.

A.2 PEAK REDUCTION SUFFICIENCY

The following figures shows the proportion of the top 100 peak loads where there is sufficient reduction capacity to reduce those peaks to the level of the 101st peak.

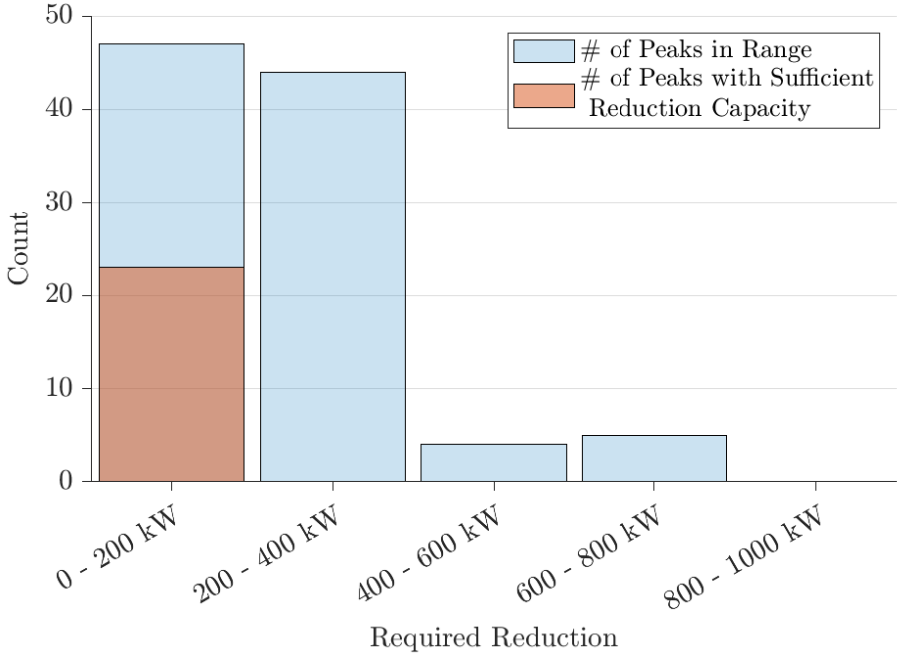

Figure A.13 Sufficiency of available reduction power to meet required reduction to reduce top 100 peaks to level of 101st peak for 5% penetration level in a network of 2212 households.

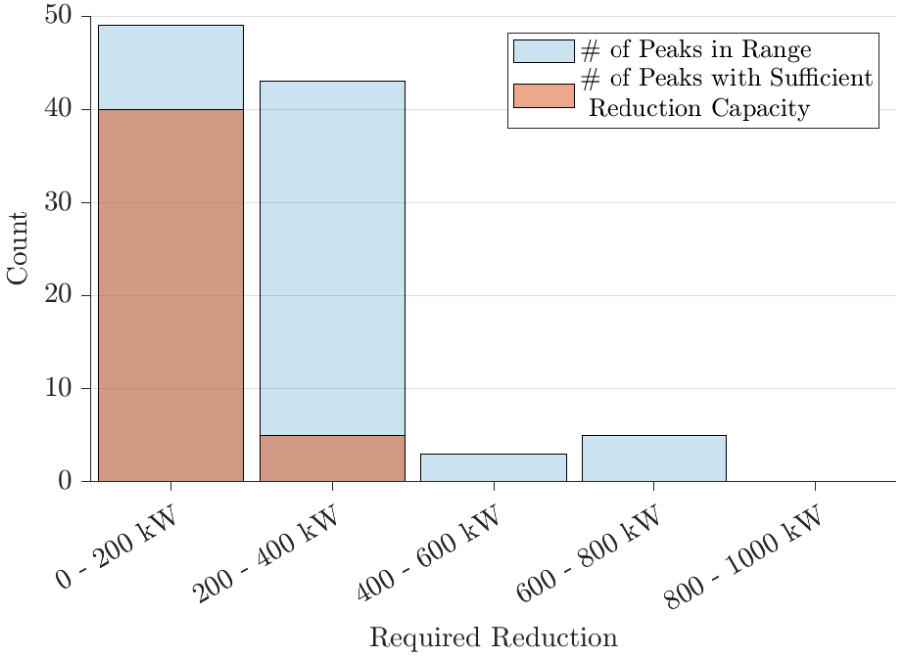

Figure A.14 Sufficiency of available reduction power to meet required reduction to reduce top 100 peaks to level of 101st peak for 10% penetration level in a network of 2212 households.

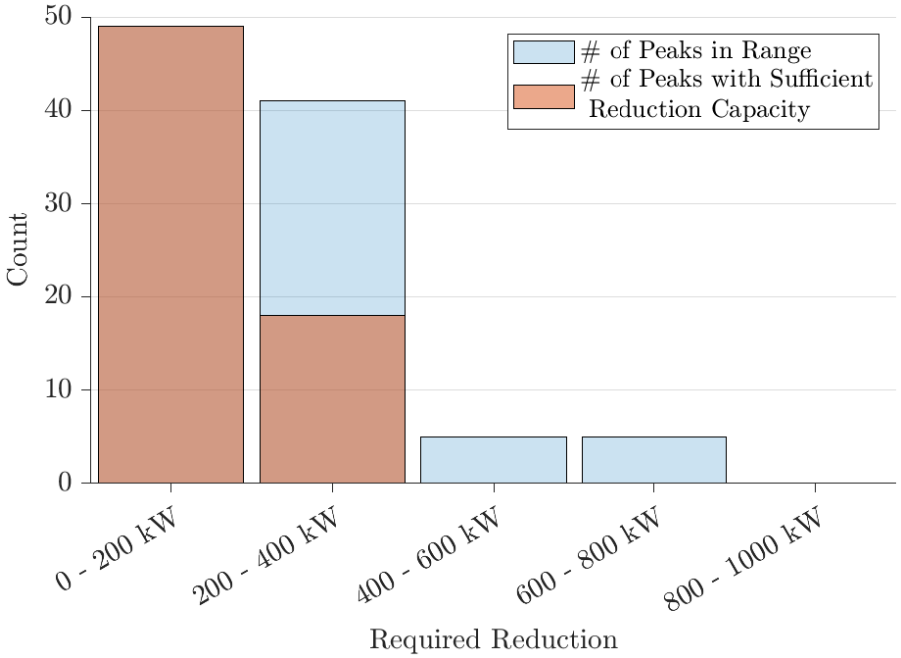

Figure A.15 Sufficiency of available reduction power to meet required reduction to reduce top 100 peaks to level of 101st peak for 15% penetration level in a network of 2212 households.

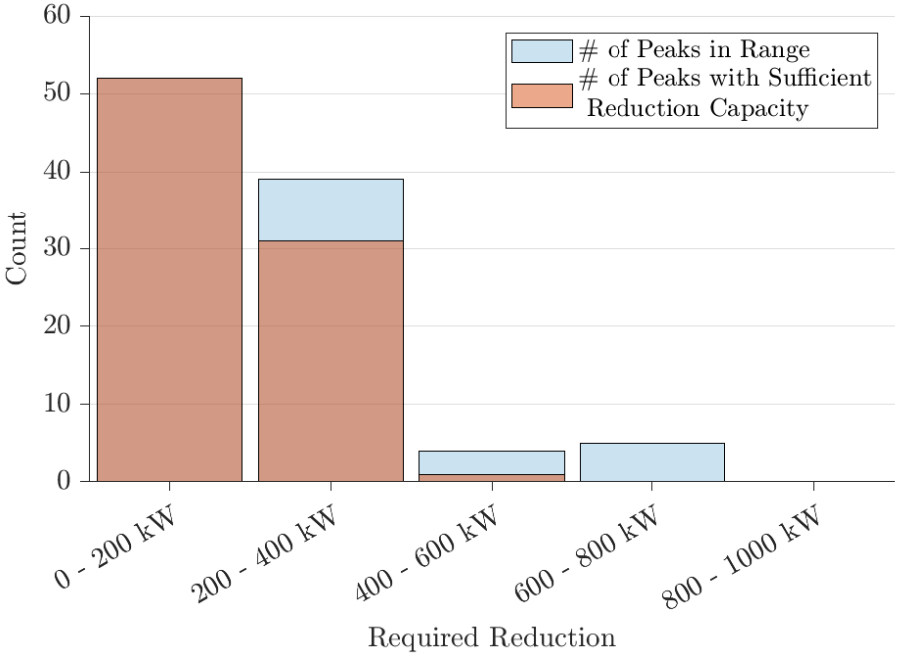

Figure A.16 Sufficiency of available reduction power to meet required reduction to reduce top 100 peaks to level of 101st peak for 20% penetration level in a network of 2212 households.

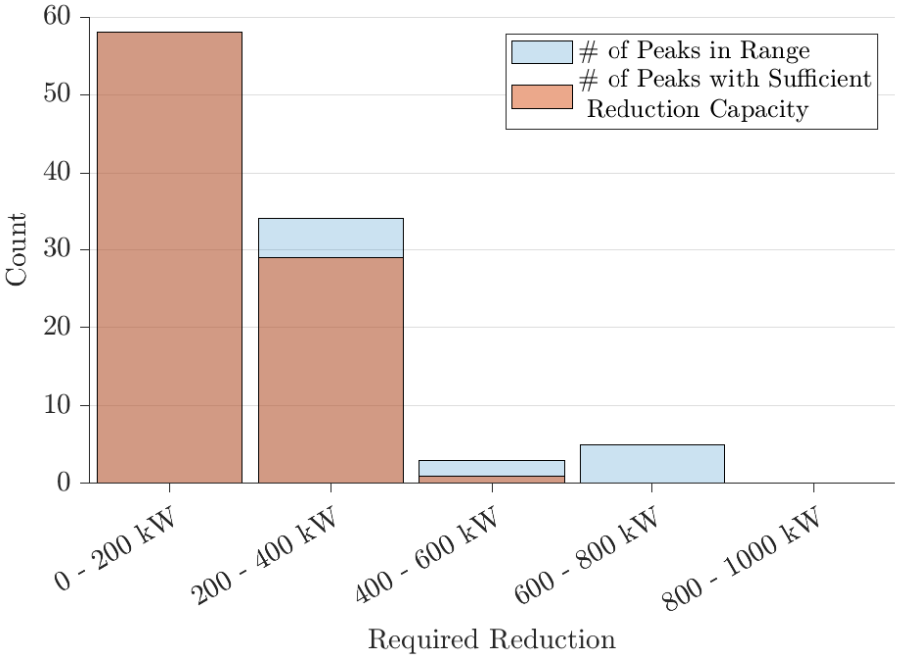

Figure A.17 Sufficiency of available reduction power to meet required reduction to reduce top 100 peaks to level of 101st peak for 25% penetration level in a network of 2212 households.

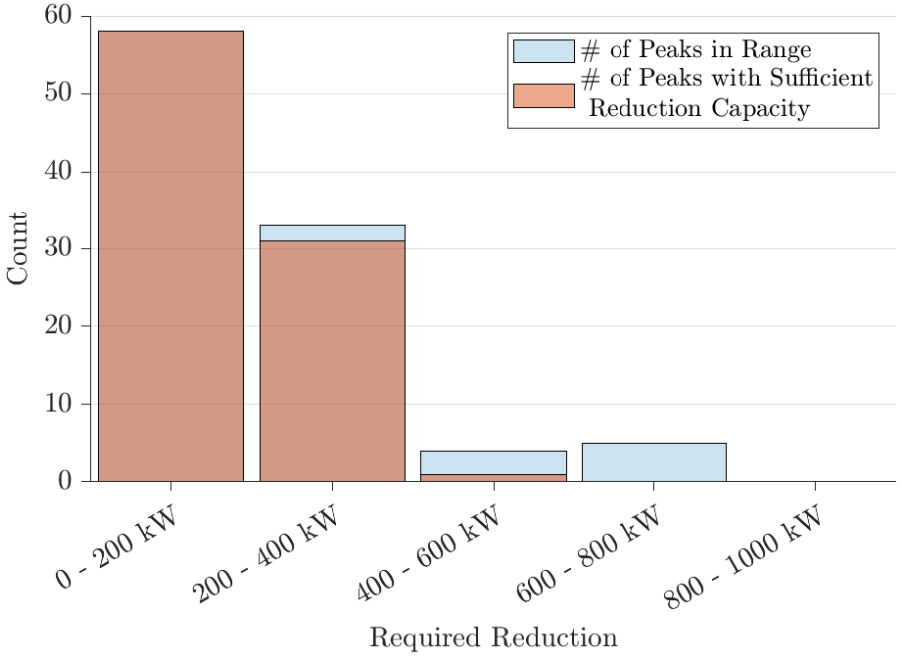

Figure A.18 Sufficiency of available reduction power to meet required reduction to reduce top 100 peaks to level of 101st peak for 30% penetration level in a network of 2212 households.

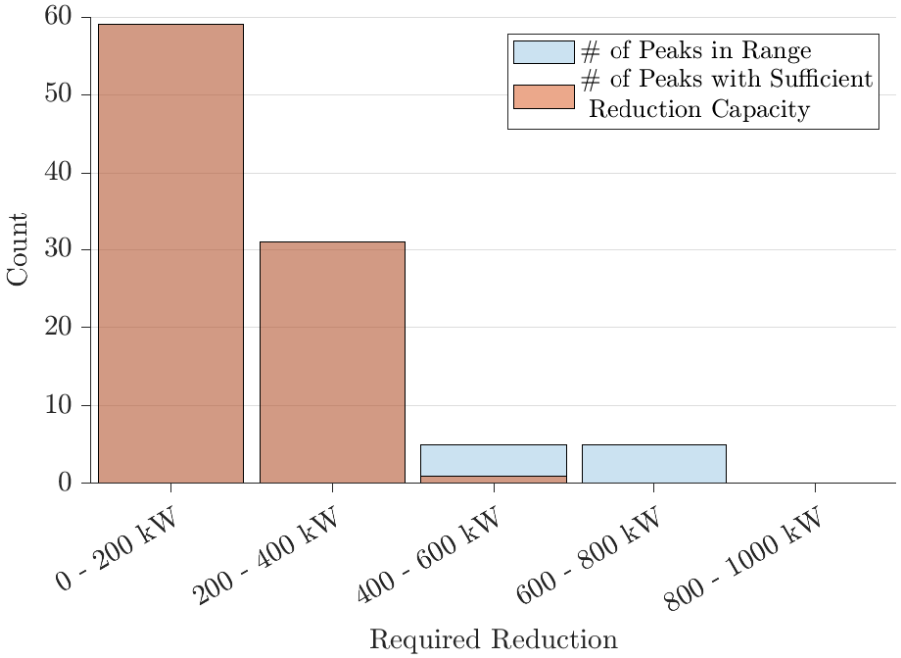

Figure A.19 Sufficiency of available reduction power to meet required reduction to reduce top 100 peaks to level of 101st peak for 35% penetration level in a network of 2212 households.

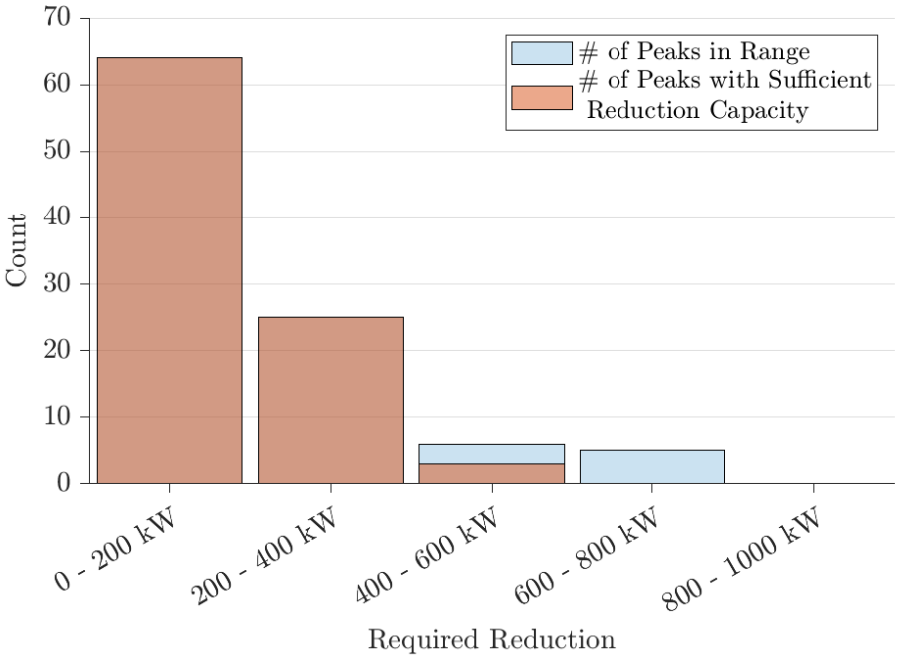

Figure A.20 Sufficiency of available reduction power to meet required reduction to reduce top 100 peaks to level of 101st peak for 40% penetration level in a network of 2212 households.

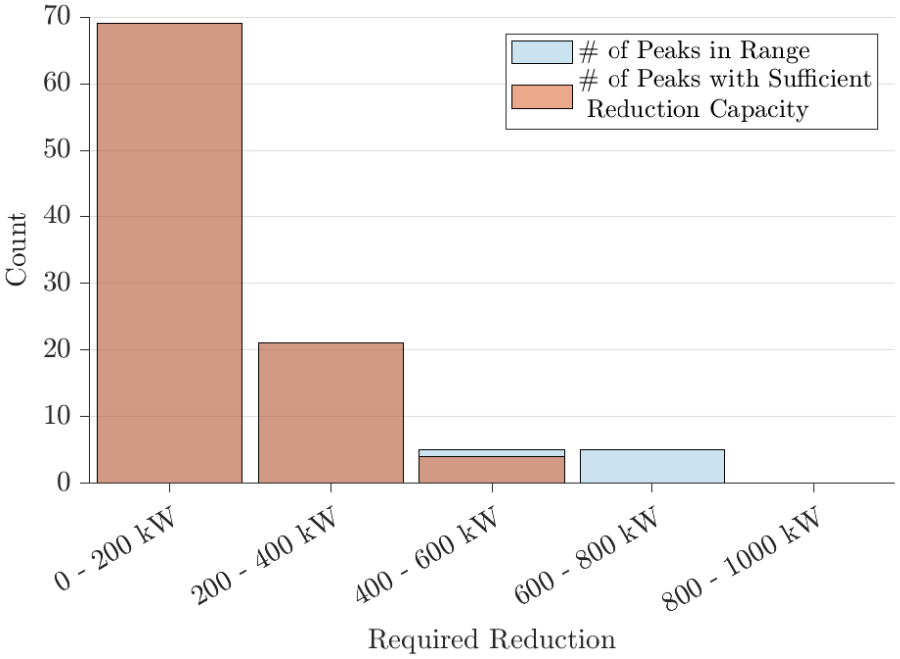

Figure A.21 Sufficiency of available reduction power to meet required reduction to reduce top 100 peaks to level of 101st peak for 45% penetration level in a network of 2212 households.

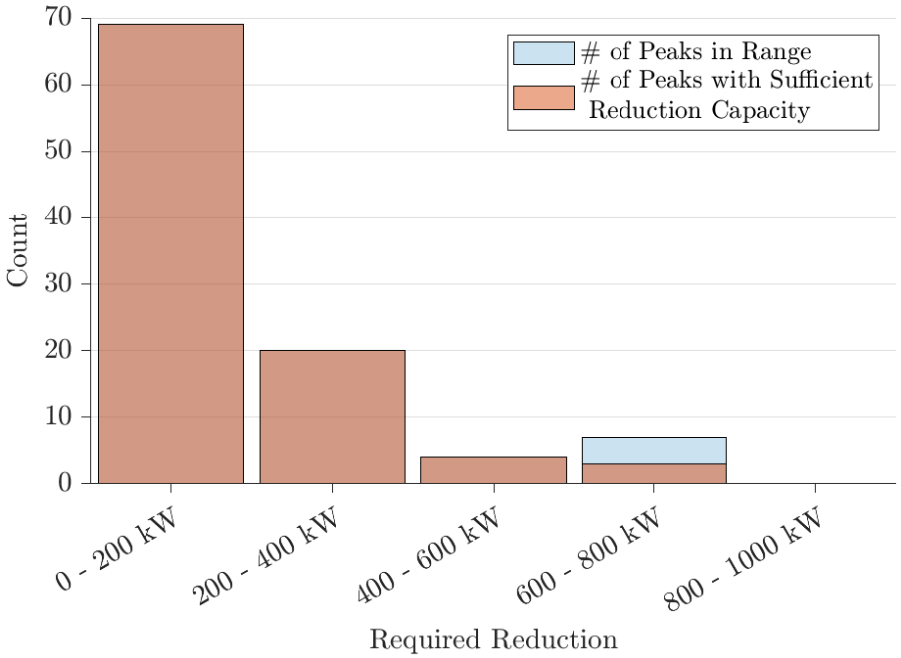

Figure A.22 Sufficiency of available reduction power to meet required reduction to reduce top 100 peaks to level of 101st peak for 50% penetration level in a network of 2212 households.

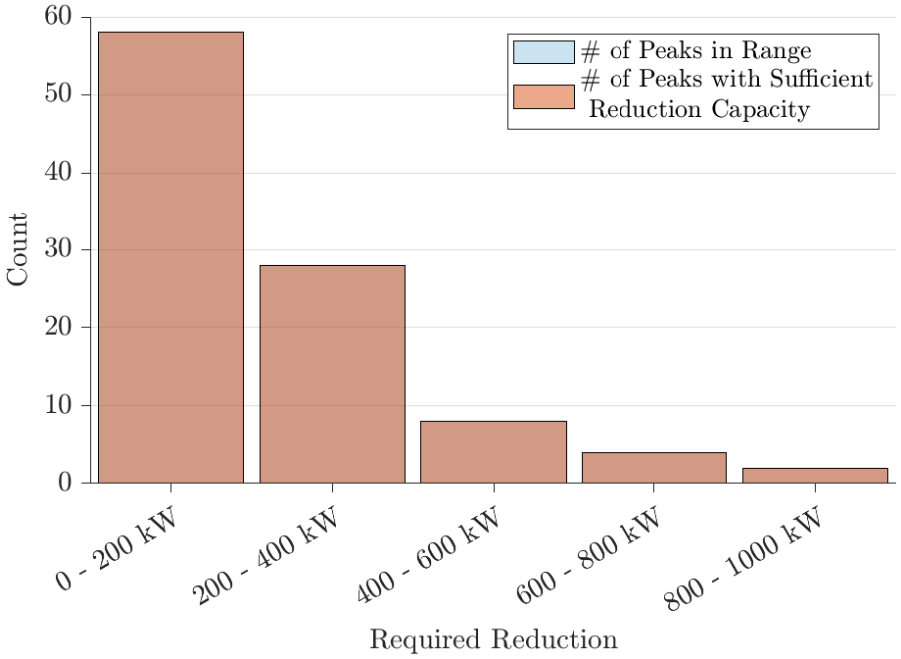

Figure A.23 Sufficiency of available reduction power to meet required reduction to reduce top 100 peaks to level of 101st peak for 75% penetration level in a network of 2212 households.

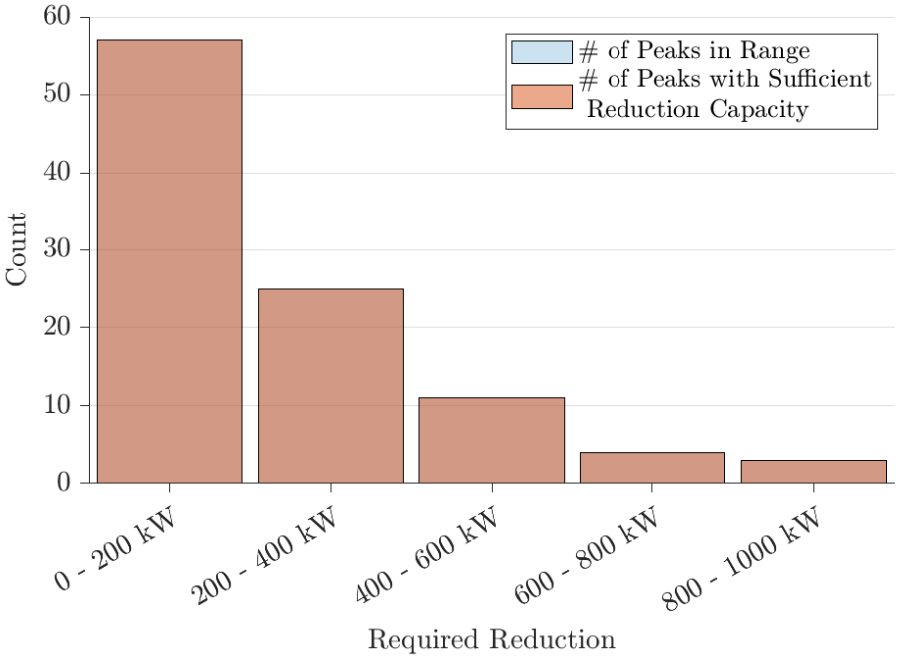

Figure A.24 Sufficiency of available reduction power to meet required reduction to reduce top 100 peaks to level of 101st peak for 100% penetration level in a network of 2212 households.

A.3 PEAK REDUCTION ACHIEVED

The following figures shows the achieved peak reduction against the required peak reduction where the required response is divided evenly amongst BESSs.

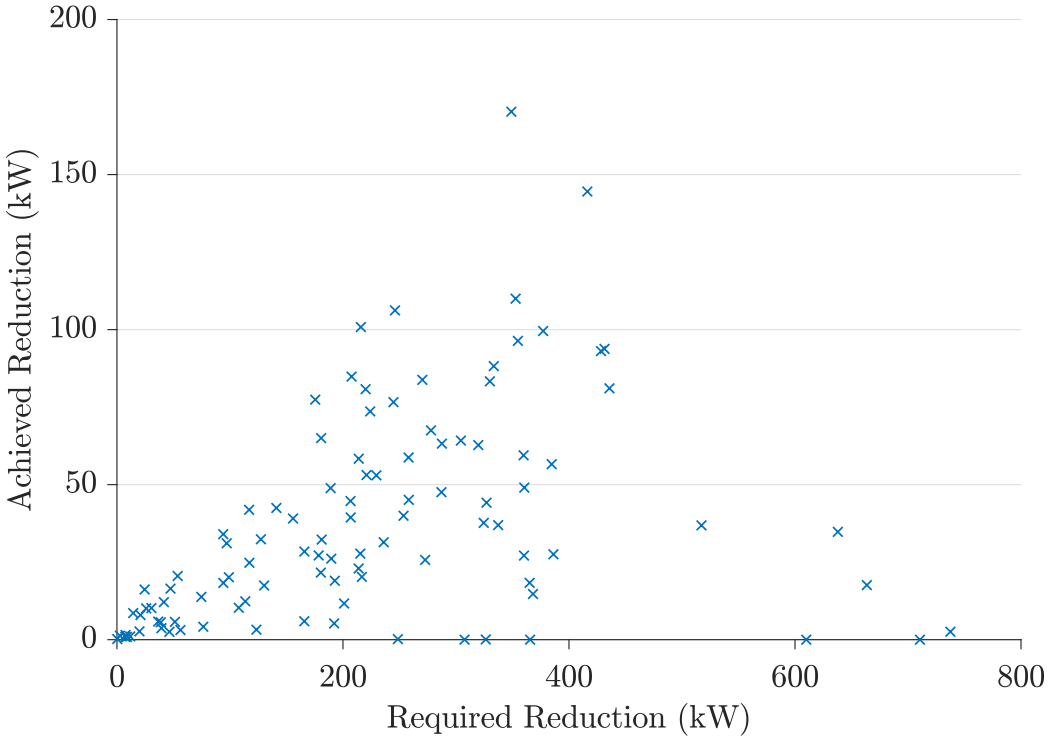

Figure A.25 Required reduction against achieved reduction to reduce top 100 peak network loads to magnitude of 101st peak for a network of 2212 households with a 5% penetration level and signalled response divided evenly between battery systems.

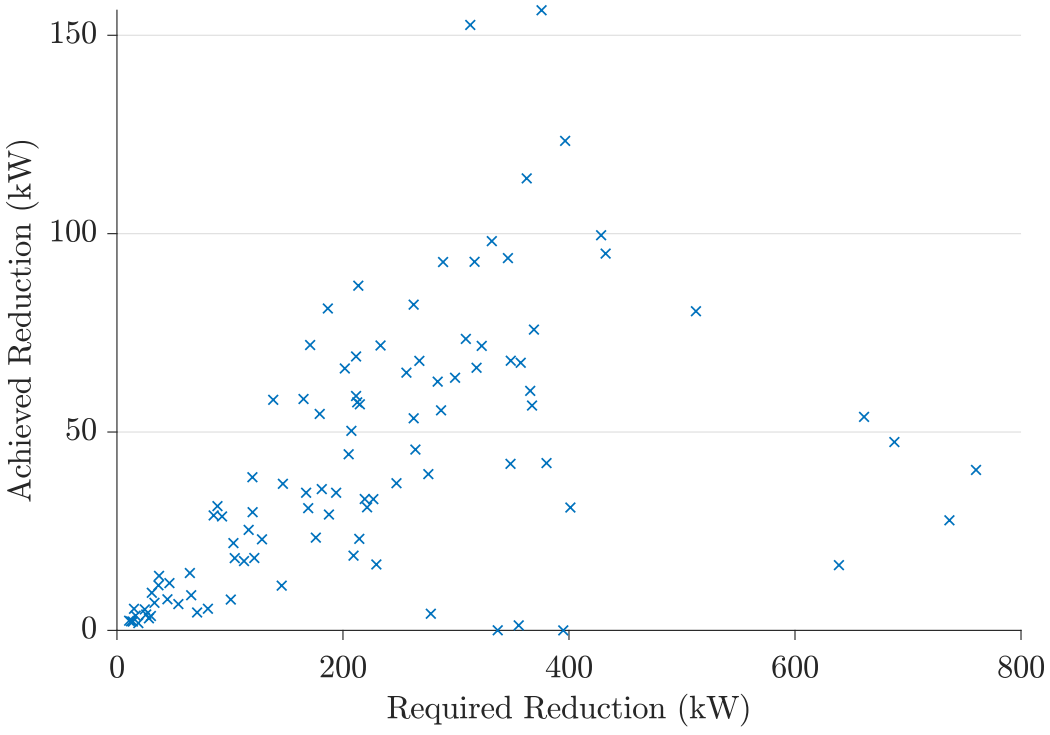

Figure A.26 Required reduction against achieved reduction to reduce top 100 peak network loads to magnitude of 101st peak for a network of 2212 households with a 10% penetration level and signalled response divided evenly between battery systems.

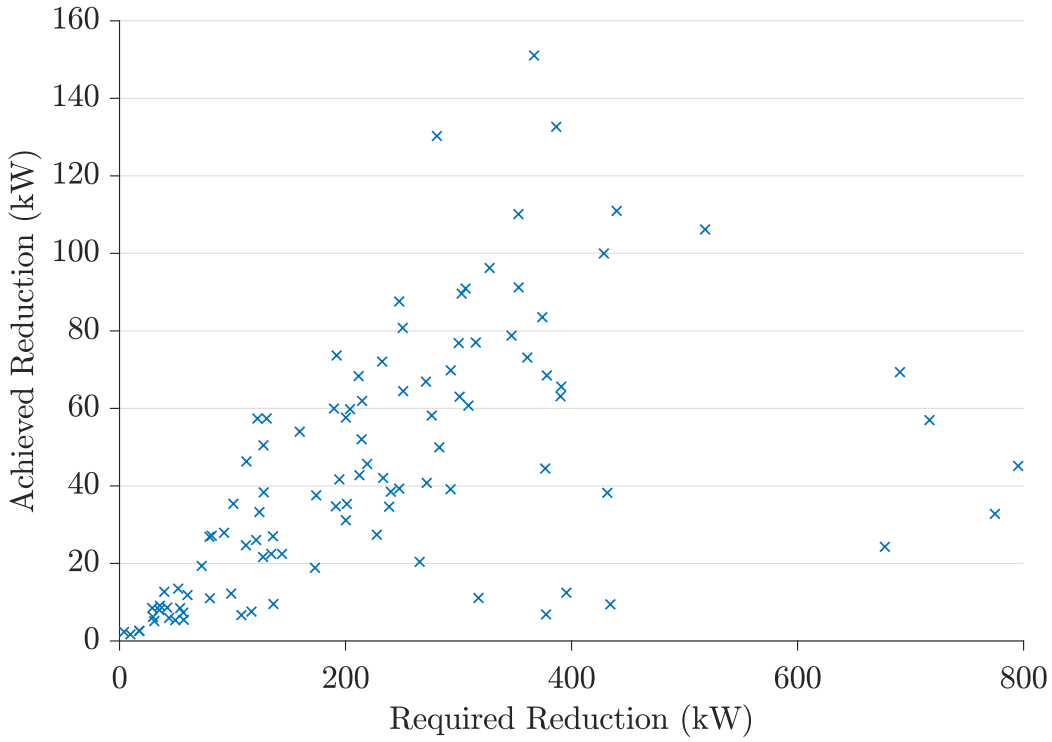

Figure A.27 Required reduction against achieved reduction to reduce top 100 peak network loads to magnitude of 101st peak for a network of 2212 households with a 15% penetration level and signalled response divided evenly between battery systems.

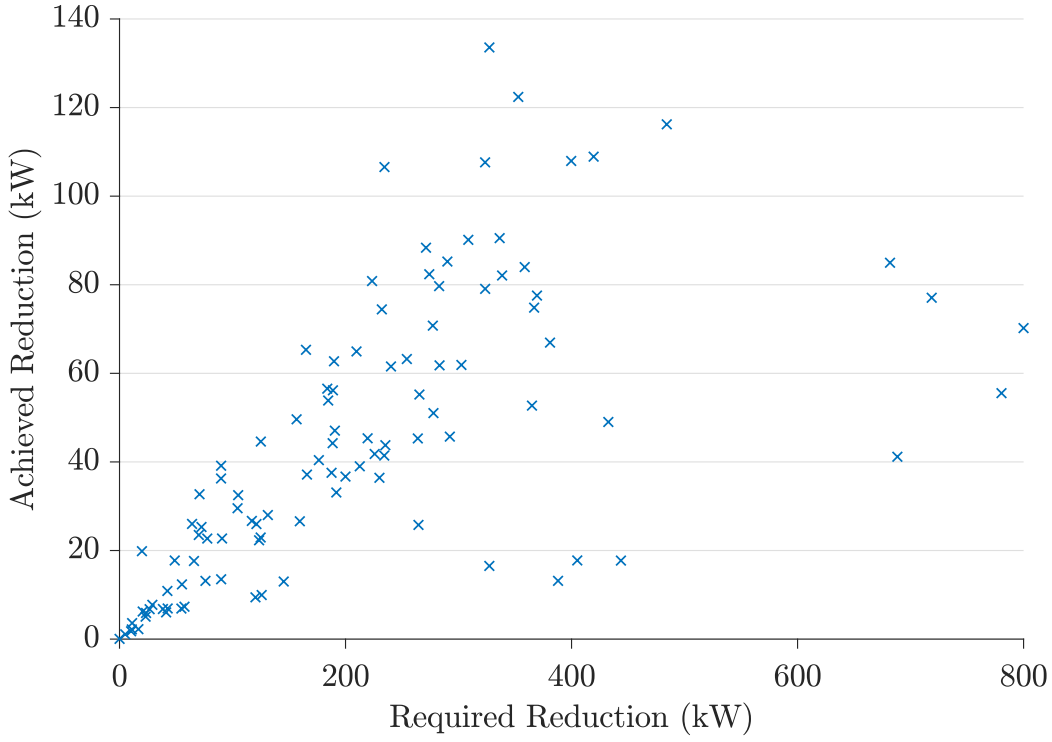

Figure A.28 Required reduction against achieved reduction to reduce top 100 peak network loads to magnitude of 101st peak for a network of 2212 households with a 20% penetration level and signalled response divided evenly between battery systems.

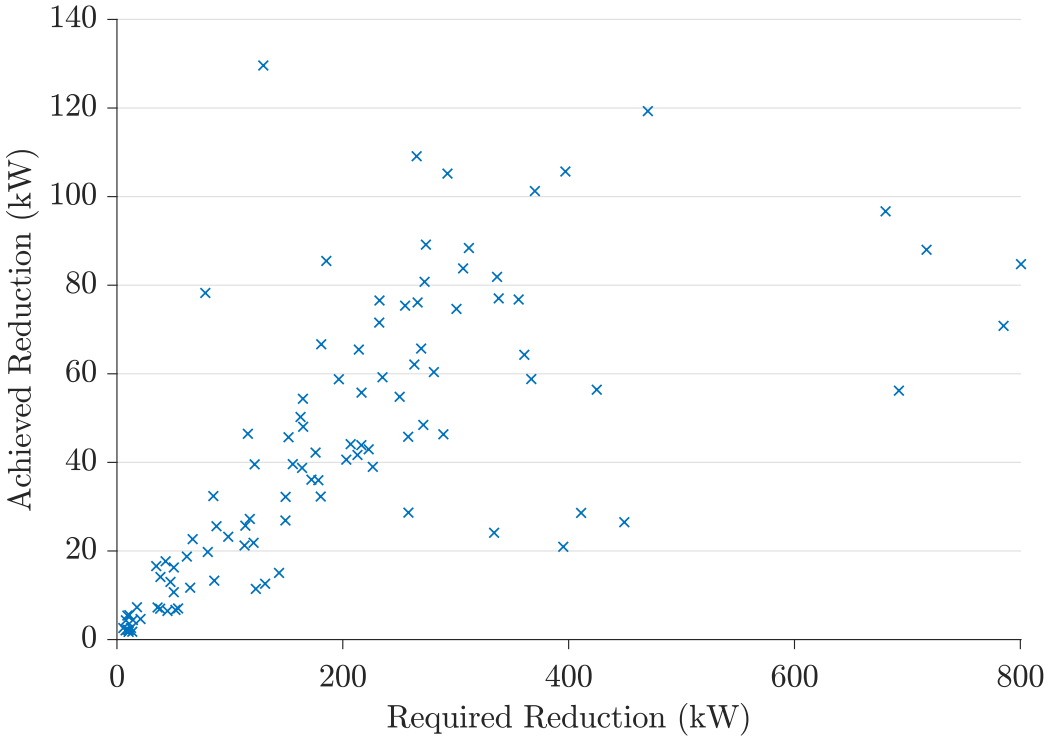

Figure A.29 Required reduction against achieved reduction to reduce top 100 peak network loads to magnitude of 101st peak for a network of 2212 households with a 25% penetration level and signalled response divided evenly between battery systems.

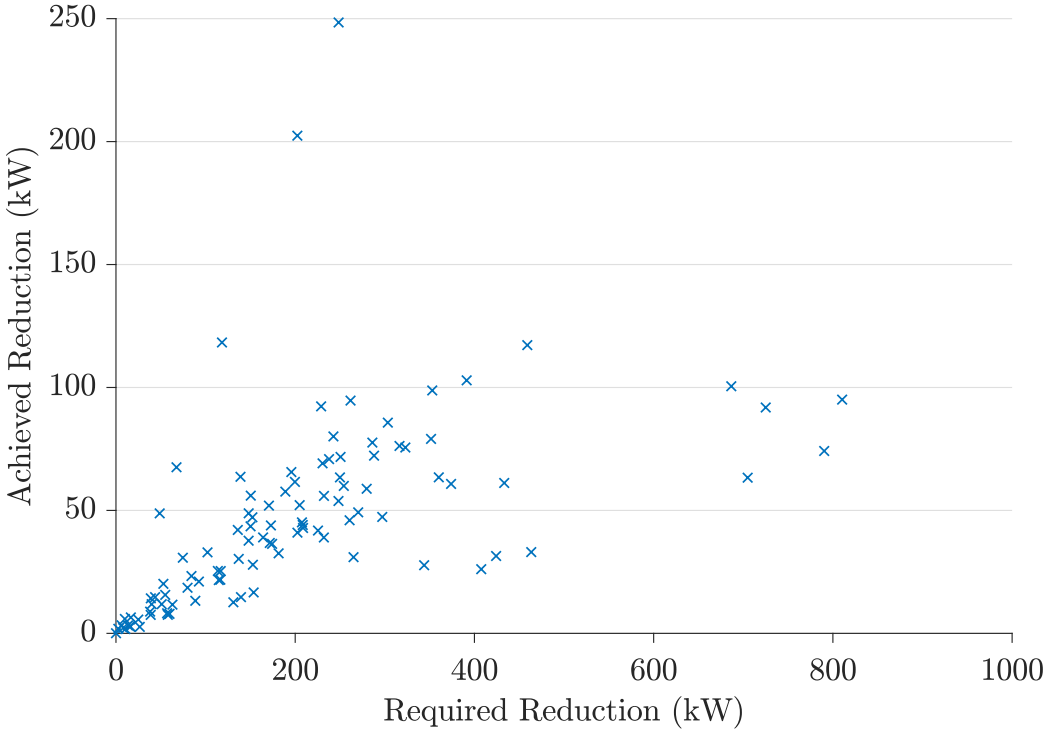

Figure A.30 Required reduction against achieved reduction to reduce top 100 peak network loads to magnitude of 101st peak for a network of 2212 households with a 30% penetration level and signalled response divided evenly between battery systems.

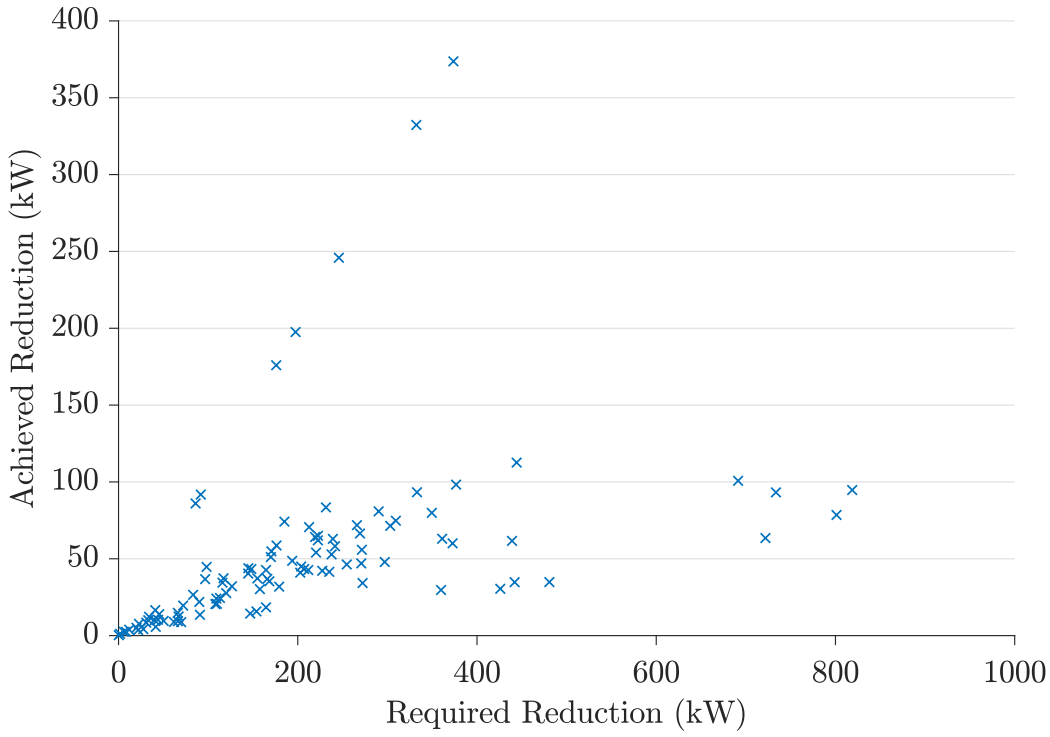

Figure A.31 Required reduction against achieved reduction to reduce top 100 peak network loads to magnitude of 101st peak for a network of 2212 households with a 35% penetration level and signalled response divided evenly between battery systems.

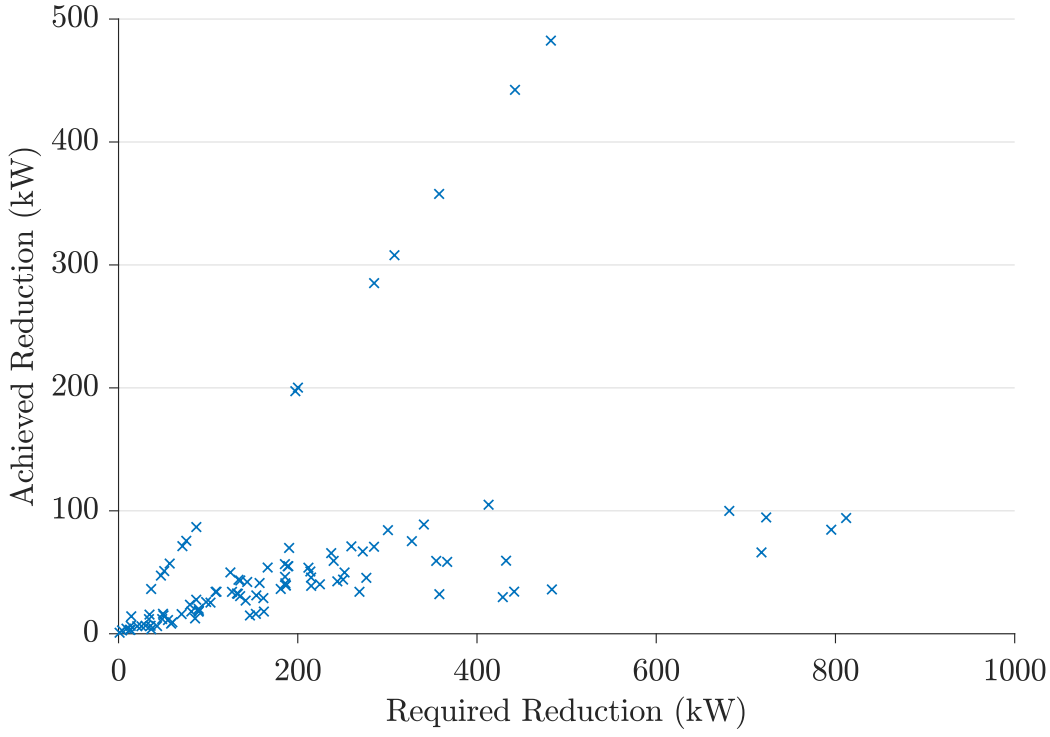

Figure A.32 Required reduction against achieved reduction to reduce top 100 peak network loads to magnitude of 101st peak for a network of 2212 households with a 40% penetration level and signalled response divided evenly between battery systems.

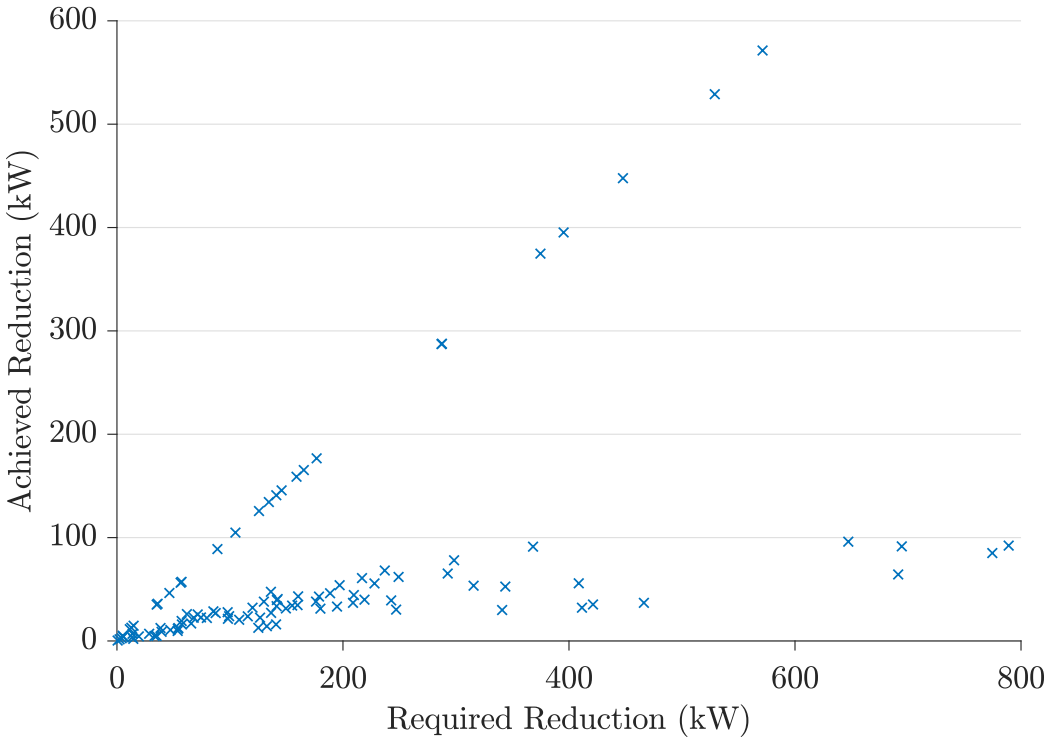

Figure A.33 Required reduction against achieved reduction to reduce top 100 peak network loads to magnitude of 101st peak for a network of 2212 households with a 45% penetration level and signalled response divided evenly between battery systems.

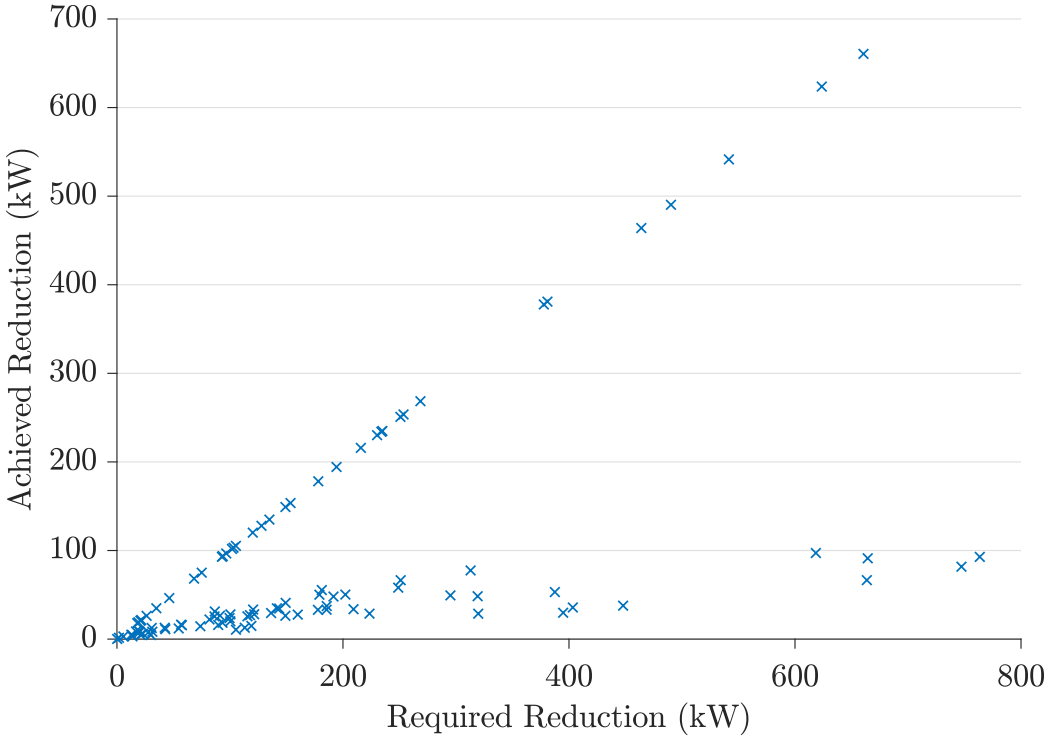

Figure A.34 Required reduction against achieved reduction to reduce top 100 peak network loads to magnitude of 101st peak for a network of 2212 households with a 50% penetration level and signalled response divided evenly between battery systems.

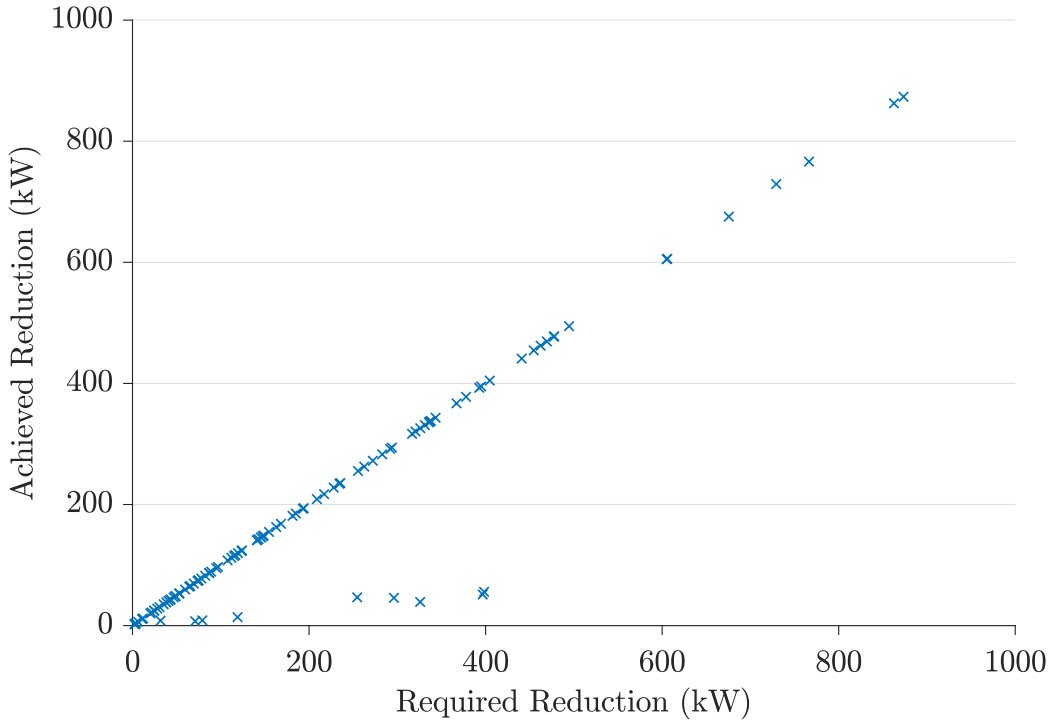

Figure A.35 Required reduction against achieved reduction to reduce top 100 peak network loads to magnitude of 101st peak for a network of 2212 households with a 75% penetration level and signalled response divided evenly between battery systems.

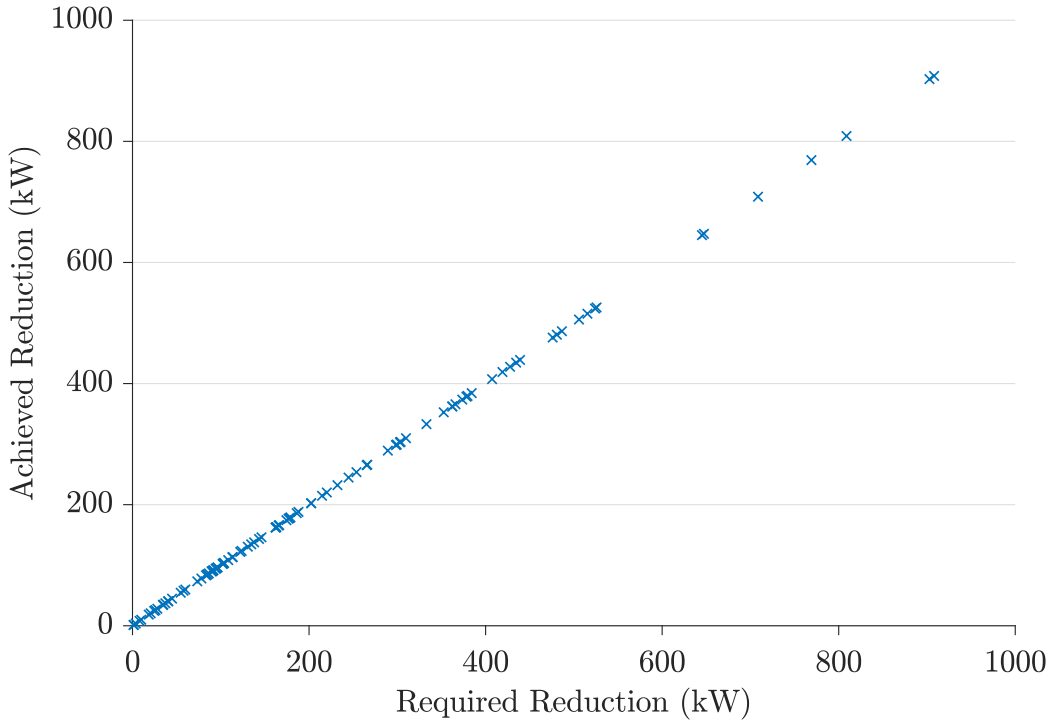

Figure A.36 Required reduction against achieved reduction to reduce top 100 peak network loads to magnitude of 101st peak for a network of 2212 households with a 100% penetration level and signalled response divided evenly between battery systems.

Appendix B

CASE 2 - SPOT PRICING

B.1 AVAILABLE REDUCTION CAPABILITY

The following figures show the available reduction power as a function of aggregate load across different penetration levels for a network of 2212 households.

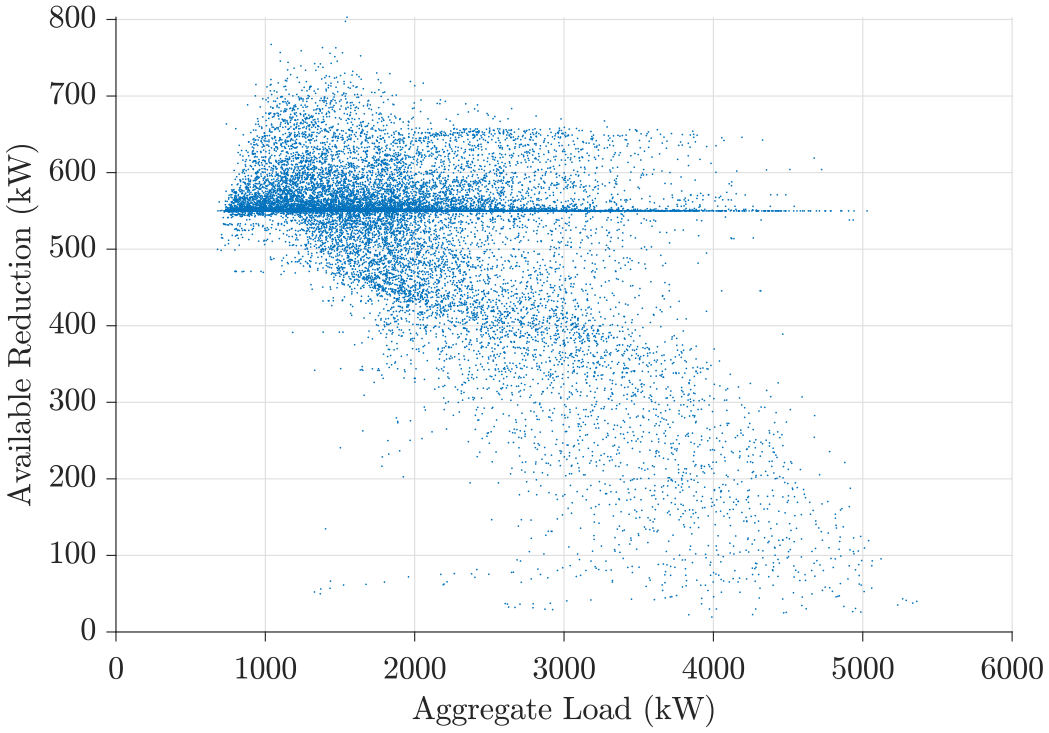

Figure B.1 Total aggregate load against available reduction capacity for a network of 2212 households with 5% PV and BESS penetration level.

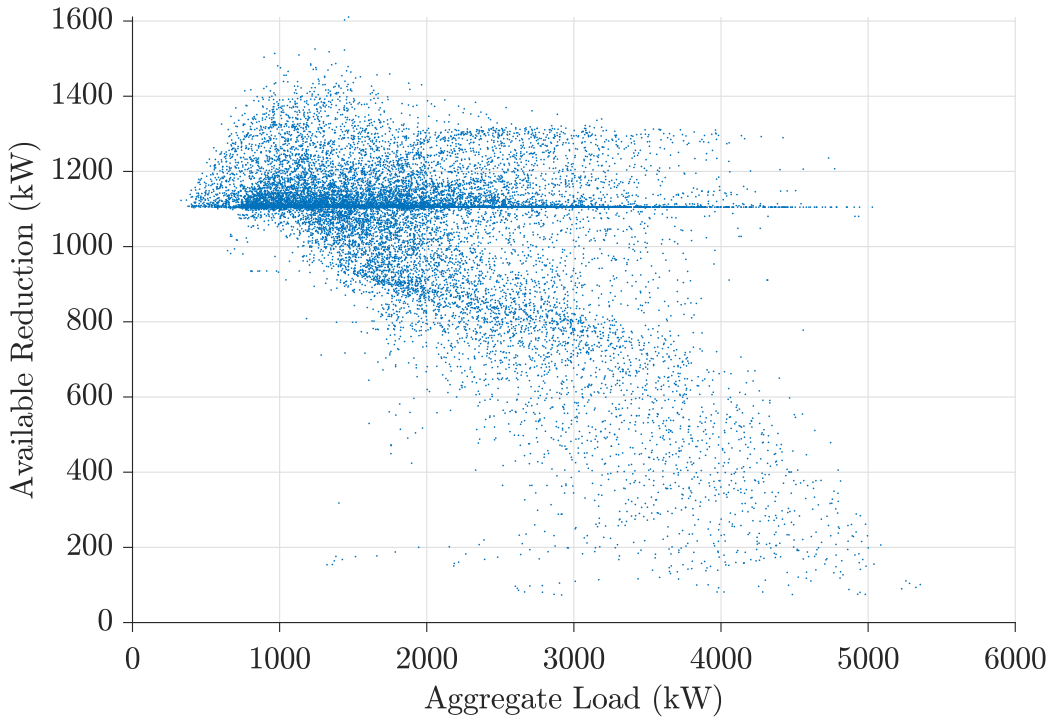

Figure B.2 Total aggregate load against available reduction capacity for a network of 2212 households with 10% PV and BESS penetration level.

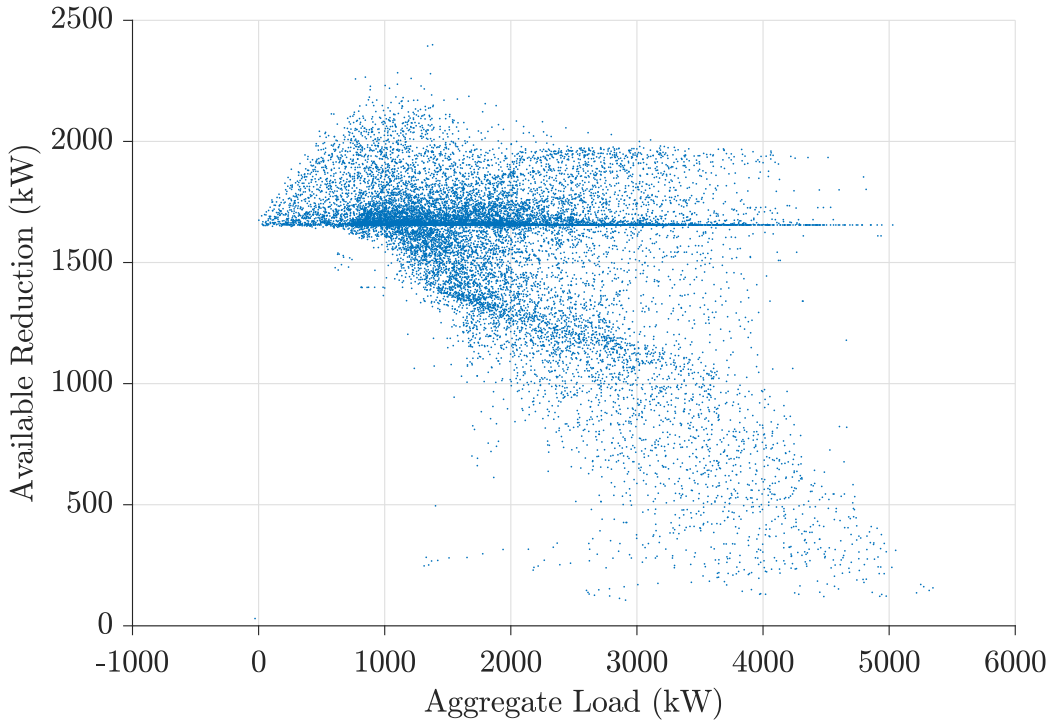

Figure B.3 Total aggregate load against available reduction capacity for a network of 2212 households with 15% PV and BESS penetration level.

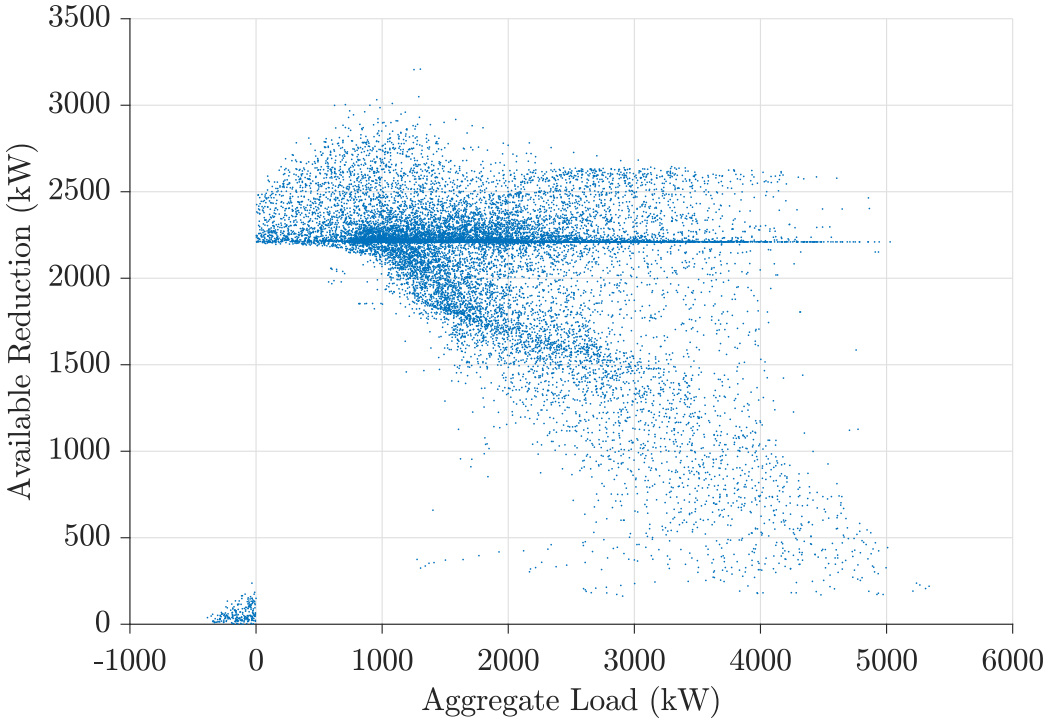

Figure B.4 Total aggregate load against available reduction capacity for a network of 2212 households with 20% PV and BESS penetration level.

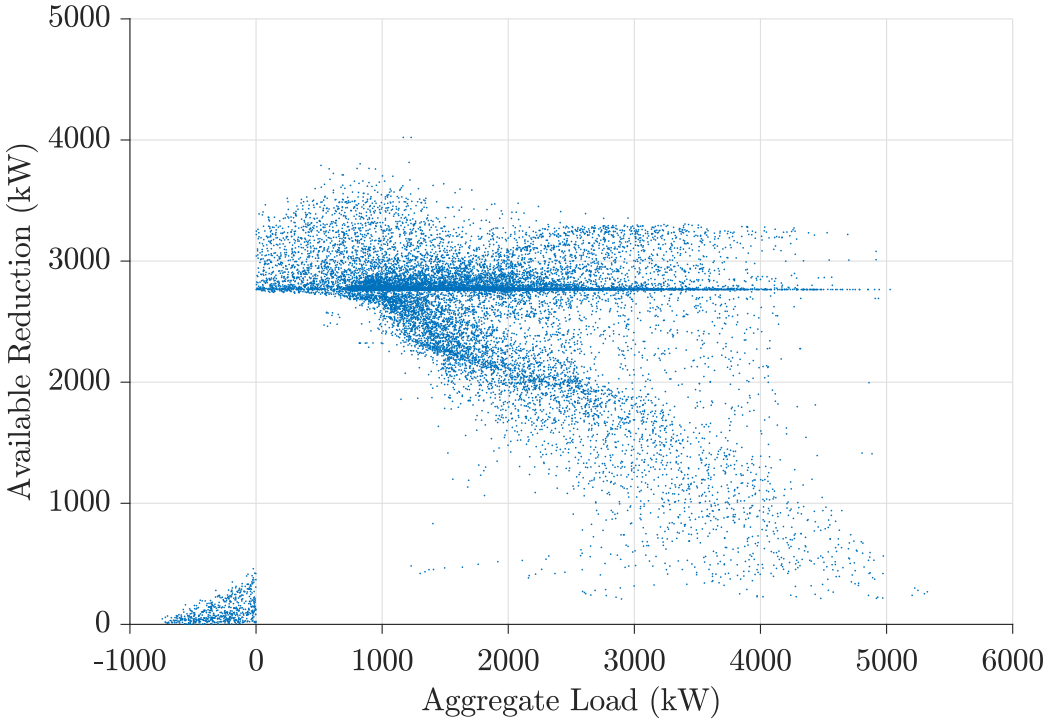

Figure B.5 Total aggregate load against available reduction capacity for a network of 2212 households with 25% PV and BESS penetration level.

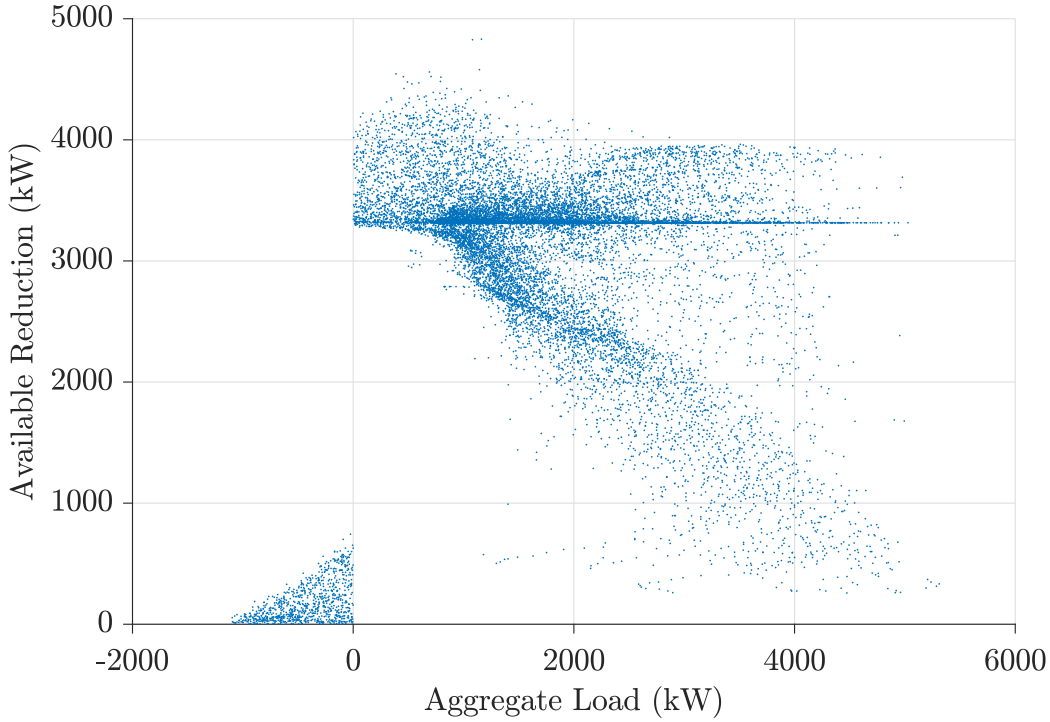

Figure B.6 Total aggregate load against available reduction capacity for a network of 2212 households with 30% PV and BESS penetration level.

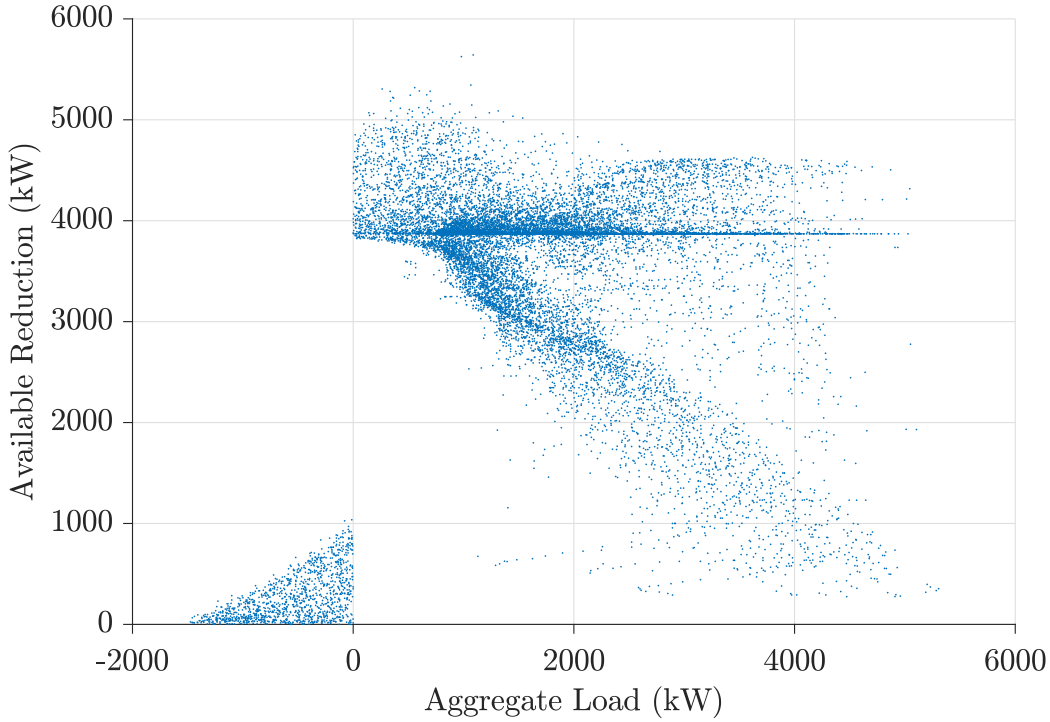

Figure B.7 Total aggregate load against available reduction capacity for a network of 2212 households with 35% PV and BESS penetration level.

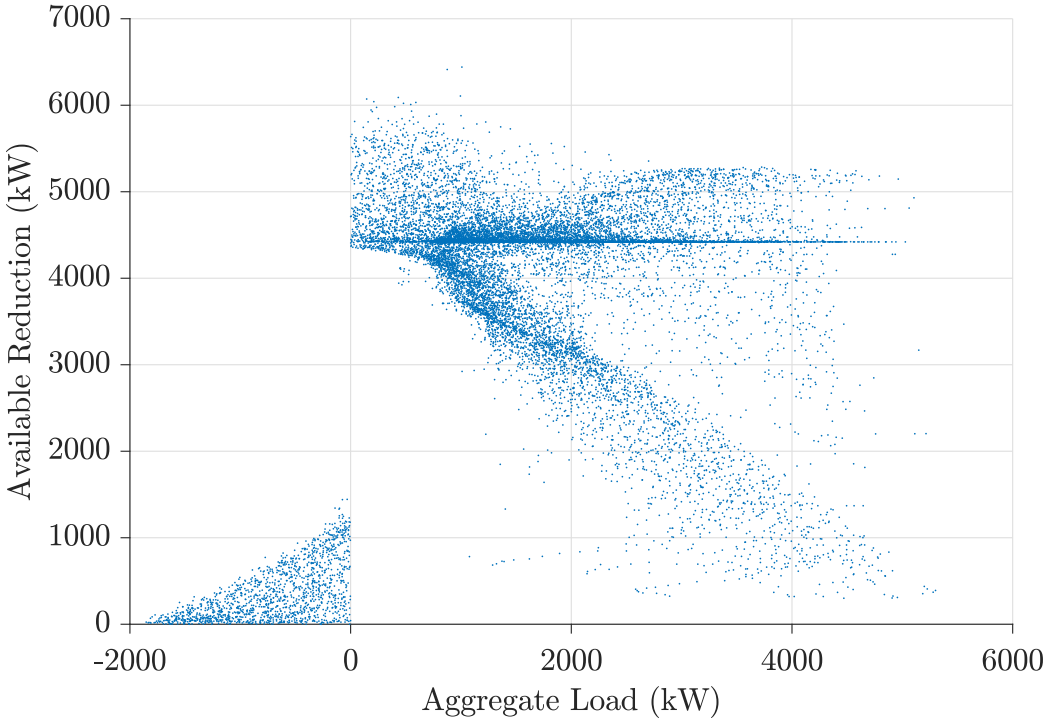

Figure B.8 Total aggregate load against available reduction capacity for a network of 2212 households with 40% PV and BESS penetration level.

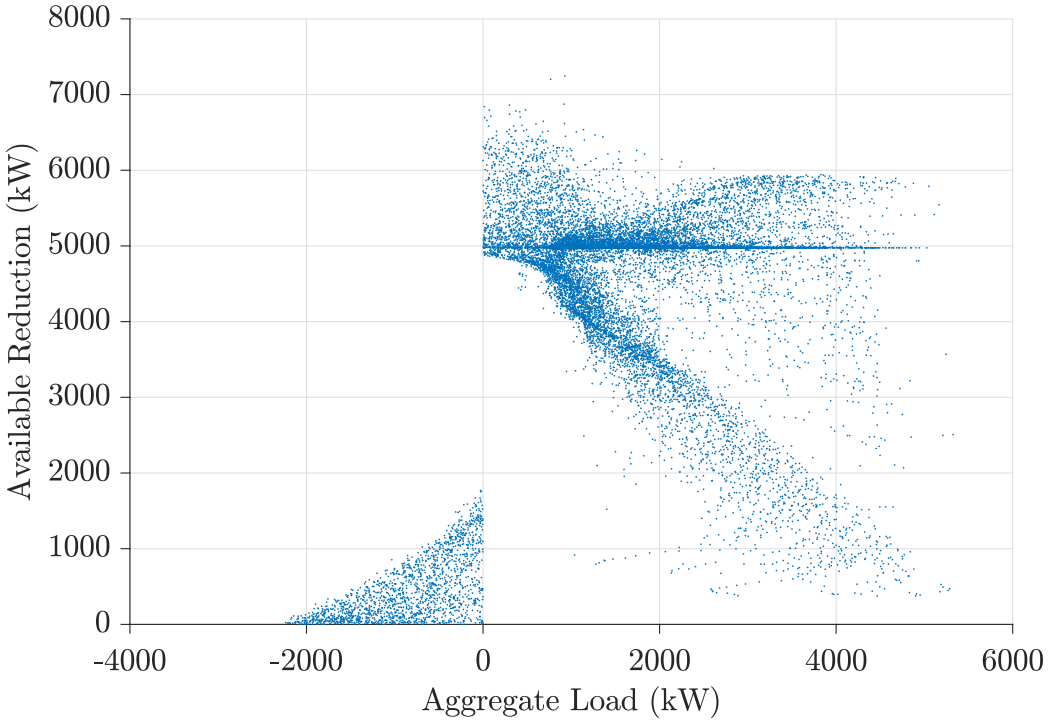

Figure B.9 Total aggregate load against available reduction capacity for a network of 2212 households with 45% PV and BESS penetration level.

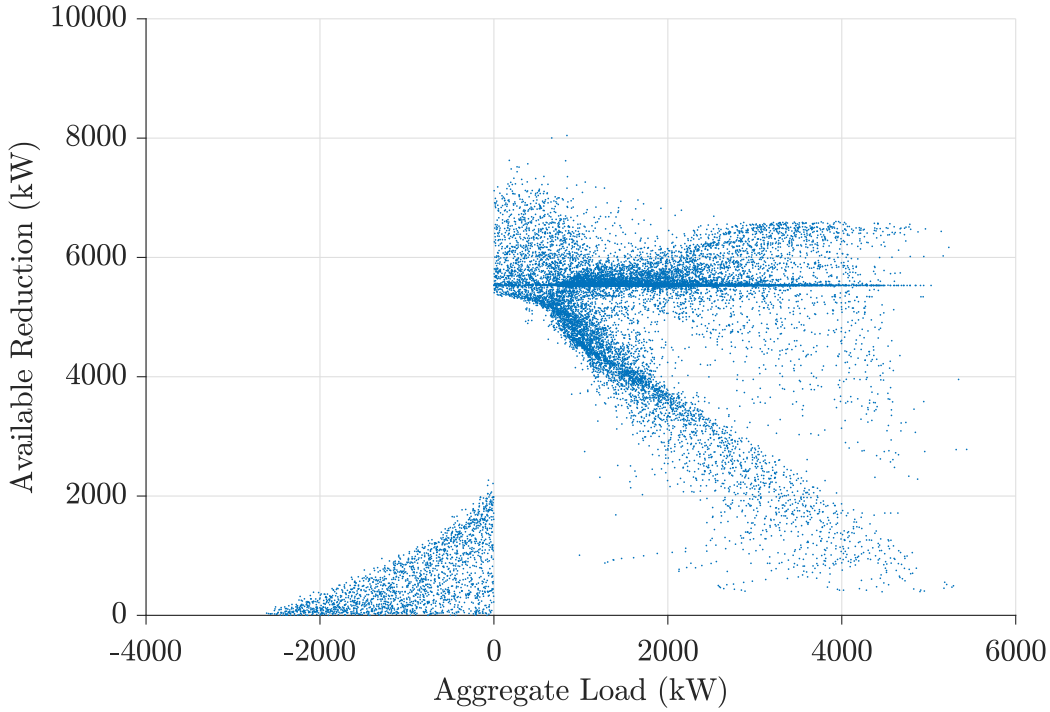

Figure B.10 Total aggregate load against available reduction capacity for a network of 2212 households with 50% PV and BESS penetration level.

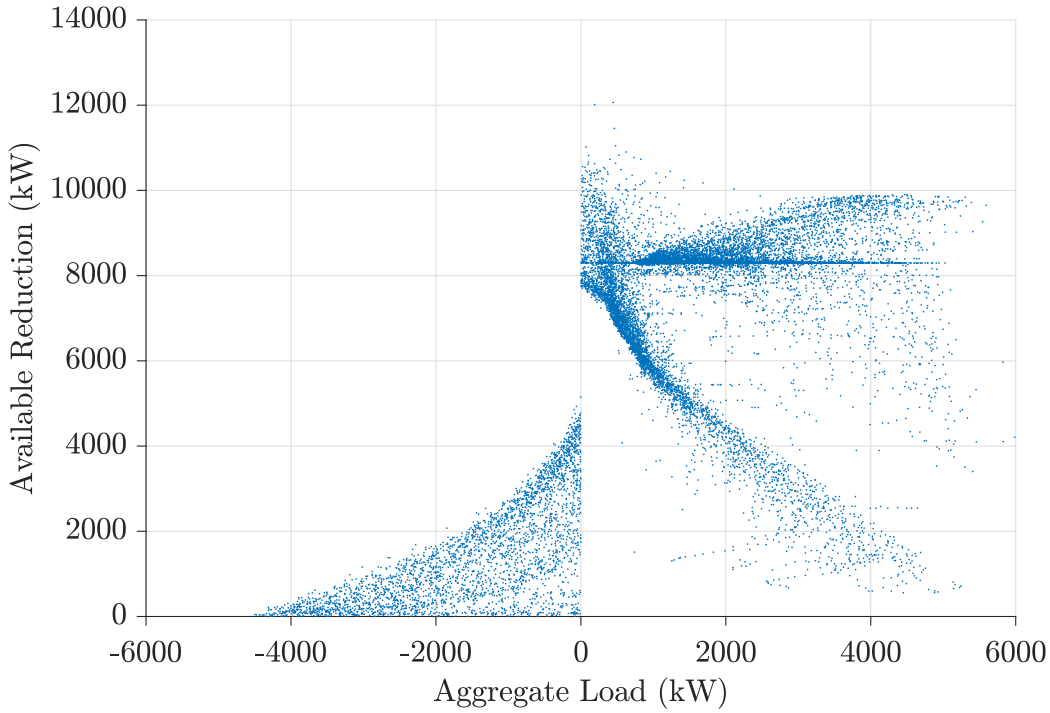

Figure B.11 Total aggregate load against available reduction capacity for a network of 2212 households with 75% PV and BESS penetration level.

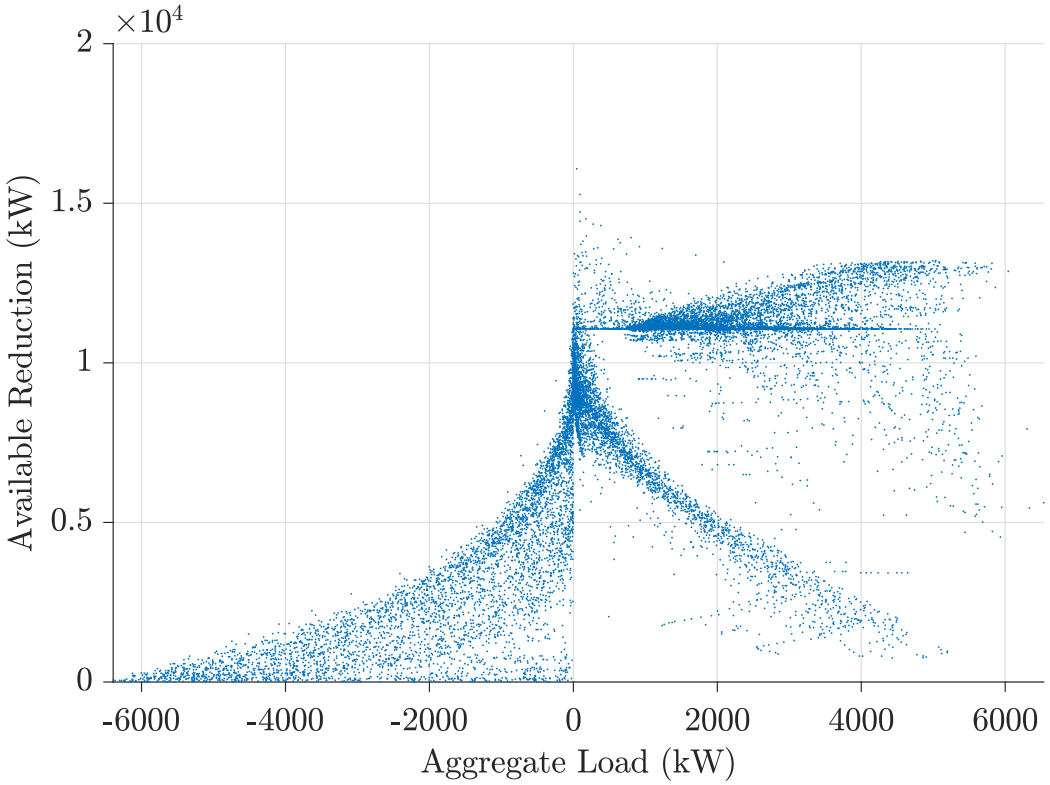

Figure B.12 Total aggregate load against available reduction capacity for a network of 2212 households with 100% PV and BESS penetration level.

B.2 PEAK REDUCTION SUFFICIENCY

The following figures shows the proportion of the top 100 peak loads where there is sufficient reduction capacity to reduce those peaks to the level of the 101st peak.

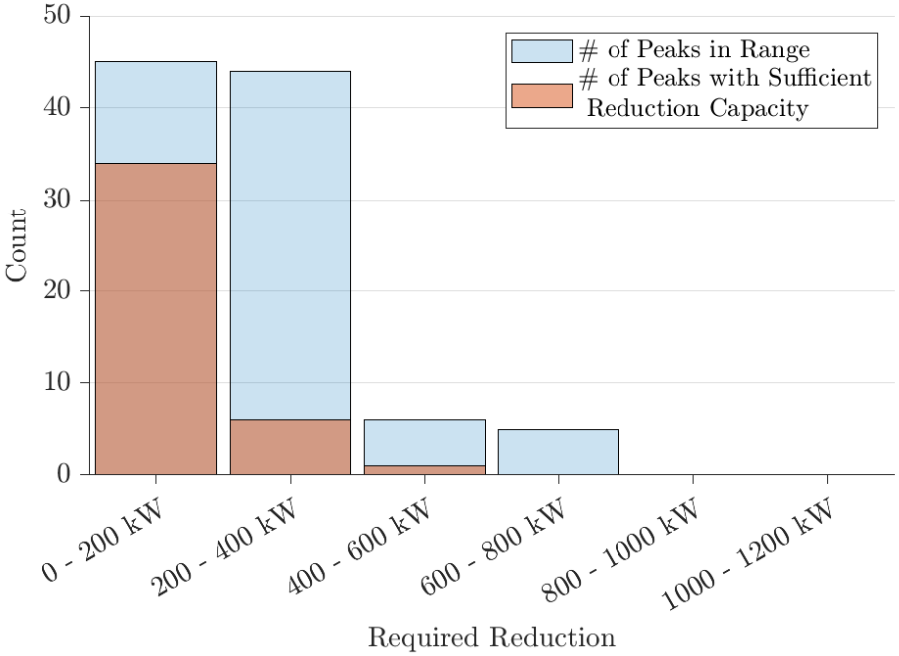

Figure B.13 Sufficiency of available reduction power to meet required reduction to reduce top 100 peaks to level of 101st peak for 5% penetration level in a network of 2212 households.

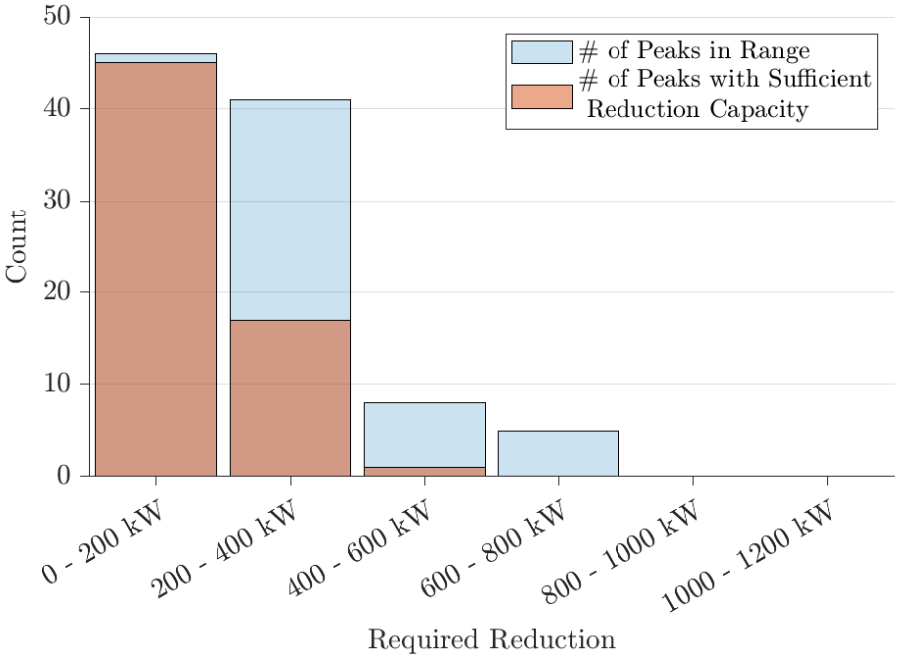

Figure B.14 Sufficiency of available reduction power to meet required reduction to reduce top 100 peaks to level of 101st peak for 10% penetration level in a network of 2212 households.

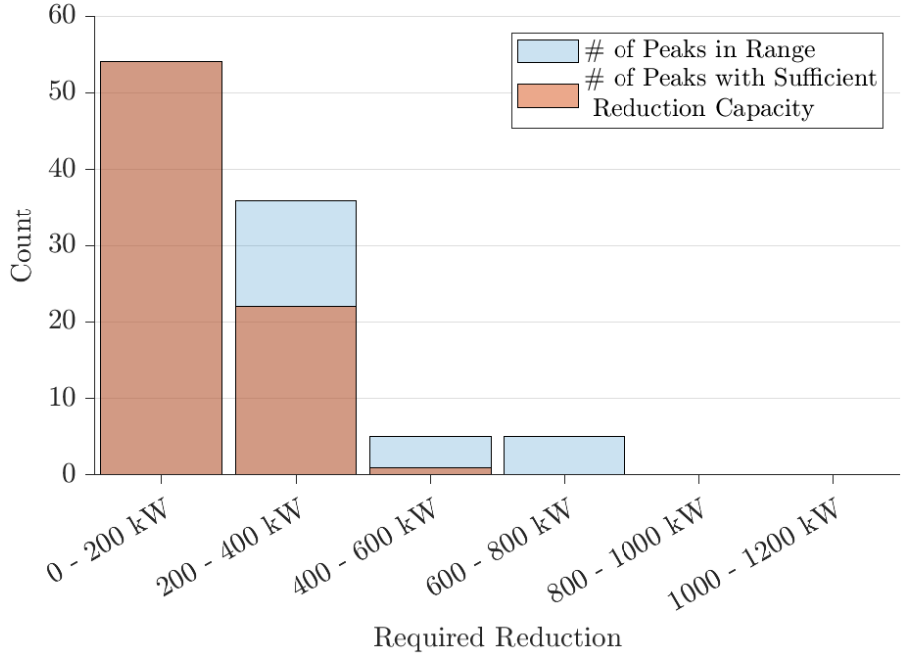

Figure B.15 Sufficiency of available reduction power to meet required reduction to reduce top 100 peaks to level of 101st peak for 15% penetration level in a network of 2212 households.

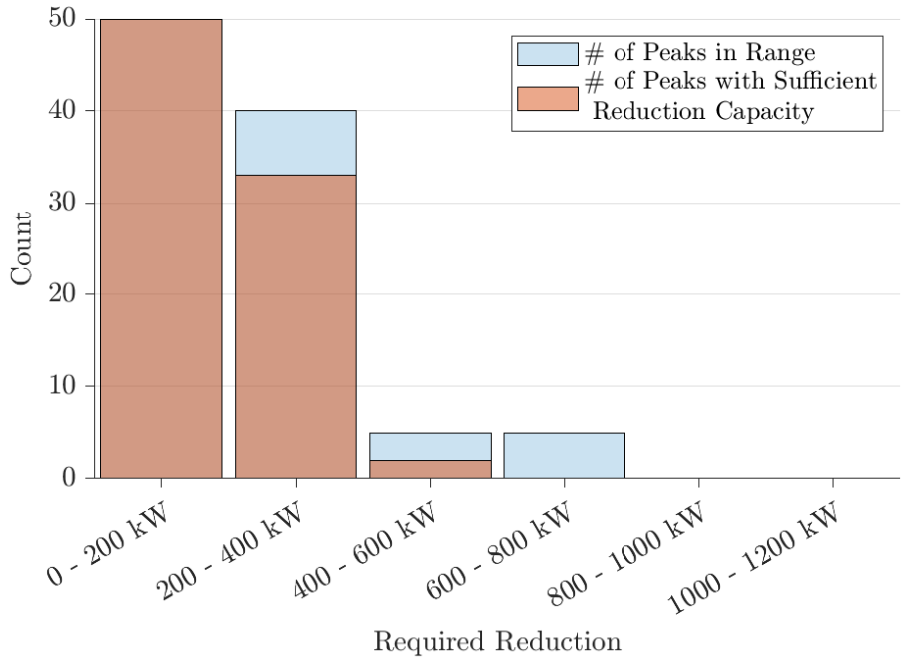

Figure B.16 Sufficiency of available reduction power to meet required reduction to reduce top 100 peaks to level of 101st peak for 20% penetration level in a network of 2212 households.

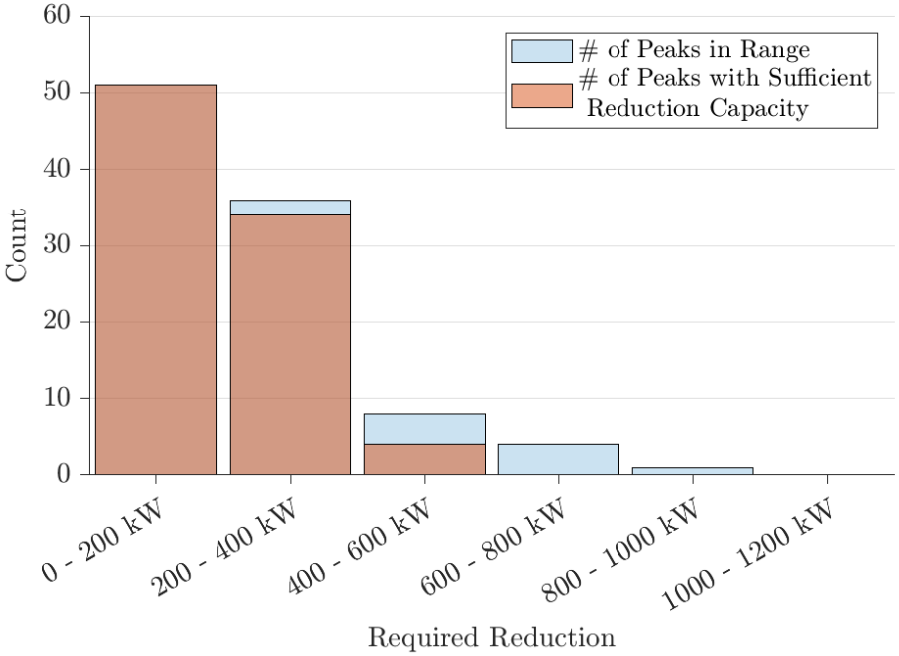

Figure B.17 Sufficiency of available reduction power to meet required reduction to reduce top 100 peaks to level of 101st peak for 25% penetration level in a network of 2212 households.

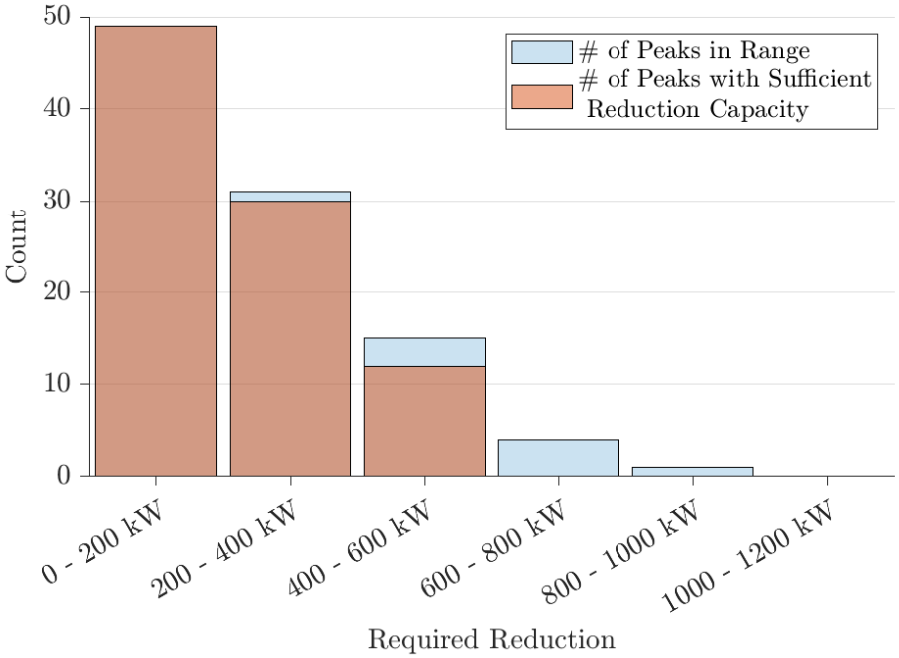

Figure B.18 Sufficiency of available reduction power to meet required reduction to reduce top 100 peaks to level of 101st peak for 30% penetration level in a network of 2212 households.

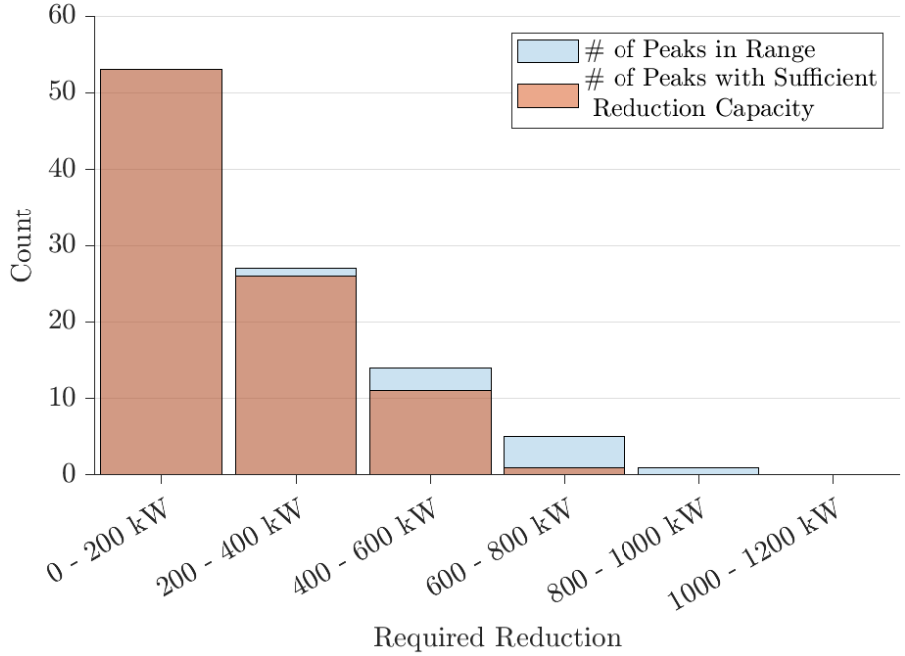

Figure B.19 Sufficiency of available reduction power to meet required reduction to reduce top 100 peaks to level of 101st peak for 35% penetration level in a network of 2212 households.

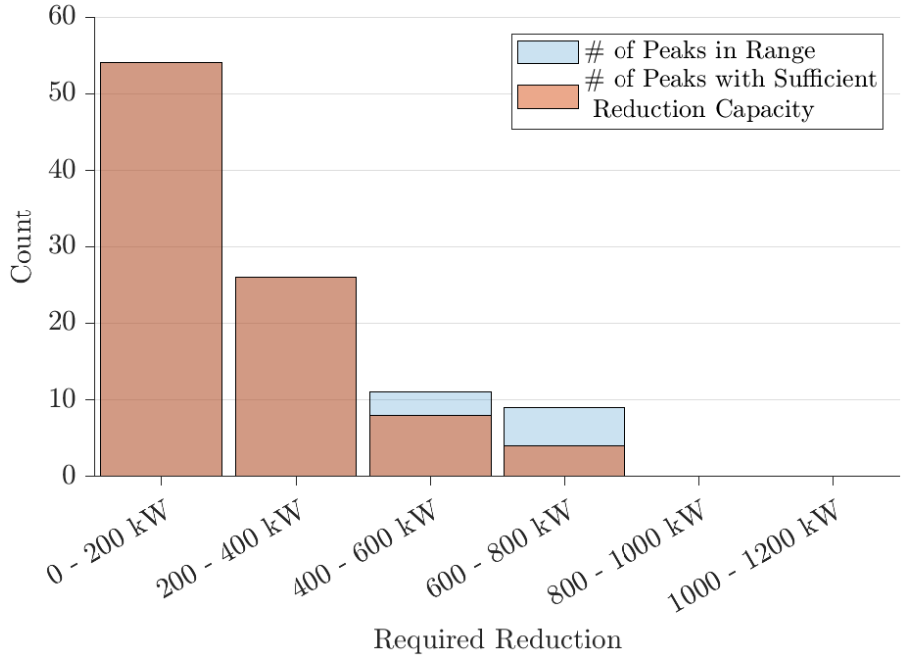

Figure B.20 Sufficiency of available reduction power to meet required reduction to reduce top 100 peaks to level of 101st peak for 40% penetration level in a network of 2212 households.

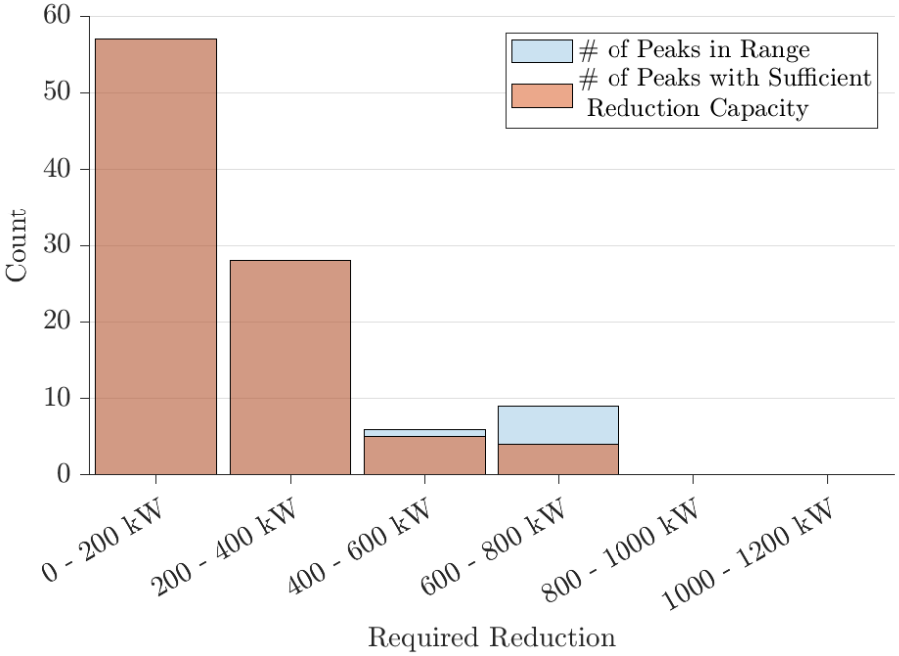

Figure B.21 Sufficiency of available reduction power to meet required reduction to reduce top 100 peaks to level of 101st peak for 45% penetration level in a network of 2212 households.

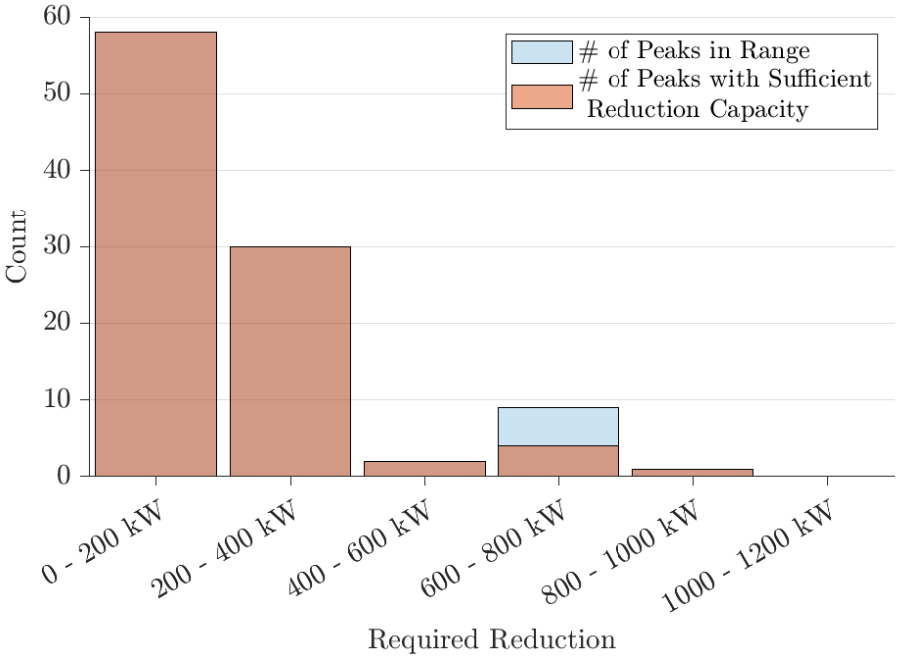

Figure B.22 Sufficiency of available reduction power to meet required reduction to reduce top 100 peaks to level of 101st peak for 50% penetration level in a network of 2212 households.

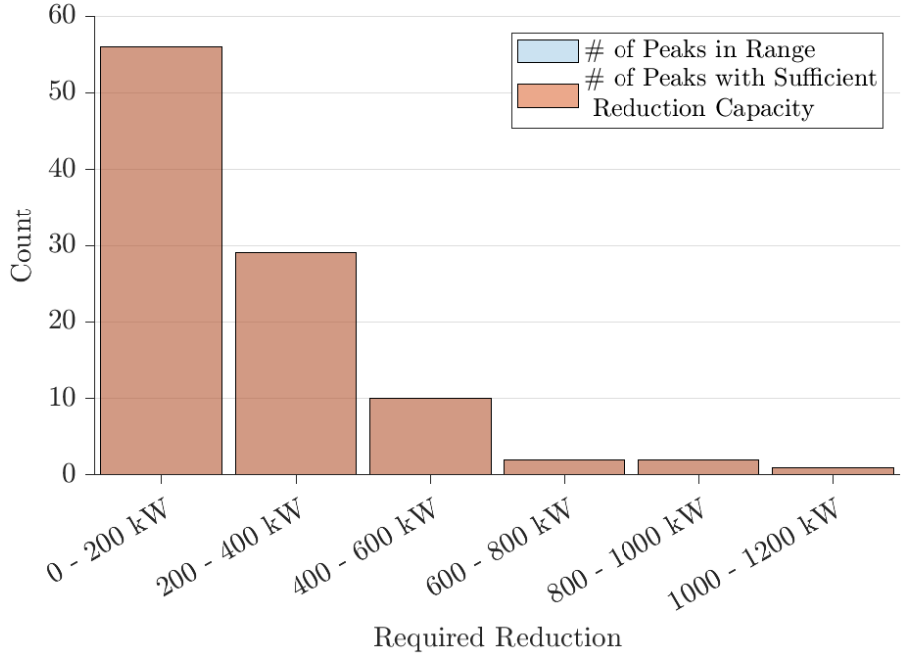

Figure B.23 Sufficiency of available reduction power to meet required reduction to reduce top 100 peaks to level of 101st peak for 75% penetration level in a network of 2212 households.

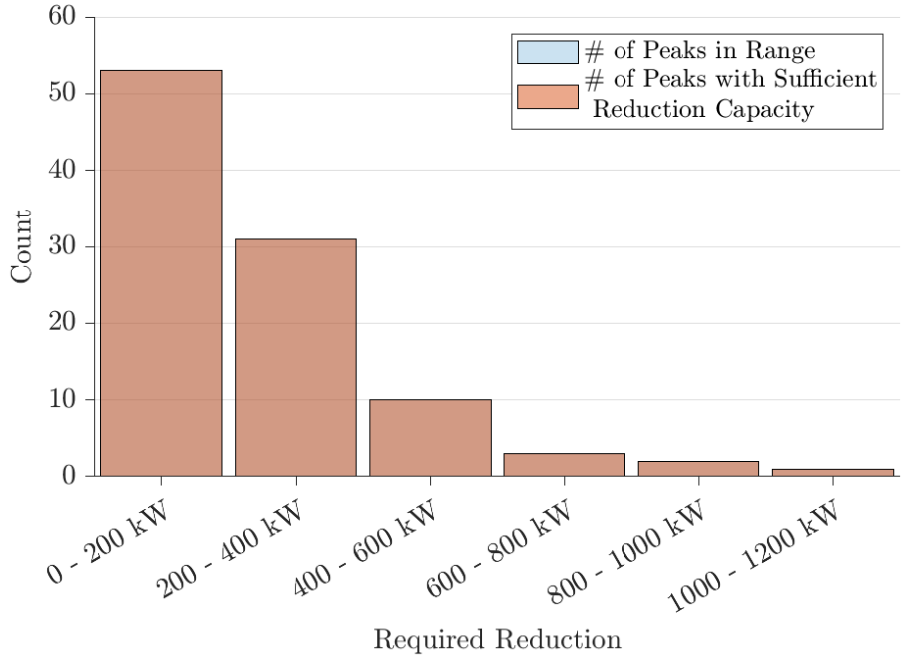

Figure B.24 Sufficiency of available reduction power to meet required reduction to reduce top 100 peaks to level of 101st peak for 100% penetration level in a network of 2212 households.

B.3 PEAK REDUCTION ACHIEVED

The following figures shows the achieved peak reduction against the required peak reduction where the required response is divided evenly amongst BESSs.

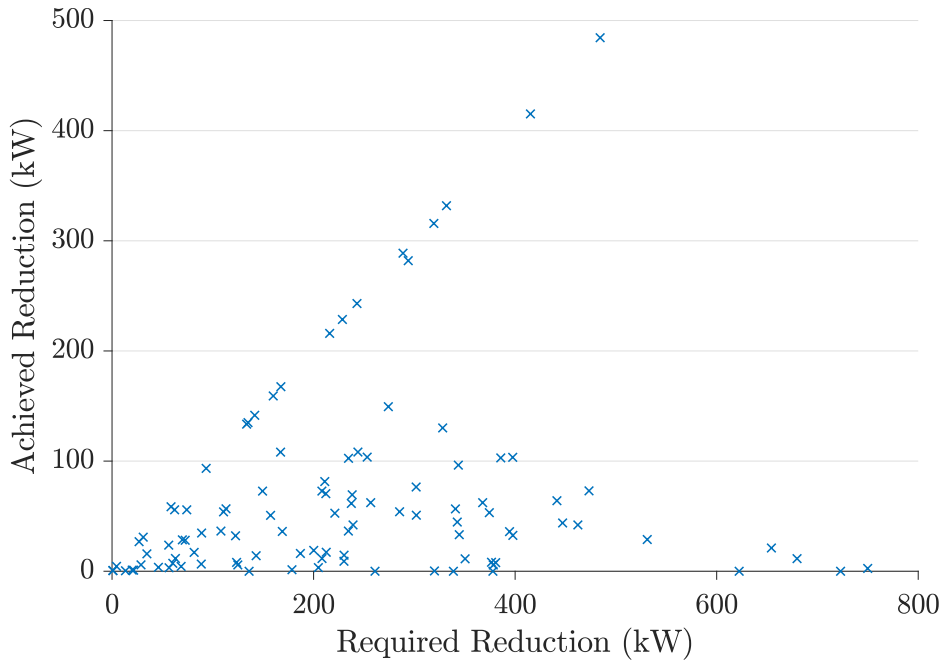

Figure B.25 Required reduction against achieved reduction to reduce top 100 peak network loads to magnitude of 101st peak for a network of 2212 households with a 5% penetration level and signalled response divided evenly between battery systems.

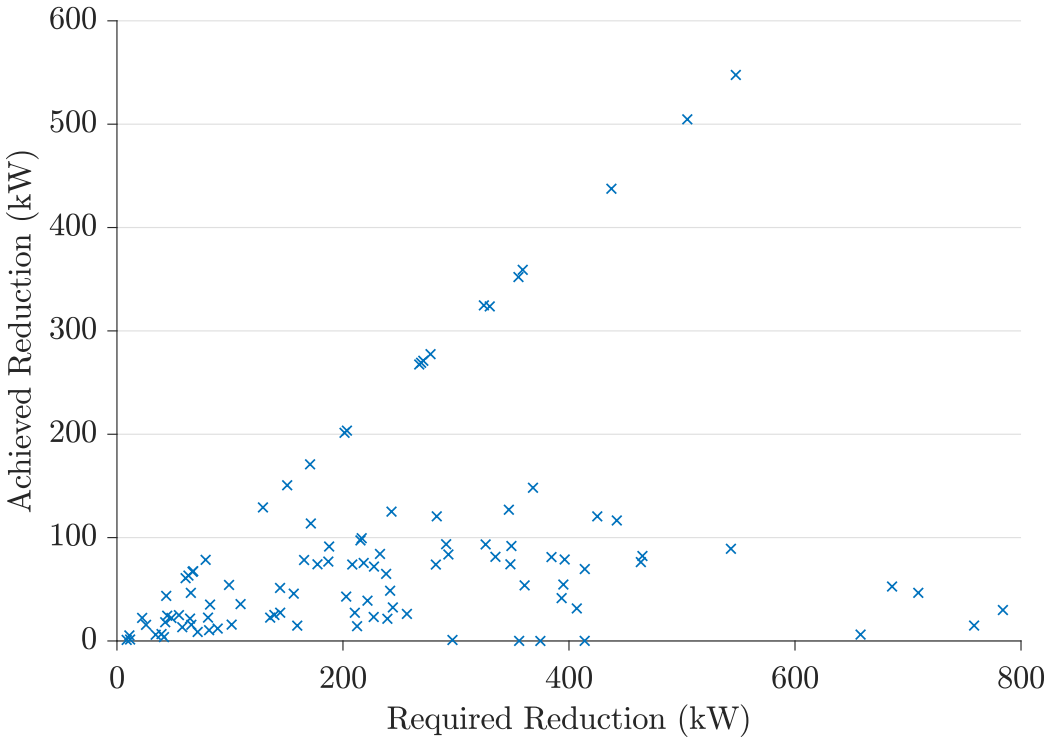

Figure B.26 Required reduction against achieved reduction to reduce top 100 peak network loads to magnitude of 101st peak for a network of 2212 households with a 10% penetration level and signalled response divided evenly between battery systems.

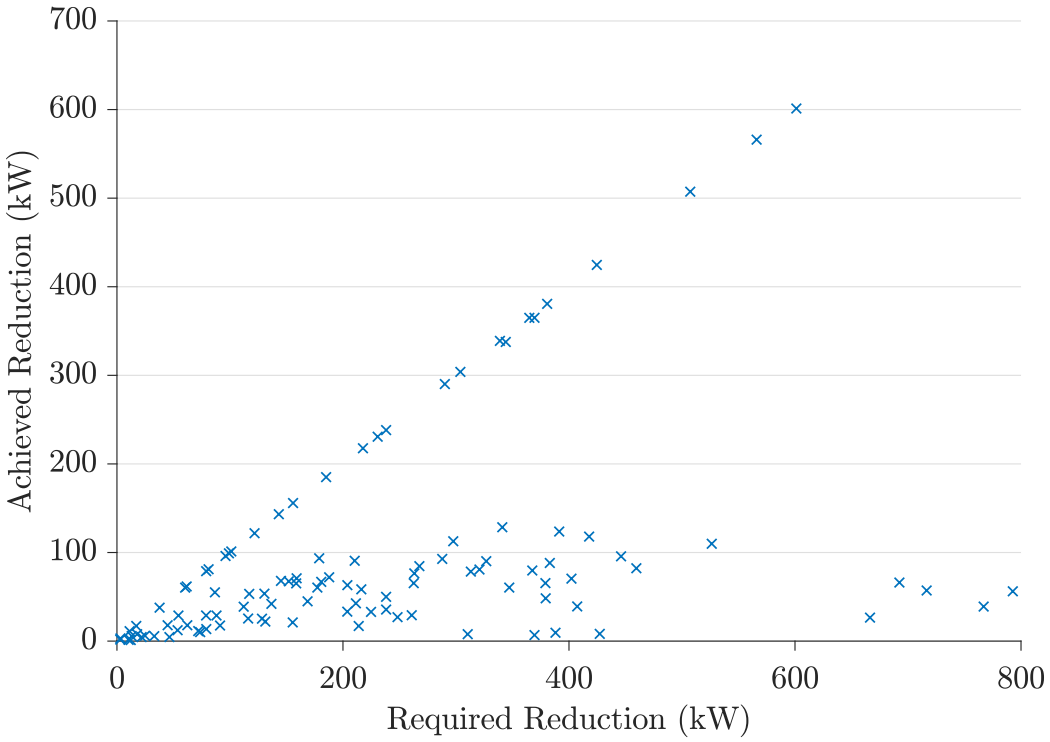

Figure B.27 Required reduction against achieved reduction to reduce top 100 peak network loads to magnitude of 101st peak for a network of 2212 households with a 15% penetration level and signalled response divided evenly between battery systems.

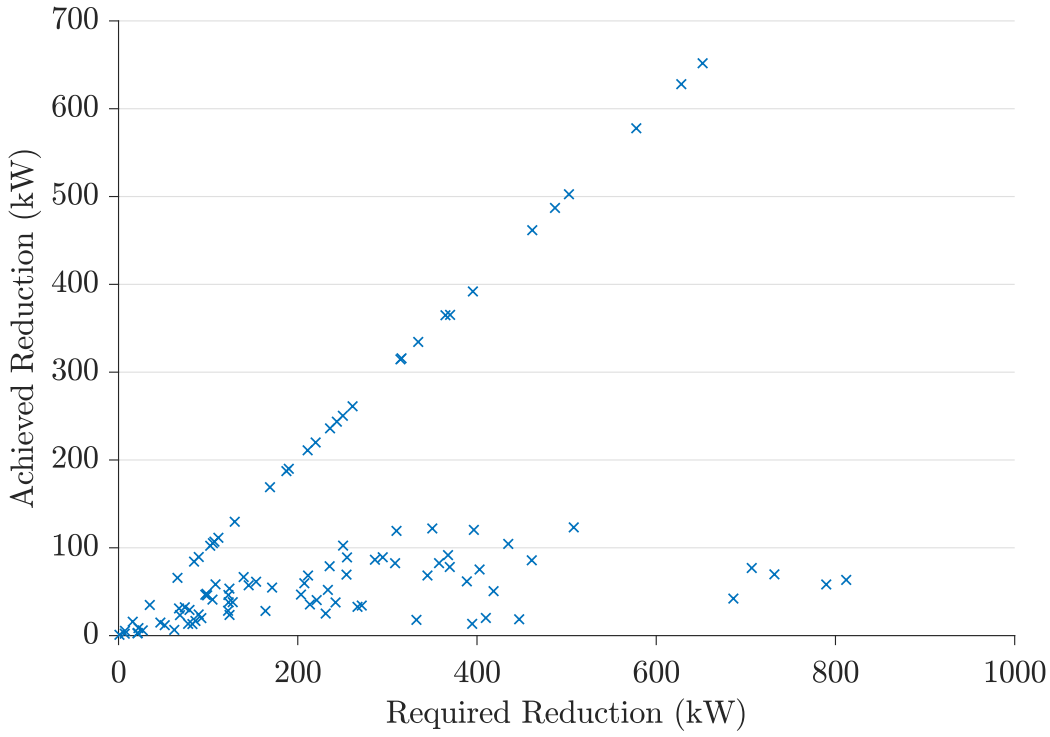

Figure B.28 Required reduction against achieved reduction to reduce top 100 peak network loads to magnitude of 101st peak for a network of 2212 households with a 20% penetration level and signalled response divided evenly between battery systems.

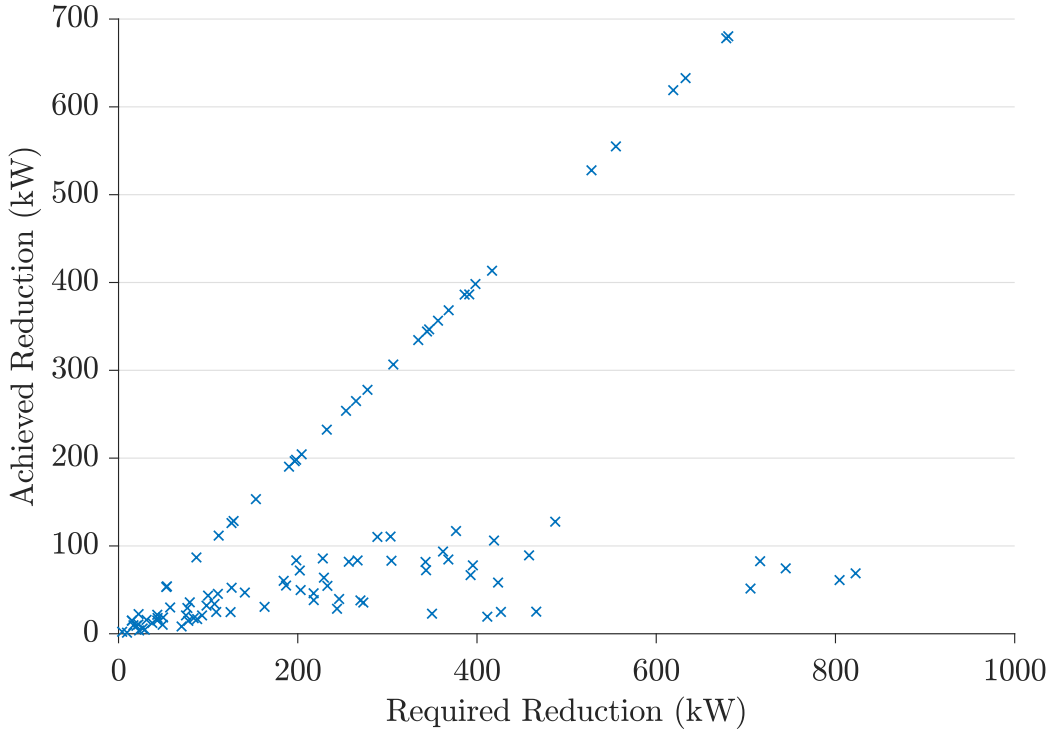

Figure B.29 Required reduction against achieved reduction to reduce top 100 peak network loads to magnitude of 101st peak for a network of 2212 households with a 25% penetration level and signalled response divided evenly between battery systems.

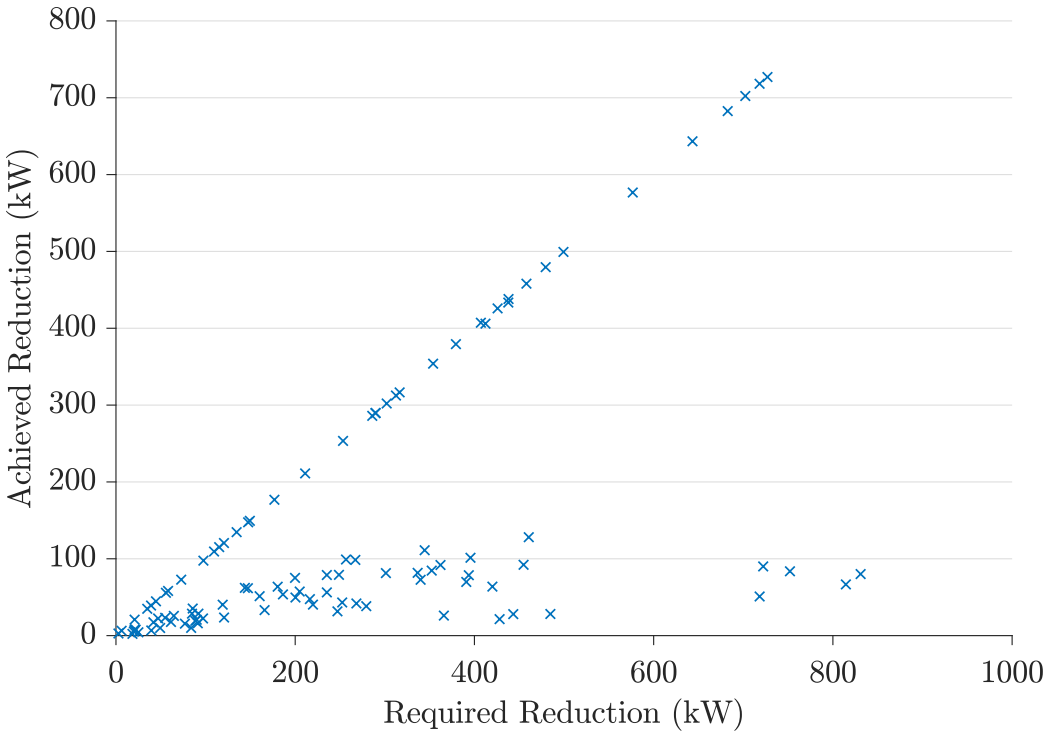

Figure B.30 Required reduction against achieved reduction to reduce top 100 peak network loads to magnitude of 101st peak for a network of 2212 households with a 30% penetration level and signalled response divided evenly between battery systems.

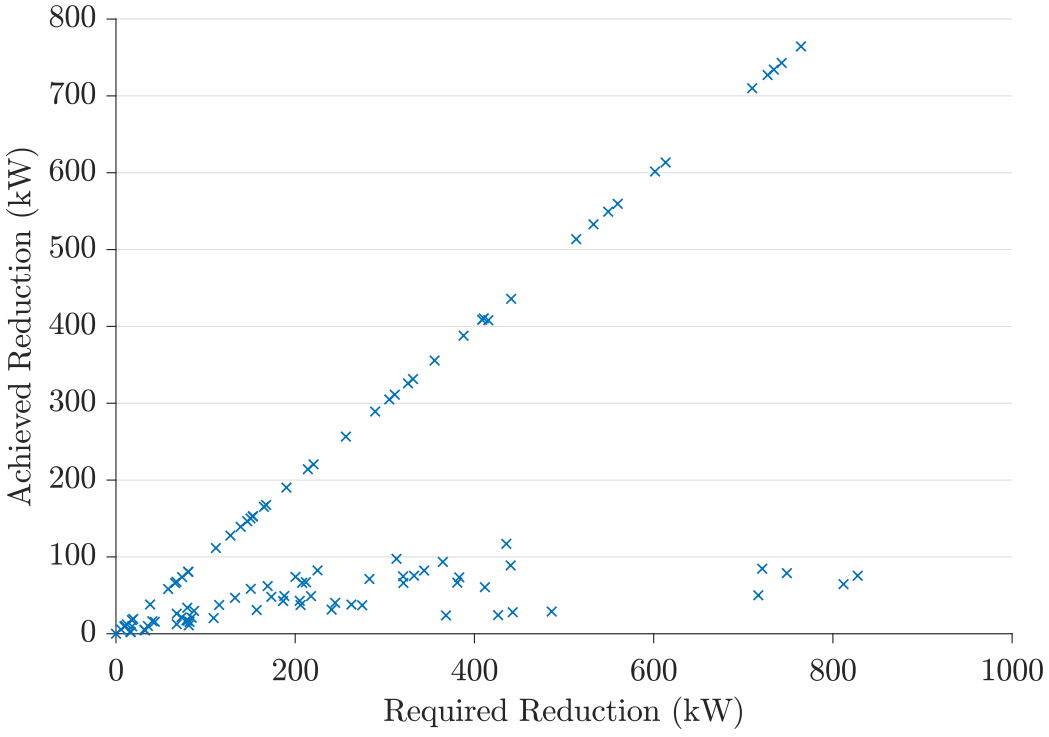

Figure B.31 Required reduction against achieved reduction to reduce top 100 peak network loads to magnitude of 101st peak for a network of 2212 households with a 35% penetration level and signalled response divided evenly between battery systems.

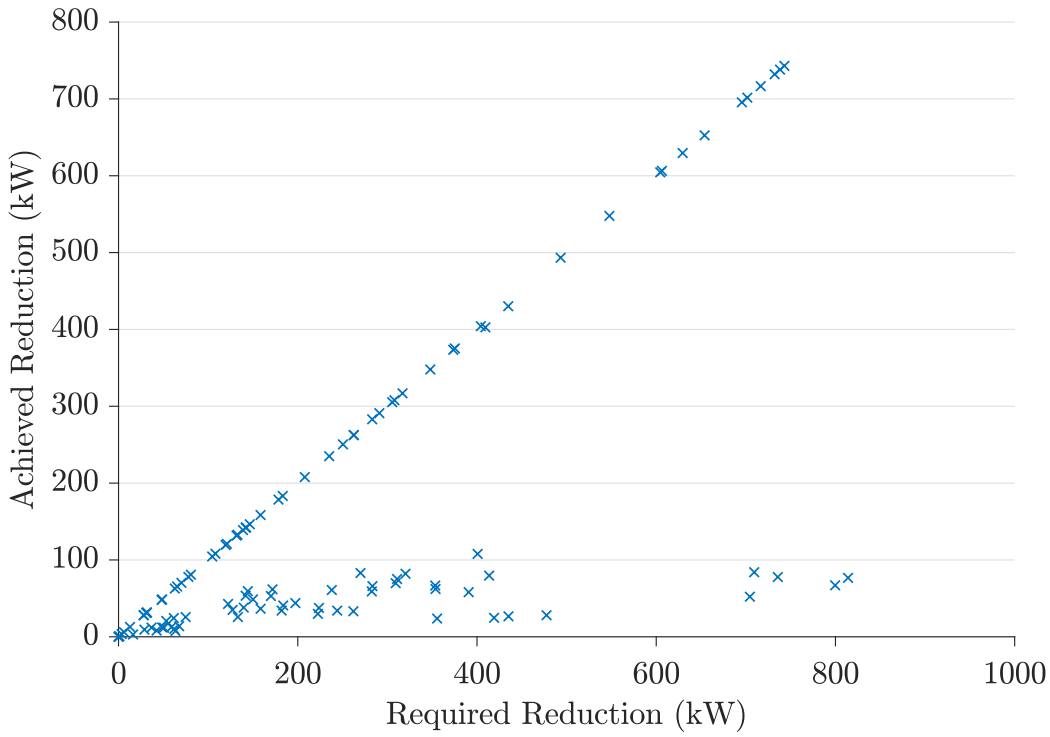

Figure B.32 Required reduction against achieved reduction to reduce top 100 peak network loads to magnitude of 101st peak for a network of 2212 households with a 40% penetration level and signalled response divided evenly between battery systems.

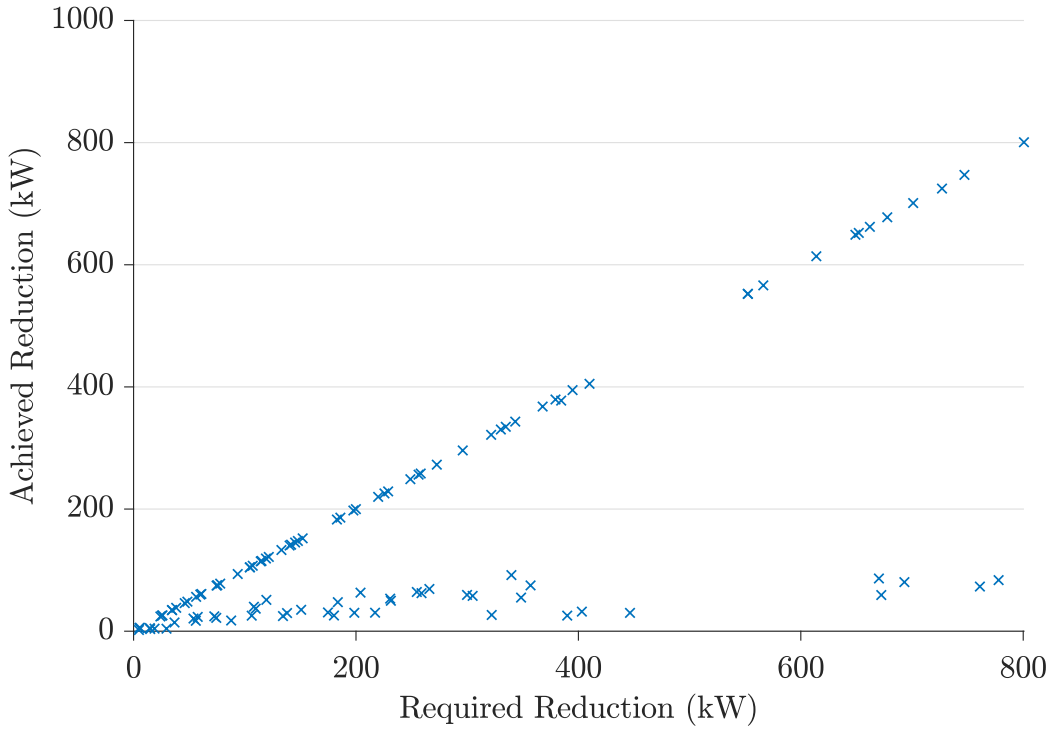

Figure B.33 Required reduction against achieved reduction to reduce top 100 peak network loads to magnitude of 101st peak for a network of 2212 households with a 45% penetration level and signalled response divided evenly between battery systems.

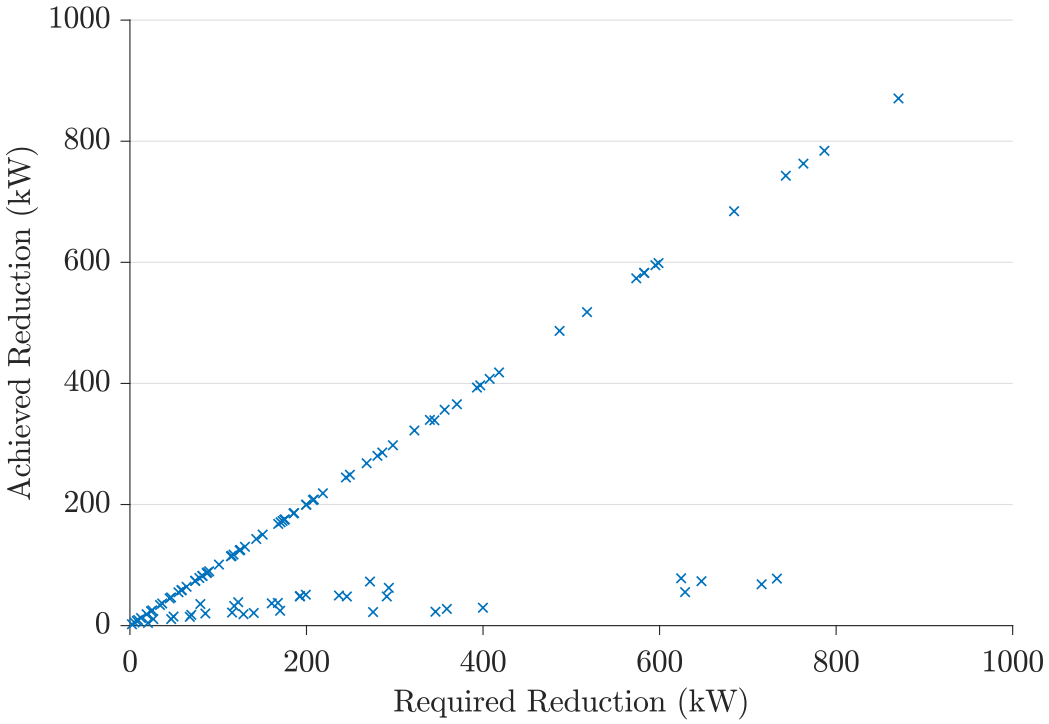

Figure B.34 Required reduction against achieved reduction to reduce top 100 peak network loads to magnitude of 101st peak for a network of 2212 households with a 50% penetration level and signalled response divided evenly between battery systems.

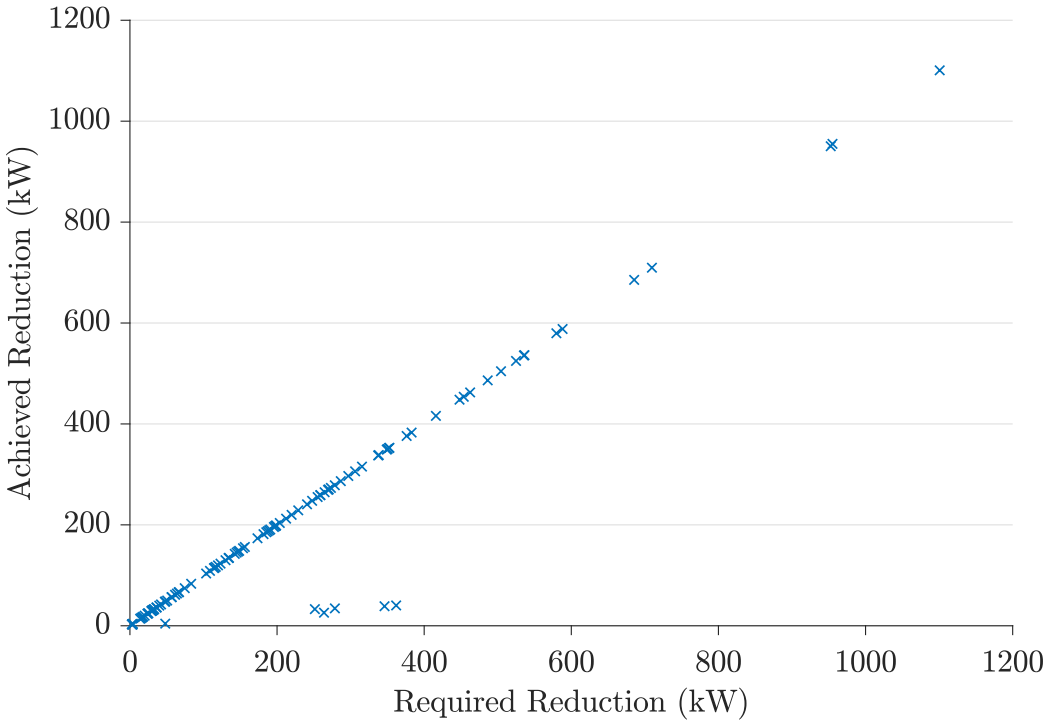

Figure B.35 Required reduction against achieved reduction to reduce top 100 peak network loads to magnitude of 101st peak for a network of 2212 households with a 75% penetration level and signalled response divided evenly between battery systems.

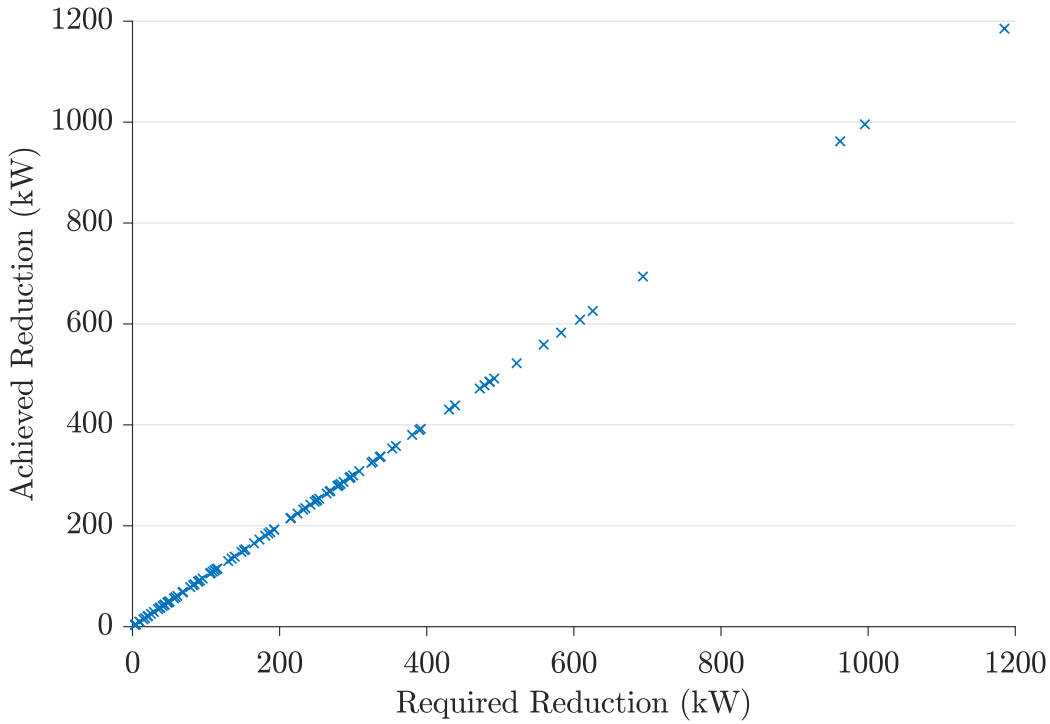

Figure B.36 Required reduction against achieved reduction to reduce top 100 peak network loads to magnitude of 101st peak for a network of 2212 households with a 100% penetration level and signalled response divided evenly between battery systems.

Appendix C

CASE 2 - PEAK/SHOULDER/OFF-PEAK PRICING

C.1 AVAILABLE REDUCTION CAPABILITY

The following figures show the available reduction power as a function of aggregate load across different penetration levels for a network of 2212 households.

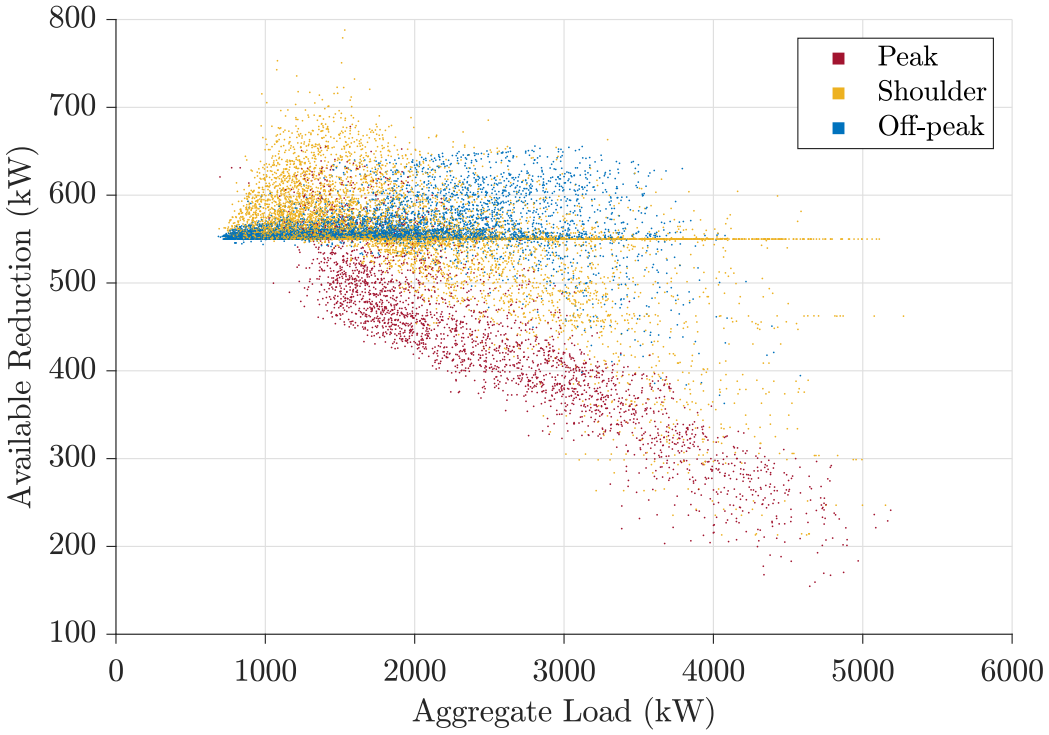

Figure C.1 Total aggregate load against available reduction capacity for a network of 2212 households with 5% PV and BESS penetration level.

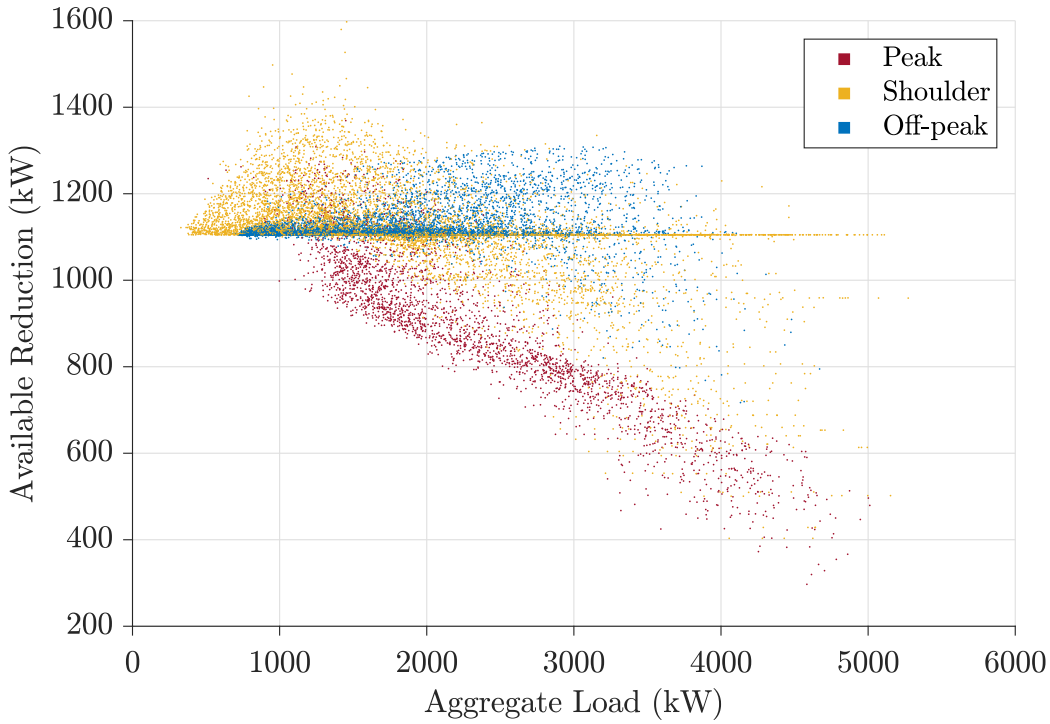

Figure C.2 Total aggregate load against available reduction capacity for a network of 2212 households with 10% PV and BESS penetration level.

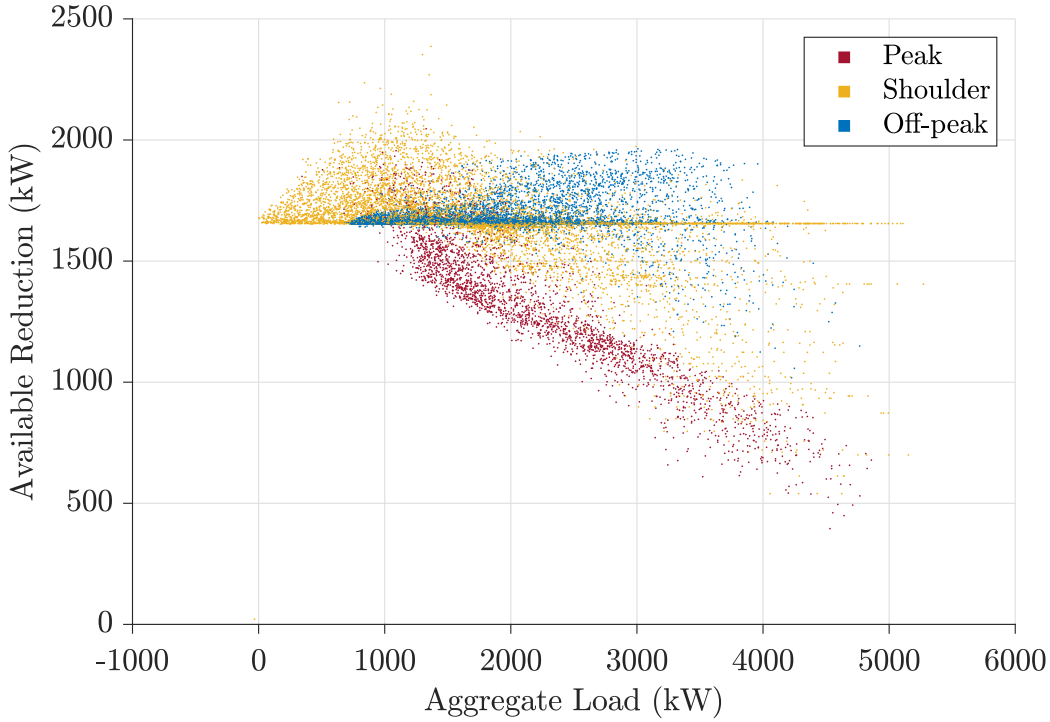

Figure C.3 Total aggregate load against available reduction capacity for a network of 2212 households with 15% PV and BESS penetration level.

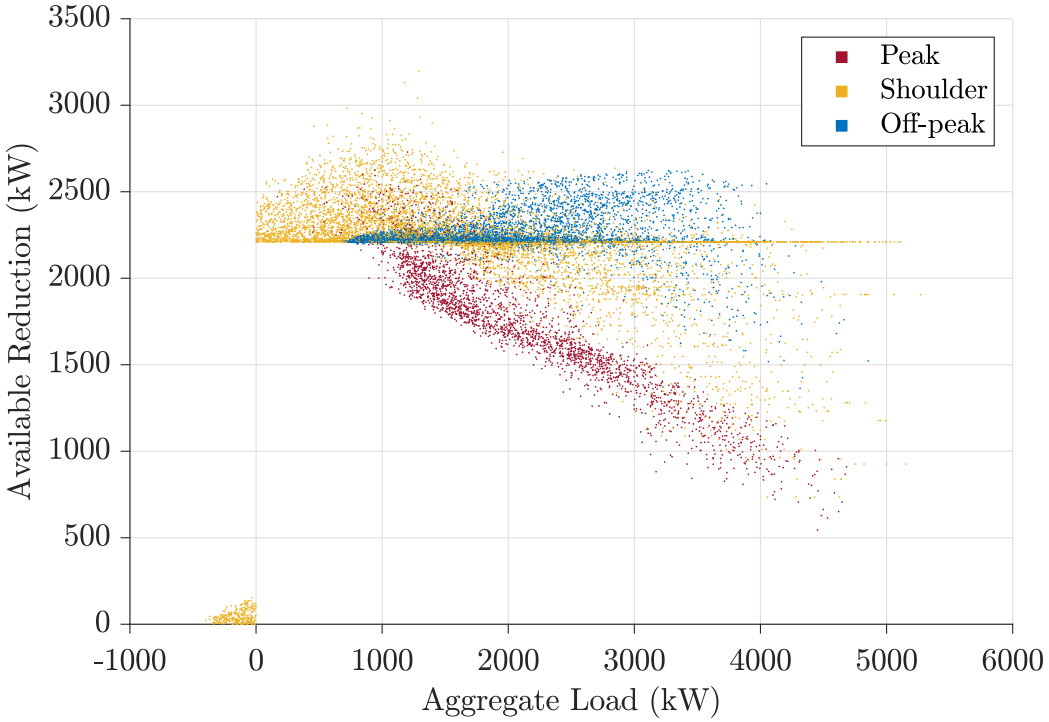

Figure C.4 Total aggregate load against available reduction capacity for a network of 2212 households with 20% PV and BESS penetration level.

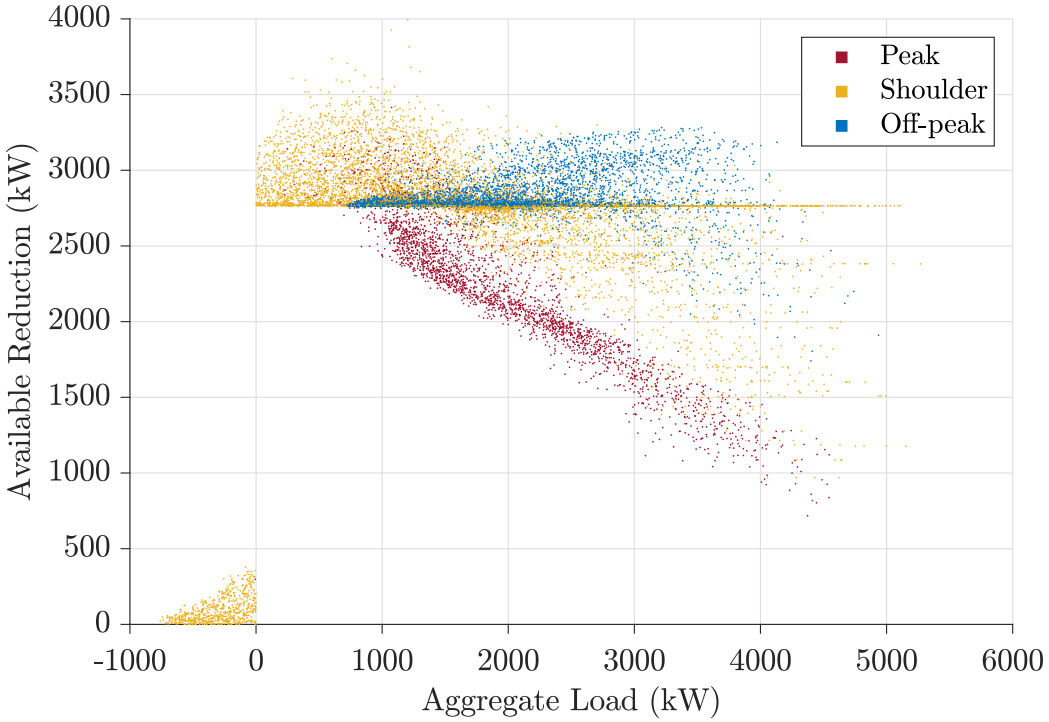

Figure C.5 Total aggregate load against available reduction capacity for a network of 2212 households with 25% PV and BESS penetration level.

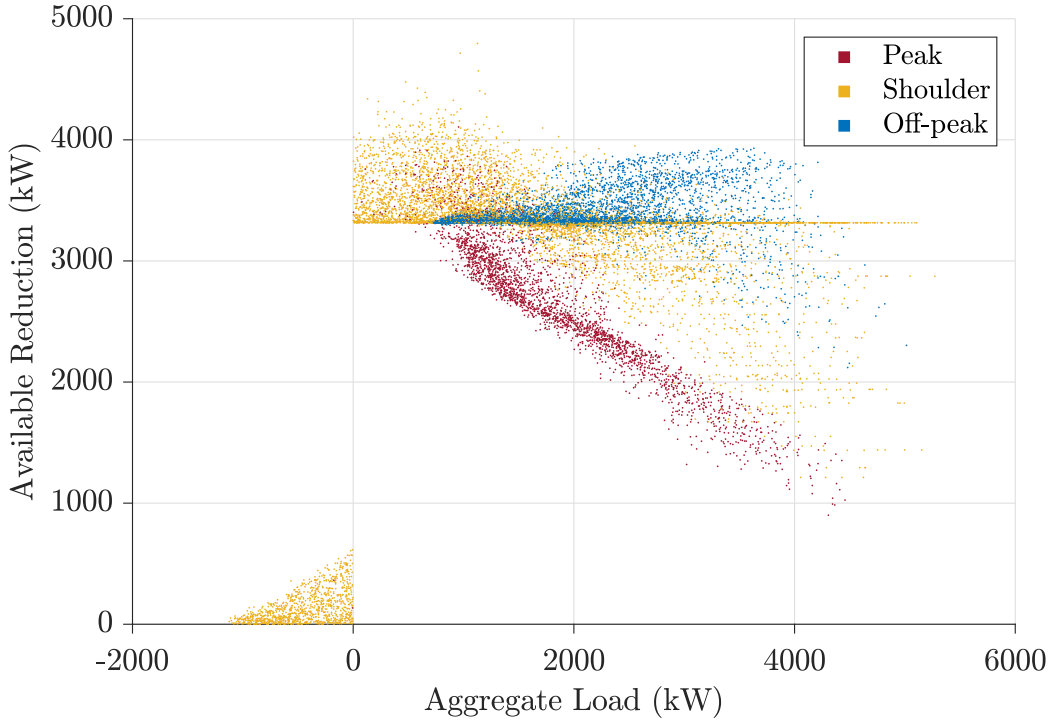

Figure C.6 Total aggregate load against available reduction capacity for a network of 2212 households with 30% PV and BESS penetration level.

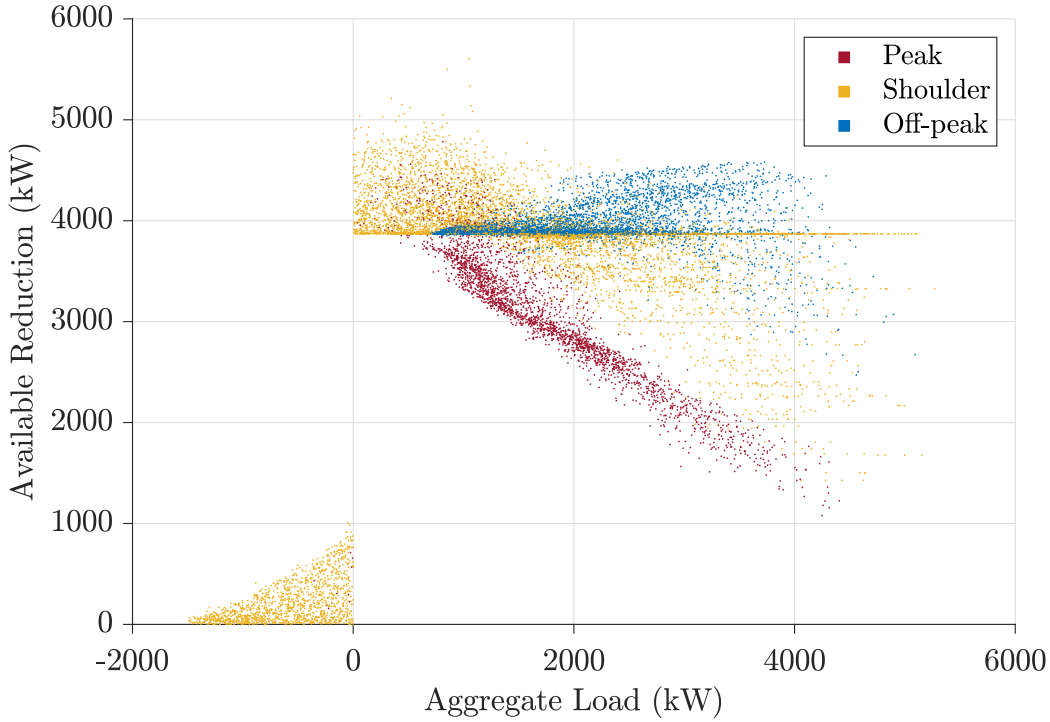

Figure C.7 Total aggregate load against available reduction capacity for a network of 2212 households with 35% PV and BESS penetration level.

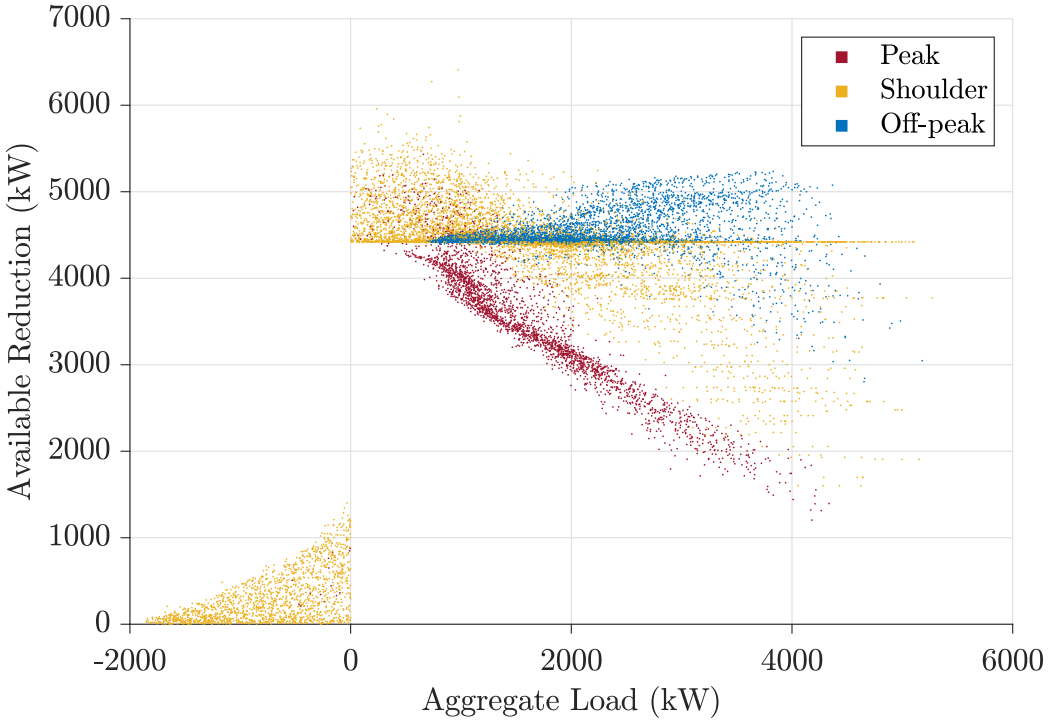

Figure C.8 Total aggregate load against available reduction capacity for a network of 2212 households with 40% PV and BESS penetration level.

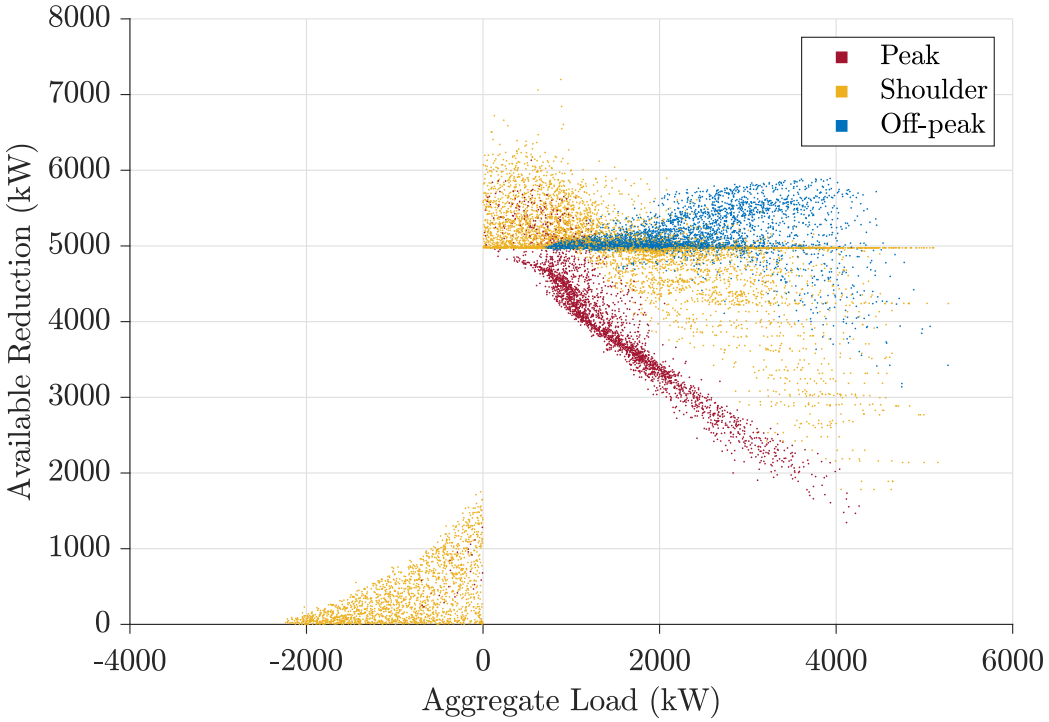

Figure C.9 Total aggregate load against available reduction capacity for a network of 2212 households with 45% PV and BESS penetration level.

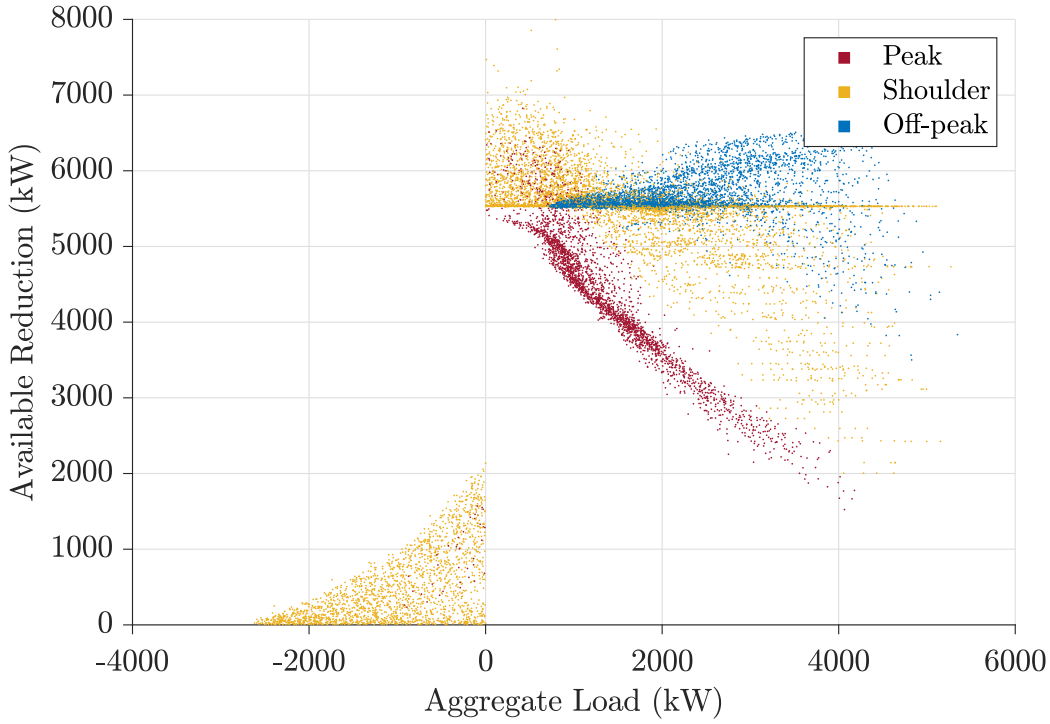

Figure C.10 Total aggregate load against available reduction capacity for a network of 2212 households with 50% PV and BESS penetration level.

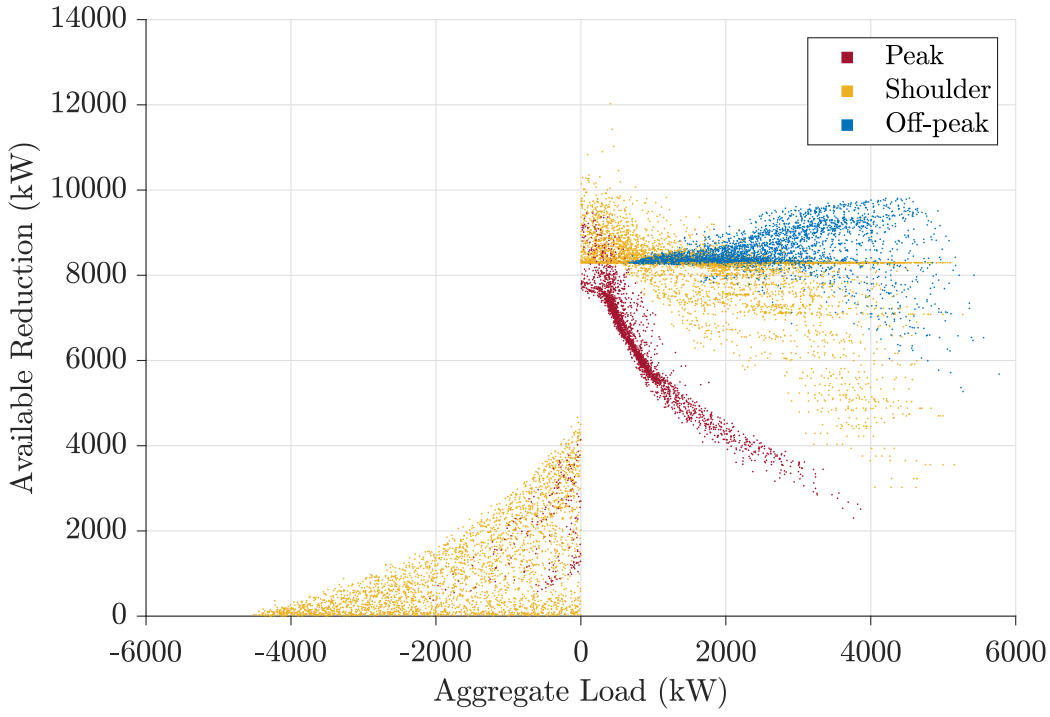

Figure C.11 Total aggregate load against available reduction capacity for a network of 2212 households with 75% PV and BESS penetration level.

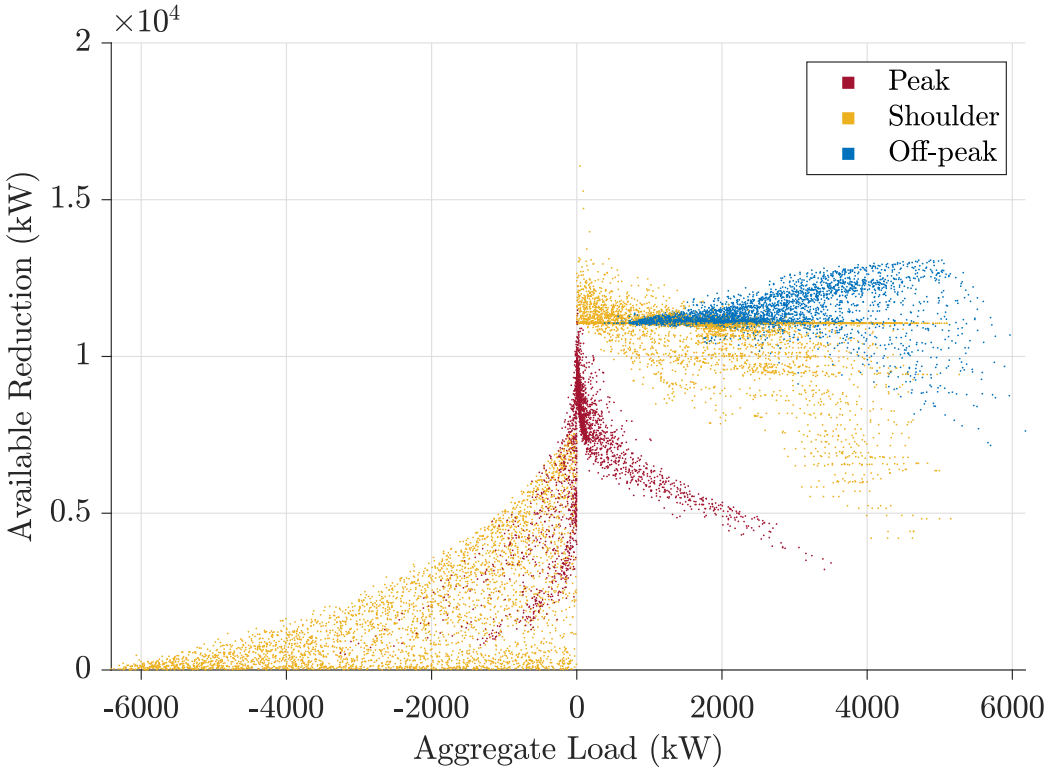

Figure C.12 Total aggregate load against available reduction capacity for a network of 2212 households with 100% PV and BESS penetration level.

C.2 PEAK REDUCTION SUFFICIENCY

The following figures shows the proportion of the top 100 peak loads where there is sufficient reduction capacity to reduce those peaks to the level of the 101st peak.

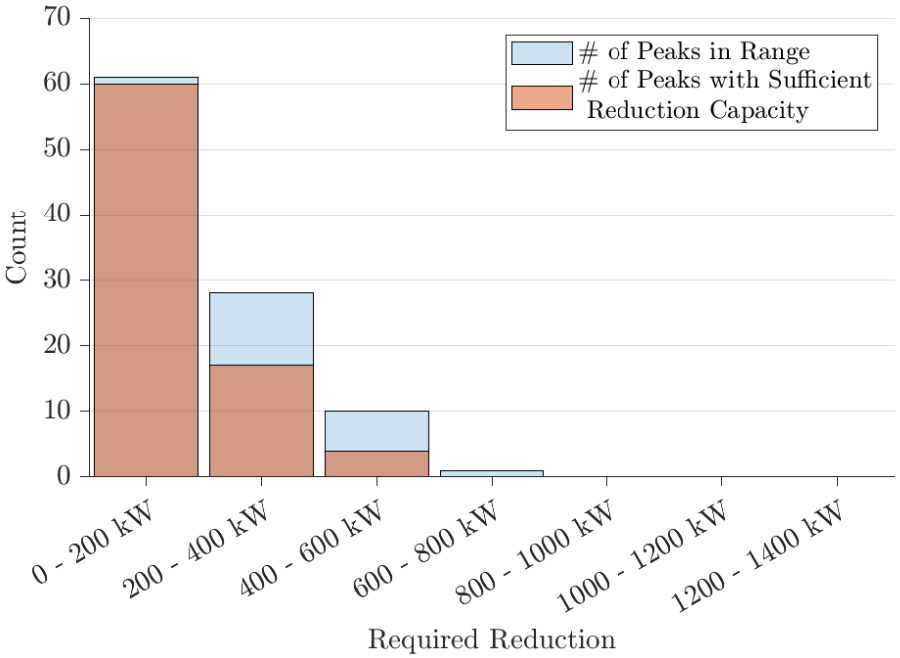

Figure C.13 Sufficiency of available reduction power to meet required reduction to reduce top 100 peaks to level of 101st peak for 5% penetration level in a network of 2212 households.

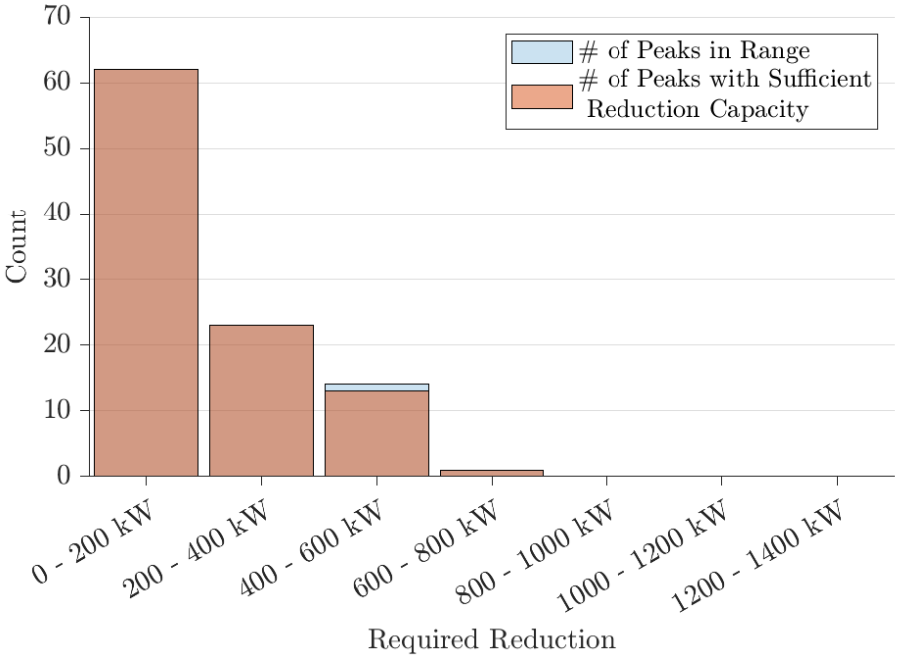

Figure C.14 Sufficiency of available reduction power to meet required reduction to reduce top 100 peaks to level of 101st peak for 10% penetration level in a network of 2212 households.

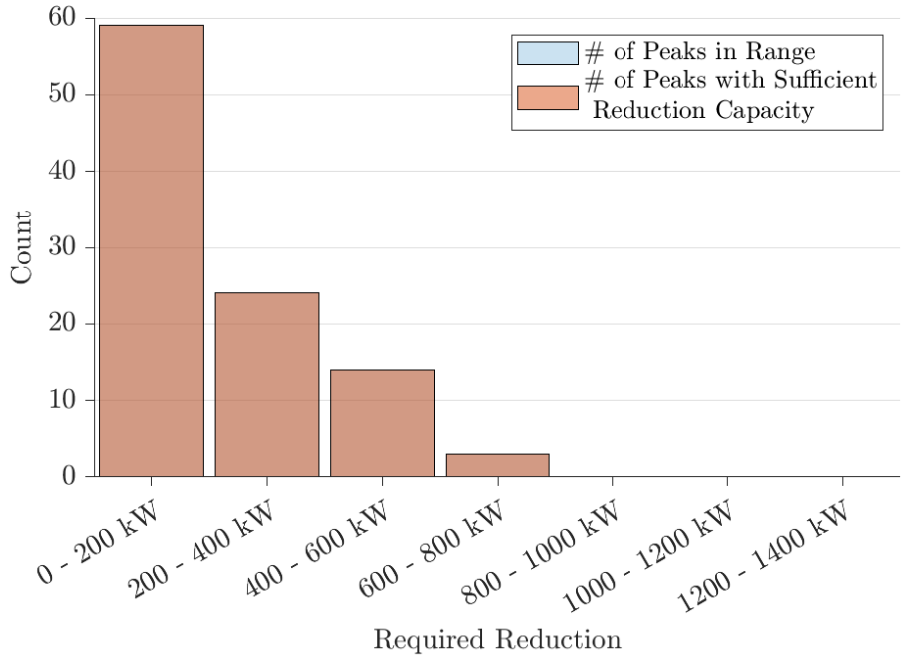

Figure C.15 Sufficiency of available reduction power to meet required reduction to reduce top 100 peaks to level of 101st peak for 15% penetration level in a network of 2212 households.

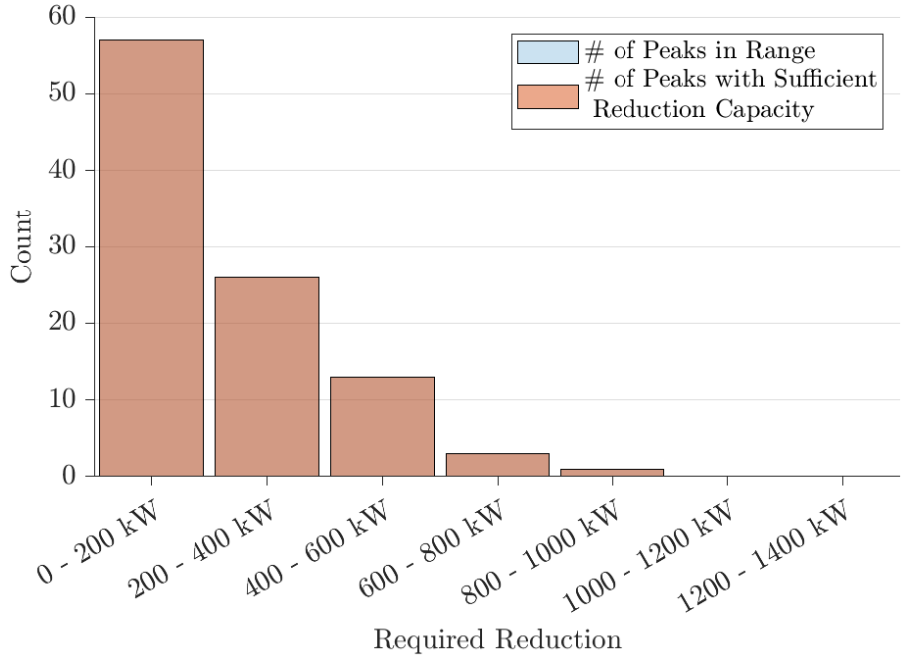

Figure C.16 Sufficiency of available reduction power to meet required reduction to reduce top 100 peaks to level of 101st peak for 20% penetration level in a network of 2212 households.

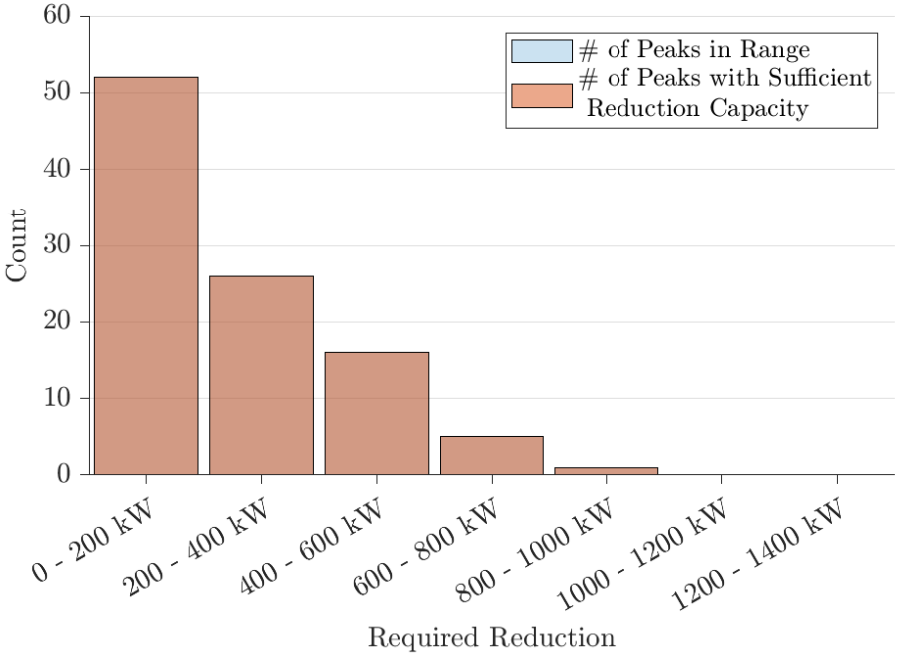

Figure C.17 Sufficiency of available reduction power to meet required reduction to reduce top 100 peaks to level of 101st peak for 25% penetration level in a network of 2212 households.

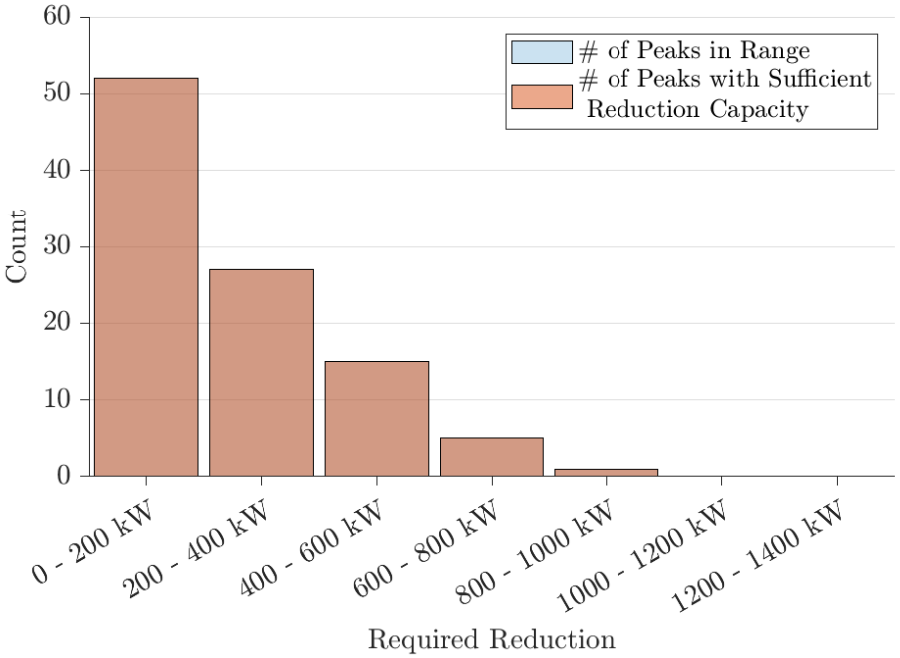

Figure C.18 Sufficiency of available reduction power to meet required reduction to reduce top 100 peaks to level of 101st peak for 30% penetration level in a network of 2212 households.

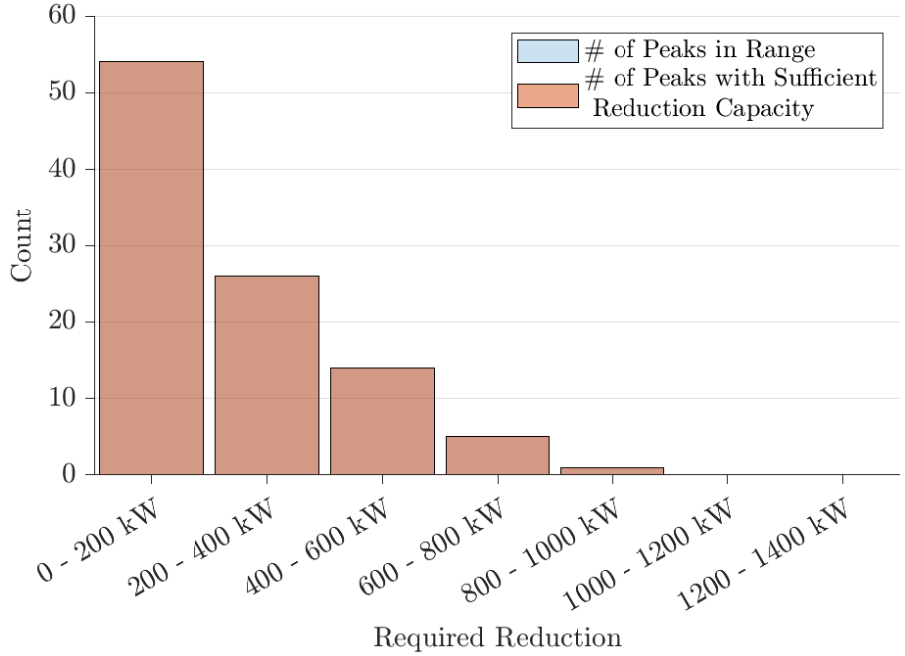

Figure C.19 Sufficiency of available reduction power to meet required reduction to reduce top 100 peaks to level of 101st peak for 35% penetration level in a network of 2212 households.

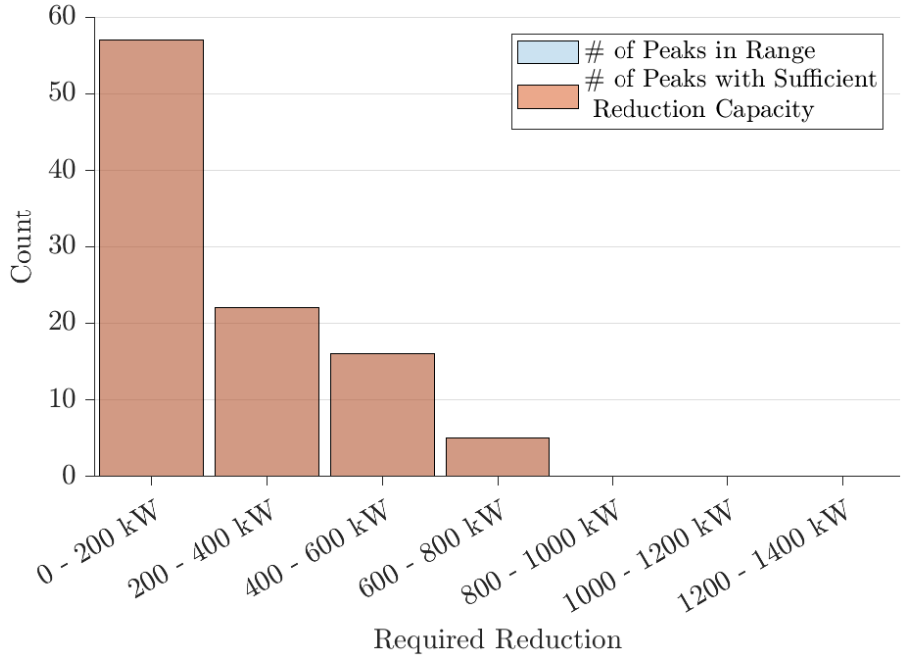

Figure C.20 Sufficiency of available reduction power to meet required reduction to reduce top 100 peaks to level of 101st peak for 40% penetration level in a network of 2212 households.

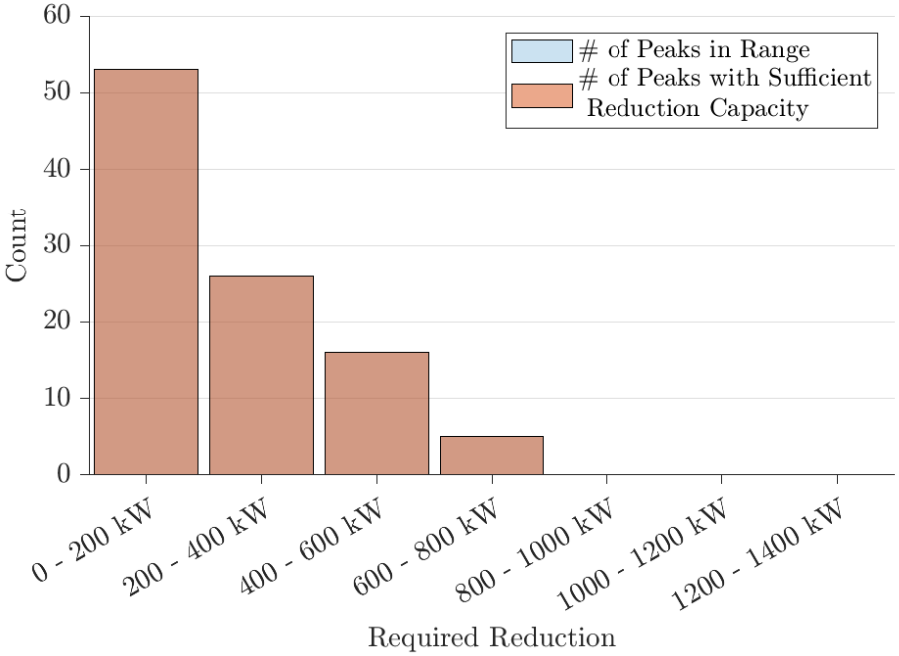

Figure C.21 Sufficiency of available reduction power to meet required reduction to reduce top 100 peaks to level of 101st peak for 45% penetration level in a network of 2212 households.

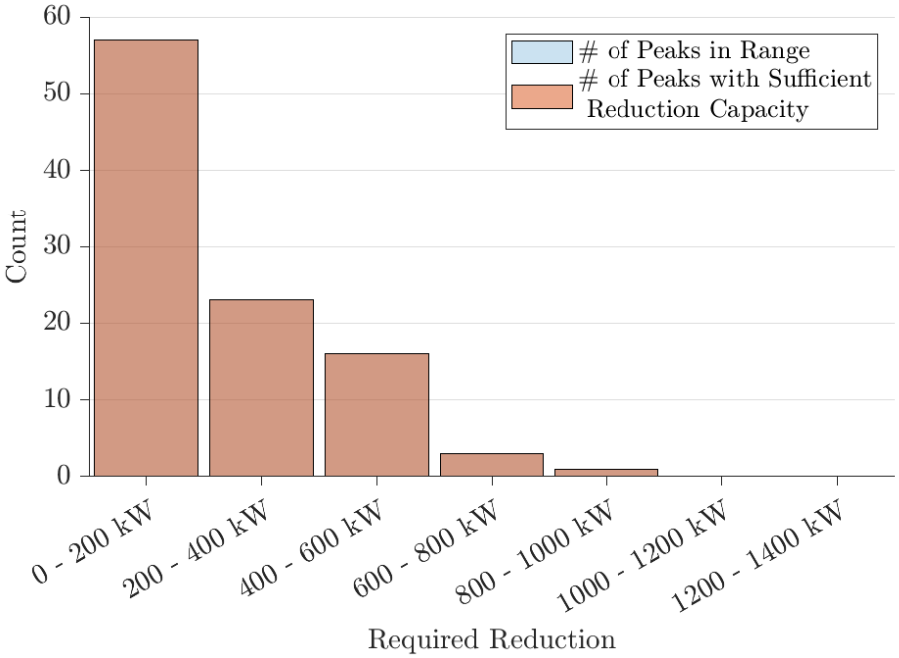

Figure C.22 Sufficiency of available reduction power to meet required reduction to reduce top 100 peaks to level of 101st peak for 50% penetration level in a network of 2212 households.

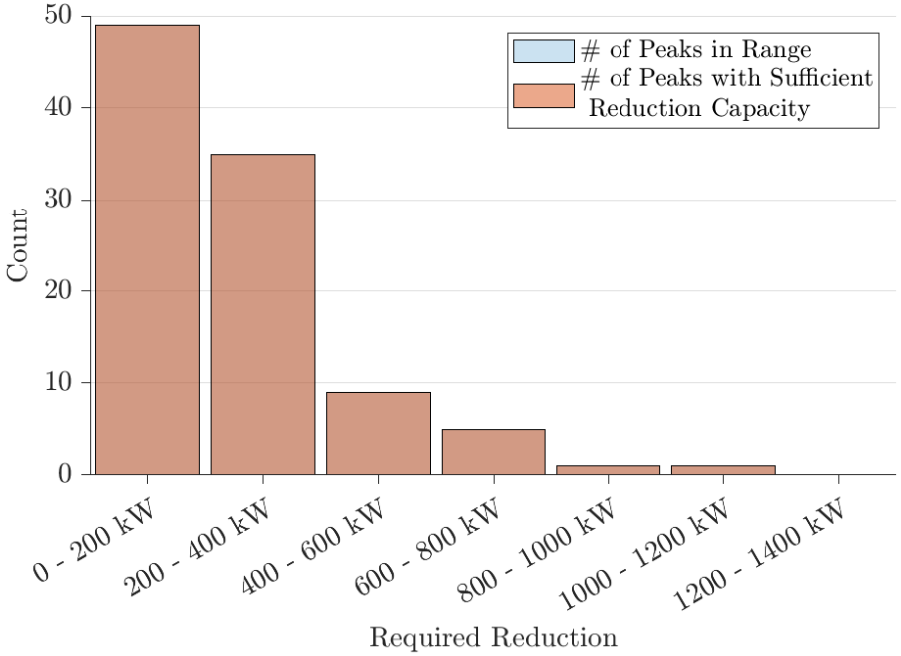

Figure C.23 Sufficiency of available reduction power to meet required reduction to reduce top 100 peaks to level of 101st peak for 75% penetration level in a network of 2212 households.

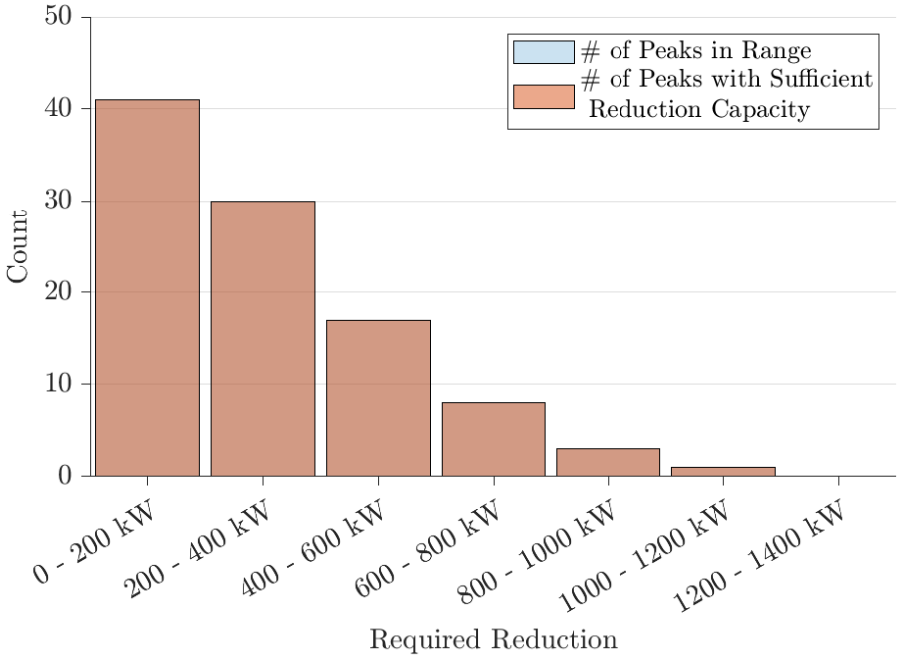

Figure C.24 Sufficiency of available reduction power to meet required reduction to reduce top 100 peaks to level of 101st peak for 100% penetration level in a network of 2212 households.

C.3 PEAK REDUCTION ACHIEVED

The following figures shows the achieved peak reduction against the required peak reduction where the required response is divided evenly amongst BESSs.

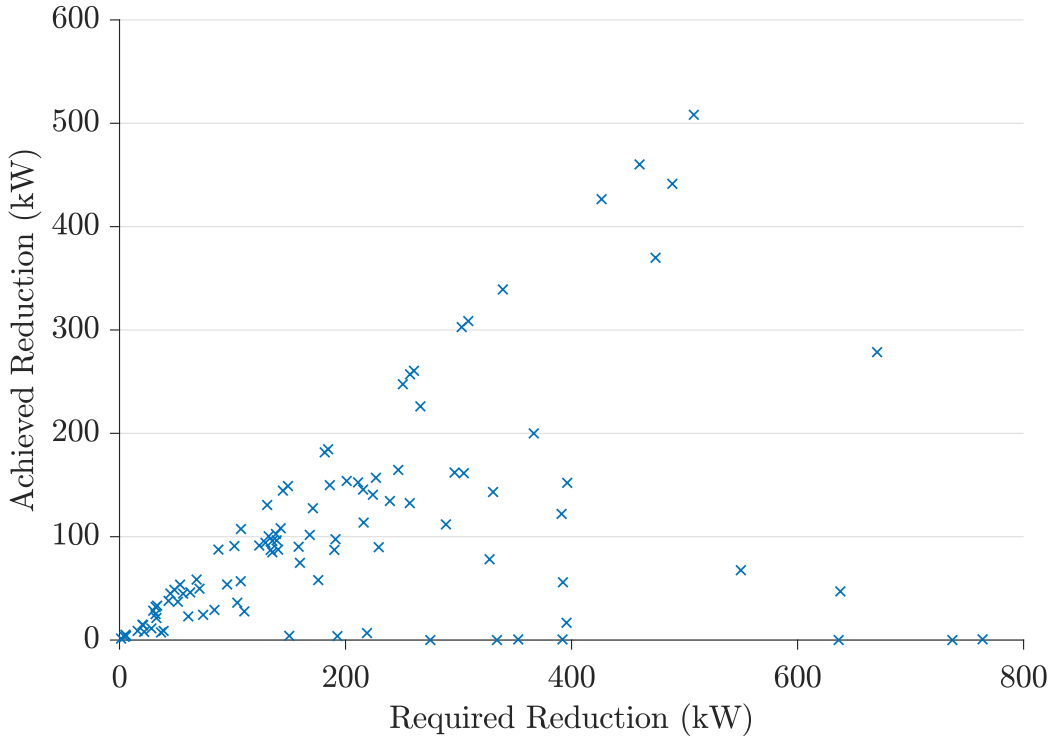

Figure C.25 Required reduction against achieved reduction to reduce top 100 peak network loads to magnitude of 101st peak for a network of 2212 households with a 5% penetration level and signalled response divided evenly between battery systems.

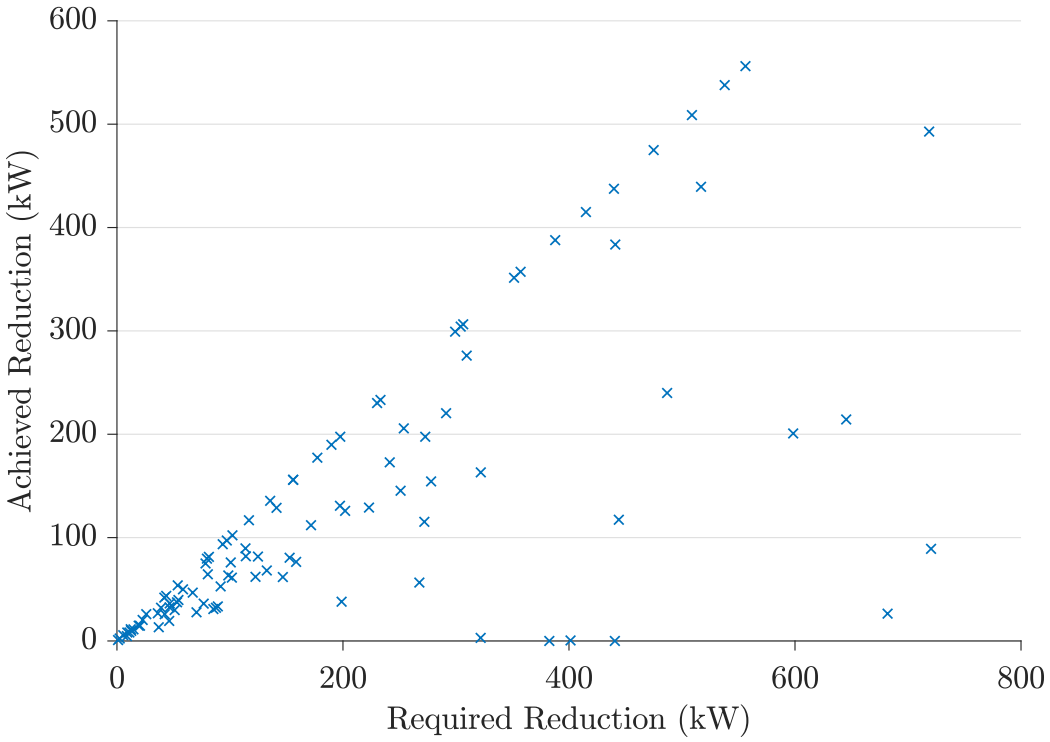

Figure C.26 Required reduction against achieved reduction to reduce top 100 peak network loads to magnitude of 101st peak for a network of 2212 households with a 10% penetration level and signalled response divided evenly between battery systems.

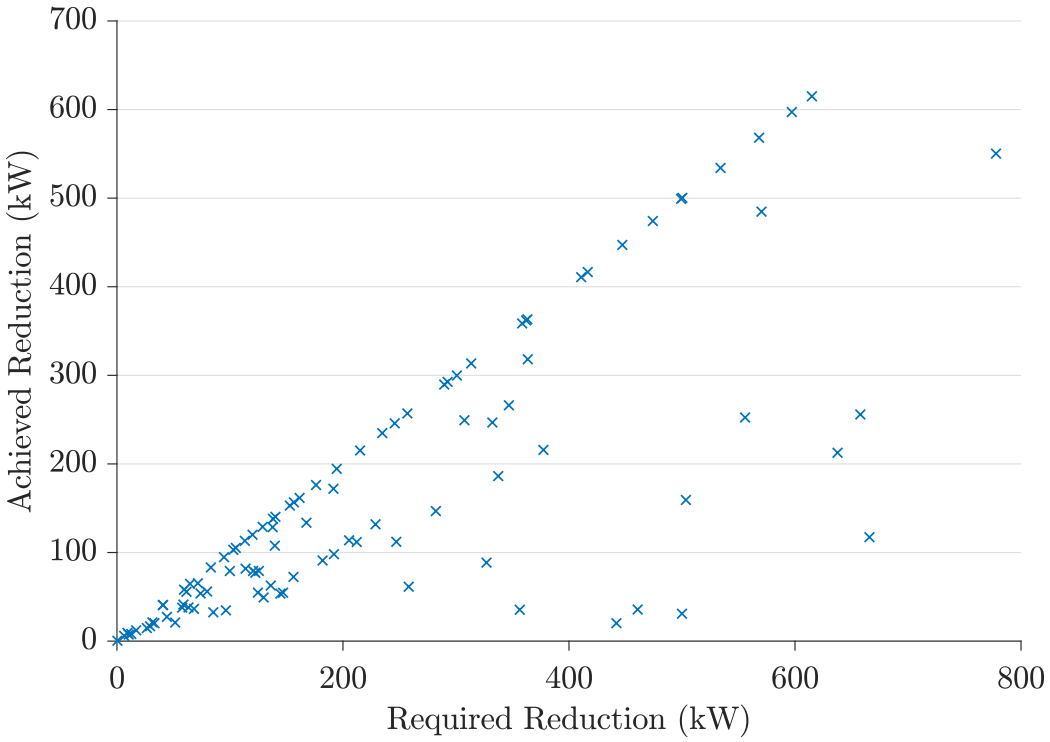

Figure C.27 Required reduction against achieved reduction to reduce top 100 peak network loads to magnitude of 101st peak for a network of 2212 households with a 15% penetration level and signalled response divided evenly between battery systems.

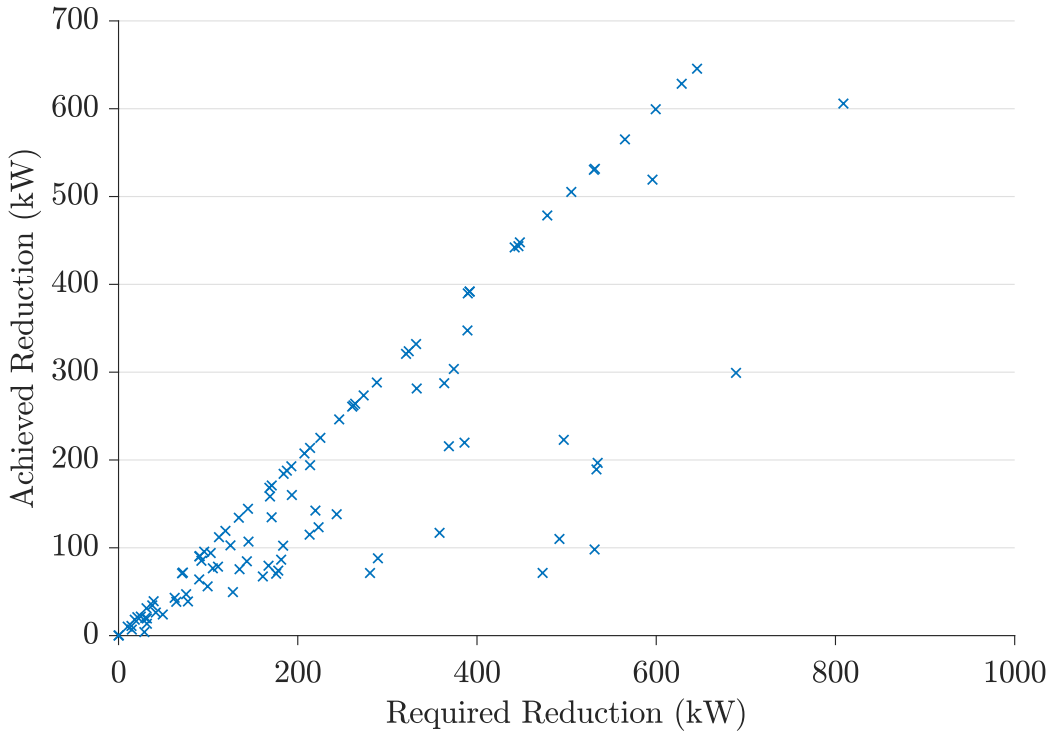

Figure C.28 Required reduction against achieved reduction to reduce top 100 peak network loads to magnitude of 101st peak for a network of 2212 households with a 20% penetration level and signalled response divided evenly between battery systems.

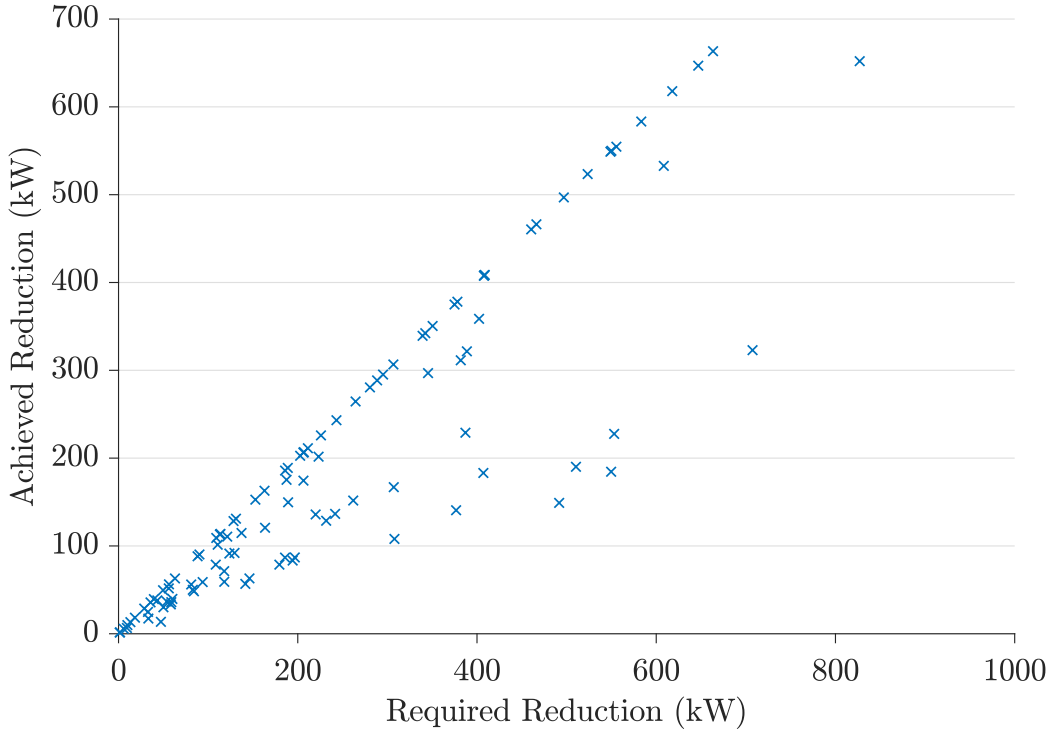

Figure C.29 Required reduction against achieved reduction to reduce top 100 peak network loads to magnitude of 101st peak for a network of 2212 households with a 25% penetration level and signalled response divided evenly between battery systems.

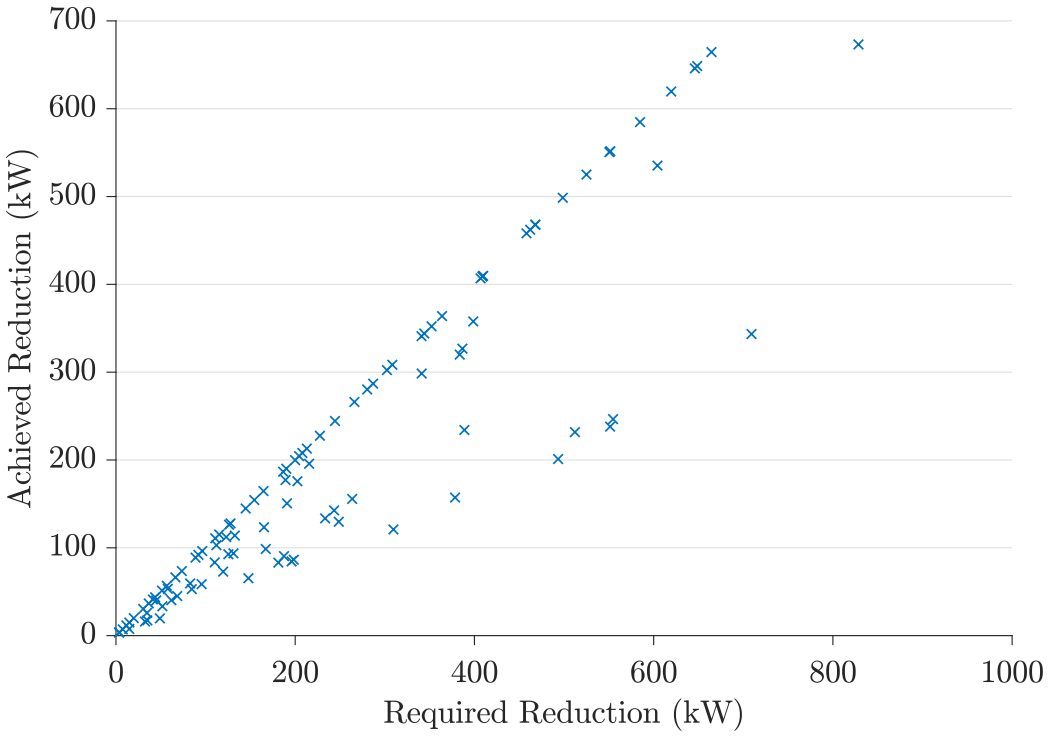

Figure C.30 Required reduction against achieved reduction to reduce top 100 peak network loads to magnitude of 101st peak for a network of 2212 households with a 30% penetration level and signalled response divided evenly between battery systems.

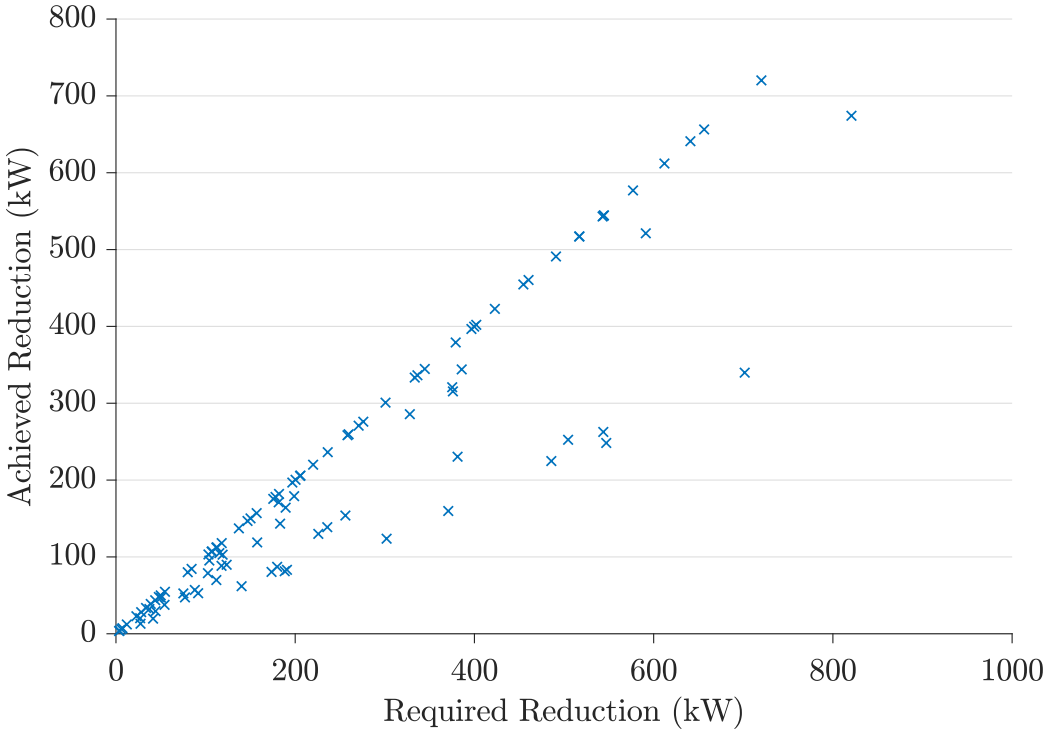

Figure C.31 Required reduction against achieved reduction to reduce top 100 peak network loads to magnitude of 101st peak for a network of 2212 households with a 35% penetration level and signalled response divided evenly between battery systems.

Figure C.32 Required reduction against achieved reduction to reduce top 100 peak network loads to magnitude of 101st peak for a network of 2212 households with a 40% penetration level and signalled response divided evenly between battery systems.

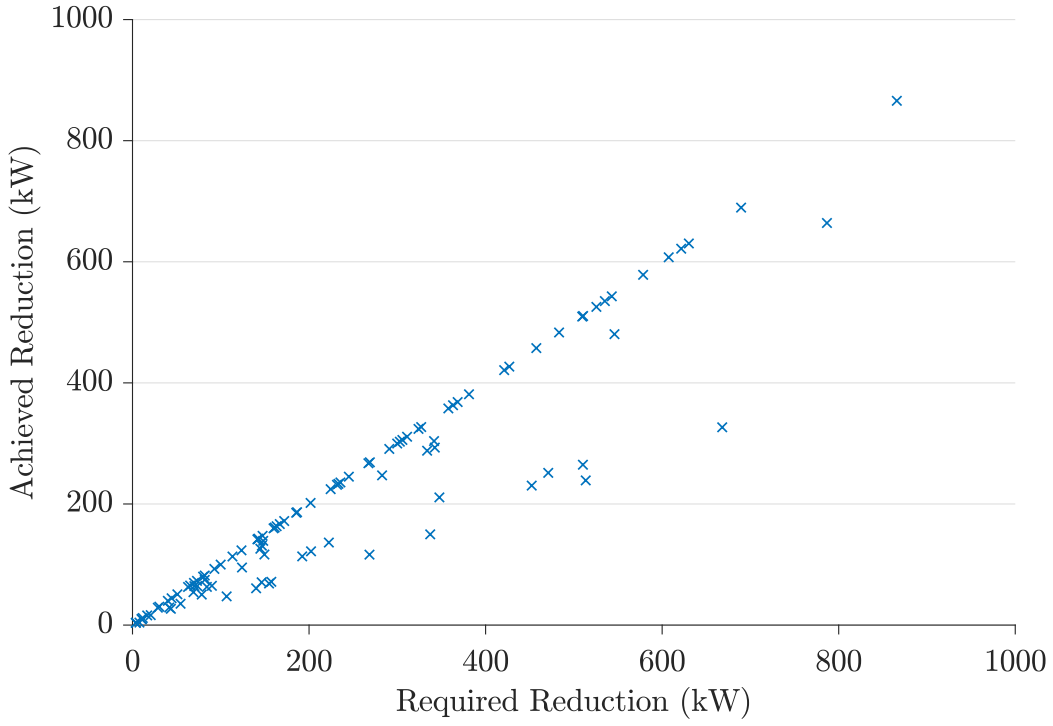

Figure C.33 Required reduction against achieved reduction to reduce top 100 peak network loads to magnitude of 101st peak for a network of 2212 households with a 45% penetration level and signalled response divided evenly between battery systems.

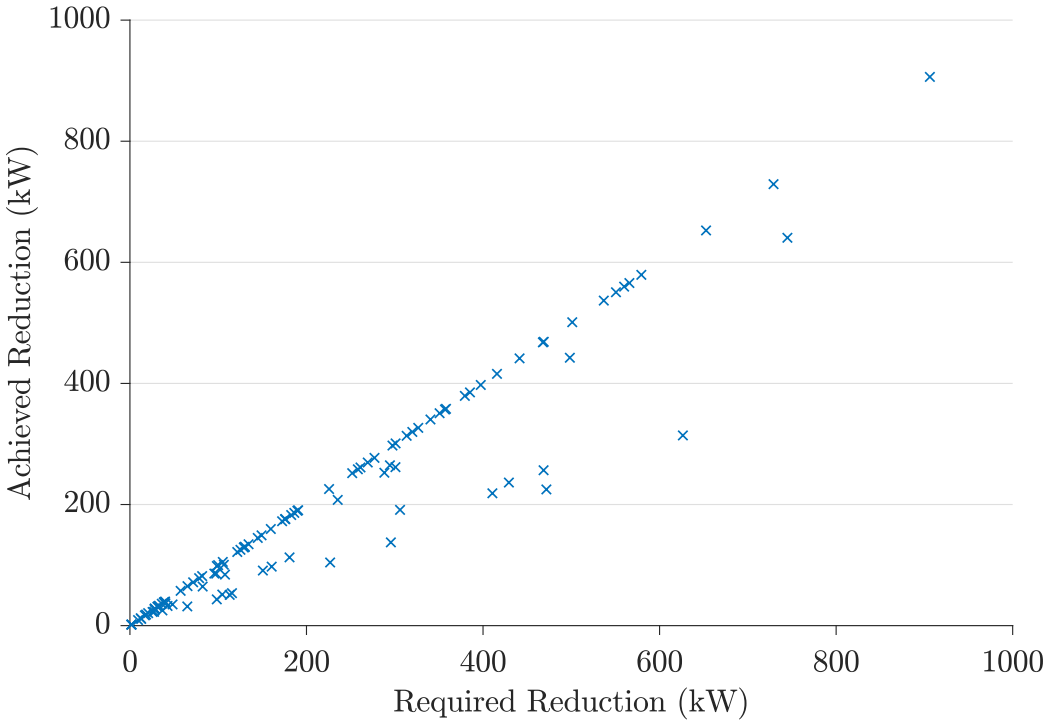

Figure C.34 Required reduction against achieved reduction to reduce top 100 peak network loads to magnitude of 101st peak for a network of 2212 households with a 50% penetration level and signalled response divided evenly between battery systems.

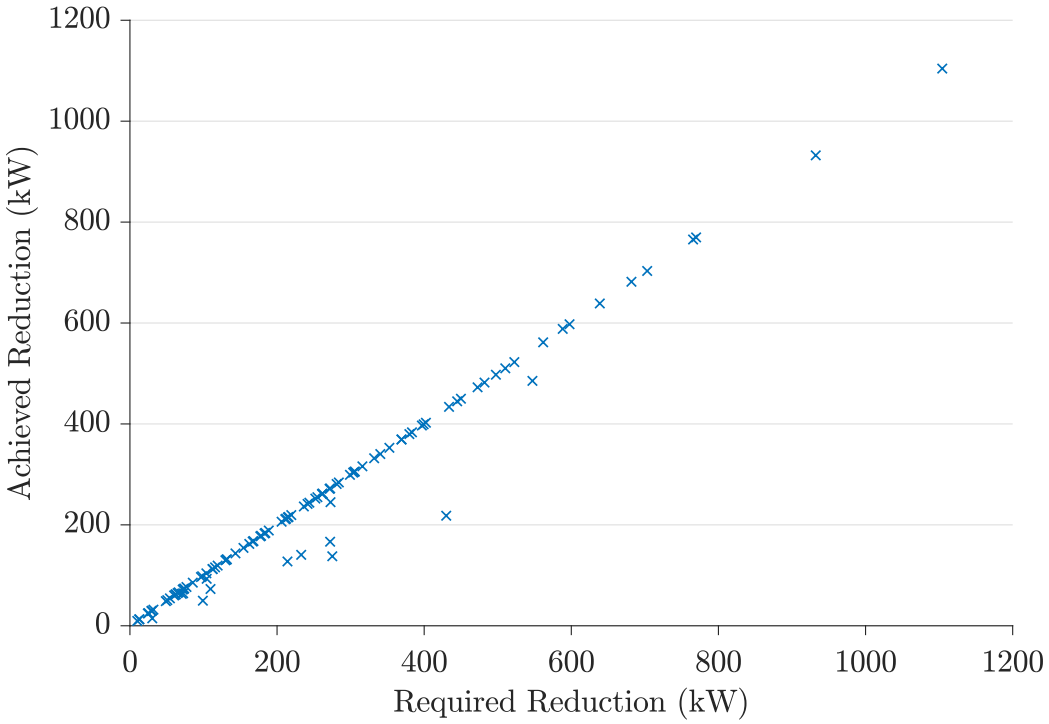

Figure C.35 Required reduction against achieved reduction to reduce top 100 peak network loads to magnitude of 101st peak for a network of 2212 households with a 75% penetration level and signalled response divided evenly between battery systems.

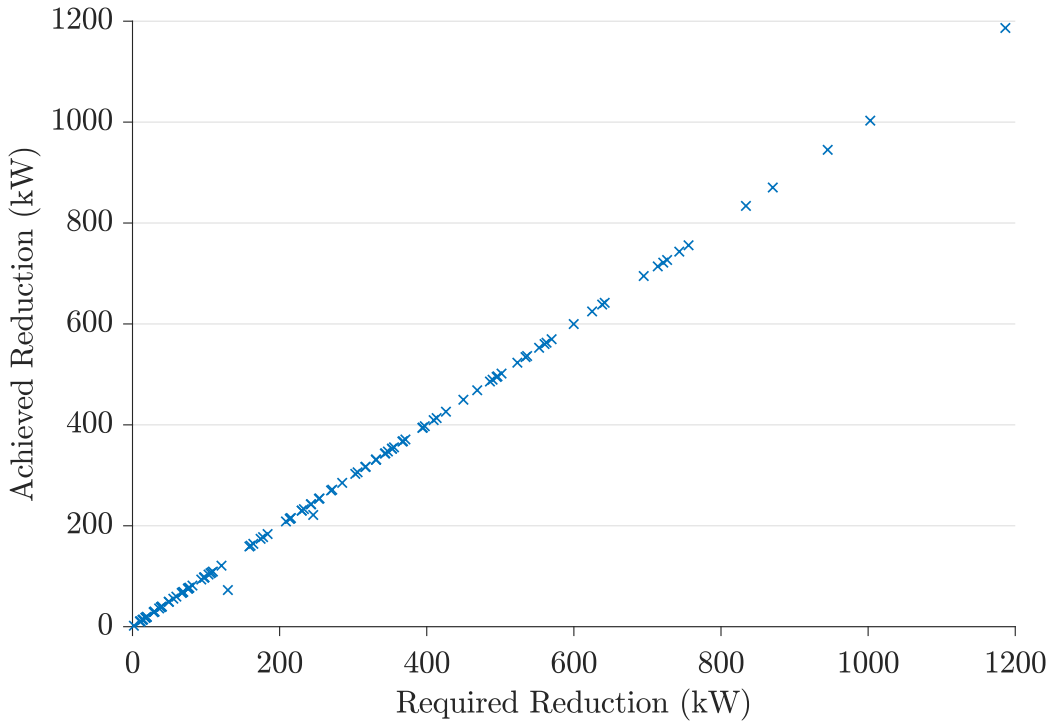

Figure C.36 Required reduction against achieved reduction to reduce top 100 peak network loads to magnitude of 101st peak for a network of 2212 households with a 100% penetration level and signalled response divided evenly between battery systems.

BIBLIOGRAPHY

[1] IEA, *Global EV Outlook 2019*, 2019. [Online]. Available: https://www.iea.org/reports/global-ev-outlook-2019.

[2] Ministry of Transport, "Monthly electric and hybrid light vehicle registrations," Wellington, New Zealand, Jul. 2020. [Online]. Available: https://www.transport.govt.nz/mot-resources/vehicle-fleet-statistics/monthly-electric-and-hybrid-light-vehicle-registrations/.

[3] Transpower, *Te Mauri Hiko - Energy Futures*, Jun. 2018. [Online]. Available: https://www.transpower.co.nz/sites/default/files/publications/resources/TP%20Energy%20Futures%20-%20Te%20Mauri%20Hiko%2011%20June%2718.pdf (visited on 02/24/2020).

[4] T. Franke and J. F. Krems, "Understanding charging behaviour of electric vehicle users," *Transportation Research Part F: Traffic Psychology and Behaviour*, vol. 21, pp. 75–89, Nov. 2013. DOI: 10.1016/j.trf.2013.09.002.

[5] S. Zoepf, D. MacKenzie, D. Keith, and W. Chernicoff, "Charging Choices and Fuel Displacement in a Large-Scale Demonstration of Plug-In Hybrid Electric Vehicles," *Transportation Research Record: Journal of the Transportation Research Board*, vol. 2385, no. 1, pp. 1–10, Jan. 2013. DOI: 10.3141/2385-01.

[6] K. Sharma and D. V. Shah, "Supercharged: Challenges and opportunities in global battery storage markets," Deloitte, 2018. [Online]. Available: https://www2.deloitte.com/content/dam/Deloitte/bg/Documents/energy-resources/gx-er-challenges-opportunities-global-battery-storage-markets.pdf.

[7] BloombergNEF, *Battery Pack Prices Fall As Market Ramps Up With Market Average At $156/kWh In 2019*, Dec. 2019. [Online]. Available: https://about.bnef.com/blog/battery-pack-prices-fall-as-market-ramps-up-with-market-average-at-156-kwh-in-2019/.

[8] Enphase Energy, *Encharge 3 Datasheet*. [Online]. Available: https://enphase.com/sites/default/files/downloads/support/Encharge-3-DS-EN-US.pdf (visited on 07/15/2020).

[9] Tesla, *Tesla Powerwall 2 AC Datasheet*, Apr. 18, 2018. [Online]. Available: https://www.tesla.com/sites/default/files/pdfs/powerwall/Powerwall%202_AC_Datasheet_en_AU.pdf (visited on 08/21/2018).

[10] J. Figgener, P. Stenzel, K.-P. Kairies, J. Linßen, D. Haberschusz, O. Wessels, G. Angenendt, M. Robinius, D. Stolten, and D. U. Sauer, "The development of stationary battery storage systems in Germany – A market review," *Journal of Energy Storage*, vol. 29, p. 101 153, Jun. 2020. DOI: 10.1016/j.est.2019.101153.

[11] Transpower, *Battery Storage in New Zealand*, Sep. 2017. [Online]. Available: https://www.transpower.co.nz/sites/default/files/publications/resources/Battery%20Storage%20in%20New%20Zealand.pdf.

[12] A. Eller and D. Gauntlett, "Energy Storage Trends and Opportunities in Emerging Markets," Navigant Consulting, 2017. [Online]. Available: https://www.esmap.org/file-download/30616/71065 (visited on 07/07/2020).

[13] T. Diaz de la Rubia, F. Klein, B. Shaffer, N. Kim, and G. Lovric, "Energy storage: Tracking the technologies that will transform the power sector," Deloitte, 2015. [Online]. Available: https://www2.deloitte.com/content/dam/Deloitte/no/Documents/energy-resources/energy-storage-tracking-technologies-transform-power-sector.pdf.

[14] G. Fitzgerald, J. Mandel, J. Morris, and H. Touati, "The Economics of Battery Energy Storage: How multi-use, customer-sited batteries deliver the most services and value to customers and the grid," Rocky Mountain Institute, Sep. 2015.

[15] Tesla, *Time-Based Control*. [Online]. Available: https://www.tesla.com/support/energy/powerwall/mobile-app/time-based-control.

[16] R. Green, "Electricity transmission pricing: An international comparison," *Utilities Policy*, vol. 6, no. 3, pp. 177–184, Sep. 1997. DOI: 10.1016/S0957-1787(97)00022-2.

[17] Frontier Economics, "International transmission pricing review," 2019, p. 42. [Online]. Available: https://www.ea.govt.nz/dmsdocument/2539-report-by-frontier-economics-international-transmission-pricing-review.

[18] Transpower, *Revenue & Pricing*. [Online]. Available: https://www.transpower.co.nz/industry/revenue-and-pricing/pricing (visited on 11/25/2019).

[19] Commerce Commission. (2019). "Commission's role in electricity lines," [Online]. Available: https://comcom.govt.nz/regulated-industries/electricity-lines/commissions-role-in-electricity-lines (visited on 07/29/2020).

[20] Electricity Authority, *Distribution Pricing: Practice Note August 2019*, Aug. 2019. [Online]. Available: https://www.ea.govt.nz/dmsdocument/25528-distribution-pricing-practice-note-august-2019.

[21] T. Stevenson and R. Le Prou, "International and domestic electricity tariffs and tariff structures," LECG, Wellington, New Zealand, May 2008.

[22] Transpower, *Demand Response: The journey so far*. [Online]. Available: https://www.transpower.co.nz/keeping-you-connected/demand-response/demand-response-journey-so-far (visited on 07/29/2019).

[23] Vector Limited, *What to do if you don't have hot water*. [Online]. Available: https://www.vector.co.nz/news/what-to-do-if-you-don-t-have-hot-water (visited on 07/30/2019).

[24] Orion New Zealand Limited, *Load management*. [Online]. Available: http://www.oriongroup.co.nz/customers/load-management-and-hot-water-control (visited on 07/29/2019).

[25] T. Weitzel and C. H. Glock, "Energy management for stationary electric energy storage systems: A systematic literature review," *European Journal of Operational Research*, vol. 264, no. 2, pp. 582–606, Jan. 2018. DOI: 10.1016/j.ejor.2017.06.052.

[26] H. Hesse, M. Schimpe, D. Kucevic, and A. Jossen, "Lithium-Ion Battery Storage for the Grid—A Review of Stationary Battery Storage System Design Tailored for Applications in Modern Power Grids," *Energies*, vol. 10, no. 12, p. 2107, Dec. 11, 2017. DOI: 10.3390/en10122107.

[27] J. Weniger, Tjaden, Tjarko, Orth, Nico, and Maier, Selina, *Performance Simulation Model for PV-Battery Systems (PerMod)*, Aug. 2019. [Online]. Available: https://pvspeicher.htw-berlin.de/wp-content/uploads/PerMod_docu.pdf.

[28] J. Neubauer, "Battery Lifetime Analysis and Simulation Tool (BLAST) Documentation," NREL, NREL/TP–5400-63246, 1167066, Dec. 1, 2014. [Online]. Available: http://www.osti.gov/servlets/purl/1167066/ (visited on 07/26/2020).

[29] D. Magnor and D. U. Sauer, "Optimization of PV Battery Systems Using Genetic Algorithms," *Energy Procedia*, vol. 99, pp. 332–340, Nov. 2016. DOI: 10.1016/j.egypro.2016.10.123.

[30] G. Mulder, D. Six, B. Claessens, T. Broes, N. Omar, and J. V. Mierlo, "The dimensioning of PV-battery systems depending on the incentive and selling price conditions," en, *Applied Energy*, vol. 111, pp. 1126–1135, Nov. 2013. DOI: 10.1016/j.apenergy.2013.03.059.

[31] A. I. Nousdilis, G. C. Kryonidis, E. O. Kontis, G. K. Papagiannis, G. C. Christoforidis, and I. P. Panapakidis, "Economic Viability of Residential PV Systems with Battery Energy Storage Under Different Incentive Schemes," in *2018 IEEE International Conference on Environment and Electrical Engineering and 2018 IEEE Industrial and Commercial Power Systems Europe (EEEIC / I CPS Europe)*, Jun. 2018, pp. 1–6. DOI: 10.1109/EEEIC.2018.8494492.

[32] Y. Ru, J. Kleissl, and S. Martinez, "Storage Size Determination for Grid-Connected Photovoltaic Systems," *IEEE Transactions on Sustainable Energy*, vol. 4, no. 1, pp. 68–81, Jan. 2013. DOI: 10.1109/TSTE.2012.2199339. (visited on 01/30/2021).

[33] S. van der Kooij, "Optimal charging/discharging strategies for batteries in smart energy grids," Vrije Universiteit Amsterdam, Nov. 16, 2016.

[34] M. N. Kabir, Y. Mishra, G. Ledwich, Z. Xu, and R. C. Bansal, "Improving voltage profile of residential distribution systems using rooftop PVs and Battery Energy Storage systems," en, *Applied Energy*, vol. 134, pp. 290–300, Dec. 2014. DOI: 10.1016/j.apenergy.2014.08.042.

[35] E. L. Ratnam, S. R. Weller, and C. M. Kellett, "Scheduling residential battery storage with solar PV: Assessing the benefits of net metering," *Applied Energy*, vol. 155, pp. 881–891, Oct. 2015. DOI: 10.1016/j.apenergy.2015.06.061.

[36] K. Kwan and D. Maly, "Optimal battery energy storage system (BESS) charge scheduling with dynamic programming," *IEE Proceedings - Science, Measurement and Technology*, vol. 142, no. 6, pp. 453–458, Nov. 1, 1995. DOI: 10.1049/ip-smt:19951929.

[37] E. L. Ratnam, S. R. Weller, and C. M. Kellett, "Central versus localized optimization-based approaches to power management in distribution networks with residential battery storage," *International Journal of Electrical Power & Energy Systems*, vol. 80, pp. 396–406, Sep. 2016. DOI: 10.1016/j.ijepes.2016.01.048.

[38] ——, "An optimization-based approach to scheduling residential battery storage with solar PV: Assessing customer benefit," *Renewable Energy*, vol. 75, pp. 123–134, Mar. 2015. DOI: 10.1016/j.renene.2014.09.008.

[39] T. Hubert and S. Grijalva, "Modeling for Residential Electricity Optimization in Dynamic Pricing Environments," *IEEE Transactions on Smart Grid*, vol. 3, no. 4, pp. 2224–2231, Dec. 2012. DOI: 10.1109/TSG.2012.2220385.

[40] A. Nottrott, J. Kleissl, and B. Washom, "Energy dispatch schedule optimization and cost benefit analysis for grid-connected, photovoltaic-battery storage systems," en, *Renewable Energy*, vol. 55, pp. 230–240, Jul. 2013. DOI: 10.1016/j.renene.2012.12.036.

[41] A. Kapoor and A. Sharma, "Optimal Charge/Discharge Scheduling of Battery Storage Interconnected With Residential PV System," *IEEE Systems Journal*, vol. 14, no. 3, pp. 3825–3835, Sep. 2020. DOI: 10.1109/JSYST.2019.2959205.

[42] N. Zhang, B. D. Leibowicz, and G. A. Hanasusanto, "Optimal Residential Battery Storage Operations Using Robust Data-Driven Dynamic Programming," *IEEE Transactions on Smart Grid*, vol. 11, no. 2, pp. 1771–1780, Mar. 2020. DOI: 10.1109/TSG.2019.2942932.

[43] L. Gong, J. Wang, L. Wang, S. Ren, Z. Zhang, and X. Yin, "Coordinated Optimization Scheduling for Photovoltaic Storage Home Energy Management System Considering User Satisfaction," in *2019 IEEE 3rd Conference on Energy Internet and Energy System Integration (EI2)*, Nov. 2019, pp. 1042–1046. DOI: 10.1109/EI247390.2019.9062274.

[44] R. Arghandeh, J. Woyak, A. Onen, J. Jung, and R. P. Broadwater, "Economic optimal operation of Community Energy Storage systems in competitive energy markets," *Applied Energy*, vol. 135, pp. 71–80, Dec. 2014. DOI: 10.1016/j.apenergy.2014.08.066.

[45] Y. Riffonneau, S. Bacha, F. Barruel, and S. Ploix, "Optimal Power Flow Management for Grid Connected PV Systems With Batteries," *IEEE Transactions on Sustainable Energy*, vol. 2, no. 3, pp. 309–320, Jul. 2011. DOI: 10.1109/TSTE.2011.2114901.

[46] M. Braun, K. Büdenbender, D. Magnor, and A. Jossen, "Photovoltaic self-consumption in Germany - Using lithium-ion storage to increase self-consumed photovoltaic energy," in *Proceedings of the 24th European Photovoltaic Solar Energy Conference and Exhibition (EU PVSEC)*, 2009, pp. 3121–3127.

[47] D. Lifshitz and G. Weiss, "Optimal Control of a Capacitor-Type Energy Storage System," *IEEE Transactions on Automatic Control*, vol. 60, no. 1, pp. 216–220, Jan. 2015. DOI: 10.1109/TAC.2014.2323136.

[48] B. Steffen and C. Weber, "Optimal operation of pumped-hydro storage plants with continuous time-varying power prices," *European Journal of Operational Research*, vol. 252, no. 1, pp. 308–321, Jul. 2016. DOI: 10.1016/j.ejor.2016.01.005.

[49] A. S. Hassan, L. Cipcigan, and N. Jenkins, "Optimal battery storage operation for PV systems with tariff incentives," *Applied Energy*, vol. 203, pp. 422–441, Oct. 2017. DOI: 10.1016/j.apenergy.2017.06.043.

[50] H. Wang, K. Meng, Z. Y. Dong, Z. Xu, F. Luo, and K. P. Wong, "Efficient real-time residential energy management through MILP based rolling horizon optimization," in *2015 IEEE Power & Energy Society General Meeting*, Denver, CO, USA: IEEE, Jul. 2015, pp. 1–6. DOI: 10.1109/PESGM.2015.7285754.

[51] R. Khezri, A. Mahmoudi, and M. H. Haque, "Optimal Capacity of Solar PV and Battery Storage for Australian Grid-Connected Households," *IEEE Transactions on Industry Applications*, vol. 56, no. 5, pp. 5319–5329, Sep. 2020. DOI: 10.1109/TIA.2020.2998668.

[52] T. Wang, H. Kamath, and S. Willard, "Control and Optimization of Grid-Tied Photovoltaic Storage Systems Using Model Predictive Control," *IEEE Transactions on Smart Grid*, vol. 5, no. 2, pp. 1010–1017, Mar. 2014. DOI: 10.1109/TSG.2013.2292525.

[53] S. Young, A. Bruce, and I. MacGill, "Potential impacts of residential PV and battery storage on Australia's electricity networks under different tariffs," *Energy Policy*, vol. 128, pp. 616–627, May 2019. DOI: 10.1016/j.enpol.2019.01.005.

[54] J. Suppers, "Impacts of new technologies on household electricity demand: From an individual household, a community, and a national perspective," University of Waikato, 2018.

[55] G. Barchi, G. Miori, D. Moser, and S. Papantoniou, "A Small-Scale Prototype for the Optimization of PV Generation and Battery Storage through the Use of a Building Energy Management System," in *2018 IEEE International Conference on Environment and Electrical Engineering and 2018 IEEE Industrial and Commercial Power Systems Europe (EEEIC / I CPS Europe)*, Jun. 2018, pp. 1–5. DOI: 10.1109/EEEIC.2018.8494012.

[56] J. Hill and C. Nwankpa, "System constraints effects on optimal dispatch schedule for battery storage systems," in *2012 IEEE PES Innovative Smart Grid Technologies (ISGT)*, Jan. 2012, pp. 1–8. DOI: 10.1109/ISGT.2012.6175634.

[57] D. Kucevic, B. Tepe, S. Englberger, A. Parlikar, M. Mühlbauer, O. Bohlen, A. Jossen, and H. Hesse, "Standard battery energy storage system profiles: Analysis of various applications for stationary energy storage systems using a holistic simulation framework," *Journal of Energy Storage*, vol. 28, p. 101 077, Apr. 2020. DOI: 10.1016/j.est.2019.101077.

[58] D. Fuselli, F. De Angelis, M. Boaro, S. Squartini, Q. Wei, D. Liu, and F. Piazza, "Action dependent heuristic dynamic programming for home energy resource scheduling," *International Journal of Electrical Power & Energy Systems*, vol. 48, pp. 148–160, Jun. 2013. DOI: 10.1016/j.ijepes.2012.11.023.

[59] N. Gudi, L. Wang, V. Devabhaktuni, and S. S. S. R. Depuru, "A demand-side management simulation platform incorporating optimal management of distributed renewable resources," in *2011 IEEE/PES Power Systems Conference and Exposition*, Phoenix, AZ, USA: IEEE, Mar. 2011, pp. 1–7. DOI: 10.1109/PSCE.2011.5772450.

[60] C. Crozier, M. Deakin, T. Morstyn, and M. McCulloch, "Incorporating Charger Efficiency into Electric Vehicle Charging Optimization," in *2019 IEEE PES Innovative Smart Grid Technologies Europe (ISGT-Europe)*, Bucharest, Romania: IEEE, Sep. 2019, pp. 1–5. DOI: 10.1109/ISGTEurope.2019.8905734.

[61] N. Mohan, *Power Electronics: A First Course*. Hoboken, N.J: Wiley, 2012, ISBN: 978-1-118-07480-0.

[62] A. Thingvad, C. Ziras, J. Hu, and M. Marinelli, "Assessing the energy content of system frequency and electric vehicle charging efficiency for ancillary service provision," in *2017 52nd International Universities Power Engineering Conference (UPEC)*, Heraklion: IEEE, Aug. 2017, pp. 1–6. DOI: 10.1109/UPEC.2017.8231947.

[63] Elena Marie Krieger, "Effects of variablity and rate on battery charge storage and lifespan," Princeton University, Apr. 2013.

[64] J. Moshövel, K.-P. Kairies, D. Magnor, M. Leuthold, M. Bost, S. Gährs, E. Szczechowicz, M. Cramer, and D. U. Sauer, "Analysis of the maximal possible grid relief from PV-peak-power impacts by using storage systems for increased self-consumption," en, *Applied Energy*, vol. 137, pp. 567–575, Jan. 2015. DOI: 10.1016/j.apenergy.2014.07.021.

[65] HOMER Energy, *Battery Roundtrip Efficiency*. [Online]. Available: https://www.homerenergy.com/products/pro/docs/3.11/battery_roundtrip_efficiency.html (visited on 11/07/2018).

[66] G. Notton, V. Lazarov, and L. Stoyanov, "Optimal sizing of a grid-connected PV system for various PV module technologies and inclinations, inverter efficiency characteristics and locations," *Renewable Energy*, vol. 35, no. 2, pp. 541–554, Feb. 2010. DOI: 10.1016/j.renene.2009.07.013.

[67] D. Bertsimas and J. N. Tsitsiklis, *Introduction to Linear Optimization*. Belmont, Mass: Athena Scientific, 1997, ISBN: 978-1-886529-19-9.

[68] Electricity Authority, *Electricty Industry Participation Code Amendment (Access to Retail Data) 2014*, Dec. 2014. [Online]. Available: https://www.ea.govt.nz/dmsdocument/19041-code-amendment-part-11.

[69] ——, "Managing electricity price risk: A guide for consumers," Wellington, New Zealand, Oct. 2012. [Online]. Available: https://www.ea.govt.nz/dmsdocument/13830-managing-electricity-spot-price-risk-guide (visited on 05/25/2020).

[70] Electricity Networks Association, *Why the Low Fixed Charge regulations should be removed*, Mar. 29, 2018. [Online]. Available: http://www.electricity.org.nz/news-and-events/news/why-the-low-fixed-charge-regulations-should-be-removed (visited on 06/30/2020).

[71] D. Hughes, "Electricity (Disconnection and Low Fixed Charges) Amendment Bill — Second Reading," *New Zealand Parliamentary Debates*, vol. 646, p. 15 113, 2008.

[72] Office of the Minister of Energy and Resources, "Progressing the Electricity Price Review's Recommendations," Feb. 13, 2020. [Online]. Available: https://www.mbie.govt.nz/assets/progressing-the-electricity-price-reviews-recommendations.pdf (visited on 06/30/2020).

[73] D. Santos-Martin and S. Lemon, "SoL – A PV generation model for grid integration analysis in distribution networks," *Solar Energy*, vol. 120, pp. 549–564, Oct. 2015, ISSN: 0038092X. DOI: 10.1016/j.solener.2015.07.052.

[74] Electricity Authority, *Electricity Market Information (EMI)*. [Online]. Available: https://www.emi.ea.govt.nz/.

[75] Orion New Zealand Limited, *Asset Management Plan 2016-2026*, Mar. 2016.

[76] J. Tipping, "The Analysis of Spot Price Stochasticity in Deregulated Wholesale Electricity Markets," University of Canterbury, Mar. 2007.

[77] *IBM ILOG CPLEX Optimization Studio*, New York, NY, USA: IBM, 2017.

[78] E. R. Bixby, M. Fenelon, Z. Gu, E. Rothberg, and R. Wunderling, "MIP: Theory and Practice — Closing the Gap," in *System Modelling and Optimization*, M. J. D. Powell and S. Scholtes, Eds., vol. 46, Boston, MA: Springer US, 2000, pp. 19–49, ISBN: 978-1-4757-6673-8.

[79] F. Domínguez-Muñoz, J. M. Cejudo-López, A. Carrillo-Andrés, and M. Gallardo-Salazar, "Selection of typical demand days for CHP optimization," *Energy and Buildings*, vol. 43, no. 11, pp. 3036–3043, Nov. 2011. DOI: 10.1016/j.enbuild.2011.07.024.

[80] J. F. Marquant, R. Evins, and J. Carmeliet, "Reducing Computation Time with a Rolling Horizon Approach Applied to a MILP Formulation of Multiple Urban Energy Hub System," *Procedia Computer Science*, vol. 51, pp. 2137–2146, 2015, ISSN: 18770509. DOI: 10.1016/j.procs.2015.05.486.

[81] G. Erichsen, T. Zimmermann, and A. Kather, "Effect of Different Interval Lengths in a Rolling Horizon MILP Unit Commitment with Non-Linear Control Model for a Small Energy System," *Energies*, vol. 12, no. 6, p. 1003, Mar. 14, 2019. DOI: 10.3390/en12061003.

[82] M. Campbell, N. Watson, and A. Miller, "Smart Meters to Monitor Power Quality at Consumer Premises," presented at the Electricity Engineers' Association Conference, Wellington, New Zealand, Jun. 2015.

[83] Electricity Networks Association, "New Pricing Options for Electricity Distributors," Electricity Networks Association, Nov. 2016. [Online]. Available: https://www.ena.org.nz/dmsdocument/38.

[84] Electricity Authority, *Installed Distributed Generation Trends*. [Online]. Available: https://www.emi.ea.govt.nz/r/jrna0 (visited on 05/28/2020).

[85] Statistics New Zealand, *2013 Census QuickStats about Housing*. 2014, ISBN: 978-0-478-40881-2.

[86] F. J. Massey, "The Kolmogorov-Smirnov Test for Goodness of Fit," *Journal of the American Statistical Association*, vol. 46, no. 253, pp. 68–78, Mar. 1, 1951. DOI: 10.1080/01621459.1951.10500769.

[87] I. T. Young, "Proof without prejudice: Use of the Kolmogorov-Smirnov test for the analysis of histograms from flow systems and other sources.," *Journal of Histochemistry & Cytochemistry*, vol. 25, no. 7, pp. 935–941, Jul. 1, 1977. DOI: 10.1177/25.7.894009.

[88] J. D. Watson, N. R. Watson, D. Santos-Martin, A. R. Wood, S. Lemon, and A. J. Miller, "Impact of solar photovoltaics on the low-voltage distribution network in New Zealand," *IET Generation, Transmission & Distribution*, vol. 10, no. 1, pp. 1–9, Jan. 7, 2016. DOI: 10.1049/iet-gtd.2014.1076.

[89] Flick Electric, *Price Schedules - Christchurch*, Oct. 2019. [Online]. Available: https://www.flickelectric.co.nz/christchurch-pricing.

[90] ——, *Home Generation Terms and Conditions - Jan 2018*, Jan. 2018. [Online]. Available: https://assets.ctfassets.net/z9mrw39mhtzh/7CrkjeJ4GI0Eim4UQGoCE6/ff336dcb7661dcf58fe8e3d5027d5f73/Home_Generation_Terms_and_Conditions_-_Jan_2018_.pdf.